Mitigation against Lateral Buckling and Axial Walking of Subsea Pipelines

Godwin Effiong Eton BSc MSc MNMGS FGS

Submitted in accordance with the requirements for the degree of

Doctor of Philosophy

The University of Leeds

Institute of Resilient Infrastructure

School of Civil Engineering

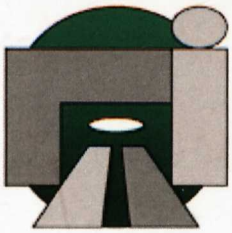

September, 2011

Declaration

The candidate confirms that the work submitted is his own and that appropriate credit has been given where reference has been made to the work of others.

This copy has been supplied on the understanding that it is copyright material and that no quotation from the thesis may be published without proper acknowledgement.

The right of Godwin Effiong Eton to be identified as Author of this work has been asserted by him in accordance with the Copyright, Designs and Patents Act 1988.

Acknowledgements

This work was made possible through support and guidance received in one way or the other from people whom I would wish to appreciate at this point. I would start by thanking my primary supervisor Prof. Barry Clarke for his immense guidance throughout this research which has significantly improved my understanding of soil mechanics concepts and has made this research a reality. My second supervisor Dr Terry Cousens was also very helpful in guiding me through all aspects of this study.

My unreserved gratitude goes to the management and staff of the petroleum technology development fund (PTDF) Nigeria, for providing the funds for this research. I thank Dr Peter Allan of Geomarine geotechnical offshore services for all the technical support and for proving the inspiration to do research in offshore geotechnics after the brief period I worked with him. My warm regards to Prof. Clifford Teme, my "second dad", for inspiration to pursue further studies in geotechnical engineering after my BSc study.

Special thanks go to Mr Mike Marsden of Leeds University geotechnical laboratory. His time, care and constant assistance made my time in the lab very enjoyable. I also appreciate the staff of the mechanical engineering workshop especially Mr Steve Caddick for fabricating all the equipment used in this study. Mr Paul Hamer, Mrs Marcia Martell, Mr Peter Flatt of concrete casting lab, members of our geotechnical research group: Tom Liu, Edet Efretuei, Kenneth Eshiet, Khairul Mohd Yusof and some MSc students in the research group: Luke Jacques and Daniel Beadnall all deserve a special thank you. Special thanks go to my bosom family friends within my house fellowship group who made my stay in Leeds very rewarding and memorable: Mr Peter Iyoko and family, Mr Tayo Fabiyi and family and Mr Dapo Olapoju and family.

My wife, Emeti-Abasi, my daughter Edidiong and my son Ubong-Abasi all deserve a big thank you for their understanding and support throughout this period. Thanks my dears for all your understanding. *Imaima*, I love you real good! I will surely make it up for you all. I also thank my parents, Mr and Mrs E. Eton and my siblings for being there for me. Finally, I return all glory to God Almighty who saw me through this journey. He was my strength and my source. Thank you Lord!

"... I cannot conceive of the time when knowledge of soils will be complete. Our expectation is that our successors will build on what has been done, as we are building on the work of our predecessors."

— R.S. Smith, Director of the Illinois Soil Survey, 1928

To my beloved wife, Emeti-Abasi
My daughter Edidiong and
My son Ubong-Abasi

And,
My late mother, Mrs Grace Eton
Who passed on to glory this September 2011
Just before I could inform her that I have finished!!

Abstract

There is a growing concern amongst offshore pipeline operators over the instability problem of lateral buckling and axial walking of offshore pipelines which is linked with elevated operating temperature and pressure. While some mitigating options are available to tackle this phenomenon, in most cases these are expensive and impracticable in deep waters, and none of them involves the modification of the ambient soil properties typically characterised by very low undrained shear strength (c_u) and high water content (w). In recent times, the use of engineered buckle solutions has become generally accepted as a cost effective and elegant solution. This option involves laying the pipeline in a snake configuration where some specific sections are designed to move during operation while others relatively stable. This option depends on accurate understanding of pipe-soil interactions which presently poses the greatest uncertainty in pipeline design. Furthermore, in order to ensure that the buckles are formed as predetermined, the ambient soil strength must be sufficient to resist the pipe motion at locations designed to be relatively stable or the entire design approach would be undermined.

This dissertation presents laboratory investigations at both small and pilot scale directed at using the electro-kinetic phenomenon (EK) to treat the soil around a partially buried pipeline with the aim of increasing the pipeline stability to lateral buckling and axial walking. The influence of the EK treatment was assessed by evaluating the changes in the soil c_u, w and the soil resistance to vertical, lateral and axial displacements of pipe sections. Additionally, large-scale pipe-soil interaction studies were conducted to study the soil deformations, especially the real time study of the berm of soil formed and the development of the soil resistance during pipe motion.

Preliminary results of the application of EK in geotechnical engineering to offshore pipelines show up to 600% increase in c_u, 14% decrease in w and 190% increase in the pullout force thus implying promising outcomes which could form the basis for subsequent research in this area.

Keywords: Pipeline, seabed, lateral buckling, axial walking, berm, electro-kinetics

Table of Contents

List of Tables

List of Figures

Chapter 2

Chapter 3

Chapter 4

Chapter 5

Chapter 6

Roman notations

A_s	embedded side surface area of object in soil
A_{xe}	embedded *b*ase surface area of object in soil
A	object plan area
A_c	contact area between pipe and soil
A	total cross-sectional area normal to the flow direction
AL	aluminium-electrode
AFT	denotes after the EK treatment
A_{ab}	area of the active berm of soil in front of the pipe
A_{db}	area of the dormant berm left behind by the pipe
B_{oi}	berm height relative to the original pipe invert after initial embedment
B_w	water buoyancy force
B_s	soil buoyancy force
$B4$	denotes before the EK treatment
c_u	undrained shear strength
c_{up}	peak undrained shear strength at the pipe invert
c_{ur}	residual undrained shear strength at the pipe invert
c_v	coefficient of consolidation of soil
CU	copper-electrode
$\mathbf{c_u}$**-P**	normalised strength profile of the as-placed soil
C-$\mathbf{c_u}$	normalised strength profile due to consolidation effect (from the control test)
$c_{u,\ invert}$	undrained shear strength at the pipe invert level
D	outer diameter of a pipeline
d	depth of foundation of footing
D_f	depth of embedment
$D_{T\text{-}bar}$	diameter of the T-bar
EK	electro-kinetic
E	elastic modulus (Young's modulus)
E	electric field intensity, i.e., ratio of the applied voltage to distance between the electrodes
EO	electro-osmosis

EK-c_u	normalised strength profile due to EK effects
FE	finite element
F_z	vertical force on pipeline used by Verley and Lund (1995)
F_{ap}^{u}	undrained conditions, peak axial resistance defined by Oliphant and Moconochie (2007)
F_{ar}^{u}	residual undrained axial resistance defined by Oliphant and Moconochie (2007)
FE	iron-electrode
F_H	horizontal force (per unit pipe length)
F_L	hydrodynamic lift force (per unit pipe length)
F_F	sliding resistance force
F_R	penetration dependent soil resistance force
F_r	peak breakout force defined by Verley and Lund (1995)
F_a	soil bearing capacity used by Finn and Byrne (1972)
F_{lib}	immediate breakout force defined by Finn and Byrne (1972)
$F_{F\,(max)m}$	maximum friction force
F_D	hydrodynamic drag force
F_L	hydrodynamic lift force
G	non-dimensional group defined by Verley and Lund (1995) as $c_u/D\gamma'$
h	horizontal pipe penetration during lateral travel
H_{ab}	height of the active berm
H	electrode insertion depth
$h_{breakout}$	normalised breakout force = $H_{breakout}/Dc_u$ defined by Bruton et al. (2006)
H_{db}	height of the dormant berm
i_e	voltage gradient, $\frac{\Delta V}{\Delta L}$
I	applied current
I (t)	electric current as a function of time, t (A)
J	current density
k_h	hydraulic conductivity
k_e	the coefficient of electro-osmotic hydraulic conductivity
k_i	amount of water moved per unit charge passed (Gal/h/Amp)
L	distance between the electrodes
L	length of pipe section
LC	location of the T-bar tests

N_c	bearing capacity factor
N	effective axial force (compressive positive)
N	vertical soil reaction
N_R	number of polarity reversal (N_R = 1 for no reversal)
N_t	T-bar factor relating shear strength and net bearing pressure
n	soil porosity
P	power consumption during EK treatment
p	internal pressure - external pressure
q_A	flow rate through a bundle of capillaries
q	T-bar bearing pressure
R	the resultant force acting on an object placed at the water-soil interface
t_{on}	power on time (min)
t_{Ri}	treatment time under each polarity defined by Micic et al. (2002a)
t_{off}	power off time (min)
S	non-dimensional group defined by Verley and Lund (1995) as W_s/LDc_u
SC	specific conductivity
SG	specific gravity
Stl_{consl}	maximum settlement at the end of consolidation of soil in the testing tank during the EK test (phase-1)
Stl_{EK}	maximum settlement due to the EK treatment of soil in the testing tank (phase-2)
S_t	soil sensitivity
S_b	width of base of active berm
S_s	soil softening index
T	wall thickness
T	residual effective tension left after construction has been completed, but before the pressure and temperature change.
T	current intermittence ratio
T_{ab}	trench level in front of active berm
U	width of dormant berm
$v_{T\text{-}bar}$	velocity of penetration
V_{max}	maximum voltage
V	voltage at any particular point
v	Poisson's ratio
v'	normalised vertical pipeload V/c_uD

v volume of treated soil, = A x H (m^3); A = treatment area (m^2)

V_o initial applied voltage (V)

V_{sl} soil level in front dormant berm

V non-dimensional velocity defined by Finnie and Randolph (1994) as $V = D_{T\text{-}bar}\, v_{T\text{-}bar}/c_v$

V vertical unit pipe load (Bruton et al., 2006)

W_S *or* W' submerged weight of pipe

w soil water content

w, a and b fitting coefficient for limiting conditions of roughness used by Aubeny et al.(2005)

W_{sl} soil level at the dormant berm

W weight of object in air

W_e energy consumption per unit volume of treated soil (Micic et al., 2002a)

x vertical pipe penetration during lateral travel

x_{max} maximum vertical pipe penetration during lateral travel

X_{sla} soil level at the top of the active berm in front of pipe

X distance from the cathode

z_{init} initial depth of penetration of pipeline used by Bruton et al. (2006)

$z_{startup}$ initial pipe embedment at startup

z_i initial depth of embedment of the pipe

z depth of pipe penetration defined by Verley and Lund (1995)

Z_{io} the original pipe invert level before start of sweep

Z_{ie} soil level after initial pipe embedment

Z_s instantaneous pipe penetration into the soil

ZOI_F calculated zone of influence below the mudline due to embedded pipe section

ZOI zone of influence

ZOI_c a non dimensional term used to relate the combined lateral and vertical extents of the EK effects

Greek notation

γ_w	unit weight of water
μ	friction coefficient
γ'	effective unit weight of soil
γ_s	total unit weight of soil
a	amplitude of pipe motion.
μ	coefficient of sliding resistance
η_p	adhesion factor which is dependent on the relative roughness of the pipe
η_r	residual adhesion factor
μ_p	peak coefficient of friction defined by Oliphant and Moconochie (2007) as f_p. $\tan\Phi_p = \tan \delta_p$
f_p	resistance factor used by Oliphant and Moconochie (2007)
Φ_p	peak drained angle of shearing resistance
δ_p	peak interface friction angle
θ	operating temperature-installation temperature
i_e	the electrical potential gradient
ζ	zeta potential
u_e	pore water pressure due to EO
σ_v'	vertical effective stress
σ	stress

Abbreviations

OSS	out of straightness features
HTHP	high temperature-high pressure
EKGs	electro-kinetic geosynthetic materials
CFA	continuous flight auger

Chapter 1

INTRODUCTION

1.1 Introduction

As the world population grows, there is an increasing demand for energy and oil and gas continue to play a leading role; no other alternatives have yet been proven to economically replace them. This high demand in oil and gas has initiated the current move to deep offshore exploration and production of the energy trapped in the seabed. The concomitant requirement of this move is a high demand for more pipeline networks, which are increasingly being required to operate at elevated temperature and pressures in order to ease the flow within these pipelines. These elevated temperatures and pressures force the pipeline to expand but this expansion is normally restricted by the interface friction between the pipeline and the seabed resulting in an imposed axial stress on the pipeline. This in most cases may result in pipeline displacements in either vertical (referred to as upheaval buckling), lateral (lateral buckling) or axial (axial walking) directions depending on the path of the least resistance.

The capacity of these pipelines to withstand the internally induced displacements depends on the weight of the pipeline and the soil strength. As the pipe moves laterally at the buckled section, a berm of soil is formed which tends to increase the resistance of the soil to further pipe motion. The deformation of soil during this berm formation and the accurate prediction of this berm effect are not fully understood. Excessive lateral buckling may lead to pipeline rupture resulting in loss of containment and release of oil/gas into the offshore environment. The financial impact of the recovery and clean-up process, lost production and repair or replacement of pipeline may be in the excess of US$200M (Griffiths et al.,2007), depending on the project specifics. This instability of offshore pipelines is currently a serious issue facing offshore pipeline operators prompting the current search for mitigating methods.

The simplest and the most straight forward means to increase pipe stability is to dig a trench and bury the pipe. However, with the increasing move to deeper waters, this becomes expensive and not feasible thus prompting a need for more cost effective alternatives. Of all the other existing methods available, none of them considers the modification of the soil properties which supports the pipeline. Additionally, the interaction between soil and pipeline during the pipeline motion is until now the greatest uncertainty in pipeline design and the mechanism of soil failure during pipeline displacement is not fully understood.

Recent studies on pipe-soil interaction and pipeline instability (Carr et al.,2003; Cheuk et al.,2007; Bruton et al.,2008; White and Cheuk,2008) suggest that a more efficient design method is to relieve the axial stress by controlling the formation of buckles along the pipeline. This is an "on-bottom" engineered buckling approach described by pipeline operators as "snake-lay". By adopting the snake-laying configuration, some sections of the pipeline are designed to buckle when the pipe is loaded as it tries to expand on the seabed, hence relieving the axial stress imposed on the pipeline. On the other hand, some sections are designed to be relatively stable otherwise the whole approach will be seriously undermined. In order to ensure that the buckles are formed as predetermined, the soil strength must be sufficient to resist pipe motions at locations designed to be relatively stable. This soil strength can be enhanced by using an approach which has been tested to be effective in enhancing the capacity of foundation soils.

Electro-kinetic improvement of soft clay soil is not new in geotechnical engineering practice. It has been successfully used in improving the foundation soil in onshore areas such as slope stability (Casagrande,1952) and improvement of pile bearing capacity and recently has been employed offshore to enhance the bearing capacity of offshore foundations. It is yet to be applied to offshore pipelines. Therefore, the focus of this research is on mitigation measures involving the modification of the soil properties around partially buried pipelines using electro-kinetics technology as well as studying the soil deformation behaviour during lateral deflection of pipeline, that is the berm effects on the soil resistance to pipe displacement.

1.2 Motivations for the study

This research was undertaken due to two major concerns facing offshore pipeline stability. These are the uncertainty relating to pipe-soil interaction and the need to increase the resistance of subsea pipelines to instability due to elevated temperature and pressure. This work investigates some of the uncertainties involving pipe-soil interactions which affect its stability on the seabed and then attempts to enhance its stability by engineering the ambient soils around the pipeline. The current study should be of direct benefit to practising offshore pipeline engineers and also presents a more cost-effective way of reducing the instability of the pipeline caused by high temperature and pressure conditions.

1.3 The aim of this study

The aims of this study are (1) to investigate the use of electro-kinetic (EK) technology to increase the stability of partially embedded offshore pipelines by increasing the soil resistance to the pipe's displacement and, (2) to study the soil deformation behaviour during large pipeline displacements which are associated with the operational induced conditions with the aim of reducing the uncertainty with pipe-soil interaction during pipeline motion.

1.4 Objectives of the study

To address the above issues, the development of the application of EK to enhance the stability of a partially embedded pipeline was investigated through a series of small-scale and pilot tests. Additionally, a series of pipe-soil interaction tests were conducted aimed at studying the resistances offered by soil to a partially embedded pipeline. Emphasis was placed on the formation, growth and influence of the berm of soil. This research will help to improve current knowledge of soil-pipeline interaction and mitigation against lateral buckling and axial walking of these pipelines.

The following objectives were set:

1) To conduct a literature review to determine current and developing practice in controlling lateral buckling and axial walking of offshore subsea pipelines

2) To investigate the use of EK technology to increase the stability of a partially embedded pipeline at pilot scale.
3) To study the effect of electro-kinetic treatment on soil resistance to vertical, lateral and axial resistances of partially embedded pipelines
4) To comment on the effects of electrical parameters and soil properties on the performance of the electro-kinetic treatment
5) To comment on the influence of electrode material on the effectiveness of the EK treatment
6) To make recommendations and suggestions on the application of the EK technology to offshore pipeline operations

On the pipe-soil interaction study, the following objectives were set out to be achieved:

7) To develop and implement a new and improved testing rig for studying pipe-soil interaction at pilot scale
8) To observe the deformation mechanism pattern of the soils surrounding the pipe section during large lateral displacements
9) To measure the resistance of a model seabed to lateral and axial motion of a partially embedded pipe section
10) To study the deformation characteristics and geometry of model seabed during pipe motion and comment on the effects on the soil resistances
11) To investigate the influence of pipeline properties such as the initial depth of embedment and the weight of the pipe on the deformation behavior of the soil during pipe motion
12) To investigate the influence of speed of pipe movement, amplitude of lateral and axial displacement, number of cycles and comment on the soil deformation patterns

1.5 Structure of the thesis

This thesis is subdivided into seven chapters which are described below:

The background to this study including motivation, aims and objectives for this study, is presented in Chapter 1.

Chapter 2 is the literature review which focuses on the instability problem of partially embedded offshore pipelines. The behaviour of high temperature-high pressure pipelines is discussed including existing methods to mitigate their instability problems. Finally, research on electro-kinetic technology in geotechnical engineering especially as applicable to soil improvement is presented.

Chapter 3 presents the experimental methodology. This is divided into two parts: part one focuses on the electro-kinetic treatment of a model seabed in small testing tanks while part two deals with the large-scale pipe-soil interaction test which is aimed at studying the soil deformation behaviour during large amplitude of pipe displacement on a model seabed. This displacement of the pipeline simulates the behaviour of partially buried pipelines on the seabed during lateral buckling and axial walking.

Chapter 4 is concerned with the results of the investigation to assess the feasibility of using electro-kinetic processes to modify a model seabed. The discussions of the results of the electro-kinetic treatment of the soil in the small and the large testing tanks described in chapter 4 are presented Chapter 5.

Chapter 6 presents the results and discussions of the large-scale pipe-soil interaction tests while Chapter 7 presents the summary and conclusions of the results of the entire research and makes recommendations for future work.

Chapter 2

LITERATURE REVIEW

2.1 Introduction

The problems associated with subsea pipeline stability have been extensively studied by many researchers. Two major areas of research have been the problem relating to the stability of pipeline under environmental loadings (mainly hydrodynamic loadings) and operational loadings (from elevated temperature and pressure) resulting in the thermal buckling of pipelines. The problem relating to hydrodynamic loadings has received significant attention in the past while the problem of the operation loadings has become an issue only recently. While a considerable amount of work has been done to investigate the problem of pipeline instability, not much research has been carried out to investigate the solutions.

This chapter presents a review of the research focused on partially embedded pipeline stability on the seabed including the mechanics and prediction methods of the pipeline-soil responses during pipe motions. It then discusses work on the nature and compositions of offshore seabed clay soils. An overview of the existing methods of controlling pipeline instability as well as some methods of soil improvement are then discussed followed by research into EK technology in geotechnical engineering. A summary of the literature review is then presented at the end of the chapter.

2.2 Stability of subsea pipelines -understanding the problem

An early attempt to analyse and predict the stability of subsea pipelines was by the use of the classical bearing capacity approach (Small et al.,1972). Figure 2 - 1 is a picture of a partially embedded pipeline on the seabed. Small et al. (1972) assumed the pipeline to be a strip footing foundation for the evaluation of the initial pipe settlement using the

ultimate bearing capacity of the soils from the classical soil mechanics bearing capacity theories proposed by Terzaghi and Peck (1948); Meyerhof (1951); and Skempton (1951). However, this theory relies on the behaviour of flat strip footing foundations and not the curved base associated with pipelines which makes direct application of these theories questionable.

Figure 2 - 1: Typical partially embedded pipeline on the seabed

Research focused on the complex problem of pipe-soil interactions and pipeline stability can be grouped into two areas: (a) stability against hydrodynamic loading where the pipe is designed to allow for limited or no movement, and (b), stability against large amplitude of displacement of the pipeline: up to ten pipe diameter (Carr et al.,2003). Most of the research on pipeline stability initially focused on the first part as in Lyons (1973) and Ghazzaly (1975) while the second part has only recently received attention from researchers due to the phenomenon of pipeline buckling which is associated with high temperature-high pressure (HTHP) operating conditions.

2.2.1 Analysis of lateral resistance of partially embedded pipeline

The horizontal capacity of embedded offshore pipeline has traditionally been estimated in industry by a Coulomb friction model (Figure 2 - 2). Here, the lateral forces attempting to displace the pipe are resisted by a friction force, assumed equal to the effective weight of the pipe times a coefficient of friction between the pipe and sediment normally assumed constant of the order of 0.4 – 0.5, (Morris et al.,1988). This approach is based on the assumption that the seabed supporting the pipe is rigid and stable and the pipe slides parallel to the surface and the soil resistance is not affected by pipe displacement. Both the deformation of the soil during pipe motion and the pipe trajectory during motion are not considered in this assumption. However, this

assumption might hold for stiff clay and dense sand but not for soft clay due to significant pipe penetration during motion.

To determine the stability of the pipeline on the seabed, the hydrodynamic drag force is computed in advance and the minimum weight of the pipe to exceed this drag force is determined. The drag force is the horizontal component of the hydrodynamic force produced when a wave or current flows across a pipeline laid on the seabed. This is shown in Figure 2 - 2 as F_D. It is this external force which attempts to displace the pipeline on the seabed. This conventional approach is still available in various design codes such as BS8010 (1993): part 3 and Veritec-RP-E305 (1988). However, (Lyons,1973), using empirical data from his test on sand and soft clay as well as finite element (FE) modelling, was the first to point out the weakness of this design approach. The test conducted in clays was typically at the depths of pipeline embedment of less than 1D. He concluded that the Coulomb friction model which relies on the weight of the pipe may be adequate to predict the soil lateral resistance to sliding of a pipe on stiff clay or dense sand but not for soft clay soil. He proposed the use of FE as a better model for predicting lateral stability on soft clays.

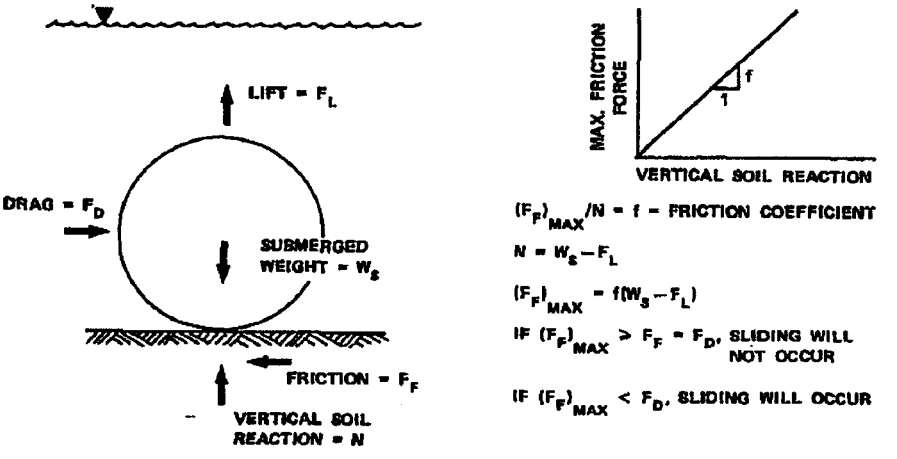

Figure 2 - 2: The conventional Coulomb friction analysis (after Lyons (1973)

Other observations noted by Lyons (1973) were that the lateral resistance in clays decreased with increasing pipe diameter and increased with increasing submerged weight of the pipeline and that the friction coefficient for clay depends on pipe diameter, weight of pipe and the coating material. The friction coefficient (μ) increases with weight of pipe and is higher for bare pipe than coated pipe. However, Lyons

(1973) attempts at using FE to predict the lateral resistance of soft clay was limited in application and was subsequently strengthened by Karal (1977) through the introduction of some geometrical, loading and material parameters.

Karal's (1977) study was the first use of a theoretical geotechnical approach to analyse pipeline stability where he used an upper bound approach of the theory of perfect plasticity to develop a method for geotechnical stability analysis of subsea pipelines in both clay and sand. He idealised the pipeline as rigid wedge indenter and presented the results in parametric forms. The effect of time on the lateral resistance of soil was studied by Karal (1983). Murff et al.(1989) extended Karal's (1977) method by developing both upper and lower bound solutions to the pipe penetration in uniform strength clay soil with the pipe idealised as a rigid cylinder. They presented a plasticity solution for pipeline penetration in cohesive soil. However, in their analysis the pipe-soil contact was below the centre of the pipeline making the solution only valid for small pipeline penetration up to 0.2D.

Still with limited data on the lateral resistance for clay soil, Wantland et al. (1979) embarked on further studies to investigate specific areas especially:- effects of pipe weight, pipe diameter (D), depth of embedment and soil type on the lateral capacity developed during lateral displacements of pipes. This work involved both field and laboratory studies which were aimed at providing a relationship between the developed lateral resistance and the variables mention above. This study did not, however, include soil deformation pattern and the effect of the soil deformation pattern were not studied. The test rig was not sophisticated enough to measure the lateral displacement directly but deduced from the rate of displacement.

Wantland et al. (1979) concluded that there was no influence of the rate of pipe displacement on the soil lateral resistance, but that the lateral resistance was influenced by the depth of embedment. The displacement before failure was highest for the relatively shallow pipes and the deepest pipes but was lowest for the intermediate values of relative penetration of the pipe. This they attributed to the fact that shallow pipes appear to fail by surface sliding, which involved the continuous build up of a soil berm.

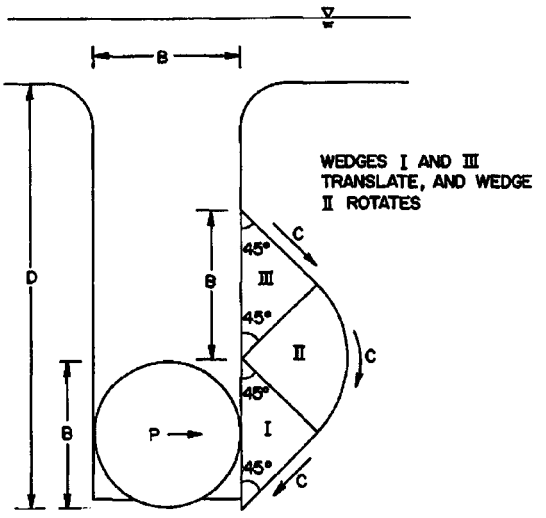

Figure 2 - 3: Assumed flow pattern for pipe embedded for more than 1D during lateral displacement of pipe, after (Wantland et al.,1979)

Deeply buried pipes fail through a flow mechanism as depicted in Figure 2 - 3. This requires considerable displacement to mobilise fully. Soil for the intermediate depth of penetration fails by producing an incomplete failure surface, approximately a Coulomb passive wedge.

The first field large-scale pipe-soil study to determine coefficient of lateral soil friction was conducted by Lambrakos (1985) for hydrodynamic stability. However, this test did not address pipe-soil interaction aspect and was only concerned with the determination of coefficient of friction of the soil during pipe displacement.

2.2.2 Effects of oscillatory pipe displacement

The effect of oscillatory pipe displacement on the pipe-soil response was investigated by Brennodden et al (1986) in a full-scale test. They came to the following conclusions: - small oscillatory motion generally increases the resistance in loose medium/ coarse sand and soft clay; large-amplitude oscillations may degrade resistance in loose silty fine sand; resistance in dense medium/coarse sand and stiff clay is less sensitive to prior cycling; consolidation of clays increases the resistance to monotonic loading but the increase is quickly broken down by cycling. Palmer et al. (1988) simulated various loading regimes during pipe installations and concluded that cyclic loading increases lateral resistance.

A laboratory study to quantitatively determine the extent that a pipeline resting on a seabed would self-bury when subjected to cyclic loading from wave and current forces was carried out by Morris et al. (1988). These studies only considered cyclic displacement between 0.05D and 0.5D which is less than the large amplitude displacement typical of a buckling pipeline. As the pipe settles due to cyclic displacement, a berm of soil forms at the sides of the pipe. Thus an additional resistive term is included in the resulting lateral resistance. To predict the amount of pipeline embedment from a given cycles of pipe displacements, Morris et al. (1988) proposed the use of Figure 2 - 4 where the embedment "*h*" is normalised by the pipe diameter, D. Apart from the fact that this study did not include the measurement of the lateral extent of the deformed soil in front of the pipe, these plots were produced from uniform loading cycles from storm waves and not likely to be applicable in the large amplitude of lateral displacement associated with HTHP pipelines.

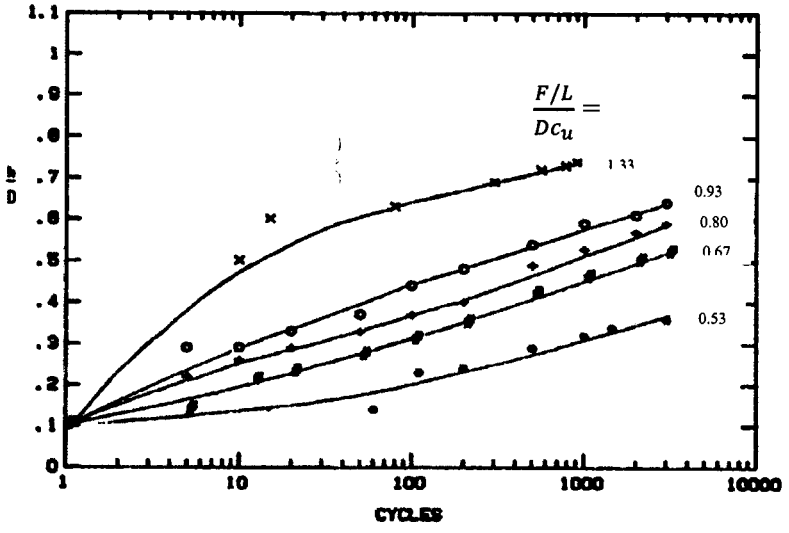

Figure 2 - 4: Embedment against time chart (after Morris et al., 1988)

2.3 Mechanics of the breakout of partially embedded objects

In offshore geotechnical engineering and in particular offshore pipelines, the need to accurately predict the amount of force needed to lift an offshore structure including pipelines embedded in seabed sediment is a vital component of the design process as this assesses the long term stability of the structure after placement. This force in excess of the submerged weight of the object is referred to as the breakout force (Muga,1967; Vesic,1971). This is sometimes referred to as the mud suction (Liu,1969). The classification for either partial or complete embedment of an object such as a pipeline is

a function of the depth of embedment with respect to the diameter of the pipeline. If the pipeline is embedded by an amount greater than its diameter, then this would be a fully embedded pipeline and its breakout resistance is partly dependent on the failure of the soil above the pipeline whereas if the depth of embedment is less than the diameter, then the pipeline is considered to be partially embedded and its breakout resistance governed by the factors below the base of the pipeline such as suction and soil strength (Lee,1973).

If an object is resting on the sea floor without embedment and no adhesion develops between the object and the ocean sediment, then the force required to lift the object will be equal to its submerged weight only. The value of the breakout force in this case is zero. If the object is embedded and an attempt is made to lift it, skin friction or adhesion which develops around the sides of the object and adhesion along the base will resist the effort to lift it. The difference between the force now required to raise the object and the submerged weight is the breakout force. The contribution from skin friction and adhesion in many cases is only a small fraction of the total breakout force. Thus the mechanism for resisting breakout cannot, in most cases, be assumed to be due to skin friction and adhesion, and other mechanisms must be sought (Vesic, 1971).

Liu, 1969, and Finn and Byrne, 1972 both argue that the behaviour of dislodging an object embedded in the seafloor is similar to bearing capacity failure of a shallow foundation. This is because the two failures are not only time dependent but also strongly dependent on the weight of the object resting on the soil surface. The resistance to which the soil offers to the breakout of an object is referred to as the soil holding strength as it is strongly dependent on the shear strength of the soil (Lui,1969). Factors affecting this force are the type of soil (cohesive and non-cohesive), rate of loading (drained or undrained), surface of embedded (object-skin roughness or skin friction) and the depth of embedment.

2.3.1 Mechanism of breakout during pullout for a partially buried object

The mechanism of breakout of a partially embedded object in the seabed has been described by Liu (1969). While this study dealt with different offshore structures including sunken submarine vessels, a direct application to a surface-laid pipeline is justifiable. A schematic of the forces acting on a partially embedded object is shown in

Figure 2 - 5. A constant lifting force is applied through the centre of gravity of the object.

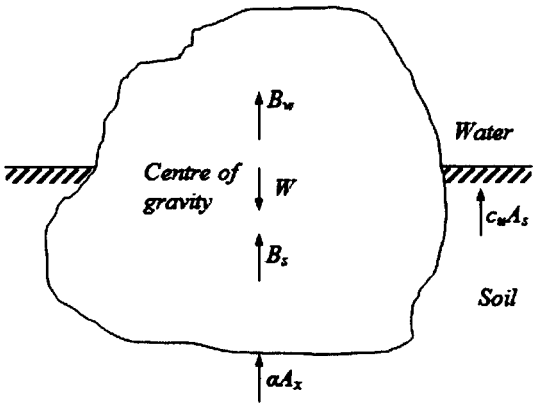

Figure 2 - 5: Forces acting on an object during breakout (after Liu, 1969)

During vertical pulling of the object from the seabed, the lifting force first relieves the soil bearing pressure underneath the object. The object remains in this position until both the bearing pressure and side friction force are counter balanced. The balance of the lift force will then produce an upward motion of the object. The vertical pulling force is normally resisted by the stationary shear stress/friction shear forces on the sides of the object and the tension resistance under the object. These determine the magnitude of the breakout resistance offered by the seabed. Thus the strength of the soil plays a major role in the breakout force.

According to Liu (1969), the resultant force (R) acting on an object placed at the water-soil interface may be expressed as:

$$R = W - B_w - B_s - c_u A_s - \alpha A_x \qquad 2\text{-}1$$

Where

W = weight of object in air

B_w = water buoyancy force

B_s = soil buoyancy force

A_s = side surface area of object

A_{xe} = base surface area of object

c_u = undrained shear strength of soil

α = bearing strength of soil.

The values of W and B_w are constant, whereas B varies with the embedded depth. The extra buoyancy force from the soil (B_s) is due to the fact that the object displaces soil that has a higher saturated density than the water (Randolph and Quiggin, 2009).

The mode of failure under pull-out is different from the deformation pattern developed under compressive load. As the embedded object is pulled upward (depending on the soil strength and suction developed) the soil mass outside the object moves laterally towards the object while the soil beneath the object moves up. This failure pattern is consistent with the failure mode observed by Byrne and Finn (1978). Finn and Byrne (1972) suggested that the conventional bearing capacity and breakout problems have similar failure mechanisms but with opposite direction of motion (Figure 2 - 6).

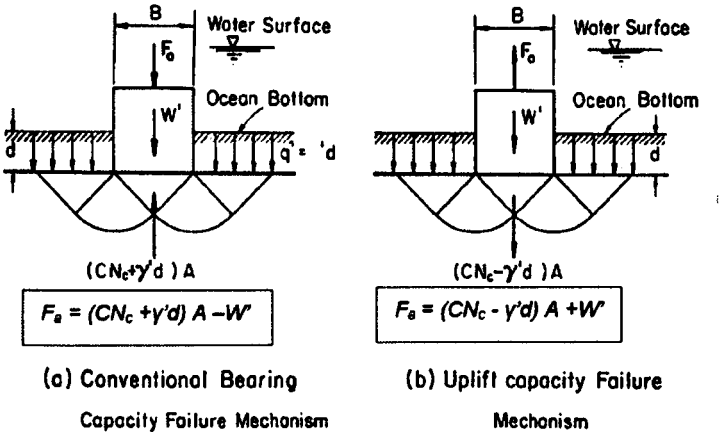

Figure 2 - 6: Plastic failure mechanisms for bearing capacity and uplift of shallow footing (after Finn and Byrne 1972)

2.3.2 Dependence of breakout force on soil strength

Finn and Byrne (1972) suggested that the mechanism of soil failure during object pullout is similar to the mechanism of shallow footing failure when loading in compression provided suction develops underneath the embedded object. This assumption lead to the proposition of a modified bearing capacity equation for determination of the breakout force as:

$$F_{lib} = (c_u N_c - \gamma_s D_f)A + W_b \quad 2\text{-}2$$

Where

c_u = soil undrained shear strength

N_c = bearing capacity factor which depends on the shape of the embedded object

W_b = the submerged weight of the object

γ_s = unit weight of the seabed soil

D_f = depth of embedment of the object

A = object plan area

The above expression indicates the breakout force of a partially embedded object in seabed is directly related to the undrained shear strength of the soil. This in turn is related to soil water content (w). Therefore the magnitude of the breakout force could substantially improve by increasing the undrained shear strength of the seabed soil.

2.4 Prediction models for soil lateral resistance and pipe penetration

2.4.1 Methods for predicting pipeline embedment

The total pipe penetration into soft seabed is dependent on the magnitude of the immediate penetration, consolidation settlement during installation and the additional settlement due to hydrodynamic forces or disturbances during installation (Cathie et al.,2005). While the level of disturbance is subject to a high level of uncertainty and could be difficult to predict, the approach for predicting the penetration caused by shearing of the soil, which contributes the largest portion of the pipe penetration, have been suggested by different researchers using analytical closed form solutions (Small et al.,1972; Ghazzaly and Lim,1975; Karal,1977; Wantland et al.,1979; Aubeny et al.,2008). The basic assumption is to idealise the pipe penetration as a bearing failure of a shallow strip footing as shown in Figure 2 - 7.

A rigorous classical analysis of pipe penetration in soft clay was presented by Murff et al. (1989) and is based plasticity solutions. They assumed a rigid-plastic response for clay and zero friction between the pipeline and the clay. Aubeny et al.(2005) extended the work of Murf et al (1989) which concentrated on uniform c_u and depth of embedment less than one-half cylinder diameter (D) to soils with linearly varying strength profile with pipe embedment exceeding 1D.

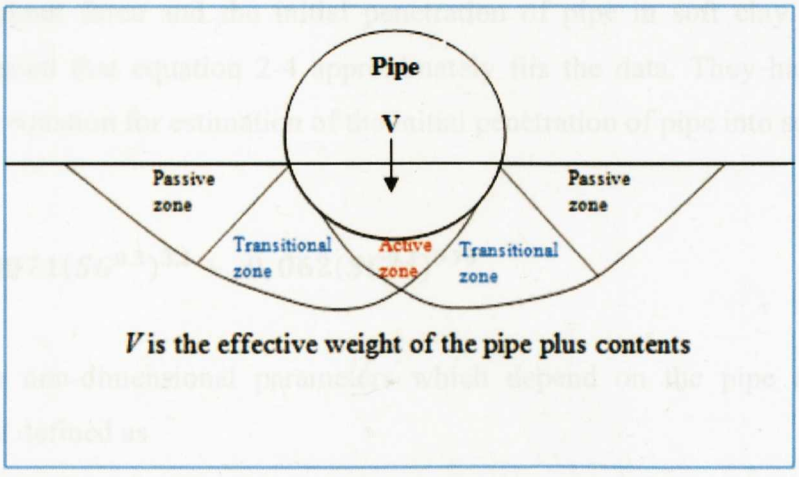

Figure 2 - 7: Schematic illustration of the mechanism of immediate pipe penetration based on the general bearing capacity failure mode

They presented a series of solutions for soil resistance versus embedment depth obtained from FE simulation and approximate solutions using classical plasticity theory. They suggested that load was expressed in terms of shear strength at the pipe invert. The limiting load at a given penetration was given as:

$$\frac{V}{c_{u,invert}D} = a\left(\frac{w}{D}\right)^{b} \qquad \textbf{2- 3}$$

Where

V = the vertical load

D = the pipe diameter

c_u = soil shear strength at penetration and

w, a and b are fitting coefficient for limiting conditions of roughness.

For a perfectly rough pipe, Aubeny et al 2005 suggested a = 7.41 and b = 0.37. For perfectly smooth pipe, a = 5.42 and b = 0.29.

The empirical equation proposed by Verley and Lund (1995) to assess the maximum penetration and soil resistance is the one most used. They suggested maximum z/D of 0.3 for the equation to be valid (z is the depth of pipe penetration). However this expression did not include the rate of cyclic motion, pipe coating, angle of applied force and the effects of seabed gradients on the penetration. This model was based on data collected from a large database of large and small scale tests and from numerical analysis used to develop models based on non-dimensional groups. The model predicts

both the breakout force and the initial penetration of pipe in soft clay. Subsequent analyses revealed that equation 2-4 approximately fits the data. They have therefore proposed this equation for estimation of the initial penetration of pipe into soft clays.

$$\left(\frac{z}{D}\right) = 0.0071(SG^{0.3})^{3.2} + 0.062(SG^{0.3})^{0.70} \qquad \textbf{2- 4}$$

S and G are non-dimensional parameters which depend on the pipe and the soil properties and defined as

$$S = \frac{W_s}{LDc_u} \qquad \textbf{2- 5}$$

$$G = \frac{c_u}{D\gamma_s} \qquad \textbf{2- 6}$$

In the same way, the maximum pipe penetration was estimated by fitting the data obtained from the database by Verley and Lund 1995 as:

$$\left(\frac{z}{D}\right)_{max} = 1.1SG^{0.54}\left(\frac{a}{D}\right)^{0.17} \qquad \textbf{2- 7}$$

Here, z is the pipe penetration (distance between bottom of pipe and original seabed) and, a is the amplitude of pipe motion.

The lower bound solutions of Murf et al (1989) are shown in Figure 2 - 8 and compared with experimental data and the Verley and Lund (1995) approaches. These solutions are very important in very soft clay where embedment may be very significant. The scatter is mainly due to difficulty in measuring the strength of the soft clay with depth (Cathie et al.,2005; White and Cheuk,2008). The plasticity solution did not account for the soil heave and berm of soil or any increase in strength with depth.

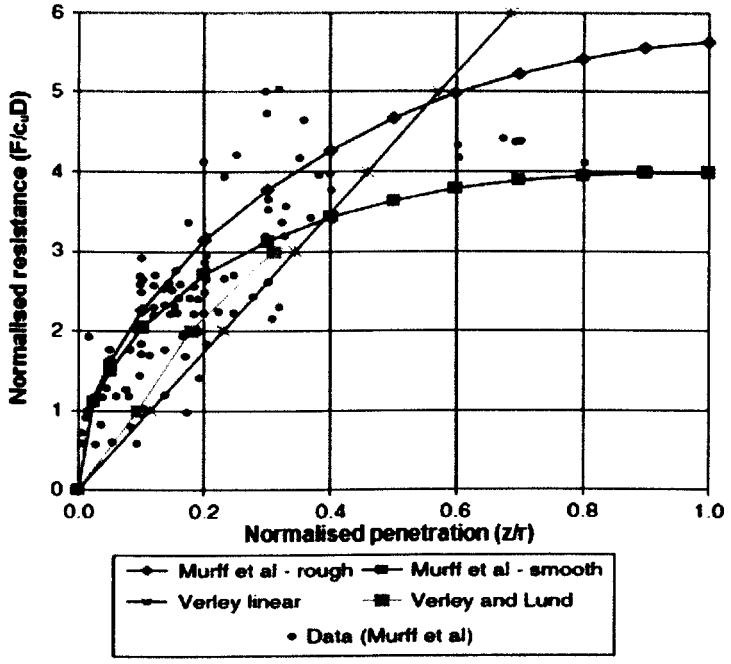

Figure 2 - 8: Lower bound plasticity solutions and empirical approaches for pipeline penetration in cohesive soils after (after Cathie et al.,2005)

While these prediction methods are widely used in the industry for design of pipeline stability, the actual field penetration after pipeline installation is often larger than the predicted value indicating a high level of conservatism in the pipe stability design (Lund,2000). This is attributed to high level of uncertainty relating to pipe loading during installation. Also, these prediction models suffer with uncertainty due to non-uniformity of the pipe responses during lateral motion.

A case is a real life field observation (Pinna et al.,2003) of the non uniformity in the self burial of offshore pipelines –where some sections of the pipeline experienced significant self-burial while some sections remain exposed. This implies that the existing prediction methods available for estimating pipeline penetration may not predict accurately the real life behaviour of these pipelines.

2.4.2 Penetration due to cyclic loads

Cyclic vertical loading was investigated by Dunlap et al. (1990) while cyclic lateral loading from environmental loading has been instigated by Morris et al (1988). In both cases, the depth of the penetration was due to the magnitude of the force or displacement and the duration of the application of the applied force.

Verley and Lund (1995) proposed an empirical equation to assess the magnitude of the maximum penetration that can be achieved for a given amplitude of motion and to assess the development of the penetration as a function of the work done by the pipe on the soil. They suggested that due to the limitations of the data (data used was from a number of previous test data), an upper limit of $(z/D)_{max}$ of 0.3 should be applied.

$$\left(\frac{z}{D}\right)_{max} = 1.1\,\frac{F_z}{Dc_u}.\left(\frac{c_u}{D\gamma}\right)^{0.54}\frac{a}{D}^{0.17} \qquad \textbf{2- 8}$$

Bruton et al. (2006) proposed an equation for initial pipe embankment for a given vertical load in a non-dimensional form to include the effect of soil sensitivity (S_t) as:

$$\frac{z_{tnit}}{D} = \frac{S_t}{45}v^2 = \frac{S_t}{45}\left(\frac{V}{Dc_{u\_tnvert}}\right)^2 \qquad \textbf{2- 9}$$

They argued that although the solutions by Murf et al. (1989) are more rigorous than a simple fit to test data and they are difficult to apply being in the form of $V/Dc_u = f(z_{init}/D)$, instead of $z_{init}/D = f(V/Dc_u)$.

Verley and Lund (1995) equation was rearranged to exclude the use of the non-dimensional parameter S and G.

2.4.3 Methods for predicting soil lateral resistance

Three approaches to the assessment of lateral soil resistance to pipe displacement have evolved over the years. These are: (1) a single friction approach where the lateral resistance is related to the effective weight of the pipelines and the soil type, (2) the two component approach where the contribution from the soil deformation is included and, (3) the plasticity model approach. The two component models are based on empirically fitting lab test data. Subsequent primary and secondary consolidation underneath the pipeline will result in additional embedment (Oliphant and Moconochie,2007).

However, Hesar (2004) argued that the separation of the lateral soil resistance into the two components has no rational basis particularly in clays since the interface friction (or adhesion) between pipeline and soil is not contact stress dependent and the strength of

clay is not constant with depth as assumed by the models. He therefore suggested the use of FE models as the best approach to predict lateral soil resistance.

Another soil model was developed during the PIPESTAB Project (Wagner et al.,1989) to predict soil resistance to lateral motion of surface-laid pipelines by including soil strength information and pipe displacement history thus improving upon the traditional Coulomb friction estimation. This consisted of two components: the sliding resistance and a penetration dependent soil resistance component. The model described the variation in total horizontal soil resistance force with lateral pipe displacement during arbitrary loading history. This model is given as:

$$F_H = \mu(W_s - F_L) + \frac{(BcA)}{D} \qquad \textbf{2- 10}$$

Where

F_H = horizontal force (per unit pipe length)

W_s = net pipe weight (per unit pipe length)

F_L = hydrodynamic lift force (per unit pipe length)

μ = 0.20 coefficient of sliding resistance

B = 39.3 for monotonic loading

31.4 - for cyclic loading (<5%D)

15.7 - for large displacement cyclic loading

c = remoulded undrained shear strength of the clay

A = one half the area of the vertical cross section of the soil displaced by the pipe

D = pipe diameter

This model is basically an empirical formula which combines a purely Coulomb friction model with a purely cohesive term for side resistance (berm). Apart from the difficulties in mixing these two approaches, the cohesive term would appear not to correspond to a plasticity approach to the actual area of shearing. In reality, deformation in soft saturated clays will be dominated by cohesive yield both for bottom sliding and lateral resistance. Their results show that increasing clay c_u decreases the lateral soil resistance since the pipeline would penetrate less into a stiffer soil. This led to their conclusion that the pipe penetration can be more important than the c_u for lateral resistance. This would therefore suggest that increasing the soil strength after the pipe penetration

should be beneficial to the pipeline stability as the passive soil lateral resistance to pipeline displacement is enhanced.

Brennodden et al (1989) developed another model based on a similar approach but using a different method for prediction of the lateral resistance. This was a research project into pipe-soil interaction conducted by SINTEF on behalf of American Gas Association (AGA) which resulted in an improved model that captures the effects of soil strength and load history on the lateral resistance shown as:

$$F_H = F_F + F_R \qquad \textbf{2- 11}$$

Where F_H is the total soil resistance force, F_F is the sliding resistance force and F_R is the penetration dependent soil resistance force. The first term in the equation depends on the net vertical pipe load, while the second term depends on the pipe penetration and the strength of the soil. The first term mimics the sliding resistance of the pipe along a flat surface. The second term (F_R) captures the soil resistance due to the failure of the passive soil wedge in front of the pipe. Their results show that the passive force term plays a dramatic role in the total resistance. They gave a general equation to describe the sliding resistance force (F_F) as:

$$F_F = \mu(W_s - F_L) \qquad \textbf{2- 12}$$

Where μ is the frictional coefficient, about 0.2 for clay soils, W_s and F_L are the submerged pipe weight and hydrodynamic lift force respectively. This was followed by energy calculation where the energy dissipated in the soil during arbitrary pipe loading was correlated with the pipe embedment.

Ayers et al (1989), described a body of research conducted by the American Gas Association (A.G.A.) which led to development of analytical models for both the hydrodynamic and pipe-soil interaction forces to be implemented in a pipe dynamic software package.

Verley and Lund (1995) have also proposed a simplification of the soil lateral resistances based on dimensional analysis. They showed that the most important

parameters are the soil c_u and the submerged weight and less important are the amplitude of hydrodynamic cyclic force and pipeline diameter. Using existing database from previous studies, they proposed that the soil resistance contributed by a given pipe embedment, z, could be estimated by:

$$\frac{F_r}{Dc_u} = 4.13G^{-0.392} \left(\frac{z}{D}\right)^{1.31} \quad \text{2- 13}$$

The peak breakout force, F_r is normalised by the pipe diameter and soil strength.
Bruton et al (2006) recalibrated the model proposed by Verley and Lund (1995) for breakout resistance based on a new database and proposed a prediction of the breakout force as:

$$h_{breakout} = 0.2v' + \frac{3}{\sqrt{c_{u\_invert}/\gamma D}} \frac{z_{startup}}{D} \quad \text{2- 14}$$

Where

v' = normalised vertical load = V/Dc_u

$z_{startup}$ = initial pipe embedment at startup

$h_{breakout}$ = normalised breakout force = $H_{breakout}/Dc_u$

c_u and γ are the soil undrained shear strength and the soil unit weight respectively.

Cathie et al.(2005) have reviewed the methods available for predicting the soil lateral resistance to pipe movement and emphasised the dependence of the soil resistance on the undrained strength of the soil which would ultimately determine the level of initial pipe penetration in the soft seabed. All the above discourse on lateral soil resistance appear to suggest that any means of increasing the strength of the soft seabed soil would considerably enhance the capacity of the soil to resisting pipeline movement.

2.5 Axial resistance on the seabed

The estimation of axial resistance of the seabed to pipe movement is a vital component of the lateral buckling design and axial walking assessment. The depth of pipe embedment, the rate and duration of pipeline loading, pipeline displacement and the relative roughness of the pipe-soil interface are determinants of the magnitude of the

axial resistance (Cathie et al.,2005; Oliphant and Moconochie,2007). It is therefore quite vital to assess the axial resistance of a partially buried pipeline at the design stage as this controls pipeline expansion and affects end connections and spool pieces.

A comprehensive discourse on the estimation of the soil axial resistance was presented by Oliphant and Moconochie (2007) where they proposed different equations for estimating axial resistance for the drained and undrained soil responses in clay as:

Undrained conditions, peak axial resistance

$$F_{ap}^{u} = A_c \cdot c_{up} \cdot \eta_p \qquad \textbf{2- 15}$$

Where A_c is the contact area which is computed as:

$$A_C = D\cos^{-1}\left(1 - \frac{2z_i}{D}\right), \text{ for } 0 < z_i \leq \frac{D}{2} \text{ and,} \qquad \textbf{2- 16}$$

$$A_C = \frac{\pi D}{2}, \text{ for } z_i > \frac{D}{2} \qquad \textbf{2- 17}$$

Where, z_i is the initial depth of embedment of the pipe, c_{up} is the peak undrained shear strength at the pipe invert, η_p is the adhesion factor which is dependent on the relative roughness of the pipe, typically between 0.7 and 1 for very soft clay. They reported that the peak axial resistance in very soft clay is typically mobilised with an axial displacement of 3 to 5mm.

Similarly, the residual undrained axial resistance can be estimated as:

$$F_{ar}^{u} = A_c \cdot c_{ur} \cdot \eta_r \qquad \textbf{2- 18}$$

Where the letter, r, denotes residual value.

c_{ur} is the undrained shear strength at the axial displacement of approximately 10cm which is related to the average sensitivity of the soil near the mudline, S_t, expressed as:

$$c_{ur} = \frac{c_u}{S_t} \qquad \textbf{2- 19}$$

The authors suggested the assumption of residual conditions for a cyclic axial displacement of the pipe with changes in direction and also advised of the use of adhesion factor at the residual displacement of 1.0.

Drained conditions

For the drained soil response, Oliphant and Moconochie (2007) and Cathie et al. (2005) suggested the use of the Coulomb friction model for estimating the peak drained axial resistance of soil to pipe displacement given as:

$$F_{ap}^{d} = \mu_p \,.\, (W' - F_L) \qquad \textbf{2- 20}$$

Where μ is the friction coefficient

$\mu_p = f_p . \tan\Phi_p = \tan \delta_p$

f_p = resistance factor

Φ_p = peak drained angle of shearing resistance

δ_p = peak interface friction angle

W' = operational submerged weight of the pipe and

F_L = the lift force

Cathie et al. (2005) reasoned that for thermal expansions, the temperature increase is likely to take several hours which may justify the need for drained analysis. The selection of appropriate friction coefficient, μ also depends on the soil friction angle and the properties of the soil-pipeline interface which could be obtained from various guidelines used in the offshore industry.

2.6 Behaviours of high temperature high pressure pipelines

Three different modes of pipe displacements are associated with HTHP pipelines namely: upheaval buckling, lateral buckling (or Euler (bar) buckling) and axial walking. Only the last two are associated with pipelines laid directly on the seabed without trenching and burial. This is because the surface-laid pipeline, unlike the buried pipeline, offers less resistance to pipeline lateral displacement and therefore the pipeline moves only laterally or axially (directions of least resistance). Figure 2 - 9 is an

illustration of the mechanism of axial walking of pipeline while a typical buckled pipeline is shown in Figure 2 - 10. Figure 2 - 9 explains the pipeline's relative movement towards the steel catenary risers (SCR).

While the solutions to the problem of upheaval buckling have received significant attention (Craig et al.,1990; Ellinas et al.,1990; Kim and Chang,1999; Andreuzzi and Perrone,2001; Nielsen and Lynberg,2004; Liming et al.,2007), relatively little has been done on the lateral buckling and axial walking phenomenon. These include (Preston et al.,1999; Perinet and Frazer,2006; Perinet and Simon,2011).

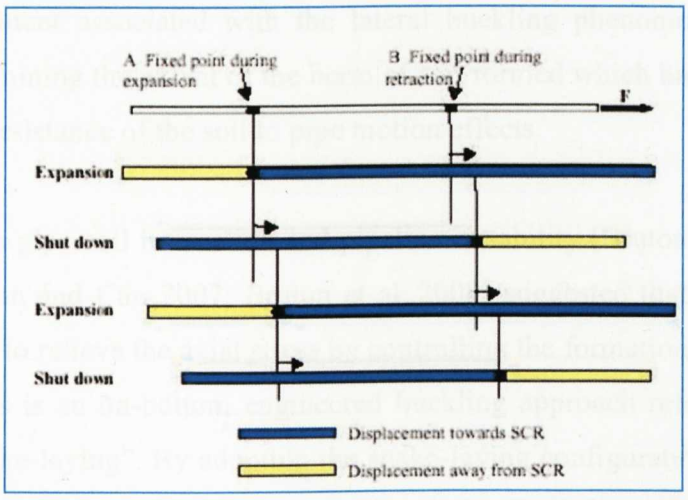

Figure 2 - 9: Illustration of pipeline walking (after Perinet and Frazer, 2006)

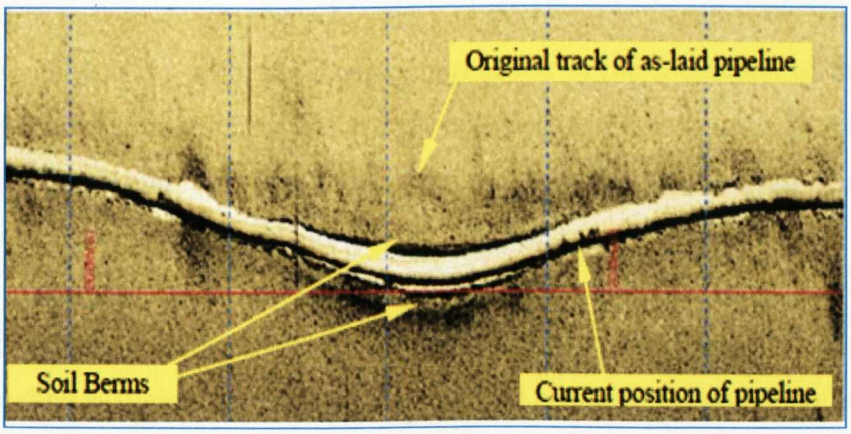

Figure 2 - 10: Side-scan Sonar Image of a Lateral Buckle
(After Bruton et al (2006)

2.6.1 Impact of pipe instability due to HTHP conditions

The pipeline movement caused by HTHP operating conditions may induce stress on the pipeline and affect connections to other subsea structures such as manifolds and connection spools. The continuous production cycles of start up and shut down may result in cyclic loading on the pipeline which could affect the structural integrity of the pipeline with time. The SAFEBUCK project (Boreas Consultant Limited,2002) is one major research programme to investigate the stability and design of submarine pipelines for lateral buckling. Significant results were gained from this project to improve the understanding of the pipe-soil interaction responses. However, uncertainties still exist on the soil deformation behaviour and the pipe-soil response during the large amplitude of pipe displacement associated with the lateral buckling phenomenon such as the problem of determining the extent of the berm of soil formed which has an effect on the resulting lateral resistance of the soil to pipe motion effects.

Recent studies on pipe-soil interaction and pipeline instability (Bruton et al.,2006; Carr et al.,2006; Bruton and Carr,2007; Bruton et al.,2008) suggested that a more efficient design method is to relieve the axial stress by controlling the formation of buckles along the pipeline. This is an on-bottom engineered buckling approach referred by pipeline operators as "snake-laying". By adopting the snake-laying configuration, some sections of the pipeline are designed to buckle when the pipe is loaded as it tries to expand on the seabed, hence relieving the axial stress imposed on the pipe. Some sections are designed to be relatively stable otherwise the whole approach will be seriously undermined.

The greatest uncertainty with this design approach is in the prediction of the pipe-soil response and the deformation pattern and the resulting soil lateral resistance during pipe movement. This solution is extremely sensitive to pipe-soil interaction as well as sensitive to the local lateral resistance (Bruton et al.,2006).

In order to ensure that the buckles are formed as predetermined, the ambient soil strength must be sufficient to resist pipe motions at a location designed to be relatively stable (Bruton et al.,2008). Typical displacement to mobilise the lateral friction is about 0.1D (Lyons,1973; Brennodden et al.,1986; Wagner et al.,1989). Marine clay in most offshore regions are characterised by very low strength and high compressibility. A method of soil improvement aimed at increasing the strength of this ambient soil around

the pipeline stands to increase the efficiency of this design. The greatest uncertainty relating to modelling, designing and enhancing pipeline stability is the uncertainties relating to pipe-soil interaction (Bruton et al.,2008).

Different approaches are available for the initiations of the engineered buckles at predefined regular intervals. This initiation will result in the compressive load on the pipe being released at the predefined buckle sites. The effectiveness of this arrangement however lies on the prediction of the lateral resistance at the buckle sites. This is currently very challenging in adopting this novel design approach. Not only that, the very soft clay with its very low effective stress makes the expected soil lateral resistance to pipe displacement quite unpredictable and sometimes lower than expected (Bruton and Carr,2007). This is why the need to understand the pipe-soil interaction is vital in the lateral buckling (LB) design approach. In addition, a means of improving the soil by way of strengthening the soil near the proposed lateral buckle location may enhance the effectiveness of this design approach.

According to (Bruton and Carr,2007), initiation of buckle is governed by three parameters: (i) the effective compressive force in the pipeline which is a function of axial resistance; (ii) out of straightness (OSS) features; and (iii) lateral breakout resistance. Lateral breakout resistance is generally the largest uncertainty.

Different techniques are employed to initiate controlled lateral buckling:

- Snake lay where the pipe is laid with regular tight-radius route curve
- Vertical upset – pipe is raised from the seabed using sleepers
- Local weight – pipe weight is reduced or increased to create local buoyancy or localised heavy pipe.

Typical lateral buckling design involves controlled lateral pipe movement of 5 – 20 D, and up to 1000 thermal cycles during the life of the pipeline (White and Cheuk, 2008). Prediction of soil resistance is complicated by the formation of soil berm at the either side as the pipe as the pipe is displaced laterally.

A study by Bruton et al. (2006) involving the sweeping of a model pipe section (283mm diameter, 99mm long) on a model seabed generated a typical large

displacement pipe-soil lateral friction response associated with the large amplitude of displacement typical of lateral buckling. Both E-grade kaolin clay and clay soil retrieved from the Gulf of Guinea offshore West Africa were used in this study. The primary aim of this study was to evaluate the large displacement cyclic responses that occur during lateral buckling. The model pipe was allowed to ride up over or embed and displace the soil in its path. The force displacement response was shown to depend on the soil and the pipe properties. The influence of the berm consolidation during pipe displacement was also evaluated. According to Bruton et al. (2006), four different stages of the pipe-soil interaction were investigated. These include the (1) embedment of the pipeline at installation (2) breakout during buckle formation, (3) the large amplitude displacement as the buckle forms and, (4) the repeated cyclic behaviour of the pipeline. Figure 2 - 11 (a and b) shows typical profile for monotonic and cyclic lateral force-displacement responses respectively. The numbers on Figure 2 - 11 represent the various stages in the force displacement response during pipe motion as defined by the authors as:

(0 – 1) First load monotonic breakout, a function of depth of initial pipe penetration.
(1 – 2) Suction release phase
(2 – 3) Steady accretion phase, characterised by the gradual increase in soil resistance
(3 – 4) Steady state residual friction
(5 – 6) Cyclic breakout including suction release from the established static soil berm
(6 – 7) Cyclic phase with a fresh active berm accretion in front of pipe
(7 – 8) Berm reaction which increases as the berm is established over initial cycles
(9 – 10) Cyclic breakout (as 5 – 6)
(10 - 11) Cyclic accretion (as 6 – 7)
(11 – 12) Cyclic berm interaction (as 7 – 8)

Another large-scale test performed at the Norwegian Geotechnical Institute (NGI) (Dendani and Jaeck,2007) considered both static and cyclic loading. They reported a peak mobilisation distance of between 0.3 and 0.8% of the pipe diameter, While 2 to 3% was reported for heavily penetrating pipe.

From available literature, the only studies that included the berm effect during the large amplitude of pipe displacement are from (Bruton et al.,2006) and (White and

Cheuk,2008). While White and Cheuk (2008) did attempt to assess the berm formation by modelling the amount of soil scraped from the trough behind the moving pipe, the real time measurement of berm and heave geometry was not conducted as part of the pipe-soil interaction studies. The model they proposed made use of data from the geotechnical centrifuge (Bruton et al.,2006; Cheuk et al.,2007).There is therefore need to account for the real time assessment of the development of the soil berm in order to fully understand the behaviour of the soil and soil deformation during the pipe motion.

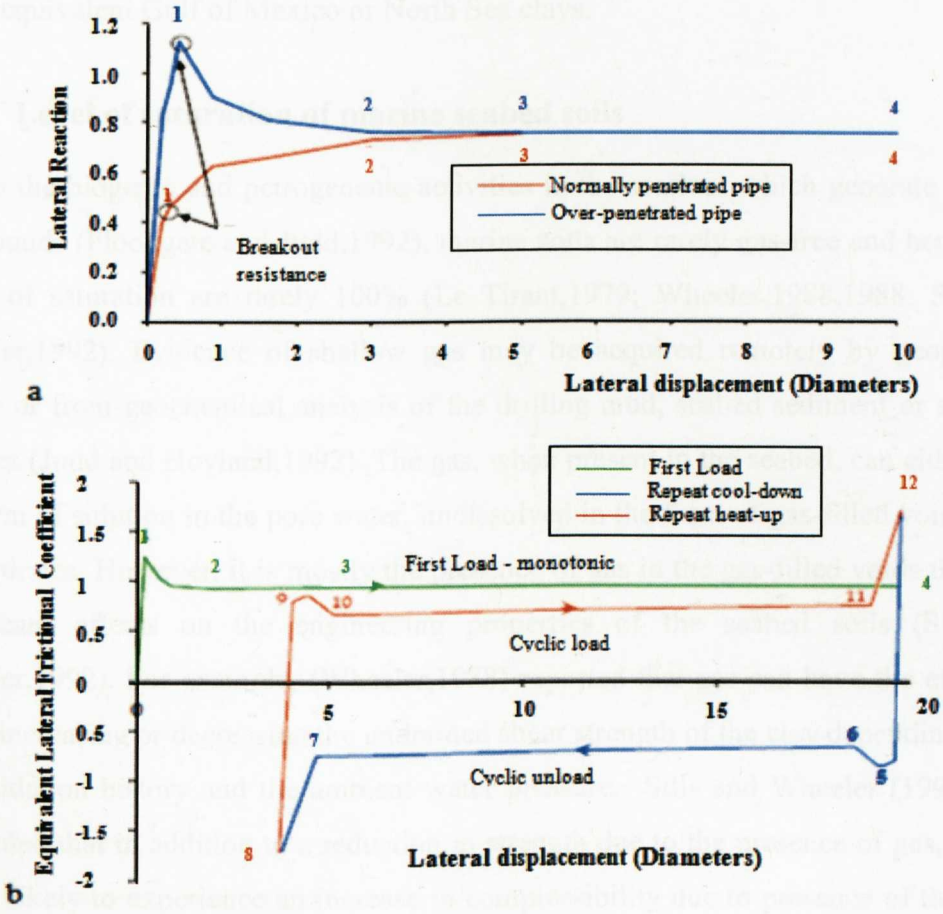

Figure 2 - 11: A typical large displacement pipe-soil lateral friction response for a) monotonic and b) cyclic lateral force-displacement response respectively after Bruton et al. (2006)

2.7 Properties and distribution of marine clays soils

The sea floor is increasingly being used as a supporting surface for offshore structures including pipelines thus necessitating a need for better understanding of the engineering properties of these soils (Ferguson and Bell,1977; Le et al.,2008). Typical deep water

field offshore clays are often made of very soft clays usually characterised by low shear strength, high water content and high compressibility resulting in considerable challenge (Bruton et al.,2008). These soft deposits occur in layers ranging from a few meters in thickness to depths of 30m below the seabed (Srinivasaraghavan and Rajasekaran,1994).

Another challenge with offshore clays is the apparent variability in the geotechnical properties from one region to the other. For instance Le et al. (2008) reported that the geotechnical properties of the soft Gulf of Guinea clays differ significantly from those of the equivalent Gulf of Mexico or North Sea clays.

2.7.1 Level of saturation of marine seabed soils

Due to the biogenic and petrogenenic activities in the seafloor which generate gaseous compounds (Floodgate and Judd,1992), marine soils are rarely gas-free and hence their levels of saturation are rarely 100% (Le Tirant,1979; Wheeler,1988,1988; Sills and Wheeler,1992). Evidence of shallow gas may be acquired remotely by geophysical survey or from geochemical analysis of the drilling mud, seabed sediment or seawater samples (Judd and Hovland,1992). The gas, when present in the seabed, can either be in the form of solution in the pore water, undissolved in the form of gas-filled voids, or as gas hydrates. However, it is mostly the presence of gas in the gas-filled voids that have significant effects on the engineering properties of the seabed soils (Sills and Wheeler,1992). For example, (Wheeler,1988) reported that gas can have the effects of either increasing or decreasing the undrained shear strength of the clay depending on the consolidation history and the ambient water pressure. Sills and Wheeler (1992) have concluded that in addition to a reduction in strength due to the presence of gas, the soil is also likely to experience an increase in compressibility due to presence of the gas in its void spaces. They also reasoned that the presence of gas in the seabed soil is particularly more severe during cyclic loading of the offshore pipeline on the soil either from hydrodynamic or operational induced (elevated temperature and pressure). This can cause a significant build of the pore pressure and a corresponding reduction in strength. Table 2- 1 is a summary of geotechnical properties of some marine deposits.

2.8 Mineralogy and structure of clay soils

Clay soils are a naturally occurring fine-grained aluminium silicate group of minerals. Some clay also contains alkalis and or alkaline earths as essential components (Bowles,1979). Its main distinguishing characteristic from other soil types is its particle sizes (< 0.002 mm) and mineralogy. Clay minerals are predominantly crystalline in that the atoms composing them are arranged in definite geometrical patterns. Apart from them being electrochemically active particles, they also exhibit characteristics of affinity for water and resulting plasticity not exhibited by other small particle minerals.

There are two fundamental building blocks (Figure 2 - 12) for clay minerals structures. One is the silica unit in which four oxygens form the tip of a tetrahedron and enclose a silicon atom. The other unit is the one in which an aluminium or magnesium (and sometimes Fe, Ti, Ni, Cr, or Li) atom is enclosed by six hydroxyls having the configuration of an octahedron.

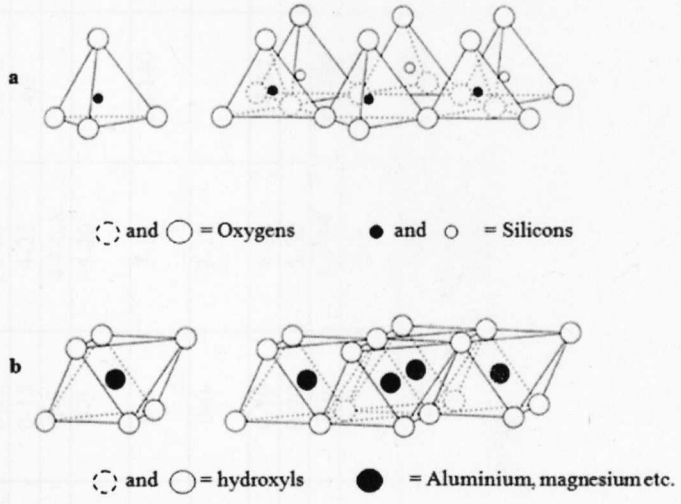

Figure 2 - 12: Fundamental building blocks for clay minerals (a): Silicon tetrahedron and silica tetrahedral arranged in a hexagonal network (b): Octahedral unit and sheet structure of octahedral units (after Mitchell and Soga, 2005)

The different types of known clay mineral groups are formed by the different patterns in which atoms are assembled into tetrahedral and octahedral units, followed by the formation of sheets and their stacking to form layers (Mitchell and Soga,2005). All the possible combinations of these basic units to form clay minerals produce a net negative charge on the exterior of the clusters. A soil-water suspension will thus have an alkaline reaction (pH >7) unless the soil is contaminated with an acidic substances (Bowles,1979).

Table 2- 1: Summary of geotechnical properties of some marine deposits

Location	Water depth (m)	Tested soil depth (m)	c_u (kPa)	w (%)	LL (%)	PL (%)	S_t	Carbonate content (%)	Source
Troll East Field, Norwegian Trench	300-330	0-15	5-40	47-70	60	37	5.5		By and Skomedal (1992)
Voring, Norwegian Sea	1225	0-15	4-25	45-60					Lacasse and Lunne (1998)
Offshore Brazil	970	0-15	4-40	50-70					Lunne et al. (1997)
Gulf of Mexico	980	0-15	4-25	60		35-40			Lunne et al. (1997)
Geojedo, South Korea	15	0-5	4.4-6.8						Cho et al. (2002)
Sagami Bay, Japan	1020	0-3	5-20		56-105	30-61		0.3-5.1	Fakue and Nakamura (1996)
Seto Inland Sea, Japan	18-25	0-6	3-12	12-140	61-129	32-58	5-15	0.3-3	Fakue and Nakamura (1996)
Tokyo Bay, Japan	12	0-6	3-12		113-120	64-70		0.6-1.7	Fakue and Nakamura (1996)
Snorre Site, North Sea	310	0-10	4-16	34-57	40-55	21-33	3-6		Dyvik et al. (1993)
Gulf of Guinea	150-200	0-20	5-30						Colliat et al. (1996)
Yulchon, South Korea (in situ)	10-15	0-9	1.9-19	90-120	62	34	2-5	1	Micic et al. (2001)
Yulchon, South Korea (remoulded and reconstituted at 15kPa)	10-15	0-9	4.5	95-130	59	27	1-2.5	1	Micic et al. (2001)
Gulf of Guinea	60 - 1500	0 - 20	5-30 up to 20m depth	150-250	200	150	3-4.3		Le et al. (2008)

Adapted and modified from (Micic et al.,2003a)

It is possible for isomophous substitution of silicon or the aluminium by lower valency ions as well as disassociation of hydroxyl ions to occur within a clay-electrolyte system resulting in the clay particle surface carrying residual negative charges. The negative charges caused the cations present in the water in the voids spaces to be attracted to the particles due to the net negatively charged surface but at the same time they tend to move away from each other because of their thermal energy. The net effect is that the cations form a dispersed layer adjacent to the particle, the cations concentration decreasing with distance from the surface until the concentration becomes equal to that in the general mass of the water in the void space of the soil as whole. This is the double layer and is discussed in detail in §2.10.1.1.

Some of the most common clay minerals are kaolinite, illite, and montmorillonite. However, only kaolinite is discussed further as it forms the kaolin soil sample employed in this study. The reader is referred to Mitchell and Soga (2005) for a comprehensive discussion on the various clay minerals while the extensive regional distribution of clay minerals in the world ocean is discussed in Griffin et al (1968).

2.8.1 Kaolinite group of clay minerals

Kaolinite is the predominant clay mineral of kaolin clay soil (Griffin et al.,1968). Its structural unit consists of alternating layers of silica tetrahedral with tips embedded in an alumina (gibbsite) octahedral unit (Figure 2 - 13a) resulting in a 1:1 basic unit. The combined silica-gibbsite sheets are held together relatively strongly by hydrogen bonding. Kaolinite is characterized by a low activity compared to other clay minerals (Bowles,1979). A diagrammatic sketch of the kaolinite structure is shown in Figure 2 - 13b. The structural formula is $(OH)_8\ Si_4Al_4O_{10}$ and the charge distribution is indicated in Figure 2 - 13c. There is very limited isomophous substitution within a kaolinite structure (Craig,2005; Mitchell and Soga,2005).

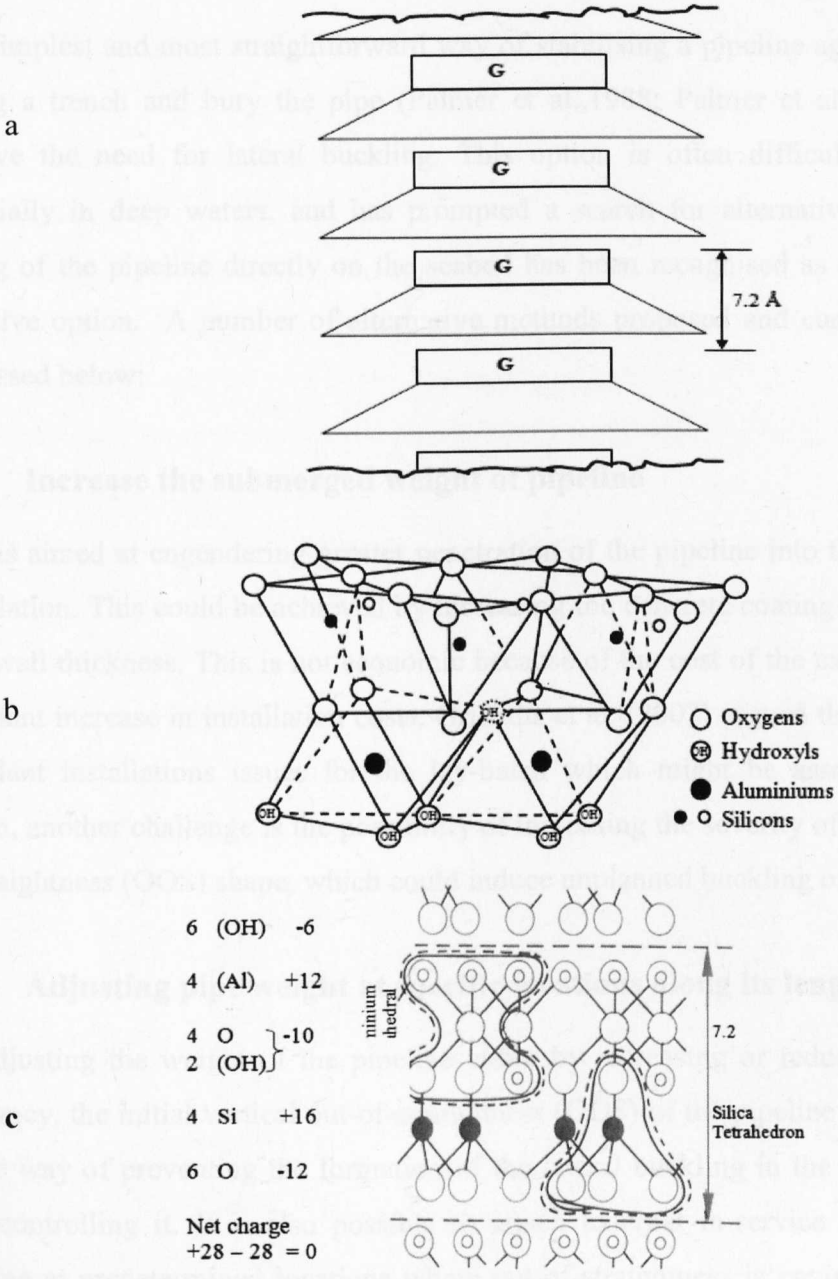

Figure 2 - 13: Kaolinite mineral; **(a)** Schematic diagram of the structure of kaolinite **(b)** Structure of kaolinite **(c)** Charge distribution on kaolinite
(After Mitchell and Soga, 2005)

2.9 Current mitigation methods for pipeline stability

The interest in the pipeline stability problem which initially revolved around instabilities due to environmental (mainly hydrodynamic) loadings, and currently on operational loadings (HTHP behaviour), have attracted considerable attention and significant research initiatives as outlined in §2.2. Some measures which have been put in place to mitigate against this phenomenon are outlined and reviewed in this section.

2.9.1 Trenching and burial of pipeline

The simplest and most straightforward way of stabilising a pipeline against buckling is to dig a trench and bury the pipe (Palmer et al.,1988; Palmer et al.,1990) and thus remove the need for lateral buckling. This option is often difficult and expensive especially in deep waters, and has prompted a search for alternative options where laying of the pipeline directly on the seabed has been recognised as an easy and cost effective option. A number of alternative methods proposed and currently in use are discussed below:

2.9.2 Increase the submerged weight of pipeline

This is aimed at engendering greater penetration of the pipeline into the seabed during installation. This could be achieved by increasing the concrete coating or increasing the pipe wall thickness. This is not economic because of the cost of the extra material with attendant increase in installation costs. Griffiths et al. (2007) argued that apart from the attendant installations issues for the lay-batch which might be associated with this option, another challenge is the possibility of increasing the severity of the pipeline out-of straightness (OOS) shape, which could induce unplanned buckling of the pipeline.

2.9.3 Adjusting pipe weight at specific locations along its length

By adjusting the weight of the pipeline either by increasing or reducing the pipeline buoyancy, the initial vertical out-of-straightness (OOS) of the pipeline is reduced. This is one way of preventing the formation of the lateral buckling in the first place rather than controlling it. It is also possible to attach external in-service structures to the pipeline at predetermined locations where out-of-straightness is envisaged in order to keep the OSS as low as possible along the length of the pipeline.

2.9.4 Preheating the pipeline

Although this method is mainly used for controlling upheaval buckling, it is also applicable to surface-laid pipelines. In this method, the pipeline is preheated and allowed to move to relax the compressive force induced by the elevated temperature and pressure conditions (Craig et al.,1990). The pipeline is continuously flushed with hot water causing it to buckle laterally to a stable position before putting into operation. By this method, tensile pre-stress is induced in the pipeline which stretches the pipeline

before it is commissioned. However, the success of this solution depends on the soil resistance being able to sustain the compressive load associated with the induced lateral buckling.

2.9.5 Increasing the vertical load on the pipeline

Stabilisation of the pipeline by dumping rocks over the pipeline is also considered by some pipeline operators (Griffiths et al.,2007). This can either be continuously over the entire length of the pipeline or intermittently at predefined intervals (Ellinas et al.,1990). This option can be improved by the use of concrete mattresses (Figure 2 - 14) or placing geotextile over the pipe before the rock is placed. The geotextile helps to increase the surface area of support offered by the rock dumps. When the pipeline begins to move, the weight of the rock on the geotextile on either side of the pipeline holds the geotextile down and keep the pipeline in place. However, the long term stability and performance of geotextile in a deep offshore environment has not yet been proven experimentally.

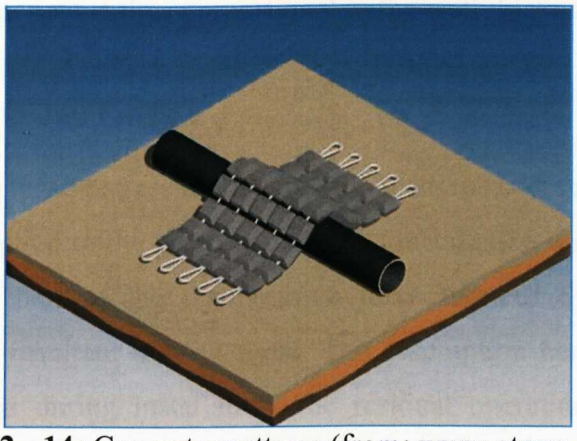

Figure 2 - 14: Concrete mattress (from: www.aterra-tj.com)

2.9.6 A reduction in the operating temperatures and pressure

This is a sort of passive mitigation approach where the causative agents for pipeline instability are eliminated or reduced considerably within the safe limit of the pipeline operation. However, reduction in the operating temperature is generally impracticable unless a heat exchanger is added to the system. This is a complex arrangement and not normally considered by deep offshore pipeline operators as it would lead to an increase in the pressure needed to pump the oil through the pipeline because of the increased friction between the oil and the pipe.

2.9.7 Reduction of the wall thickness of the pipeline

The main aim of this is to reduce the temperature component of the effective axial force, N, which is the driving force for the pipeline buckling as shown in Equation 2 - 11 . N is expressed as:

$$N = \pi R^2(1-2v)p + 2\pi RtEa\theta - T \qquad 2\text{-}21$$

Where

N = the effective axial force (compressive positive)

R = the mean radius, (1/2)(outside diameter -t)

t = the wall thickness

p = (internal pressure - external pressure)

E = the elastic modulus (Young's modulus)

T = the residual effective tension left after construction has been completed, but before the pressure and temperature change.

ν = Poisson's ratio

θ = (operating temperature-installation temperature)

The temperature component is thus proportional to the wall thickness of the pipeline.

2.9.8 Increase in the lay tension

This is to increase the tensile stress in the pipe (i.e. it stretches the pipe). The lay tension is the tensile force applied to the pipeline during its installation on the seabed. Residual lay tension balances part of the compressive force induced during operation, and therefore reduces the resultant driving force. The assumption here is that if sufficient pre-stress was applied during installation, the residual operation compressive stress could be kept within acceptable limit that could prevent pipeline buckling. A difficulty is that residual tension cannot be managed directly, but must be calculated from the lay conditions, and that its continued presence in the pipeline depends on there being no lateral movements. This approach is therefore highly unpredictable hence rejected by most pipeline operators.

Perinet and Frazer (2006) and Perinet and Simon (2011) presented a range of solutions for controlling axial walking of pipelines. These include the use of jumper /spools and use of suction anchors. The suction anchors are initially placed on the seabed before being connected to the pipelines after pipeline laying operation. The anchors hold the

pipeline in place and prevent it from moving axially. Various types of anchors were suggested which ranged from anchoring the pipeline end to suction anchors, midline restraint or use of chain restrains. This option is both expensive and unreliable in deep offshore sites. Others means suggested by the authors to increase pipeline axial and lateral stability include: increasing the depth of pipe embedment on the seabed by progressive free flooding of the pipeline. This would potentially result in higher lateral soil resistance.

2.9.9 Use of sleepers

This approach is normally used in conjunction with the lateral buckle design approach to be discussed in §2.9.10. Basically, it involved laying pipelines over pre-installed sleepers to initiate engineered lateral buckling deformations at pre-determined locations in order to initiate lateral deformation (Bruton et al.,2008). The sleepers provide an artificial vertical OOS features. The complexity of this approach as well as installation challenges is depicted in Figure 2 - 15.

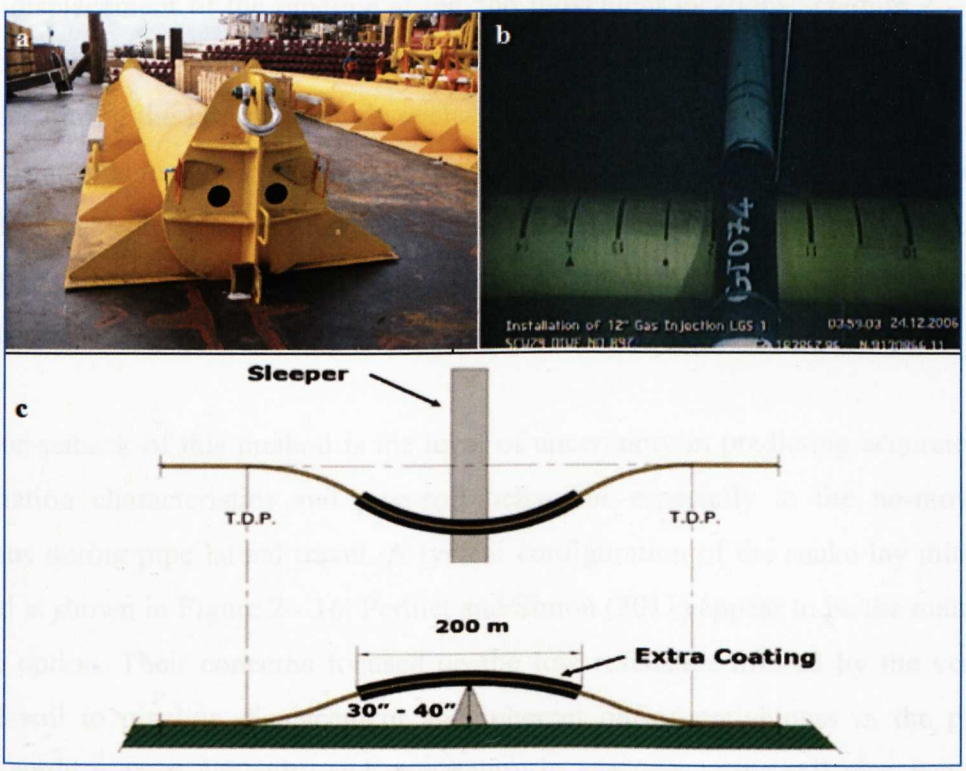

Figure 2 - 15: Control of lateral buckling using sleeper: a) sleeper before deployment; b) pipeline on sleeper on the seabed and c) schematics of the sleeper arrangement (after Perinet and Simon, 2011)

While these methods may significantly reduce pipe buckling and walking, the cost implications of their application in terms of vessel lay cost and additional elements needed are challenging. The actual cost of individual mitigation options depends on the specific situations and field conditions. Perinet and Simon (2011) reasoned that this cost can be as high as 10% of the overall cost of the flow line system. For instance, the cost of additional elements (example as in the use of sleepers, Figure 2 - 15) can substantially increase not only the operational cost of the flowline, but also the vessel time during installations. Furthermore, they may not be feasible in very deep waters.

2.9.10 Snake lay (Lateral buckling design)

This is the most current and cost effective way of controlling lateral buckling. It involves laying the pipeline in a snake configuration on the seabed without trenching (Vermeulen,1995; Bruton et al.,2006). This configuration helps to reduce excessive bending of the pipeline by effectively releasing most of the compressive loads on the pipelines at predetermined locations along the line with no additional structures required. The effectiveness of this method lies on the ability of the seabed soils to resist lateral displacement of the pipeline at the "no movement locations" (Figure 2 - 16). It therefore requires a better understanding of the interaction between the seabed and the pipelines during the large-amplitude cycles (White and Cheuk,2008). Prediction of this soil resistance is made complicated by the formation of berm on either side of the pipe, as soil is pushed ahead of the pipe during lateral movement. Designing for lateral buckling typically involves controlled lateral pipe movements of 5–20 diameters, and up to 1000 thermal cycles during the life of the pipeline (Bruton et al.,2006).

A major setback of this method is the level of uncertainty in predicting accurately soil deformation characteristics and pipe-soil behaviour especially at the no-movement locations during pipe lateral travel. A typical configuration of the snake lay mitigation method is shown in Figure 2 - 16. Perinet and Simon (2011) appear to be the main critic of this option. Their concerns focused on the low resistance offered by the very soft seabed soil to pipeline displacement and inherent out-of-straightness in the pipeline which could present difficulty and uncertainty in predicting pipe-soil response during pipe movement. These they believe could affect the formation of the curves at the predetermined locations thus potentially undermining or complicating the entire design option.

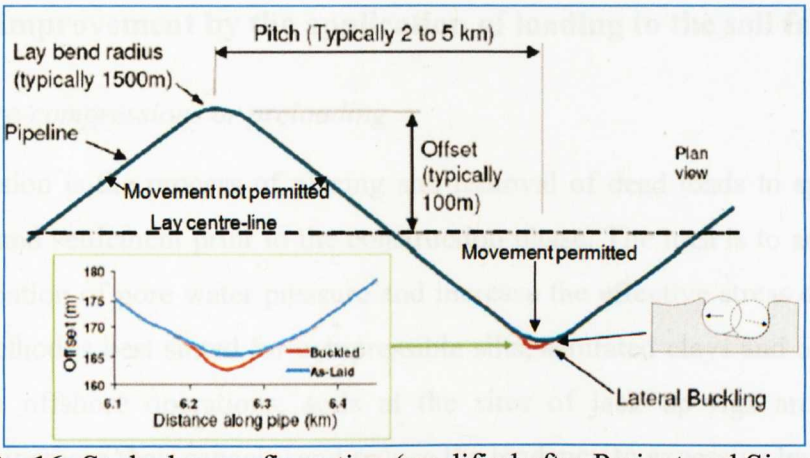

Figure 2 - 16: Snake lay configuration (modified after Perinet and Simon, 2011)

Even with the above stated challenges, the snake lay approach is currently being used in different projects in West Africa (Bruton et al.,2008). Preston et al. (1999) also reported the use of the snake lay configuration to control the compressive stress due to elevated operational temperature and pressure in pipeline location at the UK North Sea.

2.10 Overview of methods of improving foundation soils

Foundation soils which support civil engineering structures may sometimes not exist in the state and conditions adequate to safely support the structure. That is, the anticipated soil capacity may be below the expected state for safe long term function of the super-structure. In such cases, there may be a need to improve the conditions of the foundation soil. This is referred to as *ground improvement* in geotechnical engineering practise. The concept of ground improvement is not new in geotechnical engineering. It basically involves the re-engineering of the properties of the foundation soil by either introducing other elements to the internal fabric of the soil, replacing some portion of the soil with improved soil or the application of external loading to the soil with the aim of rearranging its fabric. The actual design option is mostly based on the specific site condition and the experience of the engineer.

While improvement in onshore geotechnical practice is relatively simple and well researched, soil improvement at the offshore sites poses considerable challenge and has received less attention. In this section, the existing ground improvement methods employed in the onshore sites and those used in the offshore sites are reviewed briefly. A review of the existing literature on the available techniques for soil improvement indicates that they can be broadly grouped into three areas.

2.10.1 Soil improvement by the application of loading to the soil fabric

2.10.1.1 Pre-compressions or preloading

Pre-compression is the process of placing and removal of dead loads to speed up soil compaction and settlement prior to the construction phase. The idea is to accelerate the rate of dissipation of pore water pressure and increase the effective stress of the in-situ soil. This method is best suited for compressible silts, saturated clays and organic clays and peat. In offshore operations, soils at the sites of jack up rigs are sometimes preloaded to increase their capacity and reduce the tendency to excessive leg penetration which might lead to failure. Preloading is not common in offshore operations. However, one reported case of its application is given by Yan and Cao (2005).

2.10.1.2 Vacuum preloading

Research interest in vacuum induced consolidation has attracted considerable attention mostly from onshore applications (Bergado et al.,1998; Mohamedelhassan and Shang,2002; Chu et al.,2008; Saowapakpiboon et al.,2011). The system works by using atmospheric pressure as a preload to maintain pressure beneath a sealing membrane using vacuum-generating equipment. During the process a negative pressure is produced by high speed water jetting from a water pump. It is most effective for low permeability and high compressive saturated soil by accelerating the rate of consolidation. A typical illustration of vacuum preloading is shown in Figure 2 - 17.

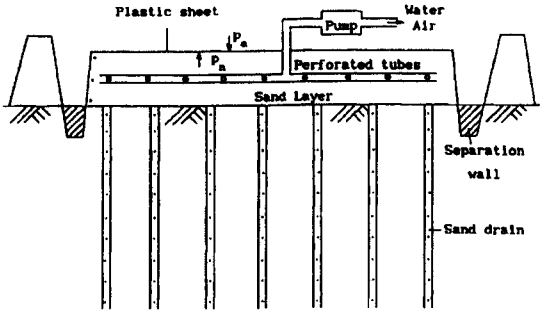

Figure 2 - 17: Field illustration of onshore vacuum preloading after Qian et al.,(1992)

Under-water vacuum consolidation

An attempt to extend the application of vacuum consolidation under water was postulated by Thevanayagam et al.(1994) The general assumption they had was that by

applying the vacuum below the water table and used in conjunction with dewatering, the equivalent preload could increase significantly. However, a full-scale pilot study has not yet been conducted to investigate this. Although Thevanayagam et al.(1994) suggested the possibility of using this technique for under-water ground improvement, it is not likely to be suitable in deep offshore sites due to the difficulty in setting up the treatment process. No direct application of this method in deep offshore sites is reported in the literature.

2.10.1.3 Vibro Compaction/vibro floatation

This is the rearrangement of granular soils particles into denser configuration by powerful deep vibrators. In this case, the load is applied laterally to the soil fabric in situ. A foundation soil is judged suitable for compaction based on its grain size analysis. In addition, the soil must have adequate permeability to allow quick drainage of the pore water during the compaction process. Sand and gravels can be compacted by the deep vibratory compaction method, while clay and silt soils cannot be compacted by vibration alone. This option is not suitable for most offshore site which is characterised by high compressibility and low permeability.

2.10.1.4 Dynamic compaction

This method is employed in the onshore ground improvement but rarely in offshore site locations. It essentially involves repeatedly impacting the ground surface with a predetermined weight from a predetermined height to increase the density of the foundation soil. This method could be applied to improve both cohesive and non-cohesive foundation soils. However, significant improvement is more likely to be achieved in granular soils than in cohesive soils.

2.10.2 Soil improvement by replacement

2.10.2.1 Vibro-concrete columns

This is the product of vibro-replacement where the in-situ non compactable cohesive soil is improved by means of special deep vibrator. It is similar to vibro-compaction technique which is mainly applied to granular soils to densify them by means of vibration resulting in direct in-situ soil improvement. Vibro-concrete column is similar to the continuous flight auger (CFA) piles. However, the advantage it has over the CFA

is that almost all the soil is displaced in-situ rather than dug. Enlarged column base and variable column diameter can also be achieved.

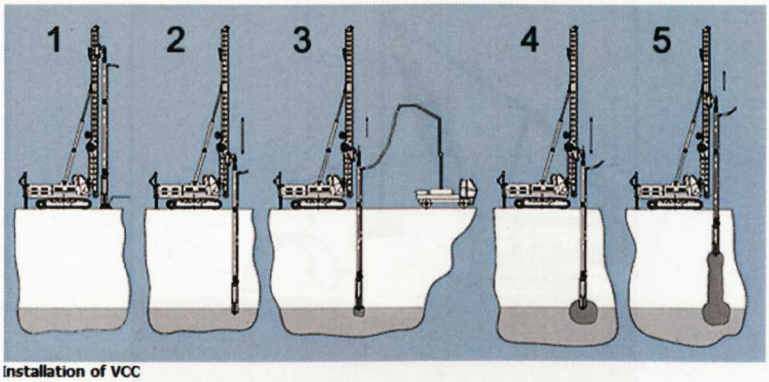

Installation of VCC

1. Locate rig over VCC point.
2. Vibrate down to depth.
3. Start the concrete pump.
4. Build the enlarged base.
5. Pull with constant speed while observing limit values for concrete pump pressure.

Figure 2 - 18: Installation of vibro concrete column (from http://www.vibroflotation.com)

2.10.2.2 Dynamic replacement

This is another method of ground improvement for treating soft compressive clayey soils which is adaptable for use in offshore sites. It is similar to the dynamic compaction technique. However, in dynamic compaction, the granular soil is compacted from the surface with no need for replacement of the in situ soil. Both techniques have been employed in offshore sites to increase the bearing capacity of offshore foundations. Figure 2 - 19 shows the schematics for the dynamic compaction process. It involves systematically dropping a heavy weight to drive a granular material into soft compressive cohesive soils (replacing the in situ soil in the process) and to compact the driven material sufficiently to meet the project design criteria. Hamidi et al.(2010) reported the first use of (about 30m water depth) dynamic replacement technique to improve seabed soils.

2.10.2.3 Stone columns

This is a relative old method of soil improvement which could be employed in any soil condition especially where washout of soil to the surface is to be avoided. A hole is drilled through the soil by vibration equipment and then filled with stone to increase the bearing capacity of the foundation soil. This method is different from the dynamic replacement method in the sense that holes are bored into the soil before being filled

with an improved material whereas in the former, no hole is bored but the soil is being replaced directly through compaction.

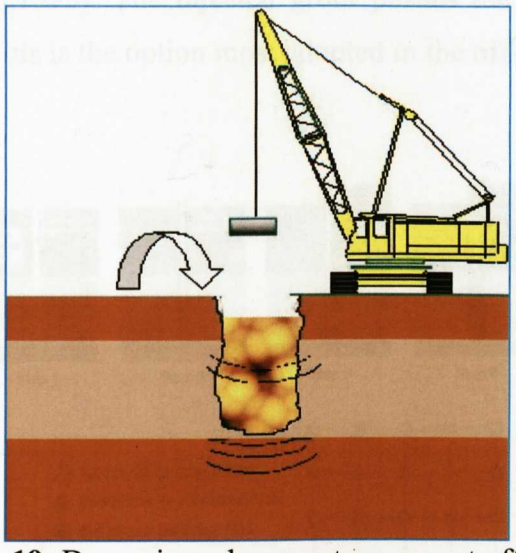

Figure 2 - 19: Dynamic replacement process at offshore site
(after Hamidi et al.,(2010)

2.10.2.4 Grouting technique for ground improvement

Grouting is one soil improvement techniques which has been extensively used to enhance the capacity of offshore foundations (Domone,1990). Littlejohn (1985) also reported the application of this technique in pipeline stability. Essentially, this method involves the injection of high-fluid (to ease pumping) materials which could be variable compositions of Portland cement/pulverised fuel ash, chalk and bentonite or sodium silicate, depending on the site requirement, into a soil formation to change the physical and chemical characteristics of the foundation soil. The grout material must be sufficiently cohesive to replace sea water and also be able to help stabilise the wall of the bore during excavation. Grouting can provide increased soil strength and rigidity. A considerable amount of laboratory research work was conducted in the 1970's before the adoption of the technique in the offshore area (Domone,1990).

The two most used injection grouting techniques are *jet grouting* and *compaction grouting*. In jet grouting, a jet of high pressure grout material is forced into the soil fabric to cause erosion of the soil structure and replace the soil particles with the grout material. The grout material, with any remaining in-situ soil, would mix together to form an improved soil mass with greater strength than the surrounding soil.

Compaction grouting on the other hand involves injection (at relatively low rate) of highly viscous grout material (Figure 2 - 20) that does not permeate the native soil thus compressing the surrounding soil resulting in a controlled growth of a grout bulb mass (Boulanger and Hayden,1995). The injected grout pushes the soils to the sides as it forms a grout column. This is the option most adopted in the offshore (Figure 2 - 21).

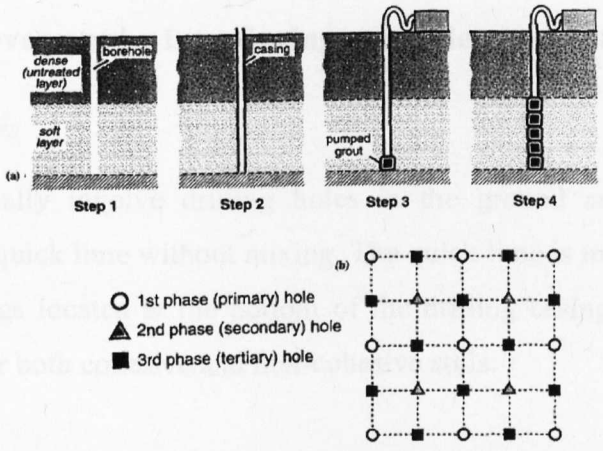

Figure 2 - 20: Schematic of compaction grouting: a) soil cross section and sequence, b) plan view of square treatment (after Boulanger and Hayden, 1995)

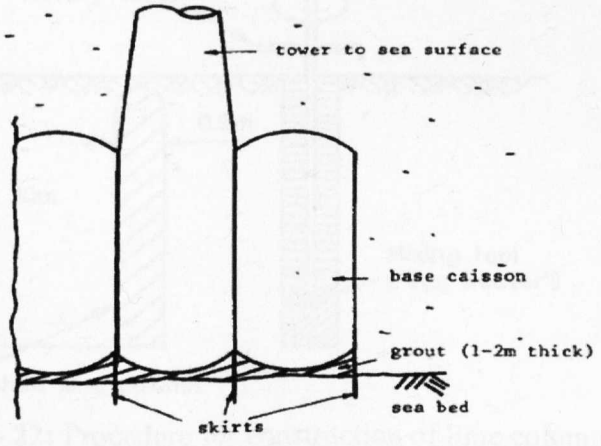

Figure 2 - 21: Use of grout for offshore foundation system (After Domone (1990)

2.10.2.5 Lime columns

In this method, holes are drilled into the ground and the soft soil allowed to mix in situ intimately with the lime to produce columns of material with greater strength and

stiffness, reduced water content and increased soil density (Rogers and Glendinning,1997). The column behaves as a conventional pile foundation system which ultimately improves the bearing capacity of the soft clay. The procedure for construction of lime column is shown in Figure 2 - 22. This technique has been suggested by Narasimha-Rao and Rajasekaran (1994) for use in stabilizing soft offshore marine clays.

2.10.3 Soil improvement by introducing other elements into the soil fabric

2.10.3.1 Lime piles

Lime piles essentially involve drilling holes in the ground and filling them with specially prepared quick lime without mixing. The quick lime is injected by compressed air through openings located at the bottom of the drilling casing Figure 2 - 23. This method is useful for both cohesive and non-cohesive soils.

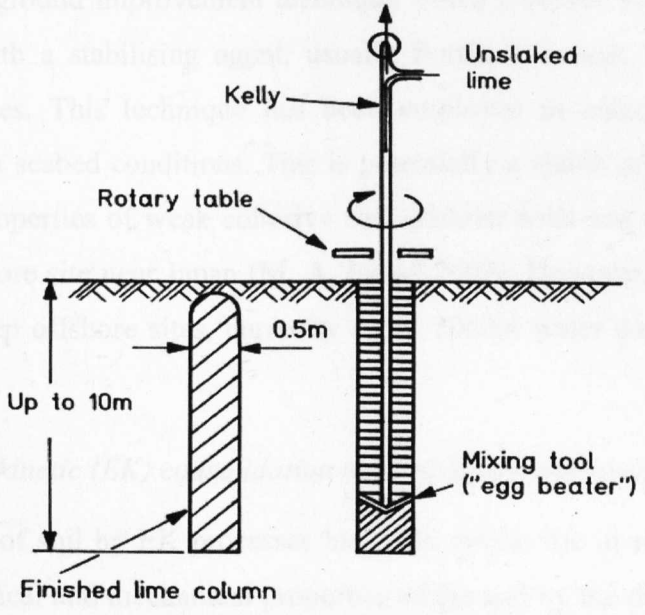

Figure 2 - 22: Procedure for construction of lime columns (after Broms and Boman (1979)

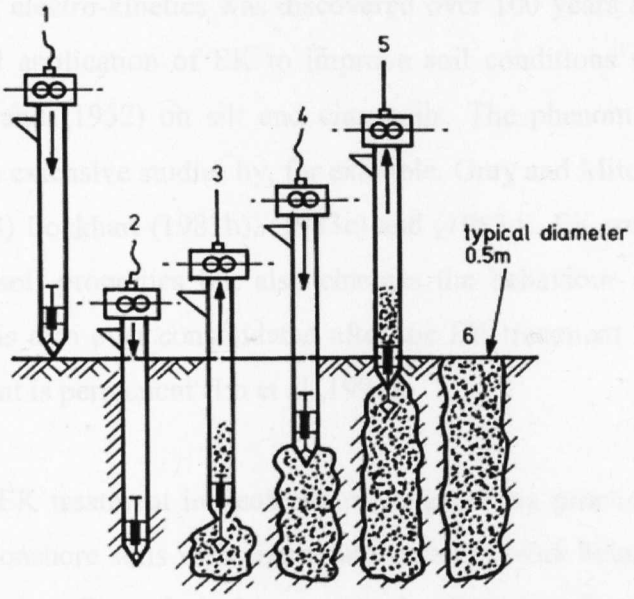

Figure 2 - 23: Chemical lime piles installation process
(after Ingles and Metcalf (1972)

2.10.3.2 Deep mixing

Deep mixing is a ground improvement technique which involves mechanically mixing the soil in-situ with a stabilising agent, usually Portland cement, to achieve certain improved properties. This technique has been employed in some offshore sites to improve the in-situ seabed conditions. This is potentially a viable option for improving the engineering properties of weak cohesive and granular soils and is reported to have been used in offshore site near Japan (M. A. Ismail,2002). However, the application of this method in deep offshore sites, currently up to 2000m water depth, would require special technology.

2.10.3.3 Electro-kinetic (EK) consolidation method of soil improvement

The improvement of soil by EK processes basically entails the in-situ modification in the physical, chemical and mechanical properties of the soil by the direct application of electric current through soil using oppositely charged electrode materials. The main electro-kinetic processes which facilitate these changes, depending on the special requirement of the treatment process, include: (a) electro-osmosis (EO) (transport of pore water towards the negative electrodes), (b) electro-phoresis (transport of negatively charged particles towards to positive electrode), (c) migration or sedimentation potential (transport of ions toward electrodes) and (d) streaming potential (electrical potential induced by movement of water under hydraulic gradient) (Mitchell and Soga,2005).

The phenomenon of electro-kinetics was discovered over 100 years ago. However, the earliest geotechnical application of EK to improve soil conditions was conducted by Casagrande (1949) and (1952) on silt and clay soils. The phenomenon is now well understood based on extensive studies by, for example, Gray and Mitchell (1967); Gray (1970); Esrig (1968) Lockhart (1983b), (1983c) and (1983d). EK treatment of soil not only improves the soil properties but also changes the behaviour of the soil (Lo et al.,1991). The clay is also over consolidated after the EK treatment indicating that the effect of the treatment is permanent (Lo et al.,1991).

The earliest use of EK treatment in geotechnical engineering practice initially centred on improvement of onshore soils with significant research work being conducted to re-engineer soils for various geotechnical issues ranging from: (a) the use of EK to solve foundation problems related to weak soils; example, (Bjerrum et al.,1967; Lockhart,1983d; Barker et al.,2004; Burnotte et al.,2004; Chew et al.,2004); (b) solving slope and walls stability issues (Glendinning et al.,2005) and (c) increase in the capacity of pipes (Milligan,1995). In recent times, emphasises has been on the application of the EK technology to improve the offshore foundations soils. This is reviewed in §2.1.1.5.

Lo et al. (1991) demonstrated that the increase in the soil strength by EK involved the expansion of the effective strength envelope and increase in the pre-consolidation pressure. Therefore, the improvement in the engineering properties of the soil would be permanent. The long term effectiveness of the EK effects was confirmed by Milligan (1995), who reported that the bearing capacity of 16.5m long steel H-piles installed in a silty clay remain unchanged 33 years after the EK treatment.

2.10.4 Interim conclusion on available soil improvement techniques

The soil improvement techniques described can improve the strength and stiffness of offshore foundation soils but many are not suitable for offshore pipelines. In order to assess the effectiveness and their applicability to seabed pipelines, the following issues were taken into consideration:

- The radial zone of influence of a pipeline is small
- The lateral extent (.i.e. length of pipeline) of the zone of influence is significant
- The technology to operate underwater and at great depth

Using these criteria, an assessment of the improvement techniques in terms of their effectiveness and applicability to offshore pipelines is presented in Table 2- 2. They are ranked from 1 to 5 with 5 implying most suitable and 1 denoting least suitable.

Assuming total cut-off scores of 8 for the purposes of this assessment, it appears that pre-compression (e.g. using rock dump), grouting, deep mixing and EK may be explored further for application to offshore pipelines.

Pre-compression is used to strengthen sea bed soils to control lateral buckling though it is the weight of the pre-compression material that remains in place that may be more relevant then the improvement in the soils. Injection grouting could be considered as the zone of influence of the pressure grouting can be continued. It has been used offshore to help stabilise platforms. Therefore there is some experience of this technique offshore. EK, however, is worth investigating further as the zone of influence can be controlled. Further it may not be necessary to install anything in the seabed. This implies that it is not necessary to use construction machinery on the seabed. The aim would be to develop a system that can be part of the pipeline thus installing it as the pipe is laid. Further EK does not require any additional material or heavy plant,

The EK technology which appears to offers a more excellent option for improving the seabed soil surrounding pipelines is discussed in detail in the following section.

2.11 Electro-kinetic phenomena in soils

When a direct current is applied across two oppositely charged electrodes embedded in a saturated or partially saturated soil mass, electro-kinetic processes namely electro-osmosis (EO), electrophoresis, streaming potential and ionic migration are generated. The prolonged application of this electrical gradient may not only induce hydraulic flow, but also cause significant changes in state and properties of the soil and flows (example, chemical flow) through the soil (Gray and Mitchell,1967; Mitchell,1991; Mitchell and Soga,2005). Figure 2 - 25 is an illustration of these electro-kinetic processes and their possible effects on the soil mass. The interplay between the electrical gradient and the induced hydraulic flow in soil (electro-osmosis) has received considerable attention in geotechnical engineering within the last 60 years.

2.11.1 Electro-osmotic phenomenon in soils

The phenomenon of EO was first observed by Reuss (1809) (cited in Lewis and Humpheson (1973). However, it was not until over 100 years before the practical significance of this phenomenon was introduced into geotechnical engineering largely due to the work of Casagrande between 1937 and 1960. A schematic illustration of the mechanism of EO consolidation is shown in Figure 2 - 25. Several theories such as the Helmholtz-Smoluchowski theory, the Schmidt theory and the Spiegler theory have been proposed to explain the phenomenon of electro-kinetics in soils. The Helmholtz-Smoluchowski theory is one of the earliest and the most widely used (Mitchell and Soga,2005).

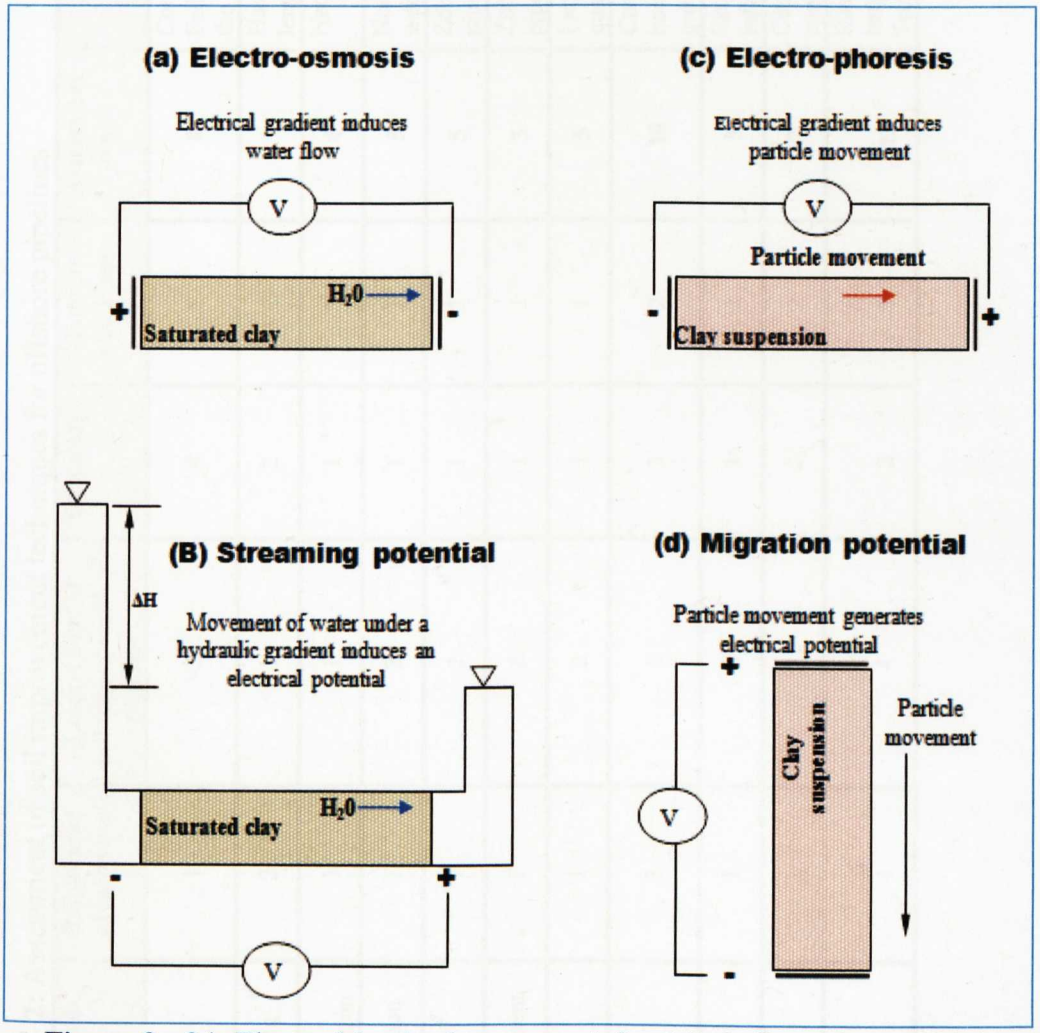

Figure 2 - 24: Electro-kinetic phenomena (after Mitchell and Soga, 2005)

Table 2- 2: Assessment of soil improvement techniques for offshore pipelines

Soil improvement method	Radial zone of influence	Lateral zone of influence (length of pipe issue)	Technology	Materials and Plant	Assessment score	Remarks
Pre-compression	1	2	4	1	**8**	Common technique in offshore engineering to stabilise pipes. Failure of the seabed could occur, the quantity and transportation of the compression materials over the length of pipe would be an issue
Vacuum preloading	2	1	2	2	**7**	Has been used for anchors offshore. Not practicable considering the length of pipelines (in km)
Vibro compaction/floatation	1	1	1	1	**4**	Not practicable considering the length of pipelines (in km)
Dynamic compaction	1	2	1	1	**5**	Not practicable because of the limitation of the effects of dropping weights in water and the need to use major plant
Vibro-concrete columns	1	2	1	1	**5**	Zone of influence much greater than the zone of influence of the pipe. Significant quantities of material over the length of the pipe
Dynamic replacement	1	2	1	1	**5**	Zone of influence much greater than the zone of influence of the pipe. Significant quantities of material over the length of the pipe
Stone columns	1	2	1	1	**5**	Large area of soil treated at great depth, thus not useful. Significant quantities of materials
Grouting	3	2	3	2	**10**	Could be applicable but the large extent of pipeline could be an issue because of need to have a number of injection points. Controlling the grouted zone could be difficult
Lime columns	1	1	1	2	**5**	Requires major plant. Zone of influence extends beyond the zone of influence of the pipe.
Deep mixing	1	2	2	2	**7**	Could be applicable but the lateral extent of the zone to be treated could be an issue; Major plant requirement.
Electro-kinetic treatment	4	4	2	3	**13**	Electric current for the soil improvement already exist along the pipe length. Could be incorporated as part of the pipe installation process. Technology has not been tried and tested offshore

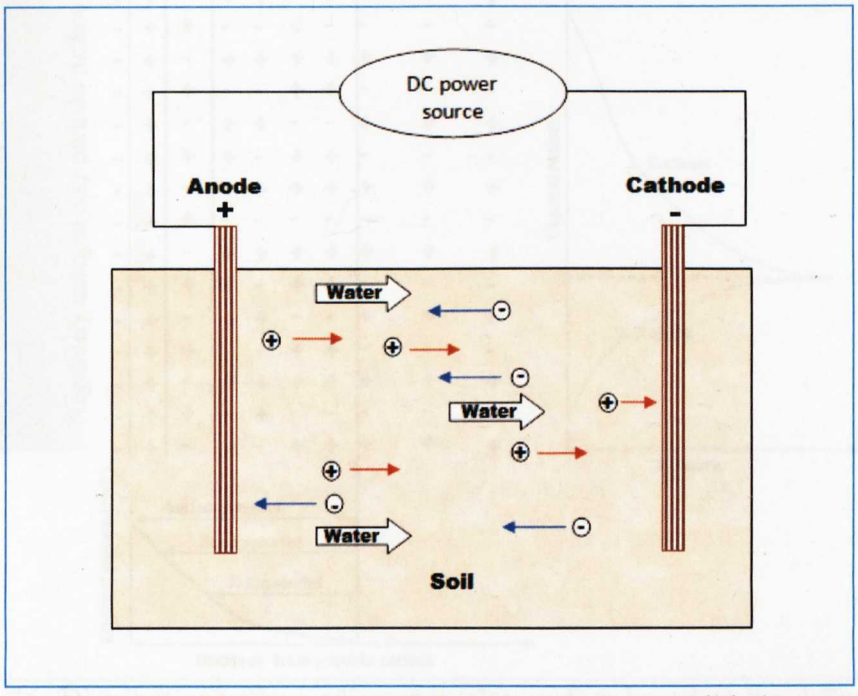

Figure 2 - 25: Schematic of electro-osmotic consolidation

2.11.1.1 The double layer concept- Helmholtz and Smoluchowski theory

The Helmholtz and Smoluchowski theory is based on the double layer (DL) theory which attempts to relate analytically the electrical and the flow parameters of electro-kinetic transport and presents a mathematical treatment of electro-osmotic flow based on the flow through capillaries. The property of the diffuse DL is an important controlling factor for the structural development, hydraulic conductivity, and other physico-chemical and mechanical properties of soil. Figure 2 - 26 is a schematic of the DL system showing the nature and distribution of charge particles on clay surfaces. It shows the surface of the clay particle as being negatively charged and the DL which is divided into two main layers. The inner wall of the DL is relatively thin compared to the outer wall with negatively charge ions on the clay surface strongly attached to the wall. The outer wall on the other hand consists of moveable positive ions.

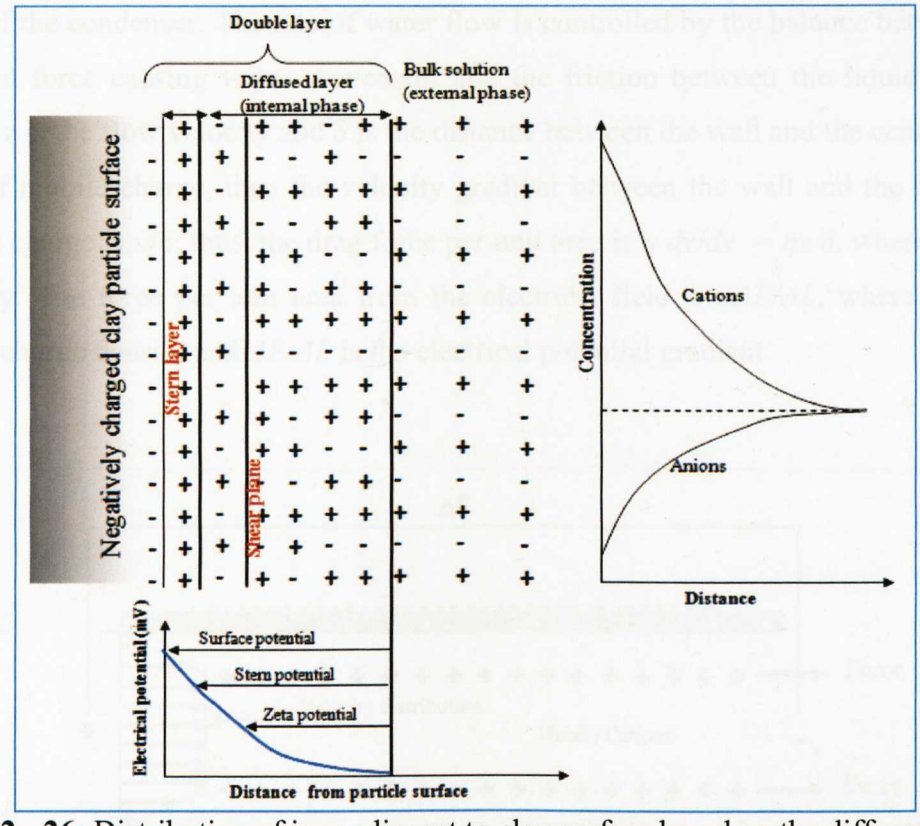

Figure 2 - 26: Distribution of ions adjacent to clay surface based on the diffused double layer concept (modified from Mitchell and Soga, 2005)

Within the diffuse layer there is an imaginary boundary inside which the ions and soil particles form a stable entity. When the soil particle moves, ions within the boundary move with it. Those ions beyond the boundary stay with the bulk solution. The electrical potential difference across this boundary (surface of hydrodynamic shear) is the zeta potential. Immediately adjacent to the double layer is a portion of free water (within the external phase). When a direct current is applied, the mobile positive ions will be attracted towards the cathode, dragging with them the free water molecules causing a general movement of water from the anode to the cathode. This is the theory on which the principles of electro-osmotic dewatering of saturated or partially saturated soil is based.

Mitchell and Soga (2005) has presented an analytical treatment of the Helmholtz-Smoluchowski theory which considers a liquid- filled capillary as an electrical condenser with charges of one sign on or near the surface of the soil particle and counter-charges concentrated in a layer in the liquid a small distance from the wall, as shown in Figure 2 - 27. The mobile shell of the counter ions is assumed to drag water through the capillary by plug flow. There is a high-velocity gradient between the two

plates of the condenser. The rate of water flow is controlled by the balance between the electrical force causing water movement and the friction between the liquid and the wall. If v is the flow velocity and δ is the distance between the wall and the centre of the plane of mobile charge, then the velocity gradient between the wall and the centre of positive charge is v/δ; thus, the drag force per unit area is $\eta\, dv/dx = \eta v/\delta$, where η is the viscosity. The force per unit area from the electrical field is $\sigma \Delta E/\Delta L$, where σ is the surface charge density and $\Delta E/\Delta L$ is the electrical potential gradient.

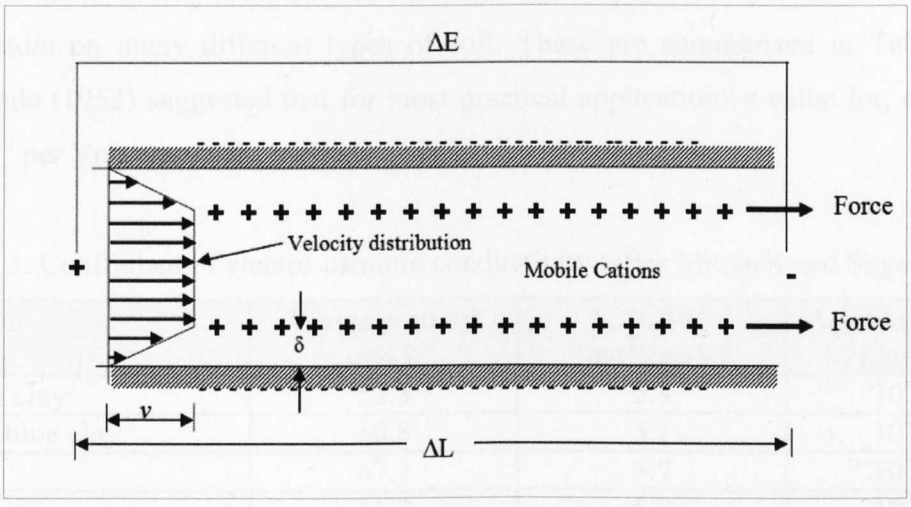

Figure 2 - 27: Helmholtz-Smoluchowski model for electro-kinetic phenomena (after Mitchell and Soga, 2005)

Mitchell and Soga (2005) presented analytical solutions using the above parameters using the analogy with Darcy's law, the flow through a capillary is:

$$q_A = k_e i_e A \qquad \textbf{2- 22}$$

Where

q_A = flow rate through a bundle of capillaries

i_e = the electrical potential gradient

A = total cross-sectional area normal to the flow direction

k_e = the coefficient of electro-osmotic hydraulic conductivity expressed as

$$k_e = \frac{\zeta D}{\eta} n \qquad \textbf{2- 23}$$

Where

ζ is the zeta potential

D is the relative permittivity, or dielectric constant of the pore fluid

n = porosity of the soil

It can be seen that Equation 2 -12 is similar to Darcy's law of fluid flow. According to the Helmholtz-Smoluchowski theory and Equation 2 - 13, k_e should be relatively independent of pore size contrary to the case of hydraulic conductivity, k_h.

Values of the electro-osmotic conductivity, k_e, have been published by many investigators on many different types of soil. These are summarised in Table 2- 3. Casagrande (1952) suggested that for most practical applications a value for, k_e, of 5 x 10^{-5} cms^{-1} per Volt/cm would suffice.

Table 2- 3: Coefficient of electro-osmotic conductivity (after Mitchell and Soga, 2005)

Material	**Water content (%)**	**k_e in 10^{-5} (cm^2/sec-V)**	**Approximate k_h (cm/sec)**
London clay	52.3	5.8	10^{-8}
Boston blue clay	50.8	5.1	10^{-8}
Kaolin	67.7	5.7	10^{-7}
Clayey silt	31.7	5.0	10^{-6}
Rock flour	27.2	4.5	10^{-7}
Na- Montmorillonite	170	2.0	10^{-9}
Na-Montmorillonite	2000	12.0	10^{-8}
Mica powder	49.7	6.9	10^{-5}
Fine sand	26.0	4.1	10^{-4}
Quartz powder	23.5	4.3	10^{-4}
As quick clay	31.0	20.0-2.5	2.0 x 10^{-8}
Bootlegger Cove clay	30.0	2.4-5.0	2.0 x 10^{-8}
Silty clay, West Branch Dam	32.0	3.0-6.0	1.2 x 10^{-8} -6.5 x 10^{-8}
Clayey silt, Little Pic River, Ontario	26.0	1.5	2.0 x 10^{-5}
Marine silty clay	37	6 - 9	10^{-7}

Sources:

1 – 10 – Casagrande (1952)
11 – Bjerrum et al. (1967)
12 – Long and George (1967) – look for all sources
13 – Fetzer (1967)
14 – Casagrande et al. (1961)
15 – Eggestad and Foyn (1983)

Table 2- 3 indicate that EO presents an excellent method of removing pore water from soil of low conductivity such as clay or silt given the fact that high hydraulic conductivity soils give lower electro-osmotic conductivity (less than 5 x 10^{-5} cms^{-1} per Volt/cm suggested by Casagrande, 1952). This implies that the treatment is not likely to be effective on a coarser grained material such as sand with a hydraulic conductivity of $k_h = 10^{-4} cms^{-1}$. However, the EO effect in low conductivity soils can be significant (Casagrande, 1952).

2.11.2 Development of pore pressure in soils due to EK treatment

The application of direct current can result in a variety of changes within the soil mass such as alteration of the clays minerals and the deposition of clay minerals. However, hardening by consolidation is the fastest to take effect and most effective in changing the soil strength (Esrig,1968). This is dependent on the generation of negative pore water pressure with the concomitant increase in the effective stress within the soil mass. Esrig (1968) argued that the application of an electric field in a soil mass may lead to the development of both positive and negative pore water pressures and that the rate of development of this pore pressure can be predicted. However, the nature of pore pressure developed depends primarily on the applied voltage, on the electrode configurations and on the boundary conditions at the electrodes. This is discussed later in this section.

The theoretical framework presented by Esrig (1968) on the development of pore pressures in soils due to application of a uniform potential field is the one most adopted in assessing the development of pore pressure during electro-osmotic consolidation. This theory, which has been validated by Wan and Mitchell (1976), is based on the assumption that flow caused by an electric field may be superimposed on flow caused by a hydraulic gradient. The effect of boundary conditions of pore water pressure as proposed by Esrig (1968) is discussed in the next section.

2.11.2.1 Boundary conditions for pore pressure development

The definition of the drainage regimes as applicable to conditions at the electrodes during EK treatment could be either an open or close system depending on the flow of water. *Open drainage* conditions are considered to exist if an electrode is open to the atmosphere or hydrostatic pressure, such that no excess pore pressure can exist at the

electrode, while a *close drainage* exist if an electrode is sealed such that no passage of fluid can take place along the length of the electrodes and excess pore pressure may develop. Three cases that could develop depending on the drainage conditions are shown schematically in Figure 2 - 28 and discussed in details below.

Case I: Anode and cathode open with free access to water

For this case both the anode and the cathode have free access to water (Figure 2 - 28a). Esrig (1968) proposed the following equation for the development of pore water pressure in a soil:

$$u_e = \frac{k_e}{k_h}\gamma_w\left(V_m\frac{x}{L} - v\right) \qquad \textbf{2- 24}$$

Where:

u_e = pore water pressure due to EO

V_M= maximum voltage

k_e = electro-osmotic conductivity

γ_w = unit weight of water

v= voltage at any particular point

L = Distance between the electrodes

x= distance from the cathode

This suggest that the term in parentheses in the Equation 2 -19 must be zero in a uniform field implying that the pore water pressure u_e, would also be zero. Therefore, in the presence of a uniform field with open boundaries that have free access to water, no pore water pressures should develop.

Case II: Anode closed, cathode open with free access to water

In this case the anode is closed while the cathode is open (Figure 2 - 28b). During EO, water flows from the anode and drains at the cathode. Since there is no water to replenish the soil at the anode, negative pore pressure will develop. Esrig (1968) proposed Equation 2 -20 for the prediction the magnitude of the negative pore pressure that could developed given this drained condition.

$$u_e = -\frac{k_e\gamma_w}{k_h}V \qquad \textbf{2- 25}$$

Equation 2- 20 therefore suggests that in an incompressible medium, a closed anode produces negative pore water pressures at any point that are proportional to the applied voltage at that point.

Case III: Cathode Closed, Anode Open With free access to water

This scenario is illustrated in Figure 2 - 28c and is based on the fact that water is available at the anode but no drainage is permitted at the cathode. During EO, as water moves from anode to cathode, positive pore water pressures are generated at the cathode. Esrig (1968) proposed Equation 2 -26 for predicting the magnitude of the positive pore pressure that could be generated.

$$u_e = \frac{k_e}{k_h} \gamma_w (V_{max} - v) \qquad \textbf{2- 26}$$

2.11.3 Factors influencing the efficiency of the electro-osmosis treatment

The efficiency and the economic viability of the EK treatment is dependent on the amount of water transferred per unit charge passed which may vary over several orders of magnitude. This is a function of a number of factors including the soil type, water content, the nature of the electrolyte concentration, the type of electrodes, electrode soil-contact and the electrode layout. These have been the focus of most EK studies aimed at improving the efficiency of the EK treatment and potential application in the field.

A method of evaluating the electro-osmotic efficiency was proposed by Gray (1966) and Gray and Mitchell (1967) This is based on the assumption that electro-osmotic water flow occurs if the momentum transfer (or frictional drag) between the ions of one sign and their surrounding water molecule exceeds that caused by ions of the opposite sign. No EO occurs in free electrolyte solutions (.i.e., if the cations and the anions are present in equivalent concentrations). The greater the concentrations of cations and anions, the greater the net drag on the water in the direction toward the cathode. This net flow of water determines the efficiency of the treatment process.

Drainage regime	Boundary conditions	Voltage distribution	Pore-water pressure distribution
a *Case I: Anode and cathode open with free access to water*	Cathode: $x = 0, V = 0, u_e = 0$ Anode: $x = L, V = V_{max}, u_e = 0$	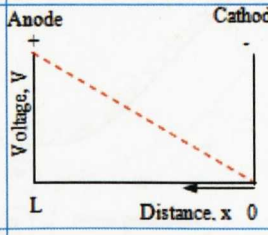	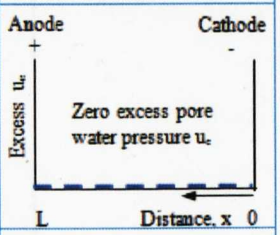
b *Case II: Anode closed, cathode open with free access to water*	Cathode: $x = 0, V = 0, u_e = 0$ Anode: $x = L, V = V_{max}$, velocity of flow $= 0$	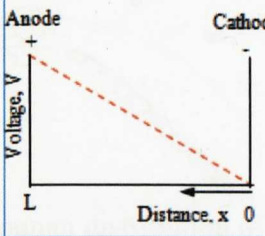	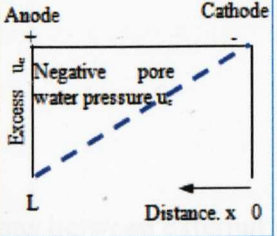
c *Case III: Cathode Closed, Anode Open With free access to water*	Cathode: $x = 0$, no flow at the boundary Anode: $x = L, V = V_{max}, u_e = 0$	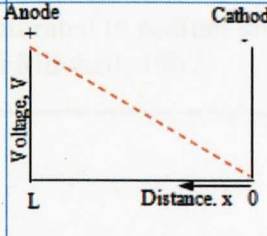	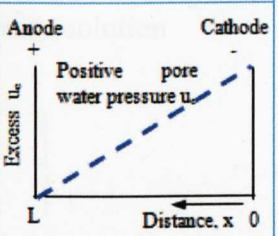

Figure 2 - 28: Pore pressure development at different electrode and drainage and boundary conditions (modified from Esrig, 1968)

Apart from the double-layer theory presented, the Donnan (1924) theory can be employed to describe the equilibrium ionic distribution in fine-grained materials. This deals with the equilibrium distribution of water and ions between two phases. A case of a sodium clay immersed in a sodium chloride solution is presented in Figure 2 - 29 while a theoretical model for predicting water transport by EO showing the effect of different activity (A) clay minerals based on this Donnan concept is shown in Figure 2 - 30.

Figure 2 - 30 therefore implies the efficiency of the EO treatment process is a function of the concentration of the ions (i.e., the electrical conductivity) of the soil mass which in turn is dependent on the water content and the cation exchange capacity (cec) of the soil. Gray and Mitchell (1967) studies indicated that electro-osmotic efficiency decreases with a decrease in water content and an increase in activity of the soil. However, in the practical sense, the type of electrode materials and the configurations of these electrodes would determine how efficient the treatment process would be (Mohamedelhassan and Shang,2000; Rittirong et al.,2008).

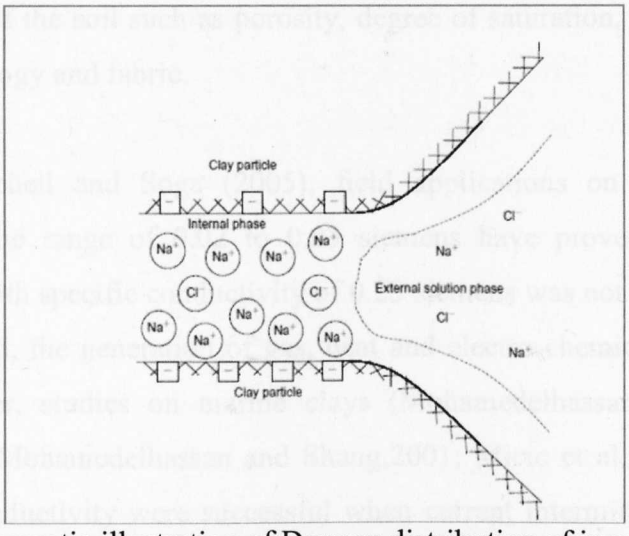

Figure 2 - 29: Schematic illustration of Donnan distribution of ions between external and internal phase for clay saturated in sodium chloride solution (After Gray and Mitchell, 1967)

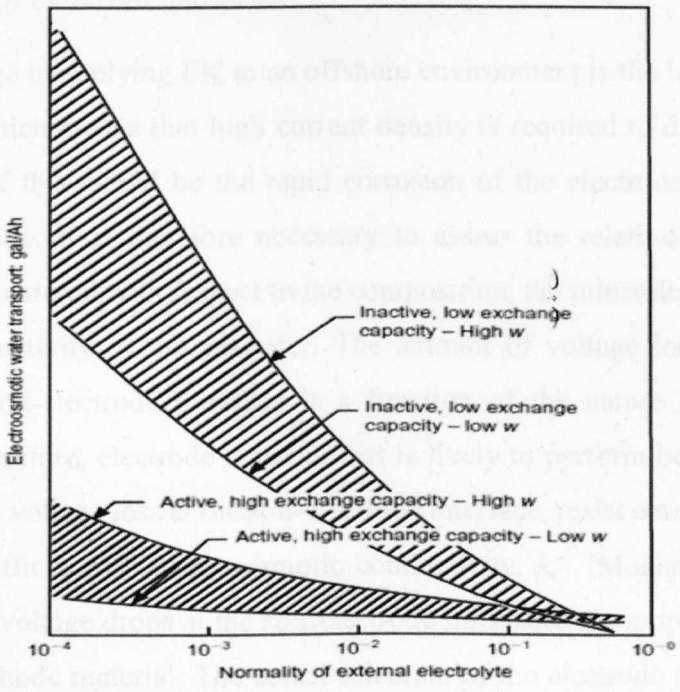

Figure 2 - 30: Schematic prediction of water transport by EO according to Donnan concept (after Gray and Mitchell, 1967)

Mitchell and Soga (2005) argued that the treatment would be ineffective in soil with a high specific conductivity (SC) as the required current to establish a voltage gradient for the treatment will be too high. SC by definition is the reciprocal of the specific resistance of the soil measured between two electrodes which is a good measure of the concentration of ions and salinity of the soil water system and thus the material's ability to conduct an electric current. The specific conductivity of a saturated soil depends on

several properties of the soil such as porosity, degree of saturation, conductivity of the pore water, mineralogy and fabric.

According to Mitchell and Soga (2005), field applications on soil with specific conductivities in the range of 0.02 to 0.03 siemens have proved successful while treatment on soil with specific conductivity of 0.25 siemens was not effective. Also, if a high current is used, the generation of gas, heat and electro-chemical effects becomes excessive. However, studies on marine clays (Mohamedelhassan and Shang,2000; Micic et al.,2001; Mohamedelhassan and Shang,2001; Micic et al.,2002b,2003c) with high pore fluid conductivity were successful when current intermittence and electrode polarity techniques were employed.

2.11.3.1 Effect of electrode materials

One main challenge in applying EK in an offshore environment is the high conductivity of the seawater which means that high current density is required to drive the process. The implication of this would be the rapid corrosion of the electrode materials used, especially the anode. It is therefore necessary to assess the relative performance of specific electrode material with respect to the composition, the mineralogy of the seabed soil and the conductivity of the seawater. The amount of voltage loss and electrode reactions at the soil-electrode interface is a function of the nature of the electrode material used. Therefore, electrode material that is likely to perform best are those that have the minimum voltage loss at the soil-electrode interface, resist corrosion and afford the maximum coefficient of electro-osmotic conductivity, k_e (Mohamedelhassan and Shang,2000). The voltage drops at the soil-electrode interfaces are more sensitive to the anode than the cathode material. The actual selection of the electrode material for field application should be a function of cost and environmental impact (Mohamedelhassan and Shang,2000; Rittirong et al.,2008).

In the experimental investigation conducted by Wrixon and Cooper (1998), three electrode materials namely steel, aluminium and copper were installed vertically in the marine soil. The aim was to increase the bearing capacity of a model offshore casing. They noted that each of the electrodes performed differently during the EK treatment. The steel electrode performed relatively well while the aluminium electrode performed poorly at high voltages, but yielded the highest shear strengths at low voltages. They

suggested that aluminium electrode should be preferred for offshore application due to the high current involved, low voltage is likely to be best suited. They concluded that copper electrodes appear to be the best performer and should be used as a coating material during offshore EK consolidation operations as it could reduce the current demand as compared to either steel or aluminium electrodes. In the Kim et al (1997) study involving iron and aluminium electrodes installed in a marine clay for EK investigation, they reported that a more homogenous degree of strength was obtained using aluminium electrode than using iron electrode, although both metals produced significant increase in the soil c_u. They attributed this to the generation of precipitates of iron oxides, aluminium oxides and aluminium hydroxides.

2.11.3.2 Current intermittence and polarity reversal

Polarity reversal is defined as the reversal of electrode or current directions while current intermittence is defined as the application of a pulsed voltage at predetermined intervals during the EK treatment process. Several researchers have investigated the effects of polarity reversal and current intermittence on the efficiency and effectiveness of the EK treatment. (Lockhart and Hart,1988; Mohamedelhassan and Shang,2000; Micic et al.,2002a).However, there appear not to be a general agreement as to the effects on the EK. While some researchers like Lockhart and Hart (1988) concluded that current intermittence has no significant impact on the EK process, others (Lo et al.,2000; Mohamedelhassan and Shang,2000; Micic et al.,2002a) have shown from their laboratory investigations that current intermittence could enhance the efficiency of the EK treatment. It could be possible that this inconsistency is due to the state of the soil sample used in the various tests.

2.11.3.3 Effect of electrode configuration and electric field intensity

The efficiency of the EK treatment depends to a large extent on the layout and the configuration of the electrode materials used. This is what determines the generation of the current and the current density which drives the EK process. Lo et al. (1991) demonstrated through a pilot test that pumping of expelled water at the cathode can be even eliminated by the appropriate design of electrodes and polarity reversals. This in agreement with Micic et al. (2002c) who demonstrated that through optimisation of the electrode arrangement and implementation of the reversal techniques, the soil strength can improve significantly. The selection of electrode configuration is vital in the design of efficient EK treatment. Soil cementation due to EK treatment has been reported to be

closely related to the electric field intensity which in turn is controlled by the electrode layout (Shang et al.,2004; Rittirong et al.,2008).

2.11.3.4 Electro-chemical effects during EK treatment

Electro-chemical changes are always associated with EK in soil-water electrolyte system. The changes in the engineering properties of soil during EK treatments have been attributed to not only electro-osmotic consolidation but also due to electro-chemical hardening of clay around the soil-structure contact (Micic et al.,2002b). Bjerrum et al (1967) reported that EO dewatering alone could not explain the increase in shear strength of quick clay after EK treatment. Other researchers (Shang and Dunlap,1998; Mohamedelhassan and Shang,2000) have all agreed as to the influence and contribution of chemical alteration in modifying the soil during EK treatment. This effect is due mainly to the migration of ionic species under the concentration gradients and continues to happen even when the electric field is withdrawn, which makes EK treatment a progressive process with time (Micic et al.,2002b). As the anodes decompose, they participate in the electro-chemical hardening of the soil. Thus the increase in strength may be higher than can be attributed to consolidation of the soil.

(Kim et al.,1997) also reasoned that if sufficient aluminium hydroxides or iron oxides were excited when aluminium or iron electrodes were employed in the EK treatment, the geotechnical properties of the clay soil could be changed due to cementation effects. In some cases, the addition of foreign chemical agents into the soil-electrolyte system could accelerate the EK treatment process. Shang et al. (2004) conducted an EK treatment with addition of calcium chloride ($CaCl_2$) in the system and reported that cementation was generated in calcareous silt by the application of an electric field through the soil.

2.11.3.5 Effect of soil type

The electro-osmotically driven water flow during EK treatment is dependent on the mineralogy of the soil, the electrical conductivity and the hydraulic and electro-osmotic conductivity of the soil. The typical hydraulic conductivity of soils suitable for electro-osmotic treatment is in the range 1×10^{-10} to 1×10^{-9}m/s, whereas the coefficient of electro-osmotic conductivity is in the range of 1×10^{-9} to 1×10^{-8} m^2/sV. To generate

electro-osmotic consolidation, the ratio of k_e/k_h (m/V) should be higher than 0.1 (Mohamedelhassan and Shang,2000).

Grundl and Michalski (1996) conducted a test using naturally occurring calcite plus illite-smectite rich glacial till and a kaolinite - water system, which is usually used in most EK tests, and reported that the results from the two test differs significantly. The mode of current conduction differs markedly also. They found out that the mechanism of flow stoppage in kaolinite was due to the cessation of current flow while electric current continues to flow through the till after the water cease to move. This was attributed to the presence of the different minerals in the clays causing the electrolytic system to respond differently to the application of an electric field. In fact the presence of calcite in the natural clay prevents the formation of low pH conditions in the sediment pore water.

2.11.4 Energy requirement

According to Mitchell and Soga (2005), if the amount of water moved per unit charge passed (Gal/h/Amp, or moles per faraday) is denoted as k_i, then

$$q_h = k_i I \qquad \textbf{2- 27}$$

Where the quantity k_i varies over a wide range unlike k_e. The power consumption P is given as

$$P = \Delta E.I = \frac{\Delta E q_h}{k_i} \text{ (in W)} \qquad \textbf{2- 28}$$

For ΔE in volts and I in amperes, the power consumption per unit volume of flow is given as

$$\frac{P}{q_h} = \frac{\Delta E}{k_i} x\, 10^{-3} \text{ (in kWh)} \qquad \textbf{2- 29}$$

K_e is related to the k_i by the following relationship

$$q_h = k_i I = k_e \frac{\Delta E}{\Delta L} A \qquad \textbf{2- 30}$$

And because $\Delta E/I$ is resistance and $\Delta L/$ (resistance x A) is specific conductivity σ, Equation 2 -17 in terms of electro-osmotic efficiency, k_i (in gallons/amp/hour) becomes

$$k_i = \frac{k_e}{\sigma} \qquad \textbf{2- 31}$$

This indicates the k_i, is a sensitive function of the electrical conductivity (σ) of the soil.

Energy consumption per unit volume

Micic et al. (2002a) presented an equation for calculating energy consumption per unit volume of treated soil during a test, W_e (Wh/m^3) as:

$$W_e = \frac{\tau V_0}{v} \sum_{i=1}^{N_R} \int_0^{t_{Ri}} |I(t)|\, dt \qquad \textbf{2- 32}$$

Where:

V_o = applied voltage (V)

τ = current intermittence ratio

t_{Ri} = treatment time under 1 polarity (h) (i = 2, … N_R);

N_R = number of polarity reversal (N_R = 1 for no reversal)

I (t) = electric current as a function of time, t (A)

v = volume of treated soil, = A x H (m^3); A = treatment area (m^2) and

H = electrode insertion depth (m)

$$\tau = \frac{t_{on}}{t_{on}+t_{off}} \qquad \textbf{2- 33}$$

Where;

τ = current intermittence ratio

t_{on} = power-on time (min)

t_{off} = power-off time (min)

For a constant applied DC current, τ = 1

2.11.5 A review of the application of EK treatment to offshore soils

The application of EK to offshore foundation soils is a relatively new move. The successful applications of EK reported in §2.10.3.3 involved soils of low salinity, i.e., the salt content in the pore water was less than 2g NaCl/*l* or the equivalent. In contrast, marine clays are characterised with high salinity, up 30g NaCl/*l* (Mohamedelhassan and Shang,2000). The earliest reported attempted case of the application of EK in the offshore was to increase the driveability of offshore piles in which pore fluid was forced to migrate towards the tips of the pile during penetration (Rose,1979). This technique of driving piles led to an investigation on the possibility of applying EK to increase the bearing capacity of soft marine sediment to support offshore casings as reported by Wrixon and Cooper (1998). They conducted an EK treatment on jet-drilled casing models and found that the bearing capacity of the model increased by 1000% within hours.

One major challenge in the use of EK in the marine environment has always been the high conductivity of the sea water which has significantly limited the application of this technology in marine soil in the past. The high conductivity of the pore fluid results in excessive power consumption and severe corrosion of the electrodes, especially the anodes, due to chemical reactions which would ultimately reduce the efficiency of the EK treatment. Srinivasaraghavan and Rajasekaran (1994) reported that the high salt contents of the marine clay could produce beneficial effects on the effectiveness of the EK process if chemical additives are added during the treatment process. However, the economy of such approach would be unfeasible in deep offshore field applications.

The earliest comprehensive study on the application of EK to offshore foundations started with the work of Lo et al.(2000) and Micic et al.(2001) in which marine clay from a coastal basin was dredged and tested for the possibility of electro-kinetically increasing its strength and for possible application in enhancing the capacity of offshore foundations. A significant increase in the undrained shear strength (c_u) and corresponding decrease in water content of the treated soil were reported.

In an attempt to enhance the effect of surcharge preloading consolidation of a marine clay soil dredged from an offshore site, Micic et al. (2001) conducted laboratory tests involving the combination of the surcharge preloading with EK treatment. They

reported up to 145% increase in the undrained shear strength and about 125% decrease in the water content of the soil when EK was combined with surcharge preloading than when the preloading consolidation was used alone. This significant change in the soil notwithstanding the high salinity (high conductivity) of the marine soil was achieved by the use of intermittent current.

The effects of polarity reversal and current intermittent current were investigated by Micic et al. (2002a). They concluded that the application of the intermittent current significantly reduced the energy consumption and electrode corrosion of the EK treatment but without reducing the effectiveness of the soil strength strengthening. In addition, they concluded that polarity reversal can generate a more uniform increase in the soil c_u during the EK treatment. They reported 185% and 80% increase in the soil c_u at the anode and the cathode zones respectively.

Micic et al. (2002a) and Micic et al. (2002b) conducted an extensive series of laboratory EK tests on marine clay recovered from a coastal basin. The tests involved both the EK phase and the post treatment phase where the ionic diffusion in the treated sample were studied. The primary aim was to strengthen the soil around an embedded steel plate which simulated a part of an offshore foundation, thus enhancing the bearing capacity of the plate. They reported a significant change in the soil properties. In addition to the decrease in the soil plasticity at the anode, the soil c_u increased from 4.2kPa to 16.5kPa during the EK phase and a further increase to 21kPa after 45 days exposure to allow for chemical diffusion phase (i.e., diffusion under the influence of a gradient in chemical composition). The soil water content also dropped from 94.3% to 74.2%, but increased to 84.9% after the 45 days diffusion phase. These changes were attributed to the combined action of electro-osmotic consolidation and chemical alteration of the soil sample during the EK treatment. The post treatment tests on the soil samples using the mercury intrusion porosimetry technique indicated that EK treatment causes a decrease in the pore size diameter of the treated soil which indicated precipitation of amorphous compounds.

Micic et al. (2003a) also presented results of a study using EK tests involving a large-scale testing facility to investigate the effects of EK treatment on the loading carrying capacity of a model skirted foundation embedded in a marine sediment and reported a

three-fold increase in both the load carrying capacity and the c_u of the treated soil. The soil-structure adhesion force was also increased as indicated by the clay strongly adhering to the wall of the model foundation due to increase bonding promoted by the EK processes in the soil. The effects were assessed though series of pull-out, water content and undrained shear strength tests conducted on both the treated and the control samples.

Micic et al. (2003b) reported a study which involved an investigation on the effect of EK in soft marine clay embedded steel plate which simulated part of a skirted foundation. From the results of the small-scale tests, a large-scale model (Figure 2 - 31) with a cylinder simulating a model skirted foundation was studied. The aim was to assess the effect of the EK treatment on the improvement of the load-carrying capacity of a model skirted offshore foundation embedded in soft marine clay. The dimensions of the small-scale test were 26.5x11.9x25.4 cm (LxWxD) while the large-scale test had dimensions of 150x75x70 cm (LxWxD). The load carrying capacity of the foundation was evaluated via axial loading and pullout tests. From the results of the investigation, they concluded that the load-carrying capacity of the model skirted foundation increased by a factor of three while the soil c_u increased by a factor of seven mainly due to the EK effects. In addition, the axial loading tests indicated a three-fold increase in the adhesion coefficient after the EK treatment.

The above studies on typical marine soil were all successful and promising. However, it should be noted here that while Esrig (1968) theorised that open electrode arrangement (i.e., the one that allows egress and ingress of pore fluid) does not promote the generation of negative pore pressure and hence little consolidation due to EO, most of the above studies on offshore EK involved an open electrode arrangement. Therefore, it can be suggested that even in the open electrode arrangement, significant improvement to the soil properties could still depend on the electrode layout.

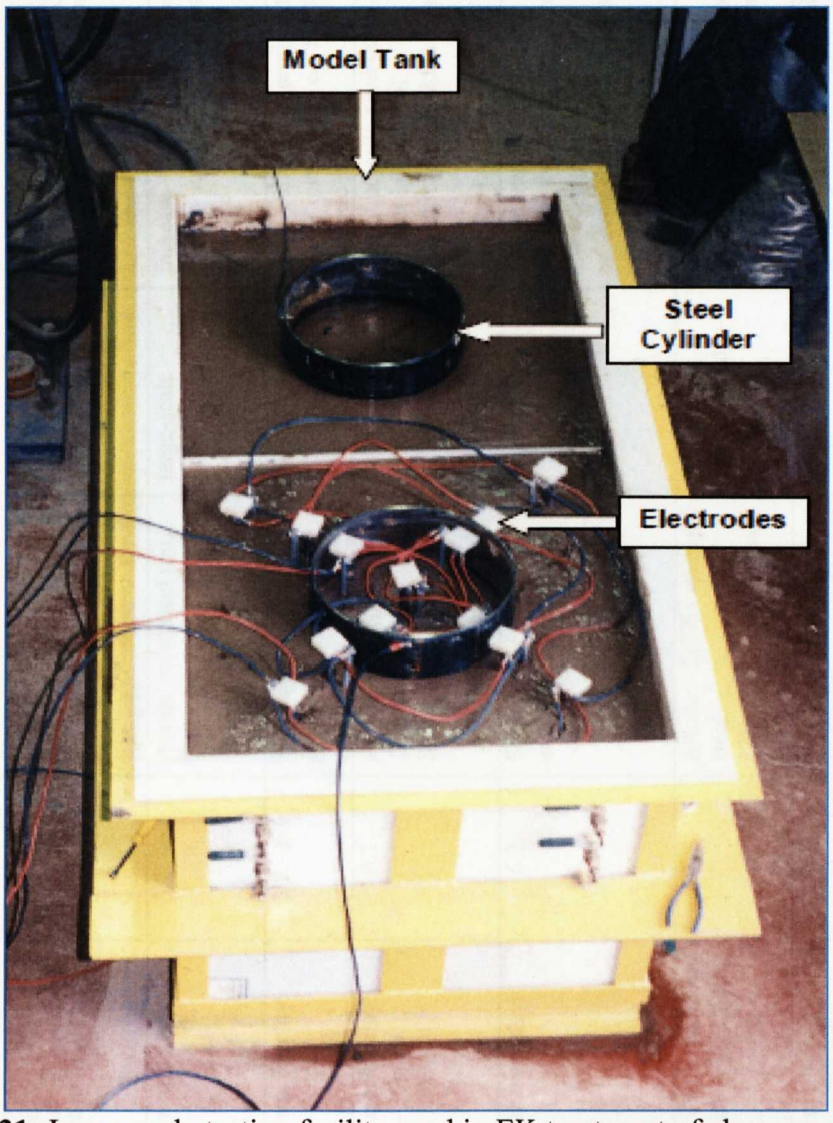

Figure 2 - 31: Large-scale testing facility used in EK treatment of clay around a skirted foundation model (Micic et al.,2003b)

This improvement is possibly due to development of suction as well as electro-chemical effects on the soil (Hamed et al.,1991; Acar et al.,1992; Eykholt,1997). In addition, changes in ionic concentration and *pH* can result in a non uniform electric field. The resultant non uniform field could generate negative pore pressures in the soil (Acar et al.,1994). Summary of electro-kinetic test conducted to enhance the capacity of offshore foundations is presented in Table 2- 4.

Table 2- 4: Summary of electro-kinetic tests conducted to enhance the capacity of offshore foundations

S/N	Reference	Application	Soil type	Voltage range (V)	Electrode material	Test type	comment
1	Srinivasaraghavan and Rajasekaran (1994)	Combined with chemical additives to enhance the EK treatment	Port Nova marine clay	30	Perforated copper plates for both anode and cathode	laboratory	3 to 8 -fold increase in the soil c_u
2	Lo et al. (2000)	To increase the bearing capacity of a marine clay to support offshore foundation	Yulchon marine clay:	3.2 – 6.6	Anode: solid steel rod Cathode: Steel pipe	large-scale experimental facility	Increase in cu in the vicinity of both anode and cathode
3.	Micic et al. (2001)	Combined with surcharged preloading	Yulchon marine clay: Salinity – 30g/l *w* – 100- 120%	3.2 – 6.6	Steel mesh for both anode and	laboratory	Use current intermittent; 145% increase in c_u, 125% decrease in *w*
4	Micic et al. (2002a)		Yulchon marine clay: Salinity – 30g/l *w* – 110- 120%	6.2	Anode: steel rod Cathode: Steel pipe		Use of polarity reversal and current intermittent Cu increase by 185% near anode And 80% near cathode
5	Micic et al. (2002b)	Embedded steel plate which simulated a part of an offshore foundation.	Yulchon marine clay:	6.2	Steel rods for both anode and the cathode	laboratory	Use current intermittent ; Studied the changes due to electro-chemical actions c_u increased from 4.2 to 21kPa *w* drop, 94.8 to 84.9%
6	Micic et al. (2003a)	To improve the load-carrying capacity of an offshore foundation	Welland River sediment mixed with high salinity solution	5.2	Anode: Solid stainless steel Cathode: perforated steel pipe	large-scale experimental facility	Used polarity reversal Load carrying capacity of the treated soil and the cu increase three fold
7	Micic et al.(2003b)	To improve the load carrying capacity of a model skirted offshore foundation	Yulchon marine clay and Welland sediment	5.2	Anode: solid steel rod, Cathode: perforated steel pipe	Small and large-scale testing facility	Significant increase in both the load carrying capacity and the soil cu for small and the large scale tests

2.12 Summary of literature review

From this review of literature, it is evident that although many authors have attempted to investigate the problem associated with pipeline instability, not much work has been done to solve this problem. Even in the reported studies on the pipeline instability, some level of divergence exists in both the assumptions employed and the reported conclusions. There is also the argument on the best approach to be used for assessing pipe-soil interaction responses. While some researchers such as Lyons (1973) and Hesar (2004) advocated the use of numerical approach as the best method, others such as Verley and Lund (1995), Bruton et al. (2006) supported the use of empirical curve fitting approach which relies mostly on results from previous laboratory studies.

While there appears to be a relative agreement amongst researchers as to the influence of depth of pipe embedment on the soil lateral resistance, other parameters such as rate of pipe displacement, pipe diameter and coating show considerable variance amongst researchers. Lyons (1973) concluded that lateral resistance of clay decreases with increasing pipe diameter, increases with pipe submerged weight and that the frictional coefficient increases with the weight of pipe and decreases with increasing pipe diameter and is higher for bare pipe than coated pipes while Verley and Lund (1995) concluded that pipe diameter has less importance on the lateral resistance of the soil. There is also little reported on the influence of the rate of pipe displacement on the ensued lateral resistance although Wantland et al. (1979) concluded on no influence of the rate of pipe displacement on soil lateral resistance. The displacement of pipeline before soil failure has not received much attention apart from the work of Wantland et al. (1979).

All workers agree to the existence of high level of uncertainty in predicting the initial embedment of pipeline into the seabed which is attributed mainly to the challenge of estimating the soil loadings during the pipeline installation process. There appears to be no conclusive solutions on this issue at present. Although various equations are in place in most cases they are on the conservative side; the actual pipe penetration is mostly greater than expected. The Verley and Lund's (1995) equation still offers the best model for pipe penetration estimation. Discrepancies between the outcomes from the various approaches of predicting pipe initial embedment could be due to the selection of the appropriate soil strength for the analysis. The review also indicates that all workers

agree on the dependency of the soil lateral resistance on the strength of the soil thus any means of increasing this strength would enhance the capacity of the pipeline to movement.

The greatest uncertainty in pipeline design is the one relating to the pipe-soil interaction especially the deformation characteristic of the soil during large amplitude of pipe displacement. While White and Cheuk (2008) have attempted to predict the additional resistance offered by the berm of soil using plasticity approach from the failure of the soil in front of the pipe, the actual real time study of the generation of the berm was not included and none of the past researchers have addressed this in their laboratory studies. The laboratory studies conducted by Bruton et al., 2006 which studied the effect of berm consolidation on soil lateral resistance did not involve real time studies of the berm generation. This present study would attempt to bridge this gap in addition to investigating some of the other parameters mentioned above.

The instability problem associated with operation conditions of the pipeline is well established. Some mitigating options are available to reduce the risk of pipeline buckling and although they may reduce the instability of pipeline, they are expensive and not feasible in deep waters. In addition, none of them deal with the modification of the soil ambient properties.

Currently, the use of engineered lateral buckles has become a generally accepted and frequently used in the industry. However, this approach depends on the ability of the soft seabed soil to resist pipe displacement at a predefined location. Electro-kinetic phenomenon is one of the methods employed in geotechnical engineering to improve the engineering properties of weak soils and may prove potentially to be used to enhance the engineering properties of the very soft offshore seabed.

It has been demonstrated through recent studies (Mohamedelhassan and Shang,2000; Micic et al.,2002a; Micic et al.,2003b; Rittirong et al.,2008) that EK can be applied to increase the capacity of offshore foundations. However, the review of literature indicated that no study has been conducted to investigate the use of EK on subsea pipelines. This research was therefore set out to investigate the feasibility of using EK to reduce the risk of subsea pipeline instability.

Chapter 3

EXPERIMENTAL METHODOLOGY

3.1 Introduction

This research focuses on the development of the application of electro-kinetic phenomenon to increase the stability of subsea pipelines, as well as studying at a large-scale, pipe-soil interaction during large cycle pipe displacement. The primary aim of this study is to mitigate against lateral buckling and axial walking of offshore pipelines which is normally associated with high temperature and high pressure pipelines. To assist in this study, a number of pieces of equipment were designed and fabricated both at small-scale and at large-scale. The chapter is divided into two major sections covering materials and methods. The first section covers the application of electro-kinetic processes to enhance subsea pipeline stability while the second section covers large-scale pipe-soil interaction test. A summary of all tests conducted is presented at the end of each section.

3.2 Design philosophy and overview of the testing programme

The main philosophy behind the test set up was to model as closely as possible a partially embedded pipeline on the seabed in two dimensions. It was decided to use small scale tests as this was an initial study of the topic and the small scale test would allow a relatively rapid test programme enabling a range of parameters to be investigated in a reasonable time. The geometric arrangements and materials of the tests were designed to reflect expected practical arrangements (depth of embedment, soil strength, loading rate etc). The larger scale tests were designed partly to confirm if the results of the smaller scale tests were applicable at a larger (nearly full size) scale and to permit a more detailed study of the soil deformation behaviour during pipe displacement, albeit of a more limited range of parameters.

In both test series EK was applied to the soil, the soil response monitored and then the pipe generally subjected to vertical, lateral or axial displacement while the force – displacement responses were monitored. The soil bed was prepared as a uniform, homogenous layer which was felt to be fairly representative of a soft seabed. Given the relatively small extent of the influence of pipelines the assumption of uniformity was felt to be reasonable, although not necessarily realistic. One typical clay type was chosen to limit the range of variable to be tested.

The existing applications of EK offshore as noted from the literature review were taken into consideration during the design of the research in an attempt to ensure the findings would be applicable. The small-scale tests were conducted in a small perspex tank which was opened to the surface. A plastic pipe was used to model the pipelines as offshore pipelines are normally non-conductive. The arrangement of the electrodes around the pipeline was designed to allow for ease of installation and to represent a feasible arrangement in line with existing technology in the offshore pipeline

Different types of electrode materials were investigated to identify the one with maximum efficiency. During the treatment, the consolidation of the sample was inferred from a dial gauge attached to the pipe while the electrical parameters were recorded manually. Only one soil type was used in all tests. A small rig was designed and fabricated to apply the various loadings of the pipe on the soil. The design philosophy of the small rig was to simulate the various pipe displacements during buckling.

The larger scale pipe-soil interaction tests were conducted in a reinforced steel tank lined with perspex sheets. At the top of the tank was a support frame which was connected to the pipe section and was able to generate controlled lateral displacement of the pipe section via a stepper motor. The resistance offered by the soil during the pipe movement was measured by a load cell while the vertical and the horizontal displacement of the pipe were measured by a draw wire displacement sensor and a posichron displacement sensor respectively. Results from all the sensors were automatically recorded by a logger connected to a PC. Different variables were investigated for the pipe-soil interaction responses. The displacement of the pipe was controlled to minimise end-effects which ensured that the soil deformation and the force-displacement responses could be modelled as a plane strain problem (two dimensions). Kaolin clay was used in all tests to

model the seabed. The soil sample was prepared in one batch but remixed and re-characterise before each test. The main task involves measuring the soil resistance of a pipeline that is partially buried in a model seabed during the pipe displacement and the real time measurement of the soil geometry and its deformation in 2D during the pipe displacement.

3.3 The equipment for the small–scale EK tests

In order to investigate this process in relation to pipeline stability, a number of pieces of equipment were designed and fabricated. The primary emphasis was on the reduction in water content of the soil around a model pipeline, increase in effective stress of the seabed as well as increase in the pipeline-soil adhesive force in order to increase the breakout force of a partially embedded model pipeline. In this section, a series of electro-kinetic tests were conducted on a kaolin clay soil model seabed using an embedded model pipe section which simulates a section of an offshore pipeline is presented. The materials used in the experiments are discussed first, followed by the test procedures and programmes. Some of the limitations of the experimental procedures are highlighted for further improvement.

3.3.1 Materials

3.3.1.1 The clay soil used

Selection of the test material

The selection of test material for this research was based on the following considerations: (a) its suitability for electro-kinetic treatment, (b) its consistency in terms of known physical and chemical compositions and, (c) potential ease to work with and produce a consistent and easily controllable tests samples that are identical in all tests and which can potentially be compared with previous studies. Although this study is aimed at modifying offshore marine clays, typical offshore soils in sufficient quantity could not be obtained within the time frame of this research due to logistical reasons. In addition, the variability in the properties of these marine soils as well as varying compositions between offshore locations (see §2.3.3) makes the choice of kaolin clay a suitable option for this preliminary studies. This material has been used in previous laboratory studies and kaolinite is a common constituent of many real clay soils.

Commercially available Polwhite E grade kaolin, a pure form of clay was therefore chosen for all the tests. This grade of kaolin was selected because it has a more uniform (in terms of its composition obtained from various sites) physical and chemical properties than most natural soils and has been reported in the literature to be suitable for electro-kinetic treatment given its chemical and geotechnical characteristics (Hamed et al.,1991; Acar and Alshawabkeh,1996; Eykholt,1997; Karim et al.,2005). This soil is produced from deposits in Cornwall (United Kingdom) and supplied by Imerys Minerals Ltd, John Keay House, St Austell, PL25 4DJ, Cornwall, (United Kingdom). The property of this clay is well documented in, for example, Acer et al (1994), Hamed and Bhadra (1997) and Lehane et al (2009).

In its natural state, kaolin is white clay comprising mainly of the hydrous aluminium silicate clay mineral kaolinite. The kaolinite minerals consist of roughly hexagonal, platy crystals ranging in size from about 0.1 micrometer to 10 micrometers or even larger. Please refer to §2.7 for a brief review on clays soil including kaolin clay. Figure 3 - 1 presents the particle size distribution characteristics of the material. Its structure is made up of one tetrahedral silicate sheet (Si_2O_5) linked through oxygen to one octahedral sheet of aluminium oxide/hydroxyl layer ($Al(OH)_4$. A summary of the chemical properties of the Polwhite E grade kaolin clay material used in this study is presented in Table 3 – 1, while a full data sheet from the supplier can be found in Appendix A.

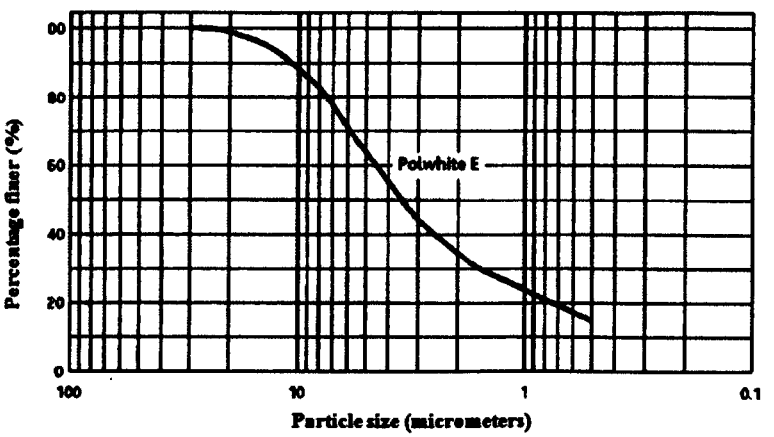

Figure 3 - 1: Particle size distribution curve for the grade polwhite E kaolin as given in the manufacturer's data sheet

Table 3 – 1 The chemical properties of the Polwhite E grade kaolin clay*

Property	**Unit**	**Polwhite E grade**
Water content max	mass %	1.5
Specific gravity	-	2.6
pH	-	5.0 ± 0.5
Water soluble salt content	Mass%	0.15
Si_2	Mass%	50
AL_2O_3	Mass%	35

*Values as given in the manufacturer's data sheet

A range of laboratory soil tests were carried out in accordance with B.S.1377:1990, Methods of Tests For Soil for Civil Engineering Purposes to determine the basic properties of the kaolin. The soil has plastic and liquid limits of about 33% and 56% respectively. Its water content varies with depth below the mudline and is about 68 % when it is allowed to consolidate (due to self weight and depending on the depth of soil) to an undrained shear strength of about 0.8kPa (from the T-bar test conducted on the soil), the corresponding unit weight is about 16kN/m^3.The hydraulic conductivity (k_h)of the kaolin obtained using the falling head method was 4.0 x 10^{-9} m/s. The electro-osmotic conductivity (k_e) of the commercial kaolin, found from previous studies, ranges between 1.1 x 10^{-5} cms^{-1} per Volts/cm and 5.7 x 10^{-5} cms^{-1} per Volts/cm (Bjerrum et al.,1967; Esrig,1968; Hamir,1997). Casagrande (1952) had also reported a k_e value of 5.7 x 10^{-5} cms^{-1} per Volts/cm for a commercial kaolin at 67.7% water content.

3.3.1.2 The small-scale electro-kinetic testing tanks

In the absence of relevant standard methods or apparatus for this type of study since no research has been published in the area of pipeline stability by EK treatment a 'fish tank' model (Figure 3 - 2) was chosen for this investigation. The rectangular, open-to-the surface tank model was considered to be more representative of actual field conditions than the traditional cylindrical closed cells used in most EK study by various researchers. In addition, this configuration allowed for post treatment tests to be conducted e.g. the various pulling tests.

Figure 3 - 2: Perspex tank models used in the small-scale EK tests

The small test tank was made from transparent perspex sheets to render it non-conductive to electrical current as well as being hydraulically and electrically impermeable. Its dimension was 410mm x 210mm x 210mm (length x width x height). These dimensions allowed for both the geotechnical and pulling tests to be conducted before and after the EK treatment. A second tank was used for the control test. The results of the control experiments were compared to those of the EK tests to assess the effectiveness of the EK treatment process.

3.3.1.3 The T-bar penetrometer and the hand shear vane devices

The selection of appropriate devices for in-situ strength measurement of very soft clays (c_u ~1 -2kPa), which is typical of most deepwater offshore sites, is currently challenging in geotechnical engineering practice and was therefore given serious consideration in this research. Currently, the most commonly used in-situ test apparatus in offshore geotechnical engineering are the vane shear and the cone penetrometer. However, these two devices have inherent limitations. For the cone penetrometer, there is need for correction for overburden pressure and pore pressure, while the shear vane suffers from the inability to measure accurately the <1kPa strength of the upper 1m depth of deepwater seabed (Randolph and Andersen,2006). In addition the vane shear can only give strength values at discrete depths.

The T-bar penetrometer (Stewart and Randolph, (1994)) which is a modified form of the cone penetrometer is considered by offshore geotechnical engineers as best suited for measuring the strength of the very soft seabed soils. It was therefore considered as the best tool to characterise the soil shear strength in this study.

a) The T-bar penetrometer

The laboratory T-bar penetrometer used in this study is shown in Figure 3 - 3. It was designed and fabricated as part of this research for assessing the undrained shear strength of the bed of clay before and after the EK treatment. The design of the T-bar was based on the original concept developed by Stewart and Randolph (1994) and gives a continuous profile of shear strength with depth. The shaft of the T-bar [1], which has a diameter of 9.6mm, was made from an aluminium rod. At the end of the shaft is a 40mm long cylindrical T-bar [2] of diameter 9.6mm which is attached perpendicular to the shaft and offers a projected area of 384mm^2 during the soil penetration.

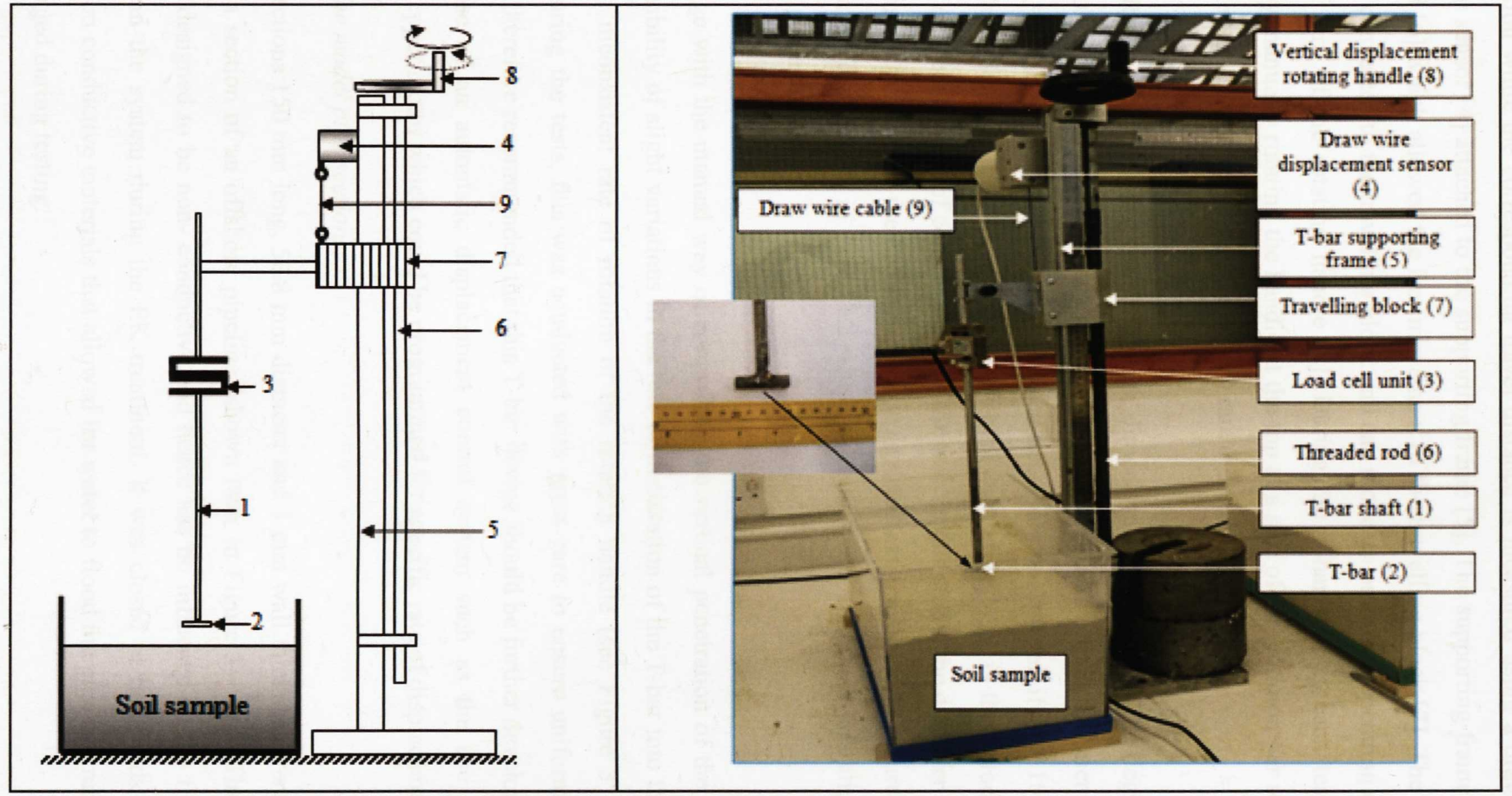

Figure 3 - 3: Schematic and photo of the laboratory T-bar penetrometer test setup

A load cell [3] attached to the top of the T-bar shaft measures the resistance during the soil penetration while the corresponding travel distance is measured using a draw wire displacement sensor [4] attached to the supporting frame [5]. The supporting frame has a threaded rod [6] which allowed the free movement of the travelling block [7]. The T-bar apparatus is connected to the travelling block and can move up or down depending on the direction of turn of the rotating handle [8]. During the T-bar testing, each test was conducted by manually rotating the handle at the top at a rate of 1 revolution per second which resulted in a penetration (and extraction) rate of 2mm/sec.

Finnie and Randolph (1994) suggested through dimensional analysis that the degree of partial consolidation during continuous penetration is controlled by the non-dimensional velocity, $V = D_{T\text{-}bar}\, v_{T\text{-}bar}/c_v$ and that an undrained behaviour will prevail if $V > 10$ (.i.e., $D_{T\text{-}bar}\, v_{T\text{-}bar}/c_v > 10$). $D_{T\text{-}bar}$ is the diameter of the T-bar while $v_{T\text{-}bar}$ is the velocity of penetration. c_v is coefficient of consolidation of the soil. In this study, the diameter of the bar is 9.6mm while the c_v of the kaolin sample is reported extensively in literature to be around $1mm^2/s$. This results in $V = 19.2$ which is enough for undrained conditions to prevail during penetration.

One challenge with the manual way of controlling the vertical penetration of the T-bar was the possibility of slight variations in the rate of penetration of the T-bar into the soil arising from inconsistent rate of rotation of the rotating handle (see Figure 3 - 3a). However, during the tests, this was conducted with great care to ensure uniformity in results. It is therefore recommended that this T-bar device should be further developed to allow for use of an automatic displacement control system such as the use of an integrated stepper motor which could be programmed for specific rate of displacement.

3.3.1.4 The model pipe sections

PVC pipe sections 150 mm long, 50.8 mm diameter and 3 mm wall thickness were used to simulate a section of an offshore pipeline (shown later in Figure 3 - 13). The pipe section was designed to be non- conductive and hence has no influence on the flow of current within the system during the EK treatment. It was closed at both ends using perforated non conductive materials that allowed for water to flood the pipe and render it fully submerged during testing.

3.3.1.5 The electrode materials

The selection of electrode materials was based on availability of the material, suitability for electro-kinetic applications and cost. A literature search showed that the material most used in previous electro-kinetic studies was copper (referred to here as CU-electrode), due to its conductivity, metallic properties and durability in a saline environment.

Experiments were conducted first using metallic copper materials as the anodes and cathodes. Mild steel (referred to here as FE-electrode) and aluminium (referred to here as AL-electrode) were also used during the later stages of the research. Although stainless steel was expected to be more suitable in the aggressive saline environment, it was not considered due to cost implications in practical field applications.

All the electrodes used were 150mm long and 3mm diameter solid metallic rods (Figure 3 - 13). Cathodes normally act as drains since the electro osmosis process forces the pore fluid to the cathode but in these tests the cathodes were in the 'sea' therefore they did not act as drains; the surface of the sea bed was the drain.

3.3.1.6 Electrode supporting units

To support and position the electrodes in place during installation for the EK treatment, two electrode positioning units (Figure 3 - 4) were designed and fabricated for each pipe section. The units were made from polypropylene materials to render them non-conductive. The rings were 4mm thick with internal and outer diameter of 50.8mm and 70mm respectively. 3mm diameter holes spaced at an angle of 10^{o} and located 30.5mm from the centre of the ring (centre to centre) were drilled through the ring. This arrangement made it possible for the electrode spacing and electrode numbers to be varied between the tests. The electrodes were horizontally installed parallel to the pipe section which serves neither as the anode nor the cathode.

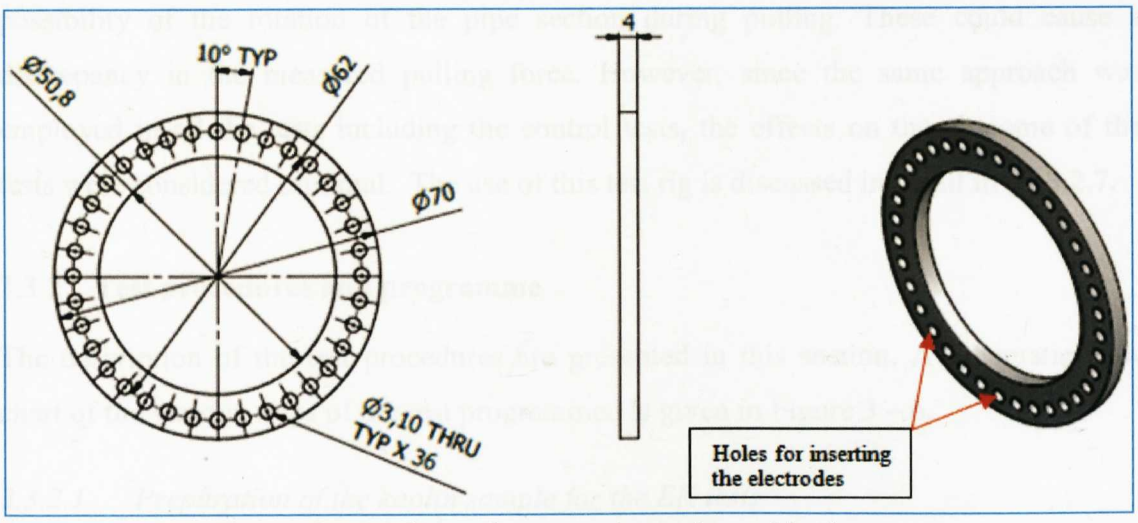

Figure 3 - 4: Electrode supporting unit used in the tests

3.3.1.7 The small test rig

To enable the three loading configurations, namely vertical, lateral and axial for the partially embedded pipeline after the EK treatment, a small test rig (Figure 3 - 5) was designed and fabricated as part of this study. Referring to Figure 3 – 5, the frame of the rig [6] was made from aluminium 25mm x 25mm box section with 2mm wall thickness. From the top of the frame runs a 25mm diameter adjustable vertical rod [7] which holds a plastic bearing at its base. A flexible wire [8] was used to connect the pipe section with the load cell via the bearing. The load cell was supported by a 9.6mm aluminium rod which in turn was connected to a travelling block attached to a supporting frame [5]. To measure the displacement of the pipe during pulling, the draw wire cable [10] was securely attached to the travelling block [11]. During the pulling tests, the rotation of the rotating handle [1] resulted in the movement of the travelling block which in turn moved the load cell and the attached pulling cable thus moving the pipe. The cable could either be attached to pull the pipe laterally, axially or vertically. The load cell measured the resistance of the soil as the pipe is forced to move.

While this arrangement offers a reasonable means of assessing the effectiveness of the EK treatment of the soil in terms of measuring the change of the soil resistances to the various pipe motions, some possible sources of inaccuracy of were noted and given consideration. These range from the error due to the possibility of introducing variable tension in the pulling cable before the pulling began, twisting and bending of the supporting stand and rods, friction losses in the bearing etc. Another factor is the

possibility of the rotation of the pipe section during pulling. These could cause a discrepancy in the measured pulling force. However, since the same approach was employed in all the tests including the control tests, the effects on the outcome of the tests were considered minimal. The use of this test rig is discussed in detail in §3.3.2.7.

3.3.2 **Test procedures and programme**

The description of the test procedures are presented in this section. A schematic flow chart of the various steps of the test programmed is given in Figure 3 – 6.

3.3.2.1 Preparation of the kaolin sample for the EK tests

The test sample was prepared by mixing the dry kaolin with saline water to form slurry with initial water contents of 70%, 90% and 120%. The saline solution was prepared by mixing 3% of Nail in 97% water to produce a 30g Nail/*l* solution which is reported as being typical of pore fluid salinity of marine offshore seabed soils (Mohamedelhassan and Shang,2000; Micic et al.,2003b; Shang et al.,2004). Most of the tests used 70% water content while the 90% and 120% water content tests were conducted at the latter stages of the research to assess the influence of water content on the effectiveness of the EK treatment process.

To reduce the time of consolidation of the clay in the tank which would be the case if the soil was prepared from a slurry state, the 70% water content was accepted although this might not guarantee 100% saturation. However, most seabed soils are rarely fully saturated due to the presence of gas bubbles (Wheeler,1988,1988; Sills and Wheeler,1992). The kaolin soil used here has a LL of 56% and at 1.4LL implies the soil would be considered fully saturated at 78% WC. Therefore the soil was therefore assumed to be partially saturated and given that seabed soils are rarely fully saturated, the 70% water content is considered adequate to represent typical offshore soils.

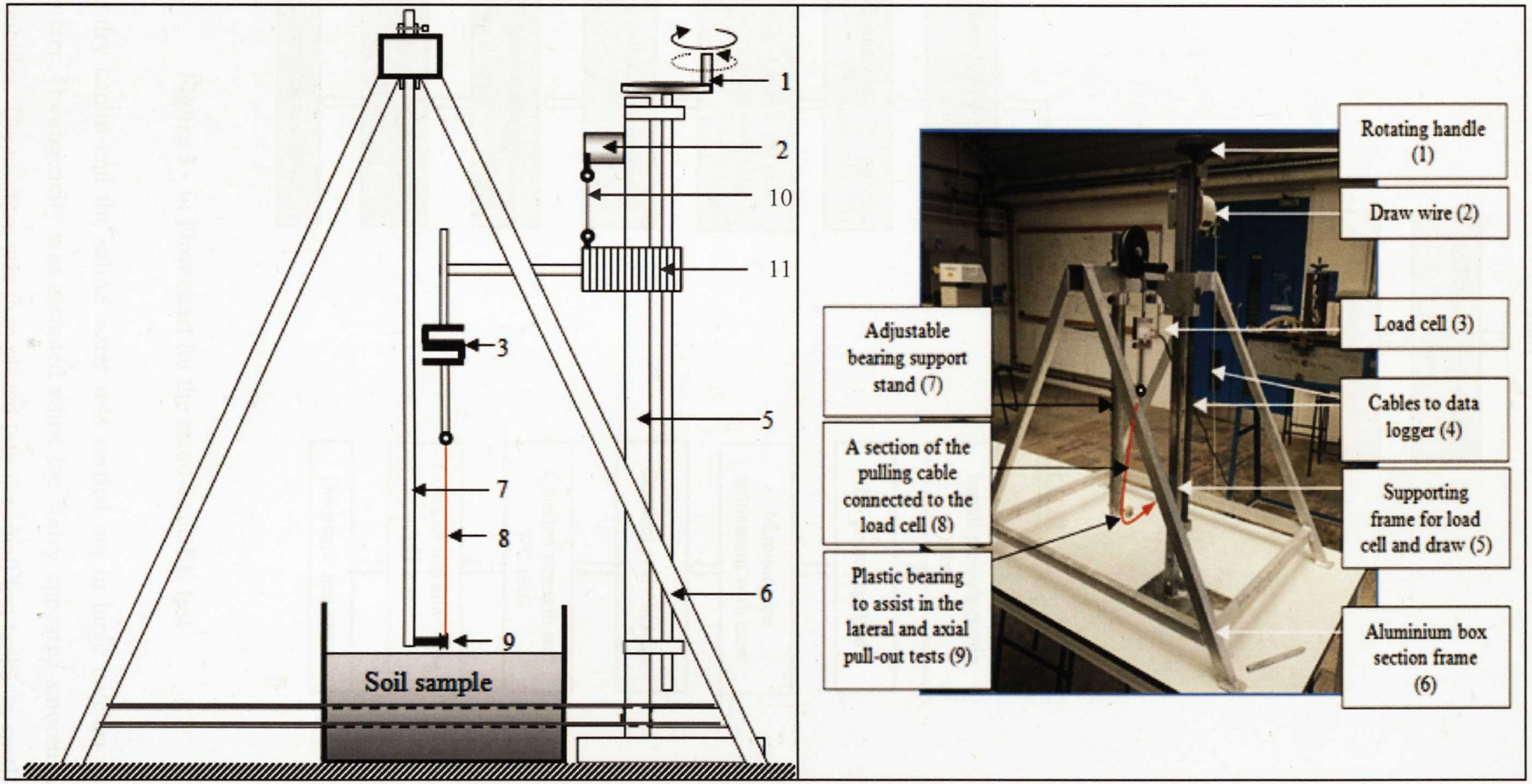

Figure 3 - 5: Schematic and photo of the small-scale pull-out test rig

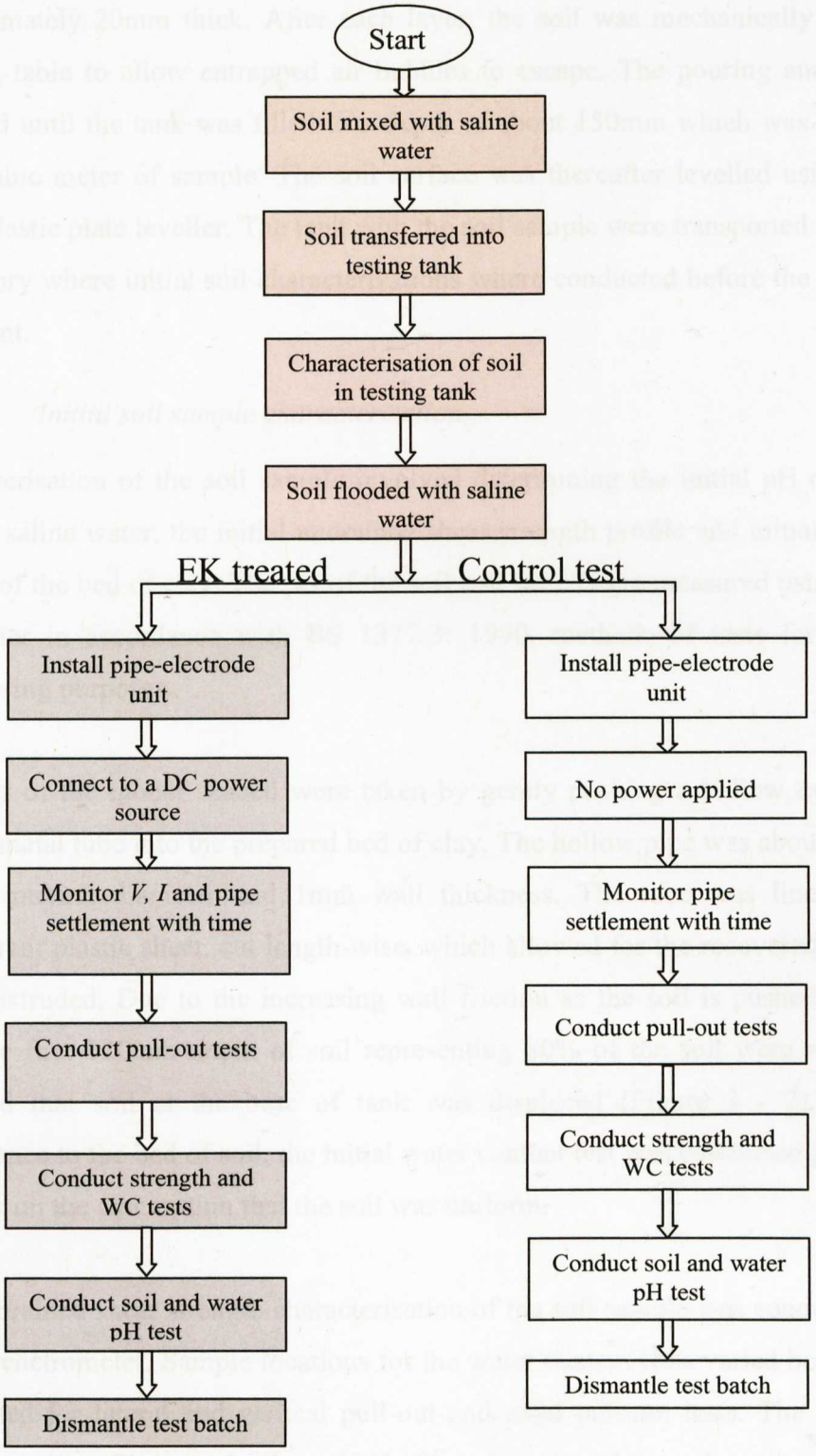

Figure 3 - 6: Flow chart for the small-scale EK test

Mixing the dry kaolin and the saline water was carried out in large batches using an industrial mixer. Homogeneity was assumed when the slurry appeared smooth with no sign of air bubbles. The mixture was then placed into the small test tanks, in small layers

approximately 20mm thick. After each layer, the soil was mechanically vibrated on a shaking table to allow entrapped air bubbles to escape. The pouring and shaking was repeated until the tank was filled to a depth of about 150mm which was approximately 0.013cubic meter of sample. The soil surface was thereafter levelled using a specially made plastic plate leveller. The tank with the soil sample were transported to the research laboratory where initial soil characterizations where conducted before the electro-kinetic treatment.

3.3.2.2 Initial soil sample characterisation

Characterisation of the soil sample involved determining the initial pH of the soil and surface saline water, the initial undrained shear strength profile and initial water content profile of the bed of clay. The pH of the soil and water were measured using a hand-held pH meter in accordance with BS 1377-3: 1990, methods of tests for soil for civil engineering purposes.

Samples of the model seabed were taken by gently pushing a hollow cylindrical thin-walled metal tube into the prepared bed of clay. The hollow pipe was about 350mm long, 20mm internal diameter and 1mm wall thickness. The tube was lined with a thin transparent plastic sheet, cut length-wise, which allowed for the recovered samples to be easily extruded. Due to the increasing wall friction as the soil is pushed into the tube, only the first 120mm depth of soil representing 80% of the soil were recovered. It is assumed that soil at the base of tank was displaced (Figure 3 - 7). To minimise disturbance to the bed of soil, the initial water content test was conducted at the corner of the tank on the assumption that the soil was uniform.

The undrained shear strength characterisation of the soil sample was conducted using the T-bar penetrometer. Sample locations for the water content tests varied between the tests conducted for lateral and vertical pull-out and axial pull-out tests. The locations were chosen to allow for investigation of EK effects based on the configuration of the pipe for each test. Figure 3 - 8 shows the water content sampling location for both vertical and lateral pull-out test while Figure 3 - 9 show sampling location for axial pull-out tests only. When testing using different electrode materials, the sampling location for the undrained shear strength were modified to reflect the observed changes in the soil c_u.

Figure 3 - 10 and Figure 3 - 11 show the modified test locations for aluminium (AL) and iron (FE) electrode respectively. These will be discussed in detail in chapter 4.

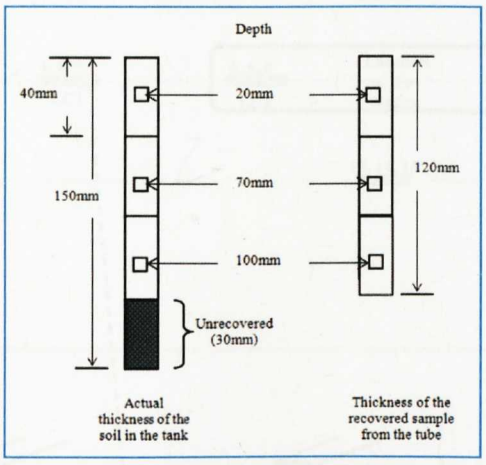

Figure 3 - 7: Recovered sample depth versus actual thickness of soil in the testing tank for the water content tests

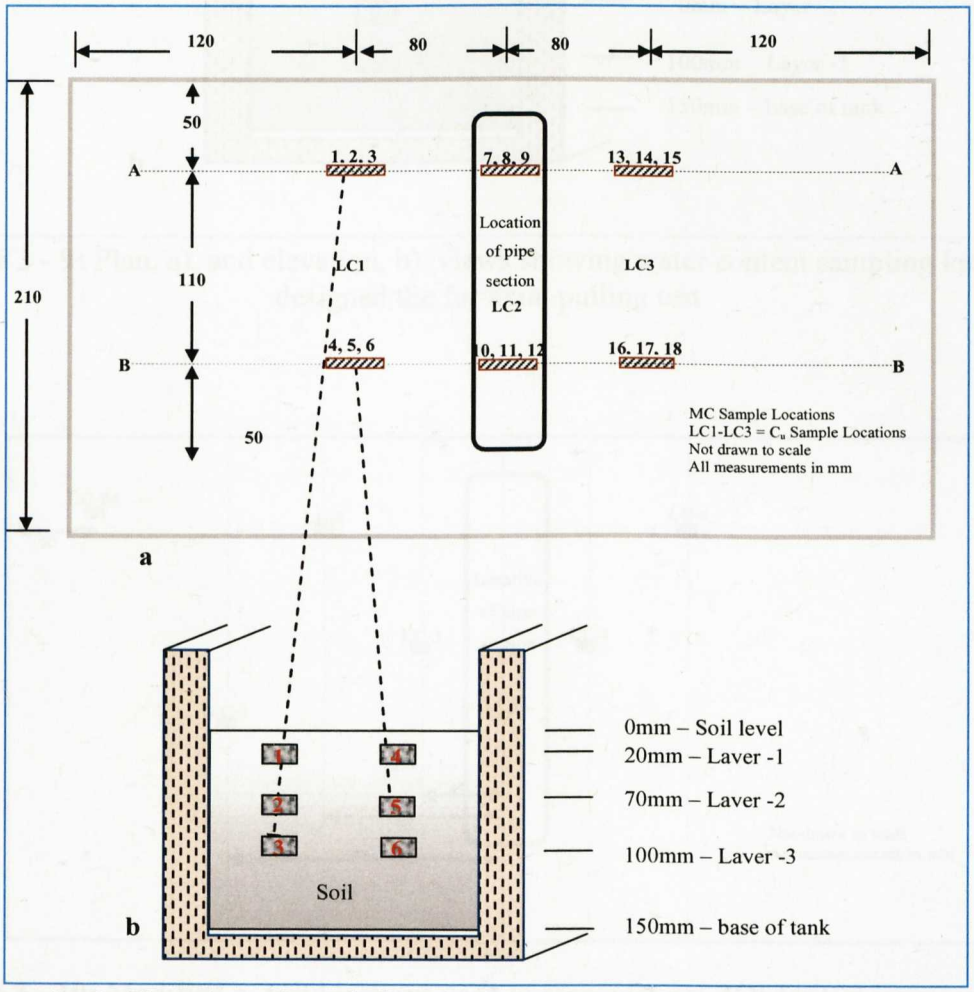

Figure 3 - 8: Plan view, a), and elevation view, b) showing water content sampling locations designed for vertical and lateral pull-out test

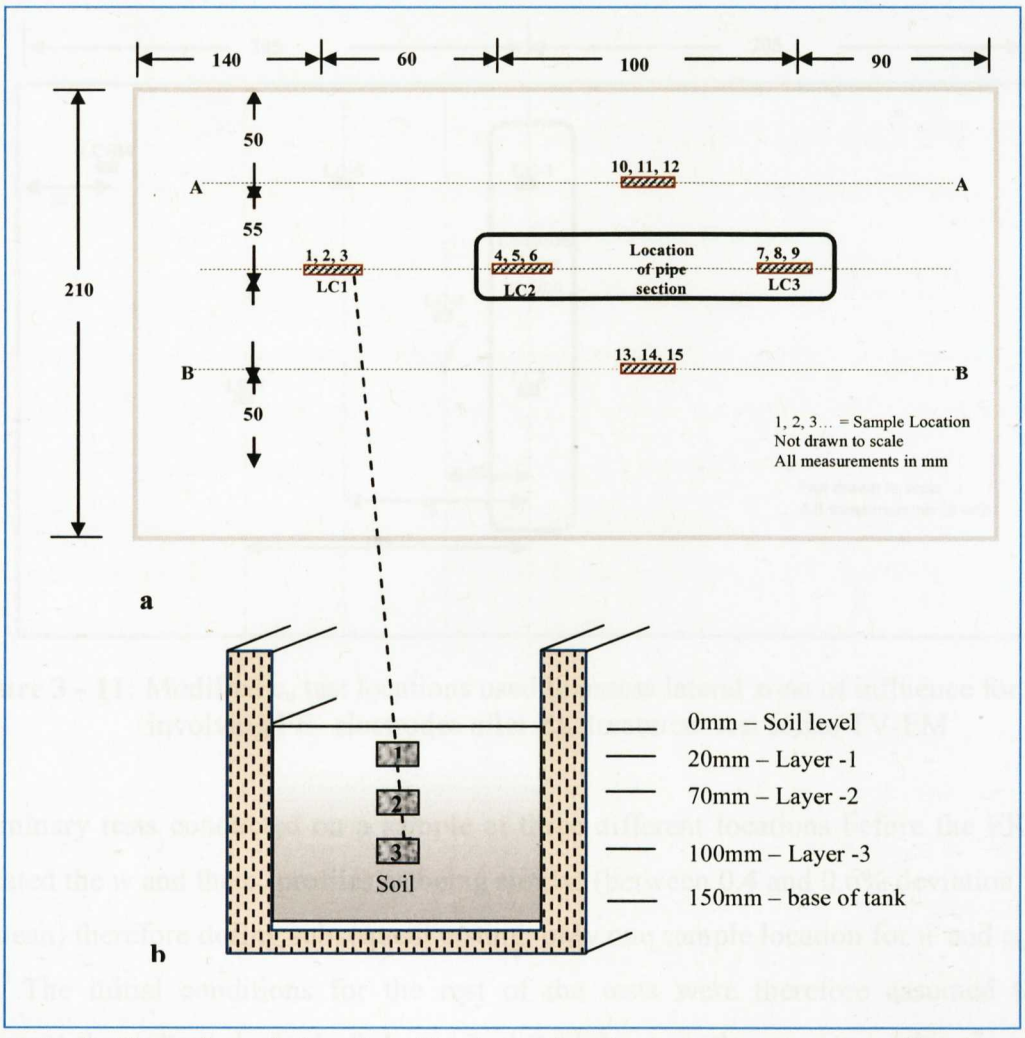

Figure 3 - 9: Plan, a), and elevation, b), views showing water content sampling locations designed the for axial pulling test

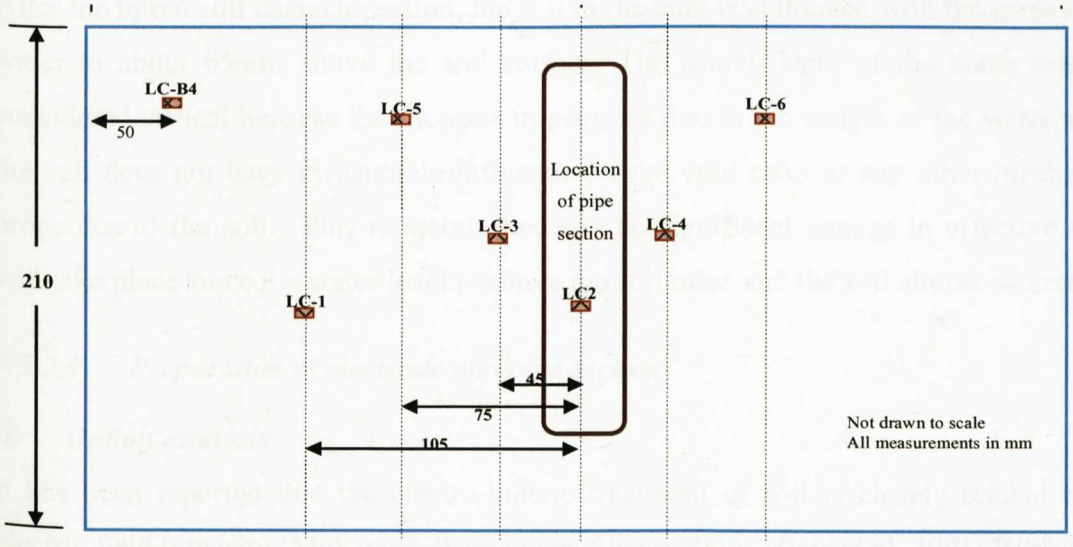

Figure 3 - 10: Modified c_u test locations used to assess lateral ZOI for test involving AL-electrodes after EK treatment test series TV-EM (Sample depths as in Figure 3-9b)

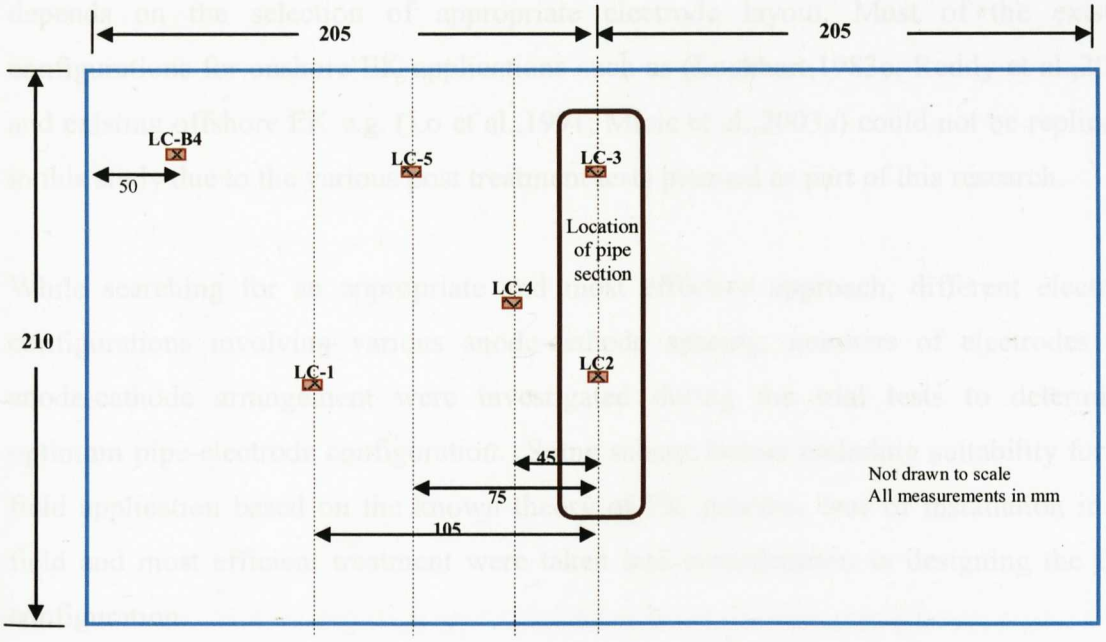

Figure 3 - 11: Modified c_u test locations used to assess lateral zone of influence for test involving FE- electrodes after EK treatment test series TV-EM

Preliminary tests conducted on a sample at three different locations before the EK test indicated the *w* and the c_u profiles as being similar (between 0.4 and 0.6% deviation from the mean) therefore during subsequent testing, only one sample location for *w* and c_u was used. The initial conditions for the rest of the tests were therefore assumed to be consistent throughout the bed of clay in each tank because the same procedure to create the test bed was followed.

After the initial soil characterisation, the soil in the tank was flooded with the same saline water to about 65mm above the soil surface. The actual depth of the water was not considered critical because the increase in pressure due to the weight of the water above the soil does not have measurable influence on the void ratio or any other mechanical properties of the soil. This is mainly because no significant change in effective stress will take place since the water level is above the soil mass and the soil almost saturated.

3.3.2.3 Preparation of electrode and pipe section

(i) Option analysis

It has been reported that the electro-kinetic treatment of soil is closely related to the electric field intensity (Mohamedelhassan and Shang,2000; Micic et al.,2001; Rittirong et al.,2008). This electric field intensity is largely a function of electrode layout. Therefore, the design of efficient electro-kinetic soil treatment suitable for offshore applications

depends on the selection of appropriate electrode layout. Most of the existing configurations for onshore EK applications such as (Lockhart,1983c; Reddy et al.,2006) and existing offshore EK e.g. (Lo et al.,1991; Micic et al.,2003a) could not be replicated in this study due to the various post treatment tests planned as part of this research.

While searching for an appropriate and most effective approach, different electrode configurations involving various anode-cathode spacing, numbers of electrodes and anode-cathode arrangement were investigated during the trial tests to determined optimum pipe-electrode configuration. Some salient factors including suitability for the field application based on the known theory of EK process, ease of installation in the field and most efficient treatment were taken into consideration in designing the final configuration.

The general design consideration was to simulate as close as possible a typical offshore pipeline laid on the sea bed surface and buried under its own weight with the proposed electrodes (for EK soil treatment) surrounding the pipe. Thus, no consolidation pressure was applied prior to the application of the electro-kinetic treatment. Also, only upward vertical drainage was allowed which simulates a consolidating seabed soil due to upward movement of pore fluid.

(ii) Electrode configuration

The layout adopted is shown in Figure 3 - 12a. This arrangement is similar to an existing model used in the industry for cathodic protection with "sacrificial elements" surrounding the pipeline during the treatment. The electrodes (anodes and cathodes) are parallel to each other. It is also thought that this option will allow for easy installation of the electrode during the main pipeline installation.

(iii) Preparation of pipe-electrode assemblage

The electrodes were prepared by cutting the electrode materials (§3.2.3.5) to 150mm length with one end of the electrode being soldered to a 2mm copper wire to ensure good electrical contact. Wire was used to ensure that no unnecessary load was imposed on the electrode/pipe arrangement during subsequent post treatment testing This was achieved by using cable-ties (see Figure 3 - 12) to hold all the wires from the electrodes in place in both the treated and the control samples in order to ensure that the arrangement of the

wires were uniform in all tests.. To prevent direct contact of this connecting point with the aggressive saline environment during testing, it was protected with a clear adhesive lined heat-shrink tubing-9mm bore - 6:1 shrink ratio (Figure 3 - 13). The connection point was still intact even after the EK treatment implying that it was protected against the saline environment.

The required number of electrodes was pushed into the holes in the electrode supporting units which held them firmly in place. Two electrode supporting units were used for each pipe section. All the ends of the wire from the electrodes to be energised as the anodes were joined together and connected to the positive terminal (+) of the DC power source. Similarly, one cable from the cathodes was also connected to the negative (-) terminal of the power source. Finally, the model pipe section described in §3.2.3.4 was pushed through the electrode supporting units and held firmly for the subsequent pipe-electrode assemblage installation (Figure 3 - 12b). To ensure that the pipe would be embedded to the equal depth in all tests, a marker was drawn axially on the pipe as shown the Figure 3 - 12b.

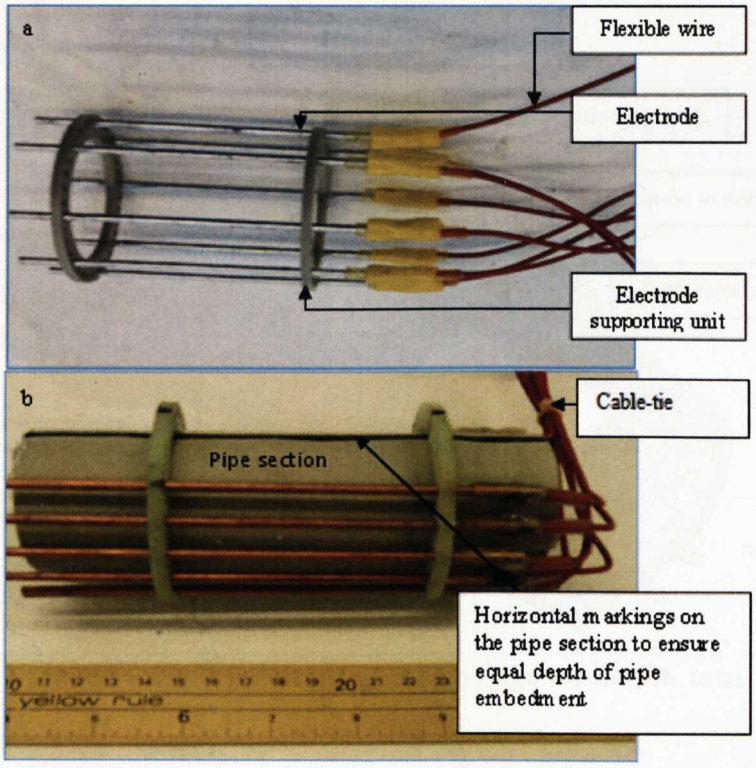

Figure 3 - 12: Pipe and electrode preparation for EK tests: a) electrode in the electrode supporting units, b) complete pipe-electrode assemblage

3.3.2.4 *Pipe-electrode assemblage installation*

The model pipe with the electrodes was inserted into the prepared soil by gently pushing it by hand into the prepared soil to the required depth of burial (30mm chosen for all tests conducted). This was considered the best simulation of actual field pipeline installation. Excavation before placement of the pipe is not applicable to surface-laid pipelines. After the installation, the anode and cathodes were connected to the appropriate terminals of the power source for a predefined voltage to be applied across the electrodes. The applied voltage was kept constant while current was monitored with time during the treatment period. A solid bar was placed on top of the testing tank to support a dial gauge whose tip extended to the middle of the pipe section. The dial gauge was used to monitor the settlement of the pipe section before the EK treatment, referred to here as phase -1, and during the EK treatment referred to here as phase 2. The set up of the EK test in the small tank is shown in Figure 3 - 14.

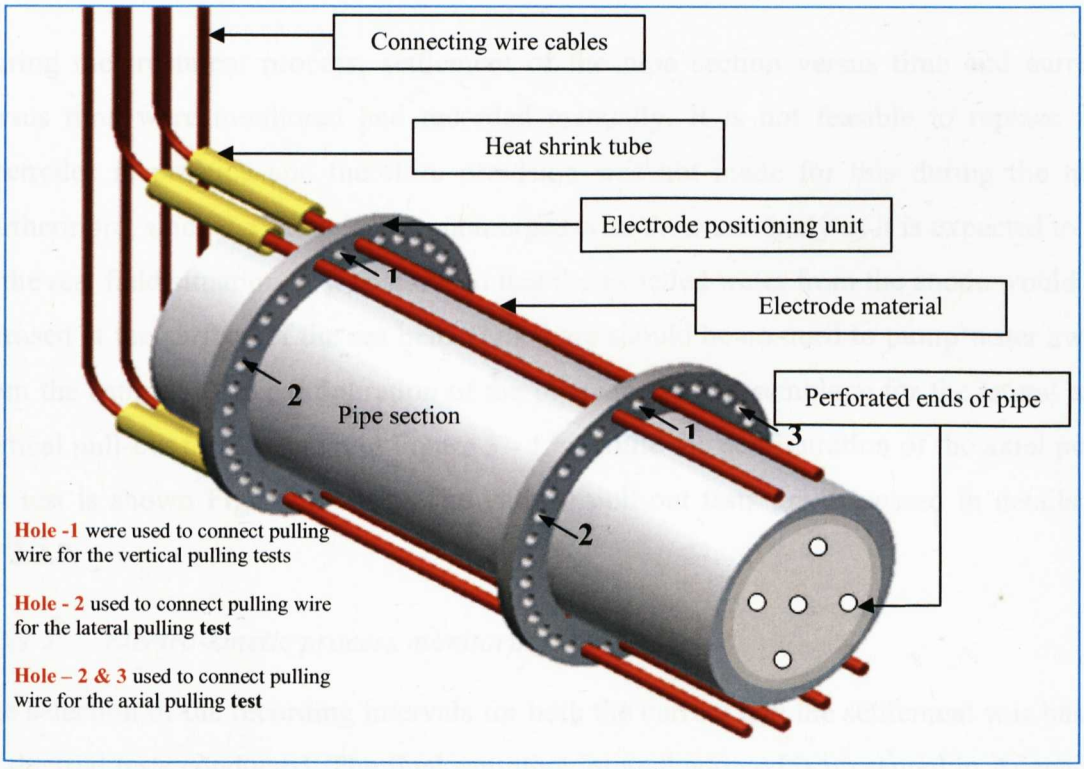

Figure 3 - 13: Pipe-electrode assemblage for the EK tests

After initial pipe installation, about 3 days was allowed for dissipation of excess pore pressure while also monitoring the settlement of the pipe section. This duration was chosen because during the trial test, the primary consolidation appeared complete during

the first three days based on the submerged pipe and soil weight only (.i.e., no external vertical loading).

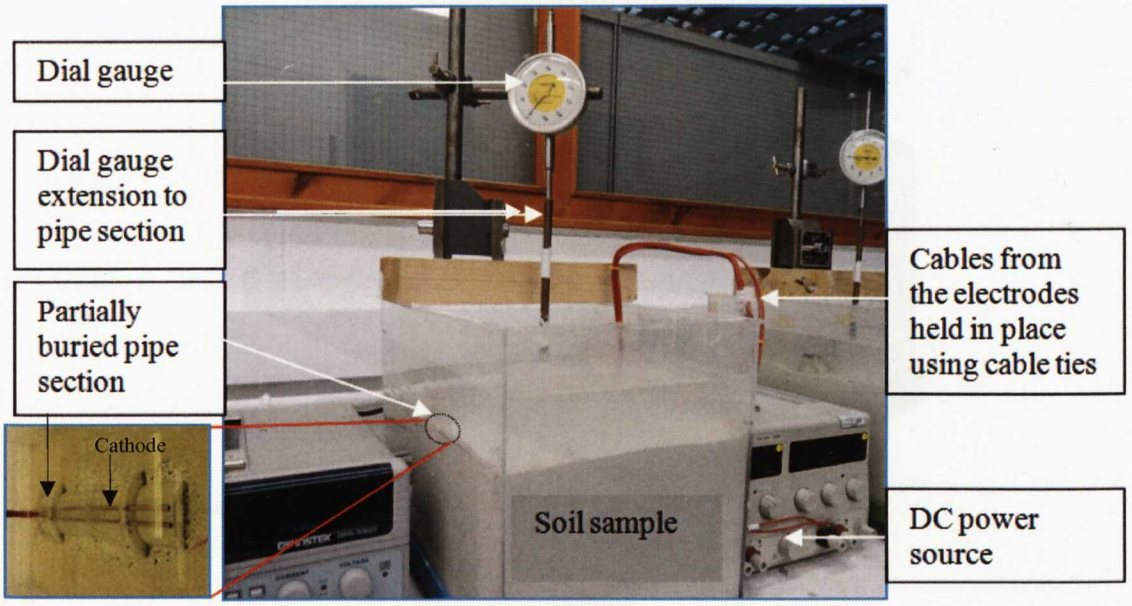

Figure 3 - 14: Test set up of the EK test in the small tank

During the treatment process, settlement of the pipe section versus time and current versus time were monitored and recorded manually. It is not feasible to replace the electrodes in practice and therefore provision was not made for this during the test. Furthermore, since the cathode was submerged with the water body as it is expected to be in the real field situation, it was assumed that the expelled water from the anode would be released at the surface of the sea bed. Thus there should be no need to pump water away from the cathode. The configuration of the pipe-electrode assemblage for the lateral and vertical pull-out test is shown in Figure 3 - 15a while the configuration of the axial pull-out test is shown Figure 3 - 15b. The various pull-out tests are discussed in details in §3.2.2.7.

3.3.2.5 Electro-kinetic process monitoring

The selection of the recording intervals for both the current and the settlement was based on the trial tests conducted. The final sampling interval adopted is presented in Appendix B (sample table for EK monitoring). This interval was used in all tests conducted. The current density, which is the ratio of the current generated to the electrode surface area, in the tests were based on the anode surface as the cathodes were not in contact with the soil.

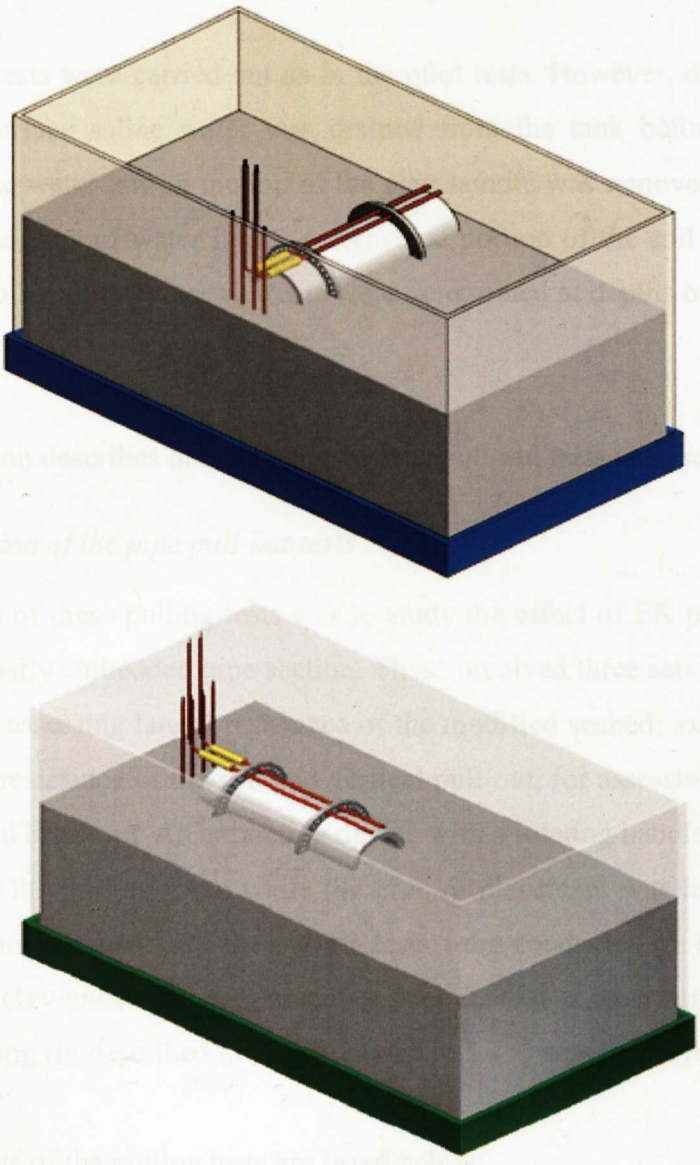

Figure 3 - 15: Pipe-electrode installation: a) lateral and vertical pull-out, b) axial pull-out

3.3.2.6 Post EK tests in the small testing tank

After the EK test, various tests were conducted to investigate the changes in the physical, mechanical and chemical properties of the soil sample. This was done with a view to assessing the effectiveness of the EK treatment on the tested soil. These tests were conducted in the order listed below.

- Measurement of pH of surface water
- Pull out tests
- The measurement of the undrained shear strength

- Determination of the soil water content
- Measurement of pH of soil samples at predefined depths

The pH, w and c_u tests were carried out as in the pilot tests. However, during the water content test, the surface saline water was drained from the tank before the test was carried out. The free water left on the top of the clay sample was removed using a paper towel to prevent the flow of water into the excavated portion of the soil where the pipe section had been pulled out. Water contents were determined at depths of 20mm, 70mm and 100mm.

The following section describes in details the various pull-out tests conducted.

3.3.2.7 Description of the pipe pull-out tests

The main objective of these pulling tests was to study the effect of EK processes on the stability of the partially embedded pipe section. These involved three sets of tests namely lateral pull-out, for assessing lateral resistance of the modified seabed; axial pull-out, for assessing the axial resistance of the soil and vertical pull-out, for assessing the resistance of the soil to vertical breakout. An extracting device with a rotating handle connected to a load cell measured the pulling force while the pipe displacement was measured with a draw wire displacement sensor. All the pulling tests were conducted on both the treated clay and untreated clay under identical conditions for ease of comparison. The specially designed small testing rig described in §3.3.1.7 (Figure 3 - 5) was employed in the tests.

Some critical aspects of the pulling tests are listed below:

- ❖ The depth of the embedment of the pipe section

  Consistency of this was maintained by making horizontal markings on the side of the pipe section and the electrode supporting unit (Figure 3 - 12). This ensured that in all the tests, including the control tests, the pipes were embedded to the same level below the mud line. The embedment depth for the model pipe section was 30mm (0.6D). This is slightly deeper than the typical depth of initial embedment of pipeline in soft offshore clay - about 0.45 diameters (Dingle et al.,2008). Nevertheless, it is considered adequate for this preliminary study.

- ❖ The flexibility of the pulling wire cable used must not affect the pulling mechanism

In order to ensure that the connections of the wire to the pipe and electrode imposed similar loads for similar pulling tests, the connecting wires were of uniform dimensions and tied together using cable-ties which ensured no variable loading was imposed on the embedded pipe section (please refer to Figure 3 - 14). In addition, the attached wires were securely attached to the sides of the tanks to reduce disturbance to the pipe and electrodes during connections to power source and subsequent post testing after the EK treatment.

- ❖ The weight of the pipe plus the electrodes must be uniform or a correction made for any differences in weight.
- ❖ The coupling of the cable to the pipe was a critical aspect of the testing programme as any irregularity will significantly distort the result of the entire test.
- ❖ The pulling rate: To ensure consistency in results, all the pulling tests were conducted at a pulling rate of 0.1mm per second.

The pulling resistance and the horizontal/vertical displacements were automatically recorded by a load cell and a draw wire displacement transducer respectively. Undrained shear strength tests and water content tests were conducted immediately after the pulling tests to assess the soil conditions. The changes in the pull-out force and the soil shear strength, compared with the control tests, were used to evaluate the effects of the EC treatment. Details of the three pull-out tests are described below.

(a) Vertical pull-out test

Figure 3 - 16 shows the schematic representation of the pull-out mechanism adopted for the vertical pull-out tests in this study. Referring to the Figure 3 - 16, a flexible steel wire [1] was made to go through the top holes of the two electrode supporting units as indicated in Figure 3 - 13. The flexible wire was then connected to a load cell [2] whose other end was connected to the travelling block [3]. The tip of the draw wire [4] was connected to the travelling block which was free to travel up or down the support stand [5] depending on the direction of rotation of the rotating handle [6]. The vertical movement of the buried pipe and the pull-out force were captured automatically using the data logger connected to the draw wire sensor [7]. At the end of the pulling test, the pull-

out force was plotted against the vertical displacement where the yield point was identified and compared with the control test in order to assess the effects of the EK treatment. The schematic of the small-scale pullout rig is shown in Figure 3 - 5 and could assist in understanding the layout of the pipe pullout.

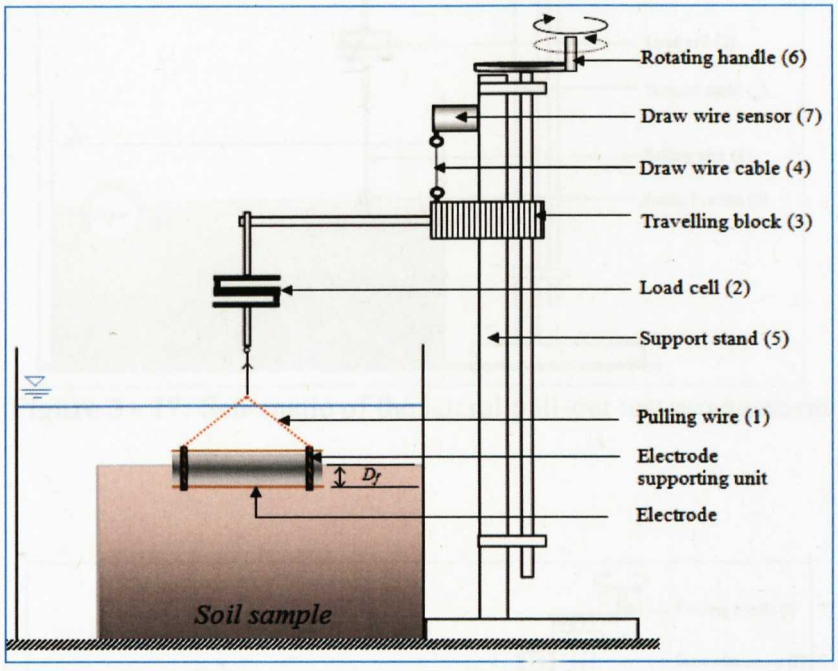

Figure 3 - 16: Schematic of the vertical pull-out test arrangement

(b) Lateral pull-out test

During the lateral pull-out tests, the flexible steel wire was made to go through hole-2 as indicated in Figure 3 - 13. The methodology for the lateral pulling test was similar to the vertical pull-out except the pipe was connected 90 degrees to the connecting points of the vertical test (Figure 3 - 17). The flexible wire was made to go round the bearing which was attached to the adjustable bearing stand (please refer to Figure 3 - 5). The wire was then connected to the load cell unit. The measurement and recording of the pulling force and the lateral movement of the buried pipe section were similar to the vertical pull-out test described above.

(c) Axial pull-out test

During the axial pull-out test, the pulling wire was connected to hole-2 and hole-3 as shown in Figure 3 - 13 before being made to passed through the bearing as shown in Figure 3 - 18. The pulling mechanism were similar to the lateral pulling tests

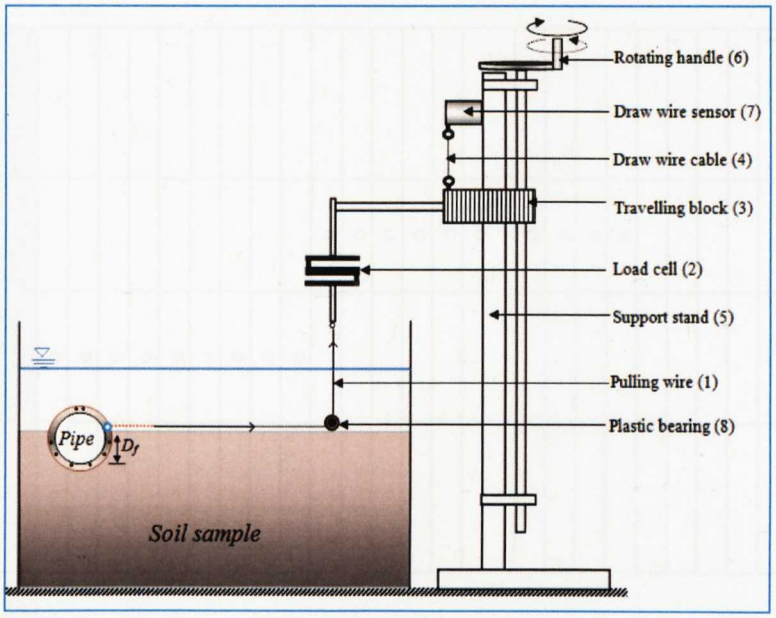

Figure 3 - 17: Schematic of the lateral pull-out test arrangement

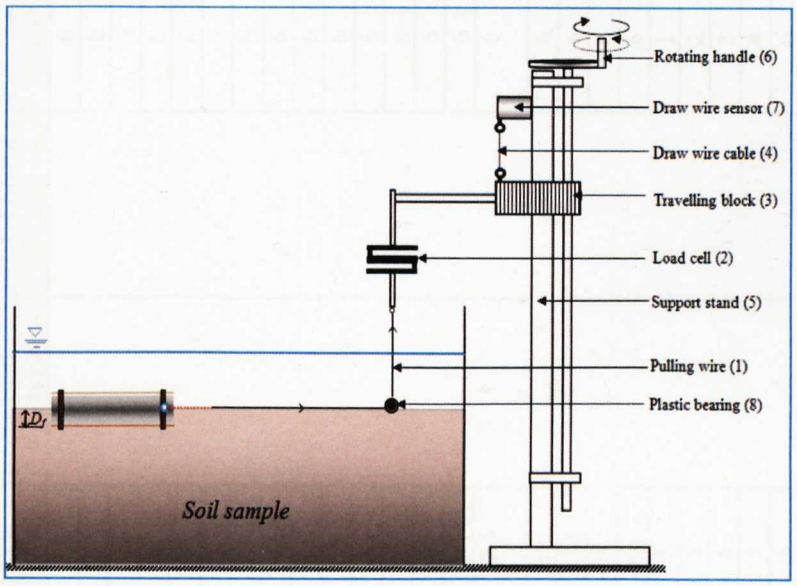

Figure 3 - 18: Schematic of the axial pull-out test arrangement

3.3.3 Summary of test conducted for the EK treatment of soil

Table 3 - 2 is a summary of tests conducted in the small testing tank

Table 3 - 2: Summary of test conducted in the small-scale tank

Test #	Test series	Purpose of test	Applied voltage (V)	Initial moisture content (%)	Electrode materials (CU/FE/AL)	number of anodes	Test duration (hrs)	Coated Pipe	Pulling test conducted		
									Vertical	Axial	Lateral
1	1 (TV-VP)	To investigate influence of voltage on vertical soil resistance	2.5	70	CU	6	end*		o		
2			5			6			o		
3			7.5			6			o		
4			no			6			o		
5			10			6			o		
6			12.5			6			o		
7			15			6			o		
8			17.5			6			o		
9			no			6			o		
10	2 (TV-AP)	To investigate influence of voltage on axial soil resistance	2.5			6				o	
11			5			6				o	
12			7.5			6				o	
13			10			6				o	
14			no			6				o	
15			12.5			6				o	
16	3 (TE-A)	To investigate the influence of number of anodes/ electric field	15			6				o	
17			17.5			6				o	
18			20			6				o	
19			no			6				o	
20			5			1					
21			5			2					
22			5			3					
23			5			4					
24			5			6					
25			10			1					
26			10			2					
27			10			3					
28			10			4					
29			10			6					

Table 3 - 2 – *continued*

Test #	Test series	Purpose of test	Applied voltage (V)	Initial moisture content (%)	Electrode materials (CU/FE/AL)	number of anodes	Test duration (hrs)	Coated Pipe	Pulling test conducted		
									Vertical	Axial	Lateral
30	4 (TE-EM)	To investigate electrode materials on vertical resistance	7.5	70	AL	6	end		o		
31			7.5	70	CU	6	end		o		
32			7.5	70	FE	6	end		o		
33			NO	70	CU	6	end		o		
34			10	70	AL	6	end		o		
35			10	70	CU	6	end		o		
36			10	70	FE	6	end		o		
37			7.5	70	AL	6	end		o		
38			NO	70	CU	6	end		o		
39			10	70	AL	6	end			o	
40			10	70	CU	6	end			o	
41			10	70	FE	6	end			o	
42			NO	70	CU	6	end			o	
43			2.5	70	AL	6	end			o	
44	5 (TV-DT)	To investigate duration of treatment and lateral resistance	10	70	AL	6	12HRS			o	
45			10	70	CU	6	12HRS			o	
46			10	70	FE	6	12HRS			o	
47			no	70	none	6	12HRS			o	
48			2.5	70	AL	6	12HRS			o	
49			2.5	70	AL	6	6HRS				o
50			2.5	70	FE	6	6HRS				o
51			10	70	AL	6	6HRS				o
52			10	70	FE	6	6HRS				o
53			NO	70	FE	6	6HRS				o
54			10	70	FE	6	12 hrs				o

Table 3 - 2 - *continued*

Test #	Test series	Purpose of test	Applied voltage (V)	Initial moisture content (%)	Electrode materials (CU/FE/AL)	number of anodes	Test duration (hrs)	Coated Pipe	Pulling test conducted		
									Vertical	Axial	Lateral
55	5 (TV-DT)	To investigate duration of treatment and lateral resistance	2.5	70	FE	6	end				o
56			2.5	70	FE	6	12HRS				o
57			10	70	FE	6	end	o			o
58			15	70	FE	6	end				o
59	6 (TWC)	To investigate the influence of initial moisture content	10	90	FE	6	end				
60			10	120	AL	6	end				
61			10	90	FE	6	end				
62			10	120	AL	6	end				
63			no	70	no	no	end				

"end" implies test allowed to come to end of electrode life

3.4 Large-scale experiment description

The greatest challenge with modelling and designing for pipeline stability is the uncertainty relating to pipe-soil interactions especially during the large-amplitude of pipe movements associated with pipeline buckling (Bruton et al.,2008). This uncertainty calls for a further understanding of the nature of soil deformation in association with large-cycle displacement of offshore subsea pipelines, especially the development of the berm of soil as the pipe moves. In order to address the above issues, a series of pipe-soil interaction tests were conducted aimed at studying the resistances offered by soil to a partially embedded pipeline. Emphasis was placed on the formation, growth and influence of the berm of soil formed during pipe motion. The details of the research materials and apparatus are presented below.

The general philosophy behind the pipe-soil interaction tests was to model as closely as possible in two dimensions the behaviour of a partially embedded pipeline on the seabed and subsequent movement of the pipeline during lateral buckling and axial walking including the resistances that the soil could offer to restrict the pipe movements as discussed in §3.2. To study this phenomenon, a model seabed was prepared in a large testing tank. The dimensions of the tank and the pipe section were carefully selected to minimize edge and end effects during the pipe various motions and to ensure that the deformation of the soil is investigated under plane strain test conditions.

In order to model pipe behaviour in two dimensions it is necessary to consider possible end effects. In axial movement of the pipe there will obviously be end resistance (at both ends). This was however taken into consideration during the design of the length of the tank. In vertical and lateral movement tests, there will be end effects, but assuming that the embedded section is subjected to a resistance equal to c_u then the end component will be:

$$Ends = 2\,x\left(\pi R^2 x\frac{\omega}{360} - 2x\left(\frac{(R-z)\,x\,R\sin\omega}{2}\right)\right)c_u \qquad 3-1a$$

$$\omega = 2cos^{-1}\left(\frac{R-z}{R}\right) \qquad 3-1b$$

$$Shaft = 2\pi R\frac{\omega}{360}xL\;x\;c_u \qquad 3-1c$$

Where L is the length of the pipe section, z is the depth of pipe embedment, R is the radius of the pipe and ω is the angle relating to the extent of the pipe-soil contact surface or depth of penetration of the pipe.

Therefore for typical pipe dimensions the percentage contributions of the ends will be minimal in relation to the total. The contribution will be similar for test with similar geometry but obviously will need to be considered if applying the results to other tests. There will be other end effects, for example soil flowing around the ends of the pipe, or affecting the ends if any build up of material occurs when the pipe is moving which is difficult to quantify but is felt not to be of major importance if the length of the pipe is large compared to the depth of embedment.

The movement of the pipe section was provided by a specially built rig (loading trolley) which was designed to provide a cyclic movement (sweeping) of the attached pipe using an actuator system. The main actuator which was coupled to the top of the tank consists of a 2.5m long belt driven linear guide controlled by a stepper motor and capable of providing variable pipe speeds. The force-displacement responses during the pipe-soil interaction tests were studied using instrumentation which is explained in detail in the following sections.

3.4.1 The large-scale laboratory testing tank

Referring to Figure 3 - 19a, a large-scale testing tank used in this study was approximately 2m long, 0.9m wide and 0.9m deep. The base and walls of the tank were made of 20mm clear perspex acrylic sheets [1]. Apart from being watertight and non-conductive during the large-scale EK tests, the clear perspex sheets render the tank walls transparent during pipe motions and therefore helped in the study of the soil deformations. Furthermore, to ensure that the tank can withstand the lateral earth pressure exerted by the soil, 50 x 50mm mild steel box sections [2] were employed to reinforce the outer walls of the tank. At the top levels of the two sides of tank, 5mm thick metal plates [3] were welded to the reinforced frame to be used to support the actuator and the stepper motor units.

In order to ensure drainage at the top and base of the tank during the clay consolidation, a 100mm thick gravel layer [4] was placed in the tank before placing the clay sample. The

gravel was covered by a sheet of geotextile [5] material which prevented mixing of the clay sample with the underlying gravel layer. The thickness of the bed of clay was approximately 450mm in all tests conducted.

3.4.2 Soil material used in the tests

Pure E-grade kaolin clay was used as the seabed material. The choice of the kaolin clay over other clay materials, the nature, composition as well as sample preparation are as discussed in §3.2.2.1. The initial plan was to also conduct tests using typical offshore soils. However, this was not possible due to the difficulty in obtaining offshore clay soils; hence only kaolin clay was used in all the tests. All the samples for the large-scale tests were mixed at 70 percent water content. Although the 70% water content does not in theory guarantee 100% saturation of the sample (that is less than 1.4LL) as already stated in §3.2.3.1, it was assumed appropriate for the investigations since in actual field conditions, ocean seabed soils are not normally fully saturated.

3.4.3 Seabed preparation

The preparation of the model seabed was carried out by placing the soil in layers. The first model seabed soil was prepared by pouring the saline kaolin clay into the tank in layers of about 100mm until the tank was filled up to the required 450mm thickness from the top of the geotextile layer. In each of the layers, the surface of the soil was levelled using a specially prepared plate before the next layer was placed. This was done in order to minimise the amount of entrapped air during pouring. Thereafter, the whole soil in the tank was thoroughly mixed again using a universal stirring mixing tool coupled to a hand held drill (Figure 3 - 19b). The blade of this mixer was designed to generate mixing effect from bottom to top of the tank which was necessary to ensure that the entrapped air was released during mixing. After mixing, the model seabed was flooded with saline water (Figure 3 - 19c).

Each of the tests series was conducted in a freshly re-consolidated bed. After the first bed of clay was used, subsequent tests commenced with pumping out the surface water using a submersible water pump and remixing the soil using the mixer mentioned above. After each consolidation, the model seabed was characterised again in terms of the soil undrained shear strength and water content. After carrying out a pipe settlement analysis

given the size and submerged weight of the model pipe section, the depth of influence of the pipe was assessed to be within approximately 300mm.

During the first test series, the soil was mixed and allowed to consolidate under its own weight for 10 and 15 days before a test commenced. However, a site investigation on the soil to investigate the effect of consolidation duration using T-bar penetrometer tests on the reconstituted soil at 3, 7 and 10 days before the test showed no significant difference in the shear strength. Hence, subsequent tests were carried out at after only three days consolidation. In all a total of 29 beds of consolidated soil were prepared comprising 19 beds for the lateral pipe-soil interaction tests, 6 beds for the axial pipe-soil interaction tests and 4 beds for the large-scale EK tests.

3.4.4 Seabed characterisation

The selection of the appropriate undrained shear strength poses considerable challenge to the pipeline design. This is because of the soft nature of the top 1m of the seabed. Although a number of devices are used to measure the soil strength, the T-bar is the most current and appears to be most effective and was therefore employed in this study.

After each model seabed was prepared, a simple site investigation was conducted across the model soil bed. This included the characterisation of the horizontal and vertical variations in undrained shear strength of the model seabed using a T-bar penetrometer as well as determination of soil water content profiles across the seabed. The specification of the T-bar is described in §3.2.2.3. The setup for the T-bar test in the large tank is shown in Figure 3 - 20 (the schematic of the setup is as shown in Figure 3 - 3) while the sampling locations for the T-bar and the hand shear vane tests are shown in Figure 3 - 21. In addition, a hand shear vane was also use to measure the soil shear strength for purpose of comparisons only. This was the conventional Pilcon type with a 33mm diameter and a 50mm long rotating blade.

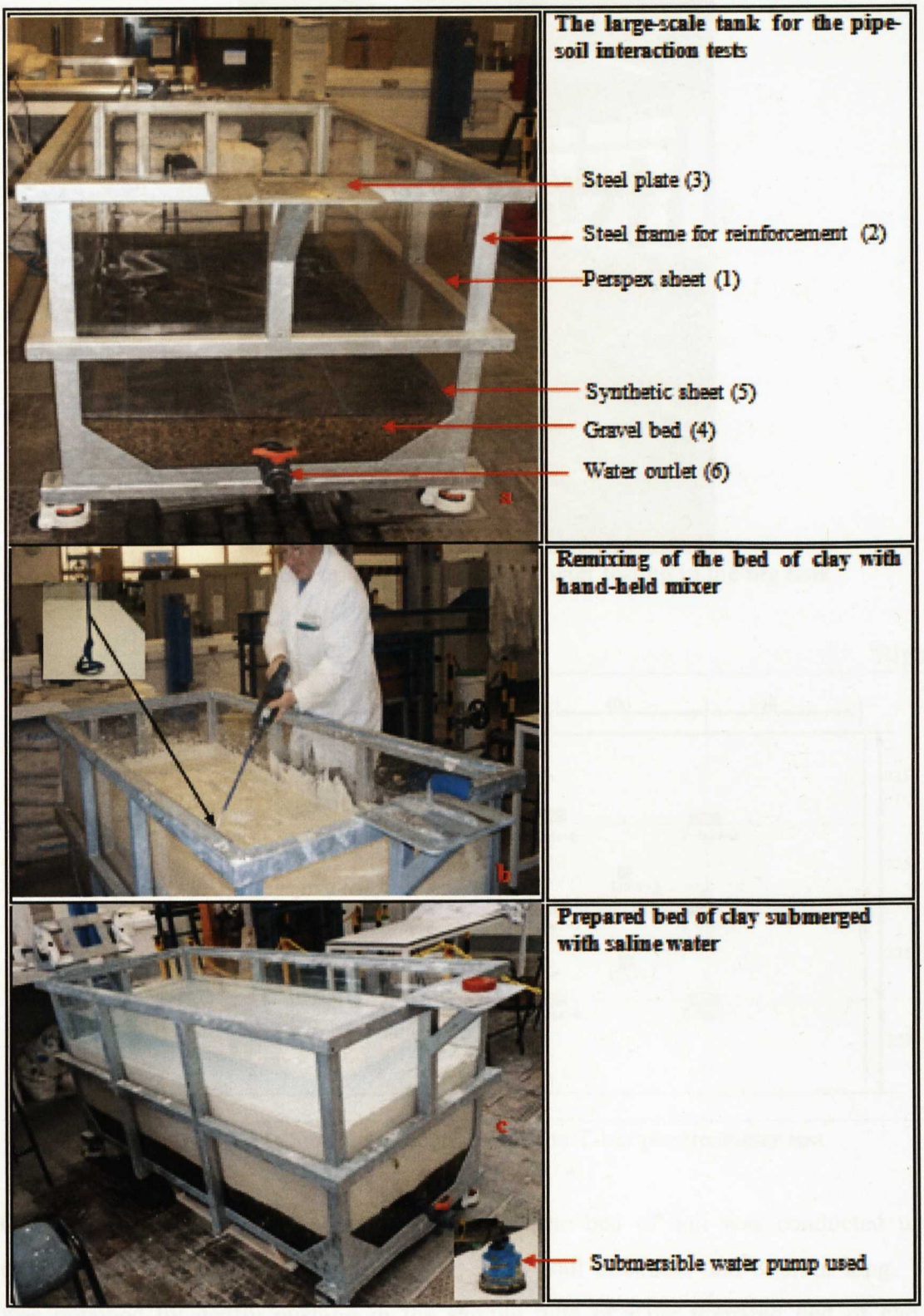

Figure 3 - 19: Equipment for the large-scale pipe-soil interaction test

Figure 3 - 20: Set up for T-bar penetrometer testing in the big tank

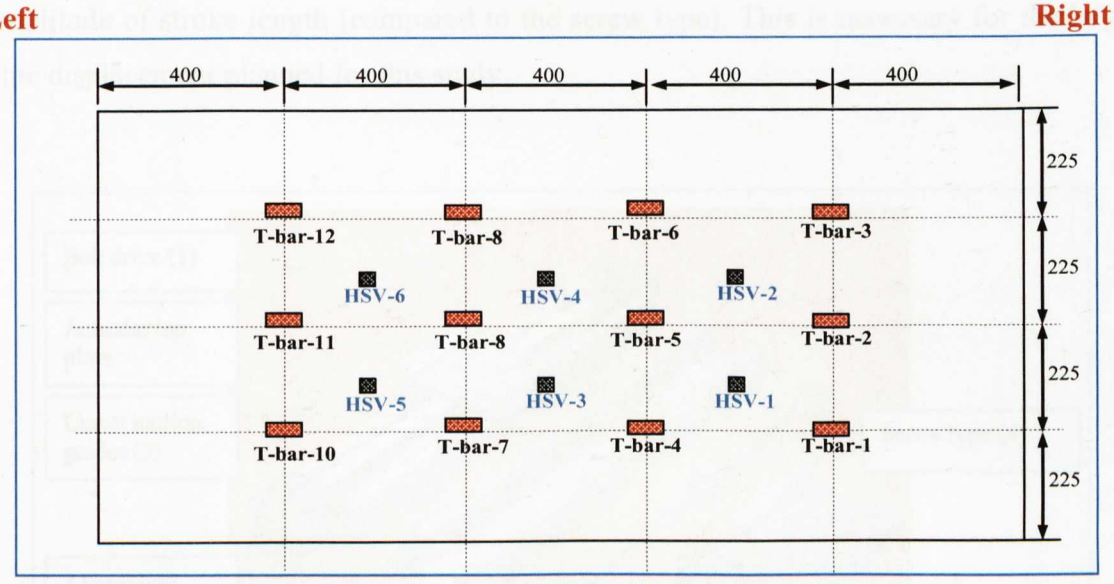

Figure 3 - 21: Sampling locations for the T-bar penetrometer test

Characterisation of the initial water content of the bed of soil was conducted using transparent plastic tubing 25mm diameter, 3mm wall thickness and 850mm long. This was obtained by gently pushing in the sample tube into the prepared bed of clay at predetermined locations. During the withdrawal of the tube, the top end of the tube was covered (to render it airtight) and to increase suction and enhance the recovery of the continuous samples. The recovered samples were analysed for water content in accordance with BS1377: 1990: Part 2. This gave an indication of the vertical and horizontal variation of water content across the model sea bed. Five water content

locations were chosen to cover the whole tank. These were located adjacent to five T-bar test locations namely LC1, LC3, LC5, LC10, and LC12 (see refer to Figure 3 - 21).

3.4.5 The actuator and the trolley pulling system

The horizontal pulling force on the model pipe section was provided by a linear motion actuator system which was attached to a loading trolley designed and built as part of this study. Components of the trolley are shown in Figure 3 - 23. The main actuator, which is a GL20-250-T4F-L-EF-C-ASSY model (Figure 3 - 22), was supplied by THK Industries Japan. It was coated with THK AP-CF layer (black chrome plating) to withstand the harsh saline environment. The actuator consists of a 2.5m long single axis actuator that allows a belt drive [1] to be integrated with an aluminium base [2] on which four units of linear motion guide [3] are mounted. The belt driven type [1] was selected because of its high rigidity as well as not being subject to restriction by high speed as opposed to ball screw type [4]. The belt type also has more rigidity and flexibility to support longer amplitude of stroke length (compared to the screw type). This is necessary for the large pipe displacement planned for this study.

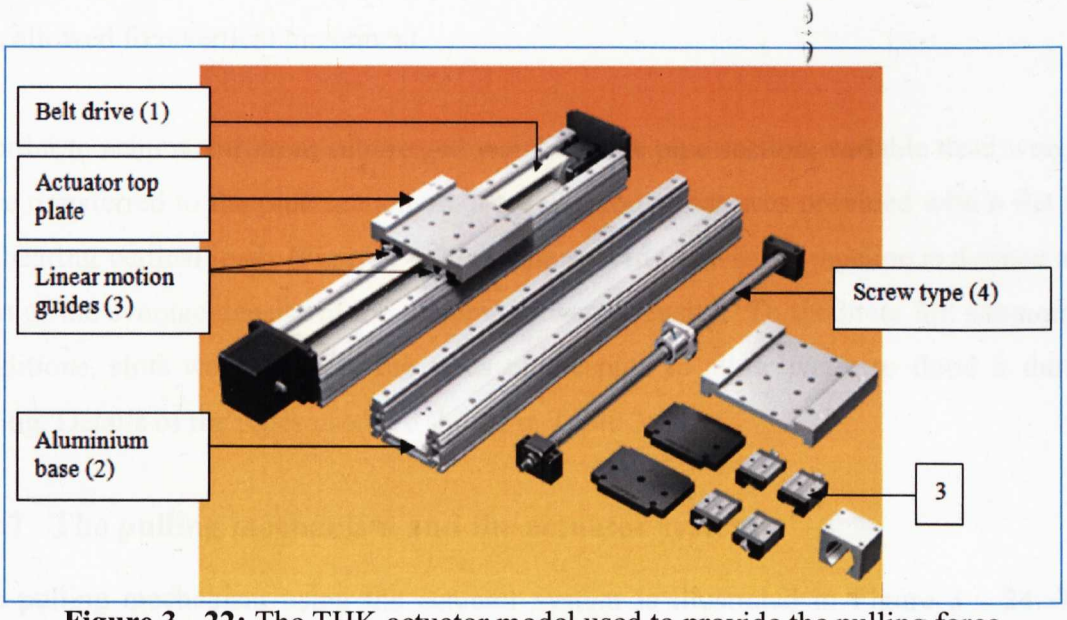

Figure 3 - 22: The THK actuator model used to provide the pulling force

The main loading trolley was made of 50x50x3mm aluminium box sections (Figure 3 - 23a), the top of which was machined to carry the actuator during pipe motion. At the two sides of the trolley there were the vertical ball splines (Figure 3 - 23c) which were designed to hold the pipe section in place (Figure 3 - 23d). The ball spline allowed free vertical motion of the pipe section but prevented rotation of the pipe section in order to

mimic the actual field motion of a typical offshore pipeline. The static permissible moment for the ball spline was given by the manufacturer as 60Nm which was in excess of the 34Nm calculated for this study. Therefore the bearing within the nut of the ball spline was believed to be able to withstand the resistance provided by the soil during pipe motion.

3.4.6 The model pipe sections

A model pipe 800mm long (Figure 3 - 26b), 130mm outer diameter, 2mm wall thickness and made from stainless steel was made to simulate an offshore pipeline. In addition, another 300mm long 130mm pipe section (Figure 3 - 26c) made of the same material was fabricated to allow for the determination of the axial resistance offered by the soil only. Details of how the axial friction was obtained will be discussed later.

The model pipe section which hangs from a loading carriage was designed to allow for the pipe's lateral and axial motion in a cyclic pattern across the surface of the model seabed using a system of actuators (Figure 3 - 26a). The ball spline ensured that that the pipe did not rotate. Thus the pipe was prevented from rolling in the horizontal plane but was allowed free vertical movement.

In order to achieve different submerged weight of the pipe section, variable dead weights were transferred to the pipe section via a loading rod which was provided with a flat top for bearing vertical loads (Figure 3 - 27a). The specific gravity of pipeline is defined as a ratio of the average density of the pipeline to water density. To facilitate full submerged conditions, slots were made at the sides of the pipe to allow water to flood it during testing. Details of the pipes used are shown in Table 3 - 3.

3.4.7 The pulling mechanism and the actuator system

The pulling mechanism using the actuator system is illustrated in Figure 3 - 24. The pulling motion which simulates the horizontal pipe displacement was provided and controlled by a stepper motor [1] attached to the pulley shaft located at the head of the linear motion actuator unit (LM) [2]. The stepper used was an MDrive34Plus integrated motor plus driver (supplied by Zapp Automation UK Ltd) with capability of about 20 micro-step resolutions up to 51,200 steps per revolution (~ ±5,000,000 steps/sec).

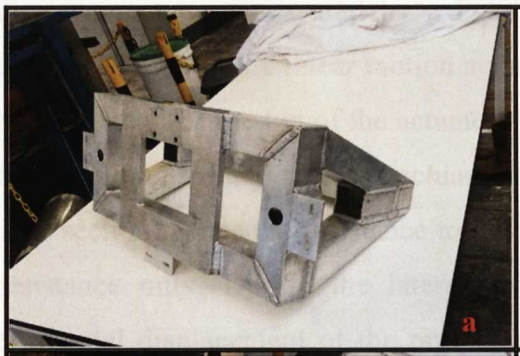	**The trolley frame**
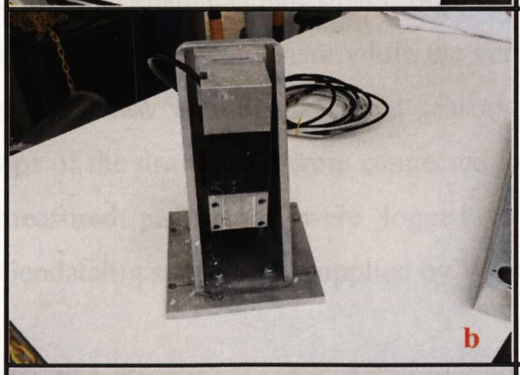	**The load cell unit inside the supporting unit**
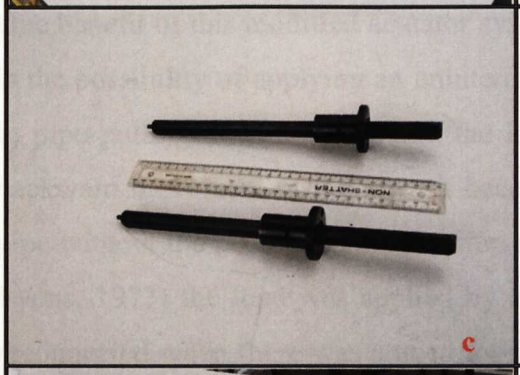	**The two ball spline used to transfer load from trolley to pipe section**
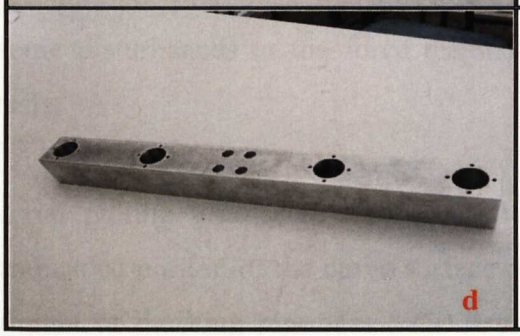	**Cross-bar used to keep the ball spline in place during the 300mm and 800mm pipe tests**

Figure 3 - 23: Parts of the trolley for the large-scale pipe-soil interaction test (a-d)

It could therefore be programmed to variable speeds as low as 0.001mm/s and therefore replaces the use of a cumbersome gear box system. Therefore, it was suitable to give the required pipe displacement of between 0.05mm/s and 24mm/s which covers the range of typical offshore speed of pipeline during pipeline buckling.

The horizontal pulling force which gives an indication of the soil resistance to the pipe displacement was measured by a PC60 load cell [3]. The load cell was designed to connect the top of the linear motion actuator [4] to the trolley unit [5] without the base of the load cell and the top of the actuator touching each other. This ensured that the pulling force was transmitted from the actuator via the load cell to the trolley (which supports the pipe section). Thus the resistance to the pulling force was considered to be from the soil resistance only. During the lateral and axial displacement of the pipe section, the horizontal displacement of the pipe was measured with a 200mm stroke Posichron [6] linear displacement sensor while the vertical displacement of the pipe was measured by a pair of draw wire displacement sensors [7] attached to the two sides of the trolley. The tips of the draw wires were connected to the pipe section as shown in Figure 3 - 26. The measured parameters were logged to the computer using a 30- WF6032 model, Geodatalog series 6000 supplied by Wykeham Ferrannce Soil Mechanic Technologies.

One benefit of this modified actuator system and the nature of the pipe-trolley connection is the possibility of applying an uninterrupted lateral and axial loading during the change in pipe pulling direction. Because the LM actuator system can maintain a forward and backward movement of the pipe, it becomes easier to apply the cyclic movement of the pipe without the need for disconnection during change of direction. In some studies, (e.g. Lyons, 1973) the load was applied by a pulling arm which had to be disconnected and reconnected when there was a need for change of pipe pulling direction. This introduced some disturbances to the force displacement response during the pipe-soil interaction tests.

Axial pulling tests were also conducted to assess the frictional force acting on the embedded portion of the curve surface of the pipe. During the axial tests, the submerged weight of the long pipe was 87N. It was anticipated that additional passive resistance acting at the end of pipe during pulling will affect the determination of the actual frictional force measured. In order to make sure that the frictional resistance is due only to the pipe-soil contact (less the passive resistance at the end of the pipe), the submerged weight of the short pipe (300mm long) was increased to 33N by adding additional 3N vertical load. This ensured that the same contact pressure as in the long section (800mm long) was applied to the soil from the two pipes. The determination of the actual friction force from the soil is illustrated schematically in Figure 3 - 25.

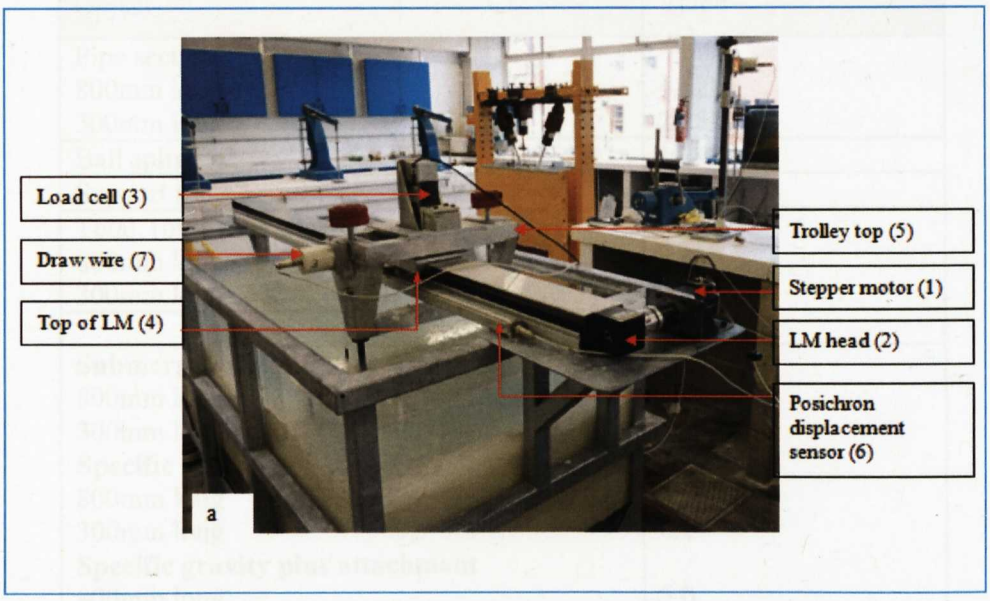

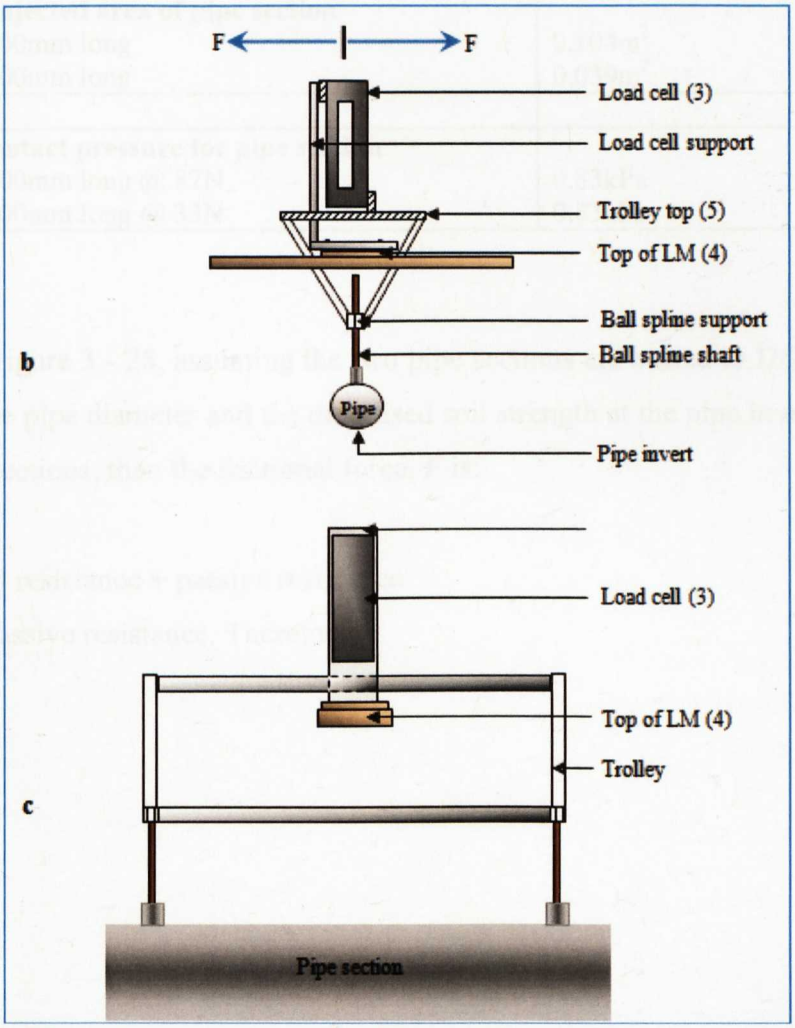

Figure 3 - 24: The actuator system and pulling mechanism during pipe-soil interaction, a): Test set up, b): cross-section, c): front view

Table 3 - 3: Weight of pipe section and attached elements

Object	Value
Pipe section 800mm long 300mm long	 4.62kg 2.28kg
Ball spline x2	1.34kg
Support rod x2	0.43kg
Total (pipe plus attachments) 800mm long 300mm long	 6.4kg 4.1kg
Submerged weight 800mm long 300mm long **Specific gravity** 800mm long 300mm long **Specific gravity plus attachment** 800mm long 300mm long	 57N 30N 3.99 4.0 5.0 6.2
Projected area of pipe section 800mm long 300mm long	 $0.104m^2$ $0.039m^2$
Contact pressure for pipe section 800mm long @ 87N 300mm long @ 33N	 0.83kPa 0.83kPa

Referring to Figure 3 - 25, assuming the two pipe sections are buried to D/2 (i.e., z is the same). D is the pipe diameter and the mobilised soil strength at the pipe invert is same for the two pipe sections, then the frictional force, *F* is:

F = frictional resistance + passive resistance

P is the soil passive resistance. Therefore,

$$\boldsymbol{R_1 = P + F_1} \qquad \textbf{3 – 2a}$$

Similarly,

$$\boldsymbol{R_2 = P + F_2} \qquad \textbf{3 – 2b}$$

This implies,

$$R_1 - R_2 = F_1 - F_2 \qquad 3-2c$$

Therefore the soil passive resistance component at the face of the pipe is eliminated and the frictional force can be computed from the two lengths of the pipe section.

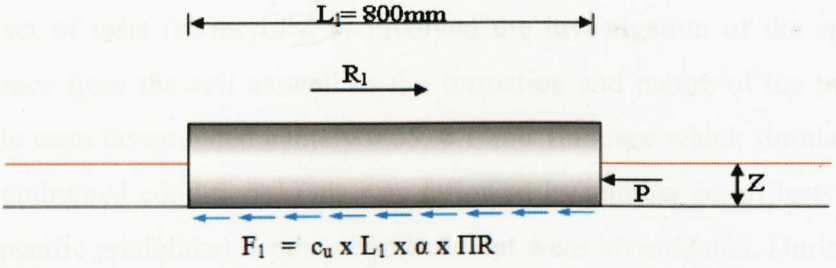

Similarly,

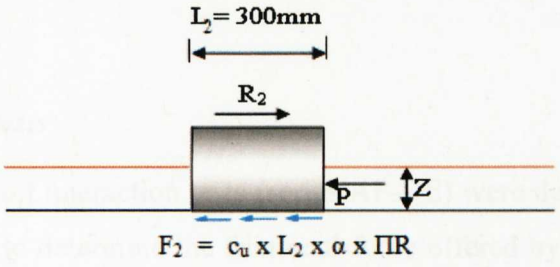

Figure 3 - 25: Schematic illustration of the determination of the actual frictional resistance of the seabed during axial pulling tests

3.4.8 Test procedures and programme

Three types of test were conducted in the large tank as part of this study namely: lateral pulling, axial pulling and the EK test (both lateral and axial). The tests are grouped to assess the influence of the pipe's submerged weight, speed of pipe travel and depth of initial embedment of the pipe on the soil resistances.

3.4.8.1 Lateral pulling tests

In the first series of tests the pipe was allowed to settle under its own weight. In order to allow the excess pore pressure generated during pipe penetration to dissipate, the test was carried out at between 20 and 24 hours after the pipe was placed on the soil surface

during which time the pipe settlement was measured. Thereafter, the pipe was swept laterally while held under constant vertical load which simulate the submerged weight of a surface laid pipeline during buckling on the seabed. These first set of tests (series LP-SW) investigated the influence of pipe submerged weight on the lateral resistance of the soil and the effects on the berm formation (see Table 3 - 4).

The second set of tests (series LP-PS) involved the investigation of the speed on the lateral resistance from the soil as well as the formation and nature of the berm. Three pulling speeds were investigated namely 0.05, 0.1 and 1mm/sec which simulates both the drained and undrained conditions. This was followed by another set of tests (series LP-DE) where specific predefined depths of embedment were investigated. During this time, the pipe was pushed into the soft seabed to three different depths of embedment namely; 1D, 1/2D and 1/4D and the same programme of cyclic pulling carried out as in the previous test set of tests.

3.4.8.2 Axial pulling tests

The last set of the pipe-soil interaction tests (series AP-DE) were designed for axial tests only where the aim was to determine the frictional force offered by the soil during axial displacement. The location of the pipe section during the lateral and the axial pulling tests is shown in Figure 3 - 28. All the tests were conducted on a reconstituted bed of clay after the necessary site investigation were conducted. The soil deformation mechanism associated with the failure of the soil during the lateral sweeping of the pipe and the associated load-displacement responses were investigated by manually measuring and recording the geometry of the seabed (soil berm) during pipe displacement.

3.4.8.3 Large-scale EK tests

In addition to the pipe-soil interaction tests conducted in the large tank, two lateral and two axial tests (one test as the control and one test on EK treated seabed each) were also conducted on the model seabed to see if the findings obtained from the small-scale tests were replicated.

The electrode configuration was similar to the small-scale test. However, only the iron electrodes were investigated here as it was deemed the best electrode material during the small scale tests. The results of the EK tests conducted in the big tank are presented in Chapter 4.

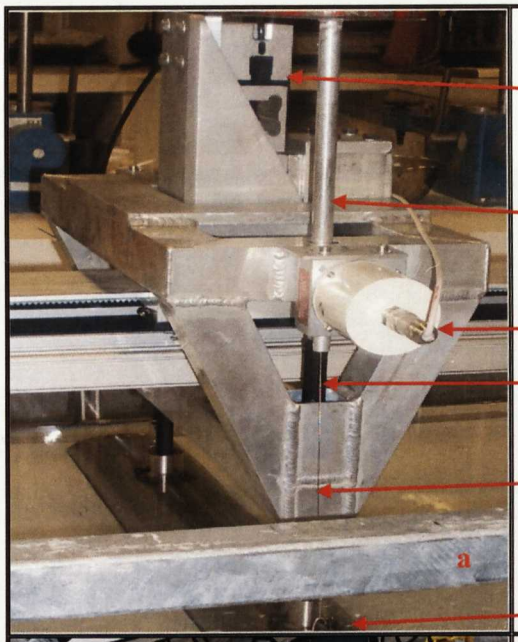

Trolley assemblage during for the pipe-soil test

Load cell for measuring the soil resistances during pipe travel

Aluminium rod for transferring variable vertical loads to the pipe section

Draw wire displacement sensor for measuring the vertical displacement of the pipe section

The ball spline

Steel wire cable from the draw wire to the pipe section

Pipe section

The 800mm pipe section

The pipe is perforated at the two sides to allow it to be fully submerged during the pipe-soil interaction tests

The 300mm pipe section

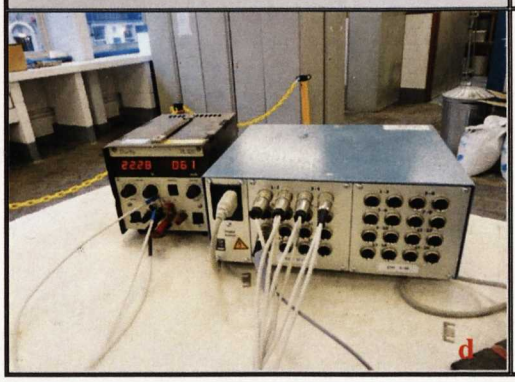

Data logger unit used for the pipe-soil interaction test

Figure 3 - 26: Equipment for the large-scale pipe-soil interaction test (a-d)

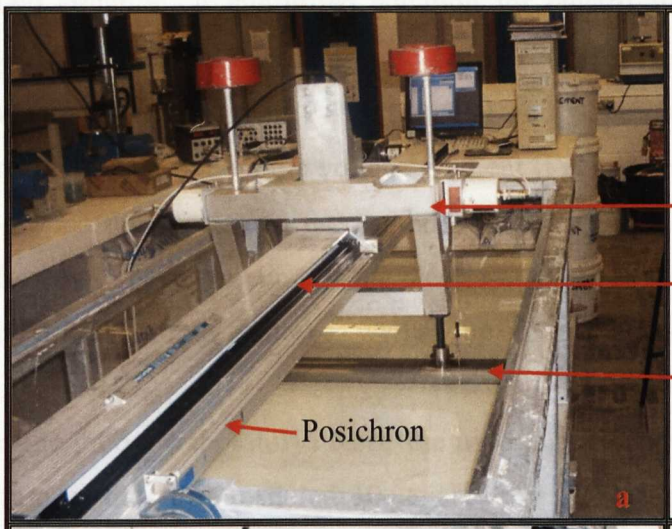

The actuator system and the trolley

The trolley

The linear motion actuator model GL20-250-T4F-L-EF-C-ASSY

Pipe configuration for lateral pulling test

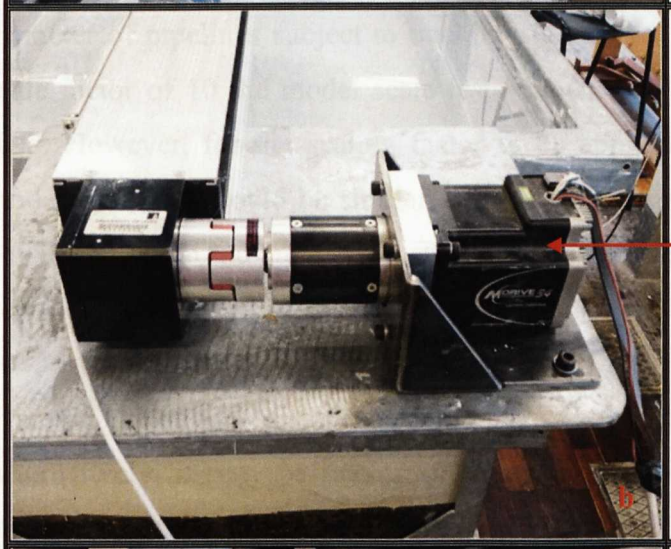

The integrated stepper motor used to control the pipe displacement during the pipe-soil interaction tests

Integrated stepper motor

Pipe configuration for axial pulling test

Figure 3 - 27: The actuator and pipe connections for the large-scale pipe-soil interaction

3.4.9 Use of models in research

This section is concerned with the scaling of the model tests presented above to a possible field situation. A simplified equation for electro-osmotic movement of water through porous soil material (analogous to Darcy's law for flow of water a through porous media) was given in Equation 2-22 (Mitchell and Soga, 2005). The effectiveness of the EK treatment depends on the voltage gradient (i.e. ratio of the applied voltage to the distance between the anode and the cathode). In addition, the magnitude of the electro-osmotic flow was also a function of the electro-osmotic conductivity of the soil (this depends on the soil conditions at site) as well as the cross sectional area of the soil treated.

In the model (laboratory) tests, the pipe diameter was 50mm while the electrodes were 3mm in diameter installed 10^{o} apart around the pipe. In field conditions, the average diameter of pipelines subject to buckling is between 0.3 to 0.5m. Therefore, applying a scale factor of 10 the model scale tests dimensions can potentially be replicated in the field. However, for the scaling factor to be applied, the voltage gradients used in the model and field should be similar. This can be achieved by adjusting the voltage at the power source. In the model tests, the distance between the anodes and the cathodes were kept constant at approximately 50mm while the applied voltage varies between 2.5 and 20V giving rise to varying voltage gradients. Most of the tests employed a 10V supply over an electrode distance of 50mm resulting in voltage gradient of 2V/cm. Alternatively, it may be necessary to select a target current density given the above dimensions of the electrodes in the field. Wrixon and Coper (1998) reported that a current density of $10A/m^2$ is sufficient to produce significant electro-osmotic flow in saline soil.

It should also be noted that increasing the voltage gradient could be beneficial to the EK treatment. This however will require further work to determine the optimum voltage gradient that can be applied to a given soil condition. The duration of the EK treatment to give the desired laboratory effects can also be scaled up by the same scaling factor assuming the same voltage gradient is applied. Esrig (1968) has demonstrated that the electro-osmotic consolidation time is proportional to the square of the anode-cathode spacing. However, if the scaling factor is applied to the applied voltage, then consolidation time becomes proportional to the anode-cathode spacing (Esrig, 1968).

As the goal of this study is in exploring the feasibility of extending EK technology in the improvement of offshore soils and hence pipeline stability, the concern is establishing the effectiveness of the process in this research. This is mainly assessed in terms of the increase in resistances of soil to pipeline displacements, to demonstrate whether the technique is feasible and may be applied to field situation.

For the pipe-soil interaction tests presented in chapter 6, the load-displacement response were normalised by the soil undrained shear strength, pipe diameter and pipe length which allows for direct application of the results in typical field situations.

3.4.10 Summary of tests conducted for the large-scale pipe-soil interaction

Table 3 - 4 is the summary of tests for the pipe-soil interaction tests.

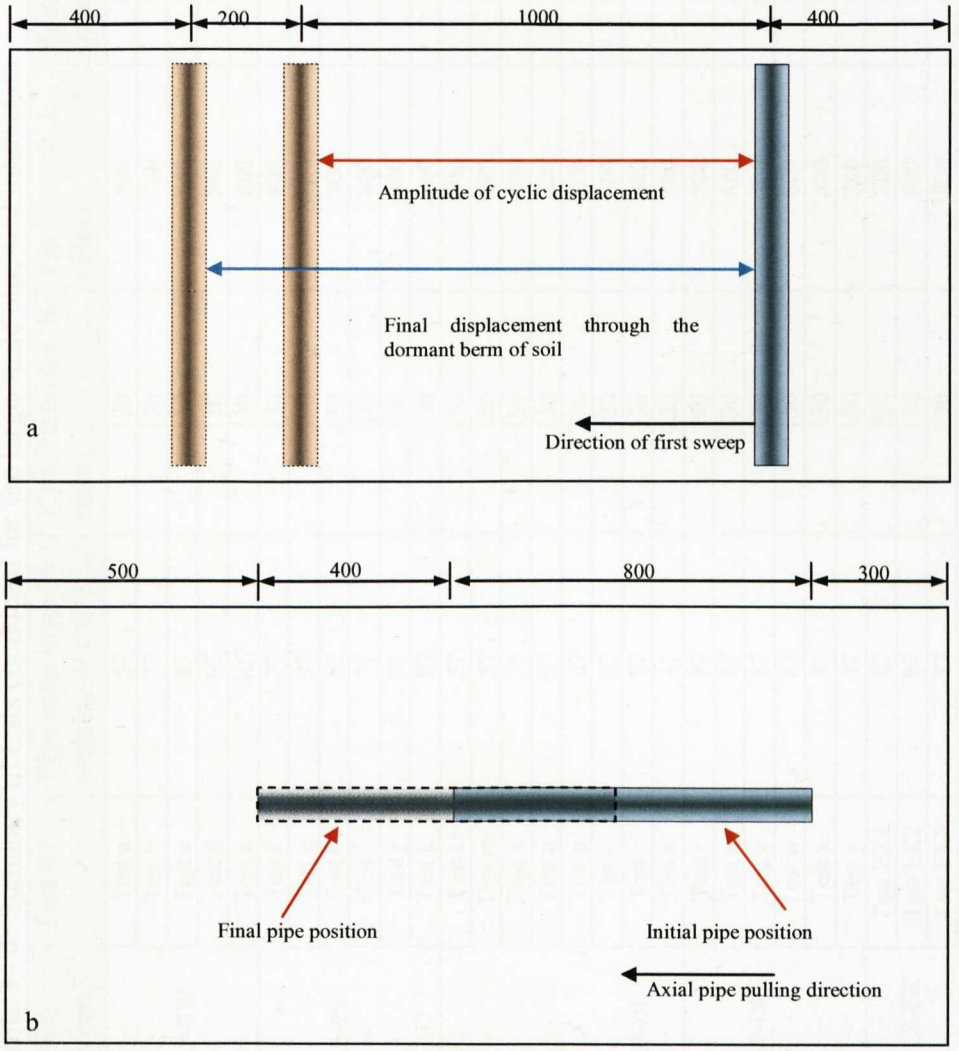

Figure 3 - 28: Pipe positions during large-scale pipe-soil interaction tests: a) Lateral pull, b) axial pull

Table 3 - 4: Summary of tests conducted for the large-scale pipe-soil interaction

Test series	Test #	Pipe submerged weight, W (N)	Pipe Diameter, D (mm)	Pipe length, L (mm)	Speed (mm/s)	Depth of initial burial, z	Remarks
LP-SW	Test a	57	130	800	0.05	Defined by the pipe settlement during installation	Lateral pulling test
	Test b	77	130	800	0.05		
	Test c	87	130	800	0.05		
	Test d	97	130	800	0.05		
	Test e	107	130	800	0.05		
LP-PS	Test f	77	130	800	0.1		
	Test g	97	130	800	0.1		
	Test h	87	130	800	0.1		
	Test i	77	130	800	1		
	Test j	97	130	800	1		
	Test k	87	130	800	1		
LP-DE	Test l	57	130	800	0.05	1/2D	
	Test m	57	130	800	0.05	1D	
	Test n	57	130	800	0.1	1/2D	
	Test o	57	130	800	0.1	D	
	Test p	87	130	800	0.05	1/2D	
	Test q	87	130	800	0.05	D	
	Test r	87	130	800	0.1	1/2D	
	Test s	87	130	800	0.1	D	
AP-DE	Test t	87	130	800	0.05	1D	Axial pulling tests
	Test u	87	130	800	0.05	1/2D	
	Test v	87	130	800	0.05	1D	
	Test w	87	130	800	0.05	1/4D	
	Test x	87	130	**300**	0.05	1/2D	
	Test y	87	130	**300**	0.05	1D	
LS-EK	Test EK1	87	130	800	0.05	1/2D	Control EK tests
	Test EK2	87	130	800	0.05	1/2D	Control EK tests
	Test EK3	87	130	800	0.05	1/2D	EK test
	Test EK4	87	130	800	0.05	1/2D	EK test

Chapter 4

RESULTS OF ELECTRO-KINETIC TREATMENT OF SOIL ON PIPELINE STABILITY

4.1 Introduction

In this chapter the results of the experimental investigations to study the effects of electro-kinetic (EK) treatment of soils around partially embedded pipe sections are presented. Six series of tests were conducted as presented in Table 3 - 2. The effects of EK treatment on the soil are assessed with respect to: (a) evolution of current density with time, (b) pipe settlements with time during the EK treatment, (c) spatial changes in water contents of the soil specimen, (d) development of undrained shear strength (c_u) after EK treatment and (e) pullout force after the EK treatment of the soil.

The chapter starts by investigating at a small-scale, the feasibility of using EK processes to modify a model seabed by studying the influence of voltage and current density on the EK processes. The effects of using different electrode materials as well as the effects of treatment time and initial water contents are then presented. Finally, the results of the large-scale tests where the small-scale tests are replicated are presented. Detailed discussions and analyses especially with respect to subsea pipeline stability are presented in Chapter 5.

4.2 Effect of using different voltages

Two test series (TV-VP and TV-AP) comprising 15 individual EK tests were carried out to study the influence of voltage on the modification of the mechanical and chemical properties of a model seabed. The investigations included monitoring and recording of pipe settlement with time and variation of current with time. In addition, changes in soil water contents, undrained shear strength and soil/water pH were investigated.

The impact of voltage on vertical and axial breakout resistances of the treated soil is assessed from series of pull-out tests conducted on the model seabed.

4.2.1 Voltage and generation of current density

The variations of current density with time for test series TV-VP and TV-AP are shown in Figure 4- 1a and Figure 4- 1b respectively. The two series were conducted under the same conditions except for orientations of the pipe sections where one was for vertical pulling test and the other for axial pulling test. The applied constant voltages ranged between 2.5V to 20V generating initial currents of between 0.9A to about 4.09A. The current density, which is defined as the ratio of the current generated to total surface area of the electrode, was assessed only from the anode surface area since the cathodes were not in contact with the soil. Given this voltage range, the soil conditions and electrode specifications, the maximum time for all the tests to come to an end (.i.e. when the anodes are depleted) was about 100hours (~6000 minutes).

The general shape of the current density curve from the two test series is comparable for the same applied voltage. This can be divided into four main stages. In the first stage, as soon as the specified voltage gradient is applied, the initial current drops almost instantaneously and then rises gradually to a peak value. This is normally followed by the second phase which is characterised by a gradual rise in current density. The third stage is depicted by gradual decline in current density while the last phase which is characterised by low current density lasts longer and gradually declines to almost zero as the test comes to an end. The decay in current density is probably due to increase in resistivity of the soil with time and is discussed in detail in chapter 5.

The effect of voltage on the generation of current density is more evident in the second stage of the current density curves. This is where the peak in the current density is always observed. The height of this peak is directly proportional to applied voltage and the higher the applied voltage the sooner the occurrence of the peak in the current density. Moreover, the pattern is less noticeable for applied voltages below 10V. Therefore it does appear that the applied voltage affects the generation of current density which is necessary to drive the EK processes. The trend of the current density for 17.5V and 20V is quite similar in their peak values. This is possibly due to the capacity of the power source used where the maximum allowable current is 4.10A. It is

therefore likely that the maximum current density for 20V would have been higher if the available current capacity was greater. However, the similarity in the curves for the two applied voltages differing by only 2.5V is worthy of note which may suggest that the difference in the effect of applied voltage is minimal for these two voltages.

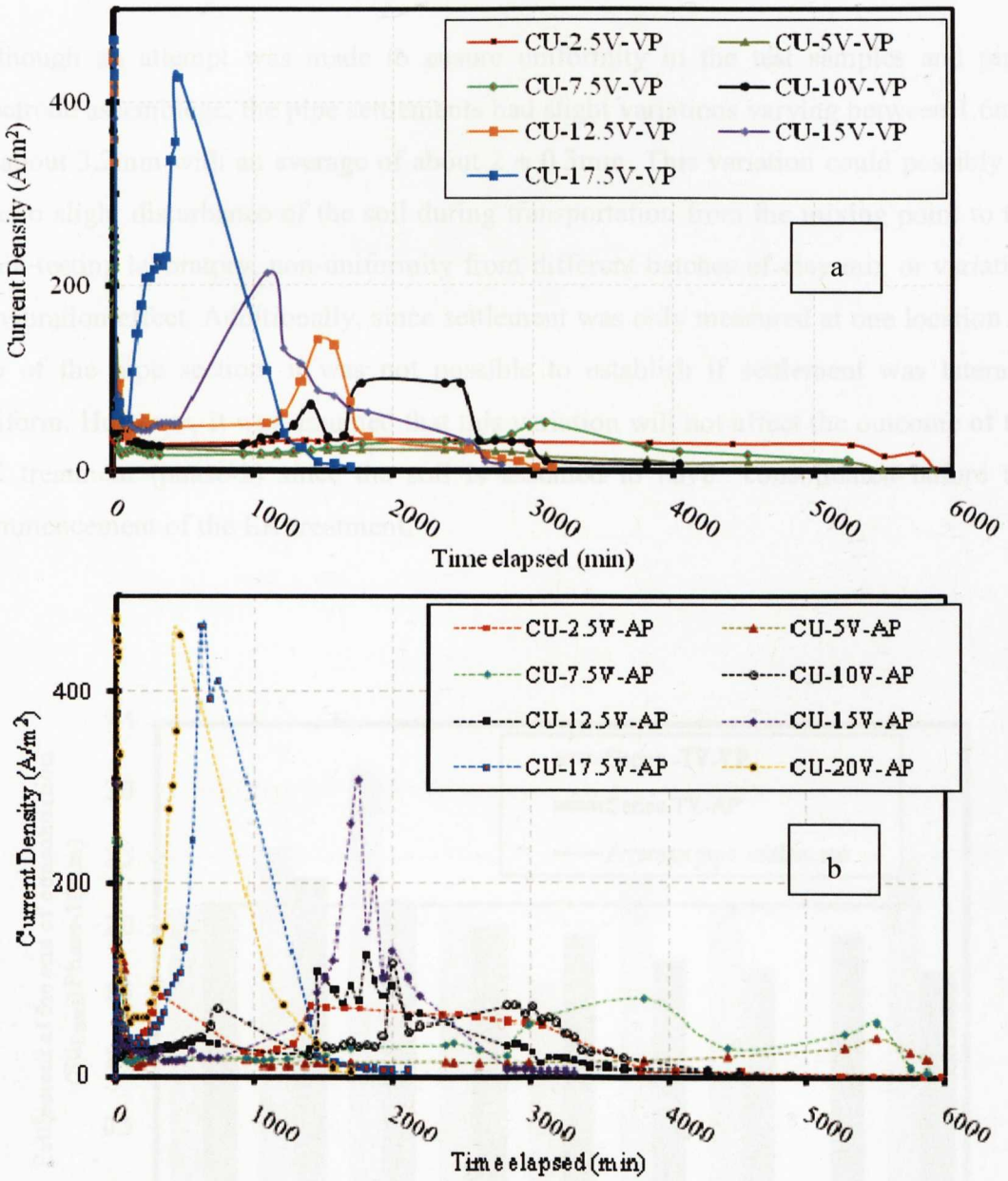

Figure 4- 1: Evolution of current density with time using different voltages: (a) series TV-VP and (b) sereis TV-AP

4.2.2 Voltage and soil settlememt

Soil settlement was inferred from a dial gauge placed at the top centre of the embedded pipe section. The primary aim of monitoring soil settlement was to use it to deduce the consolidation and dewatering of the soil during the EK treatment. Figure 4- 2 shows the plot of maximum pipe settlement against applied voltage for the two test series at the end of consolidation (phase-1).

Although an attempt was made to ensure uniformity in the test samples and pipe-electrode assemblege, the pipe settlements had slight variations varying between 1.6mm to about 3.2mm with an average of about 2 ± 0.3mm. This variation could possibly be due to slight disturbance of the soil during transportation from the mixing point to the main testing laboratory, non-uniformity from different batches of clay mix or variation in vibration effect. Additionally, since settlement was only measured at one location on top of the pipe section, it was not possible to establish if settlement was laterally uniform. However, It was assumed that this variation will not affect the outcome of the EK treatment (phase-2) since the soil is assumed to have consolidated before the commencement of the EK treatment.

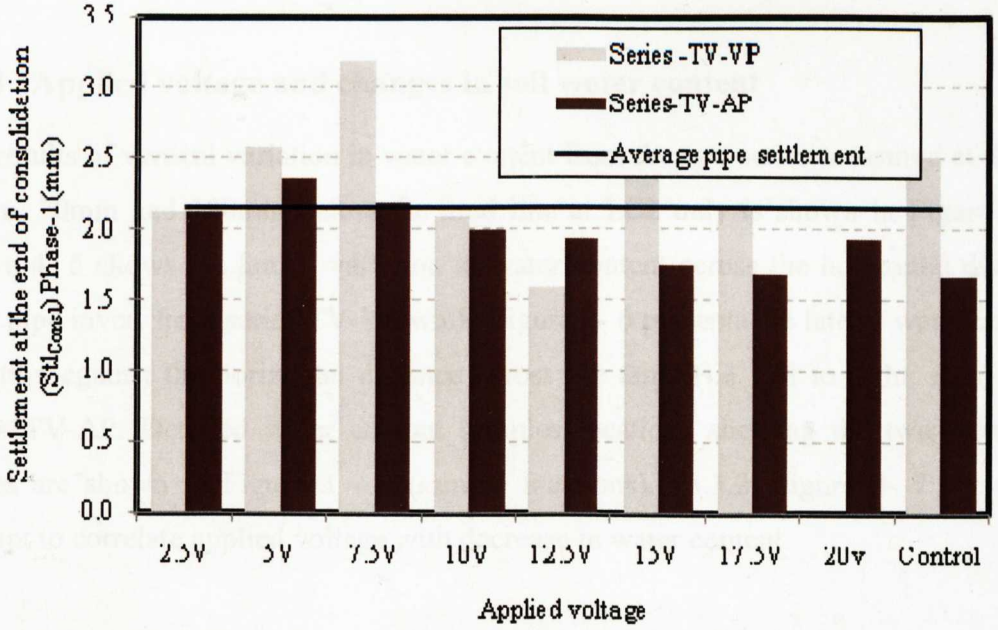

Figure 4- 2: Plot of overall settlement with time at the end of consolidation

The results of the maximum pipe settlement after the EK treatment (phase-2) are presented in Figure 4- 3. The plot suggests a gradual increase in pipe settlement with increase in applied voltage possibly due to increasing dewatering with increasing voltage application. It also appears to indicate that the settlement was very nearly independent of applied voltage after 5V.

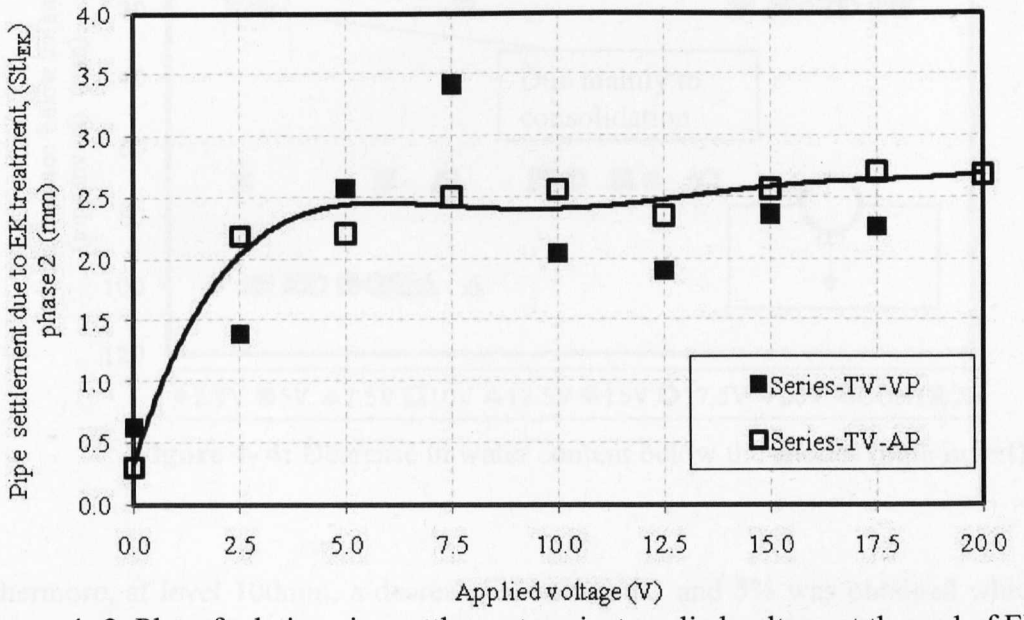

Figure 4- 3: Plot of relative pipe settlement against applied voltage at the end of EK treatment

4.2.3 Applied voltage and changes in soil water content

The results of vertical variation in water content from the two series measured at depths 20mm, 70mm and 100mm below the mud line at LC2 only is shown in Figure 4- 4. Figure 4- 5 shows the lateral variation in water content across the horizontal distance from pipe invert from series TV-VP while Figure 4- 6 presents the lateral water content variation against the horizontal distance across the tank, (i.e. left to right, R-L) from series TV-AP. Detailed water content samples locations showing the two reference planes are shown in Figure 3 - 8 (sample locations), §3.3.2. Figure 4- 7 shows an attempt to correlate applied voltage with decrease in water content.

It can be seen from the Figure 4- 4 that while the control tests had between 1 and 2% decrease in water content within the soil mass due to consolidation those treated by EK

showed a significant decrease. About 5 -13% decrease in water content occurred for the sample taken at depth 20mm level while between 4 and 11% decrease occur for sample taken at 70mm level.

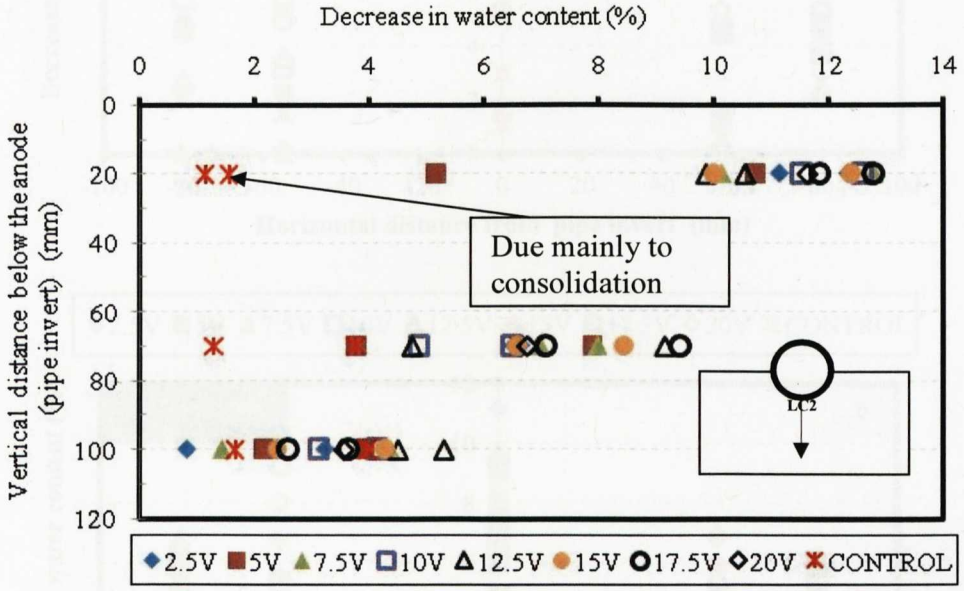

Figure 4- 4: Decrease in water content below the anodes (pipe invert)

Furthermore, at level 100mm, a decrease of between 2 and 5% was obtained which is still higher than the results from the control tests. It should be noted here that the water content samples from the treated bed soil clay had significant chemical alterations especially at the top 35mm level (Figure 4- 8). This alteration, which was caused by the degradation of the electrode materials and noticed by the discolouration of the water content sample, may have some influence on the engineering properties of the treated soil and is discussed in chapter 5.

The various water content profiles shown demonstrate that there are variations in changes in water content both vertically and laterally after the EK treatment of the soil mass. These variations do not appear to show constant relationship with the applied voltage which theoretically should be the case since the applied voltage should be the driven force for the electro-kinetic processes. However, the apparent difference with the results from the control tests indicates the feasibility of using EK to promote a decrease in the water content of the soil around a partially embedded pipe section.

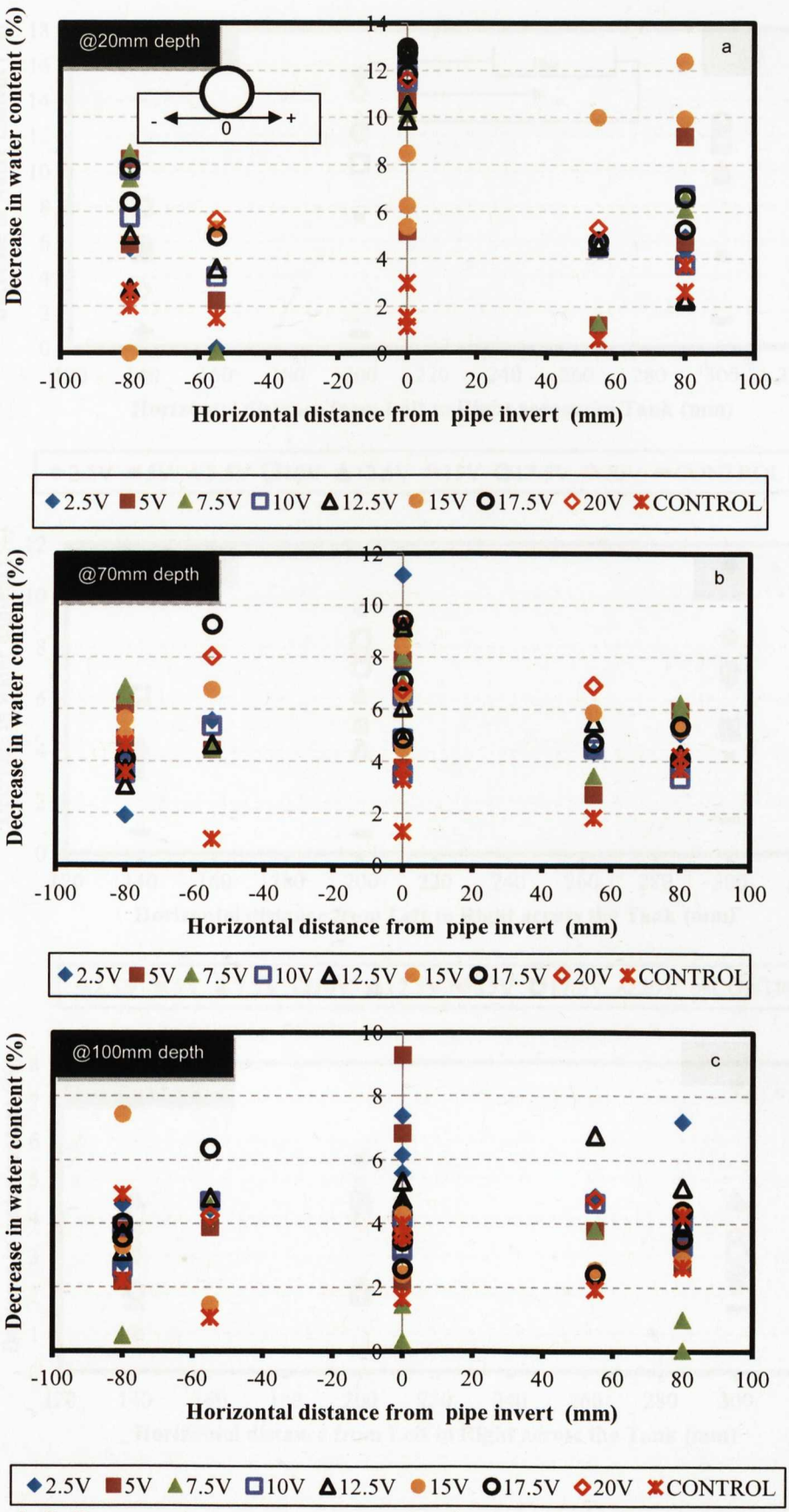

Figure 4- 5: Decrease in water content against horizontal distance from pipe invert

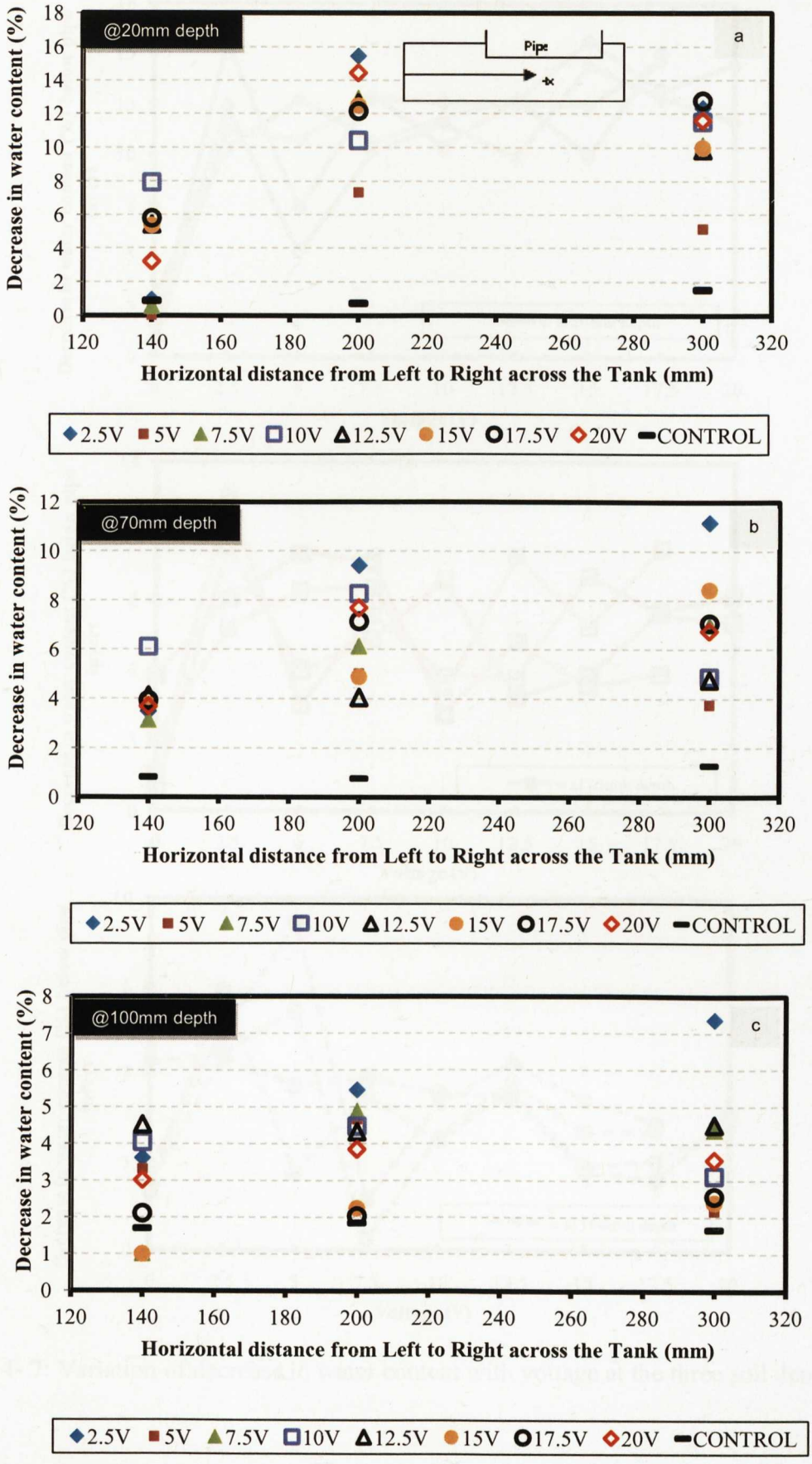

Figure 4- 6: Decrease in water content against horizontal distance across tank, L-R

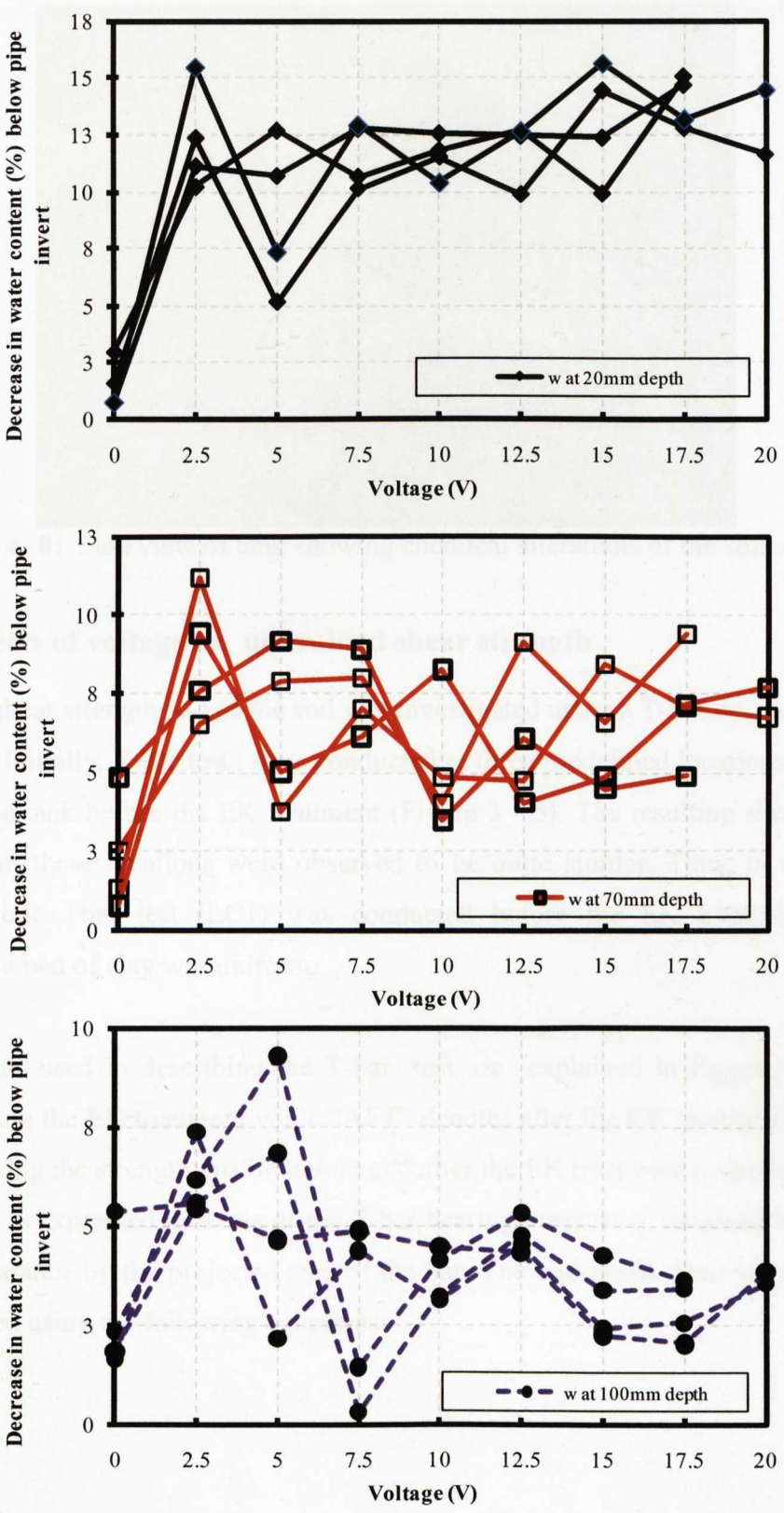

Figure 4- 7: Variation of decrease in water content with voltage at the three soil depths

Figure 4- 8: Side view of tank showing chemical alterations of the soil sample

4.2.4 Effects of voltage on undrained shear strength

Undrained shear strength (c_u) of the soil was investigated using a T-bar device discussed in §3.2.1.3. Initially, T-bar tests were conducted at three predefined locations across the length of the tank before the EK treatment (Figure 3 - 5). The resulting shear strength profiles from these locations were observed to be quite similar. Thus, in subsequent tests only one Tbar test (LC1) was conducted before the EK treatment on the assumption a bed of clay was uniform.

The notations used in describing the T-bar test are explained in Figure 4- 9. "B4" denotes before the EK treatment while "AFT" denotes after the EK treatment. A typical c_u plot showing the strength profile before and after the EK treatment is shown in Figure 4- 10. This is expressed in terms of the T-bar bearing pressure q, obtained by dividing the soil resistance by the projected area of the bar. The undrained shear strength (c_u) is then obtained using the following equations:

$$c_u = q/N_t \qquad \textbf{4 -1}$$

Where, N_t is a factor representing the relationship between shear strength and net bearing pressure. Typically, an average value of 10.5 is used in most offshore geotechnical analysis involving low strength seabed soils and is used in this research.

The reporting of the changes in c_u before the EK test is explained with respect to the test locations .ie. LC1, LC2 and LC3, as shown in the insert.

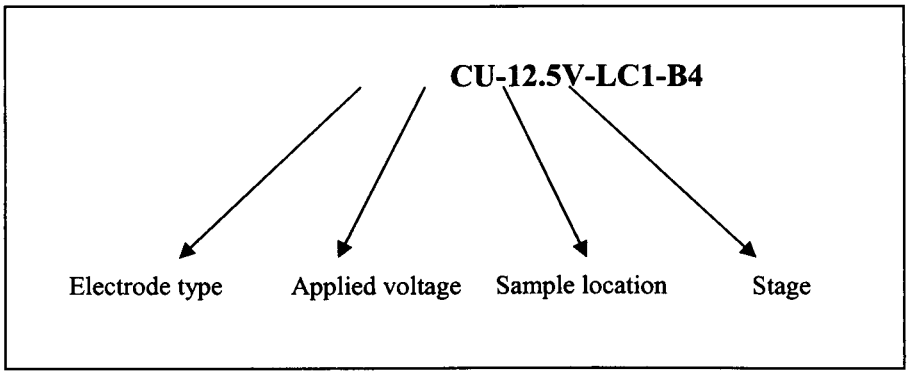

Figure 4- 9: Notations used in describing the T-bar/c_u test

Results of the undrained shear strength profiles conducted on all the beds of clay (from series TV-VP and TV-AP) before the EK treatment including the average shear strength profile is shown in Figure 4- 11. The results lie in a band of between +/-33% of the mean. The observed variation in the c_u profile from different tanks could be due to different batches of clay mixes used and other factors associated with the mode of preparation such as placement of the clay in layers, levelling of the clay surface and subsequent vibration effects. Additionally, since the T-bar tests were conducted shortly after the placement of the soil in tank, the soil had therefore not consolidated before the T-bar test. As stated earlier, the individual beds of clay were virtually uniform in strength which suggests that comparisons can be made before and after EK treatment for each bed of clay tested to assess the effects of EK on the soil.

Results of the undrained shear strength tests after the EK treatment for series TV-VP are shown in Figure 4- 12 and Figure 4- 13 for LC1 and LC2 respectively. It can be seen from the two plots that there are considerable increases in the soil c_u.Taking the c_u at 30mm depth as a reference (depth of pipe burial), the undrained shear strength ranges between 0.2 and 0.6kPa for LC1 while it is about 0.25 and 0.7kPa for LC2. Therefore, the maximum strength appears to occur below the pipe invert. At LC2, the control profiles appear to converge with the treated soil from about 80mm depth. The plots also suggest that there is a trend between applied voltage and increase in the c_u.

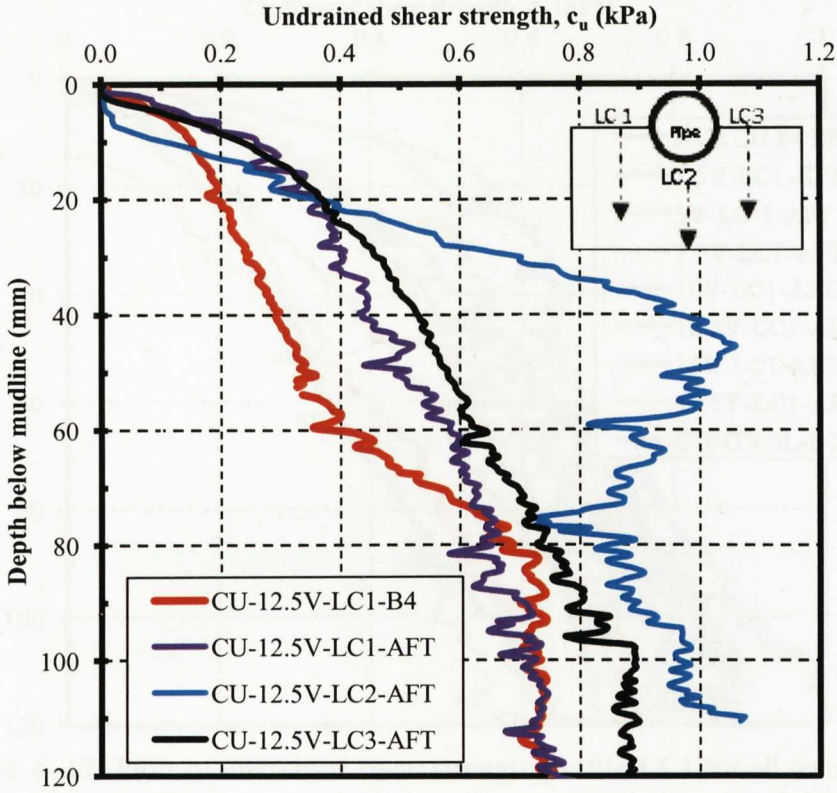

Figure 4- 10: Typical c_u profile before and after EK treatment

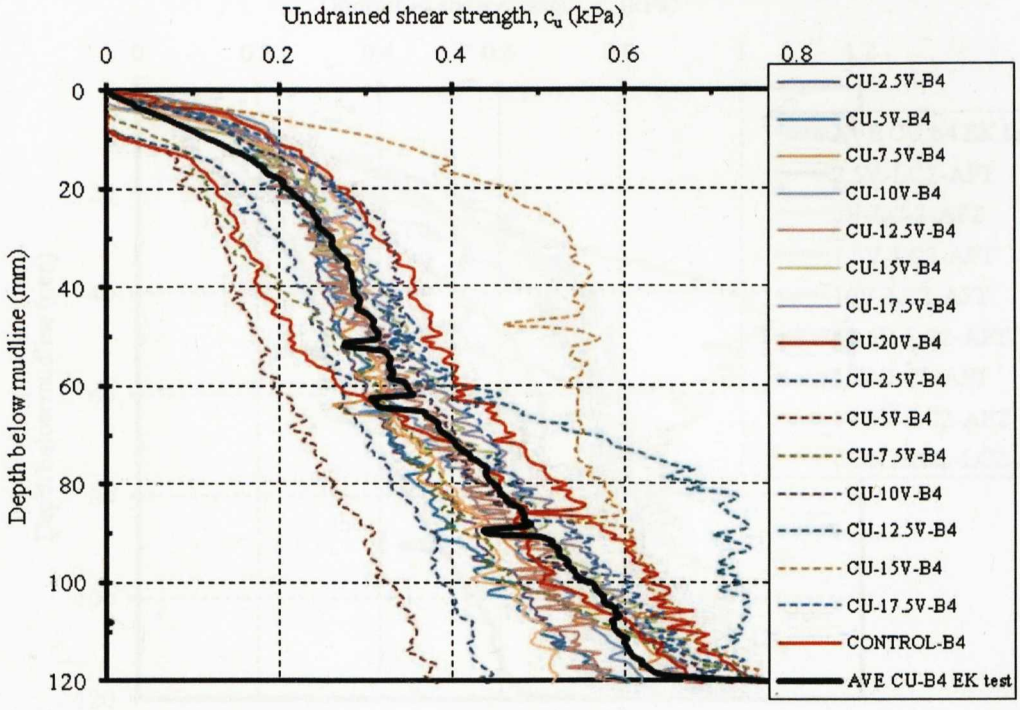

Figure 4- 11: Plots of undrained shear strength profile for tests in series TV-VP & TV-AP before EK treatment (dotted lines show profiles from TV-VP while the solid lines show profiles from TV-AP)

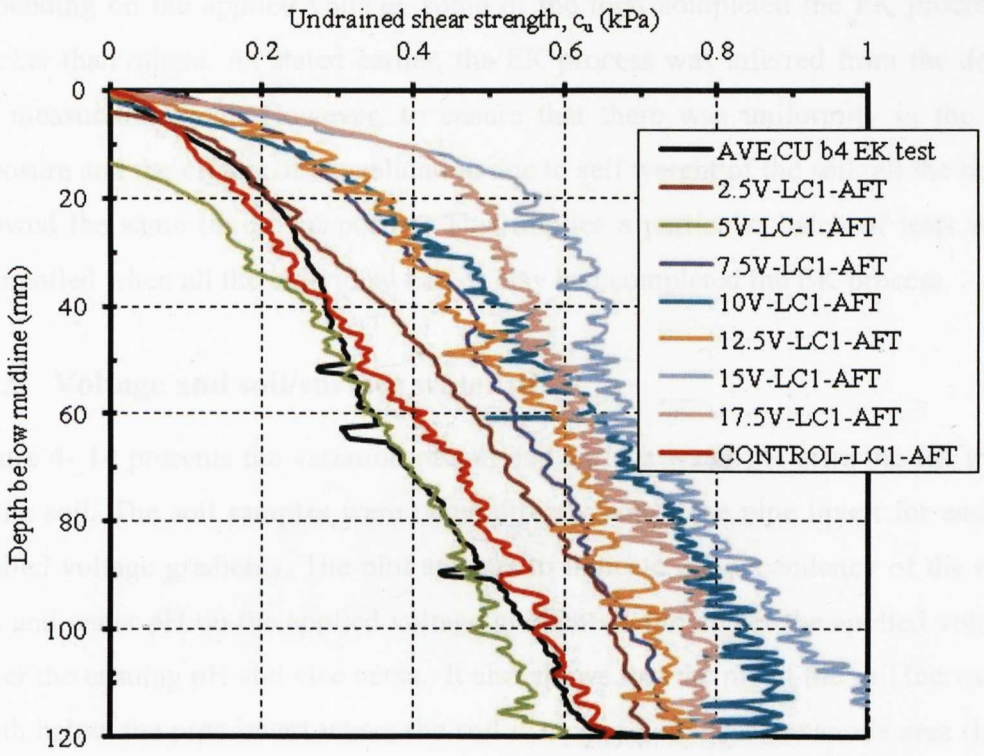

Figure 4- 12: Plots of undrained shear strength profile **LC1** for all tests in series **TV-VP** after EK treatment including the average shear strength before EK test

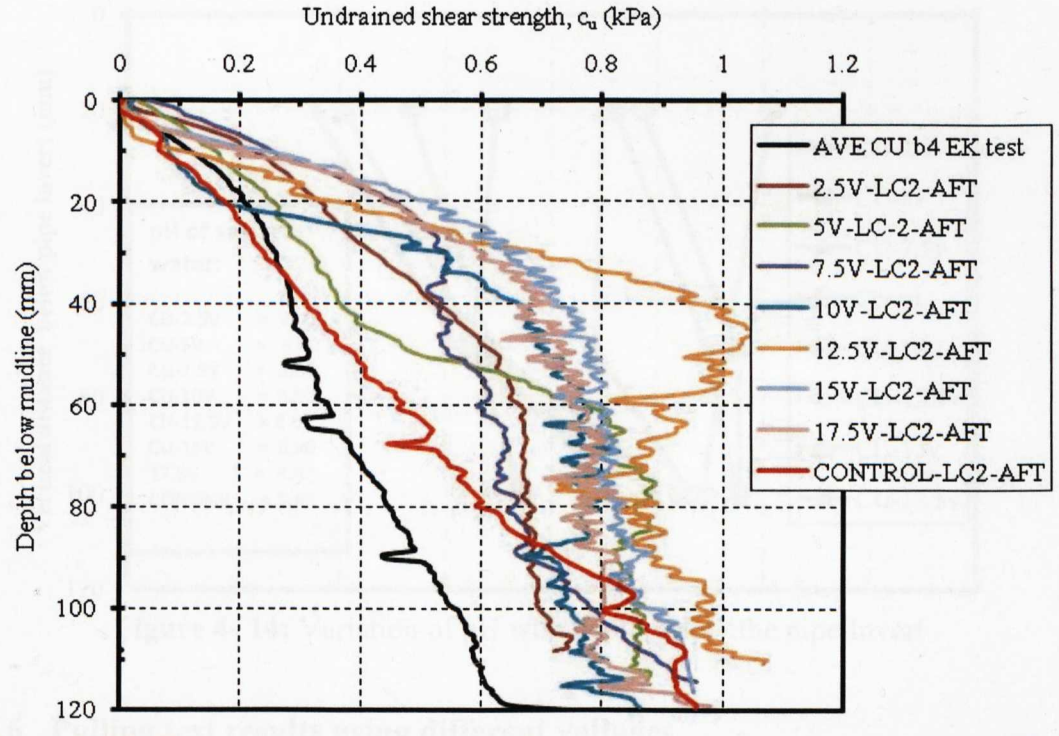

Figure 4- 13: Plots of undrained shear strength profile **LC2** for all tests in series **TV-VP** after EK treatment including the average shear strength before EK test

Depending on the applied voltage, some of the tests completed the EK process much quicker than others. As stated earlier, the EK process was inferred from the decline in the measured current. However, to ensure that there was uniformity in the time of exposure and the effects of consolidation due to self weight of the soil, all the tests were allowed the same time of exposure. This implies a particular batch of tests was only dismantled when all the individual bed of clay had completed the EK process.

4.2.5 Voltage and soil/surface water pH

Figure 4- 14 presents the variation of soil and surface water pH after the EK treatment of the soil. The soil samples were taken directly below the pipe invert for each of the applied voltage gradients. The plot appears to indicate the dependency of the resulting soil and water pH on the applied voltage gradients – the higher the applied voltage, the lower the ensuing pH and vice versa. It also shows that the pH of the soil increases with depth below the pipe invert where the soil is more acidic near the anode area (i.e. close to the embedded pipe section).

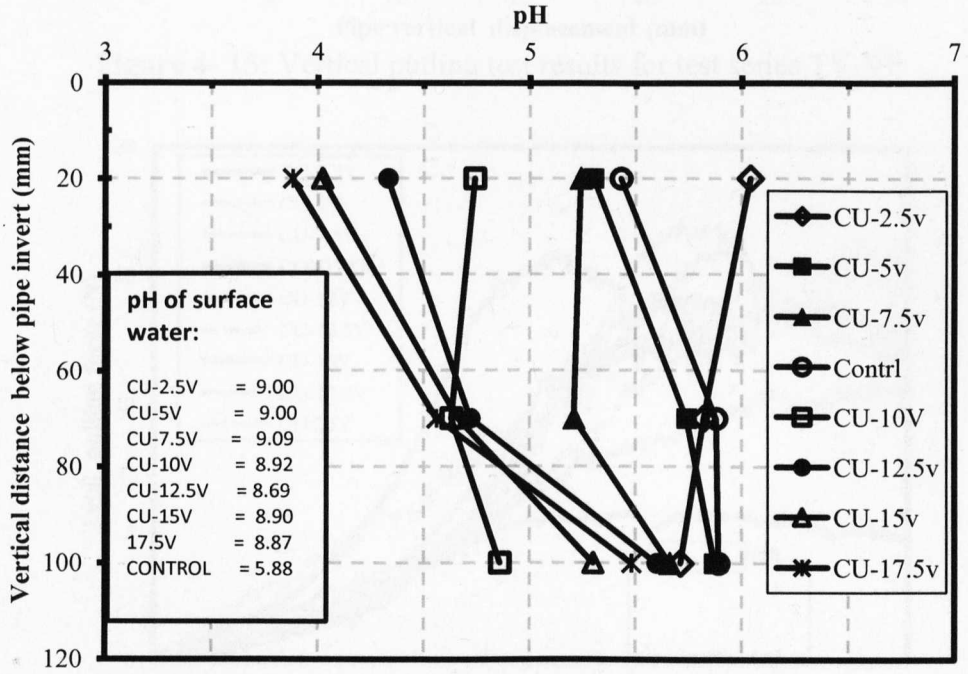

Figure 4- 14: Variation of pH with depth below the pipe Invert

4.2.6 Pulling test results using different voltages

The main aim of the pulling test was to investigate the effects of the EK treatment on soil resistances to pipe displacement in order to assess its impact to enhance pipeline

stability on the seabed. Results of vertical and the axial pullout tests are presented in Figure 4- 15 and Figure 4- 16 respectively. The results indicate an increase of between 70% to about 210% for the vertical pullout and between 90% to about 209% for the axial pullout. In all, the two types of pulling tests indicate an average of about 140% increase in pipe resistance to displacement due to EK treatment effect.

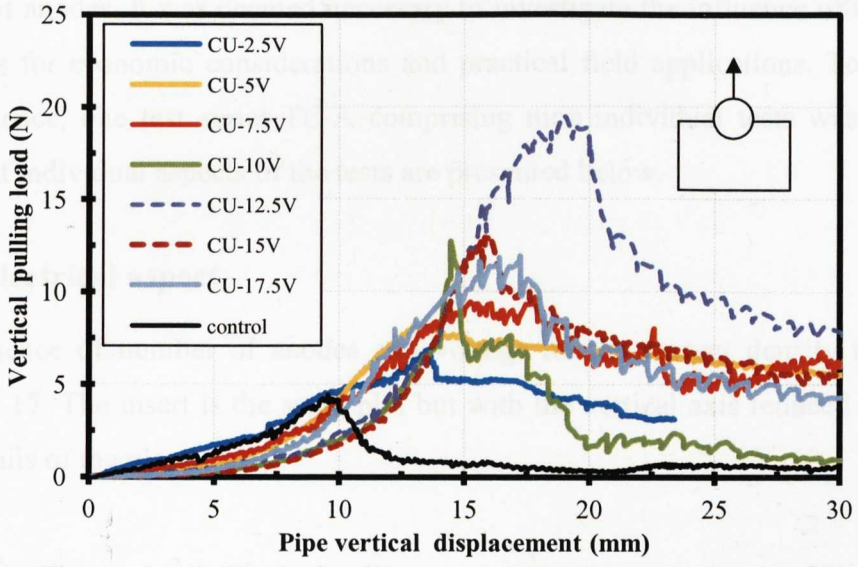

Figure 4- 15: Vertical pulling test results for test series TV-VP

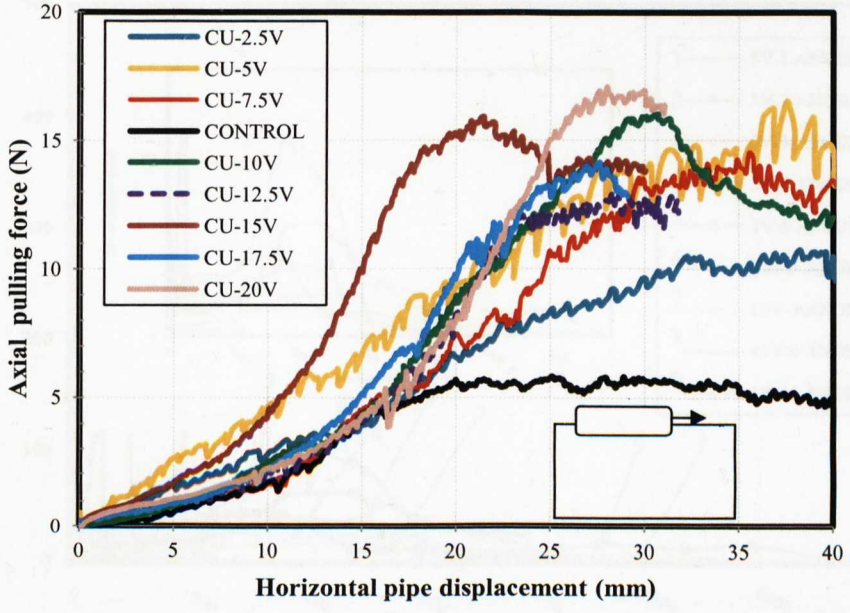

Figure 4- 16: Axial Pulling Test Results for Test Series TV-AP

The resistance of the soil to pullout is related to the applied voltage. However, unexpectedly higher vertical pullout force is measured for the 12.5V test. This could

possibly be due to chemical alteration of the soil leading to increase pipe-soil adhesion not explained by electro-osmotic dewatering alone.

4.3 Current density/number of anodes

The effectiveness of the EK treatment process is a function of the current density generated during the treatment which is the main driving force for the various electro-kinetic processes. At constant voltage, the current density is directly related to the number of anodes. It was deemed necessary to investigate the influence of the numbers of anodes for economic considerations and practical field applications. To investigate this influence, one test series-TE-A comprising nine individual tests was conducted. Results of individual aspects of the tests are presented below.

4.3.1 Electrical aspect

The influence of number of anodes and voltage on the current density is shown in Figure 4- 17. The insert is the same plot but with the vertical axis reduced to highlight more details of the plot.

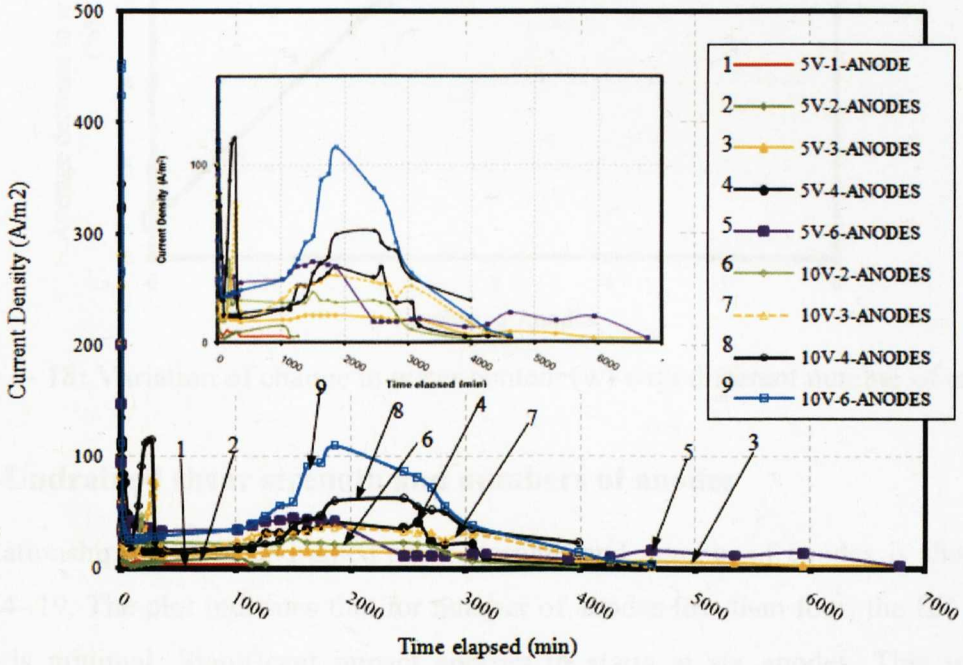

Figure 4- 17: Variation of current density with number of electrodes and voltage

The plot demonstrates the dependency of current density generated on the number of anodes employed. It indicates that the higher the number of anodes, the higher the current density generated. However, the current density generated by 4 anodes at 10V application has a higher peak than 6 anodes at 5V. Similarly, 2 anodes at 10V have a higher peak than 3 anodes at 5V. This trend appears to suggest that increasing the applied voltage could compensate for increasing number of electrodes although this will need to be evaluated further in terms of cost of applied voltage to cost of electrode materials.

4.3.2 Changes in water content with number of anodes

Figure 4- 18 shows the effect of numbers of anode/current density on the dewatering of the model seabed. It should be noted here that the water content samples were taken from the top 20mm only and not the entire soil mass. This indicates that the higher the current density the greater the amount of water removed from the soil.

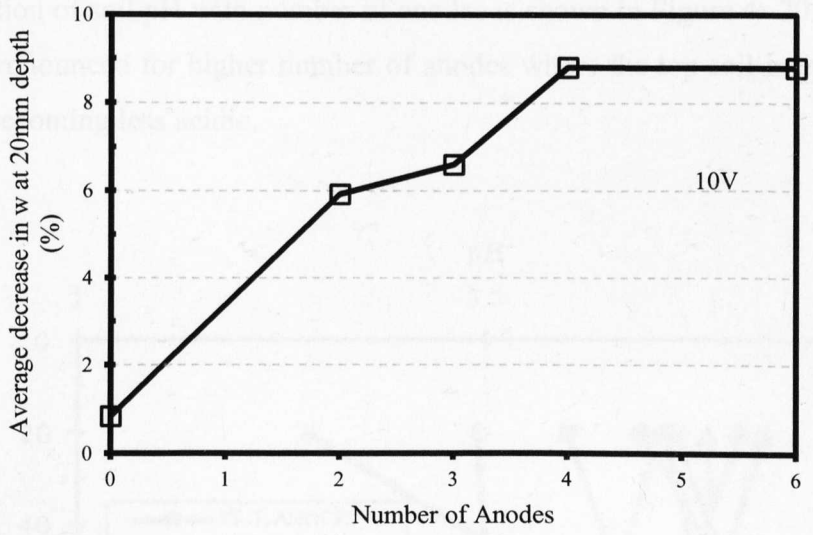

Figure 4- 18: Variation of change in water content (w) with different number of anodes

4.3.3 Undrained shear strength and numbers of anodes

The relationship between undrained shear strength and number of anodes is shown in Figure 4- 19. The plot indicates that for number of anodes less than four, the EK effect of soil is minimal. Significant impact appears to starts at six anodes. This will be discussed further in chapter 5.

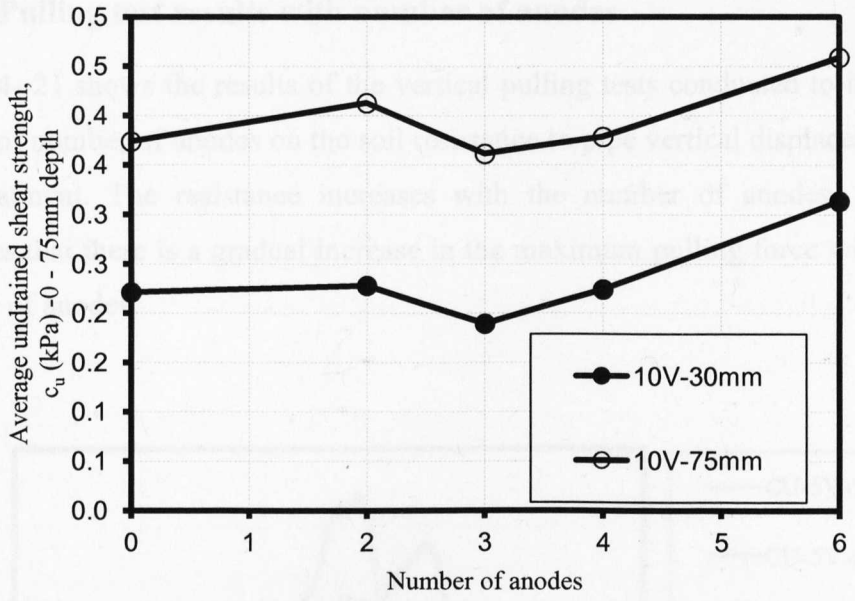

Figure 4- 19: Variation of change in shear strength using different number of anodes and voltage

4.3.4 Effect of number of anodes on soil pH

The variation of soil pH with number of anodes is shown in Figure 4- 20. The influence is more pronounced for higher number of anodes where the top soil is more acidic and the base becoming less acidic.

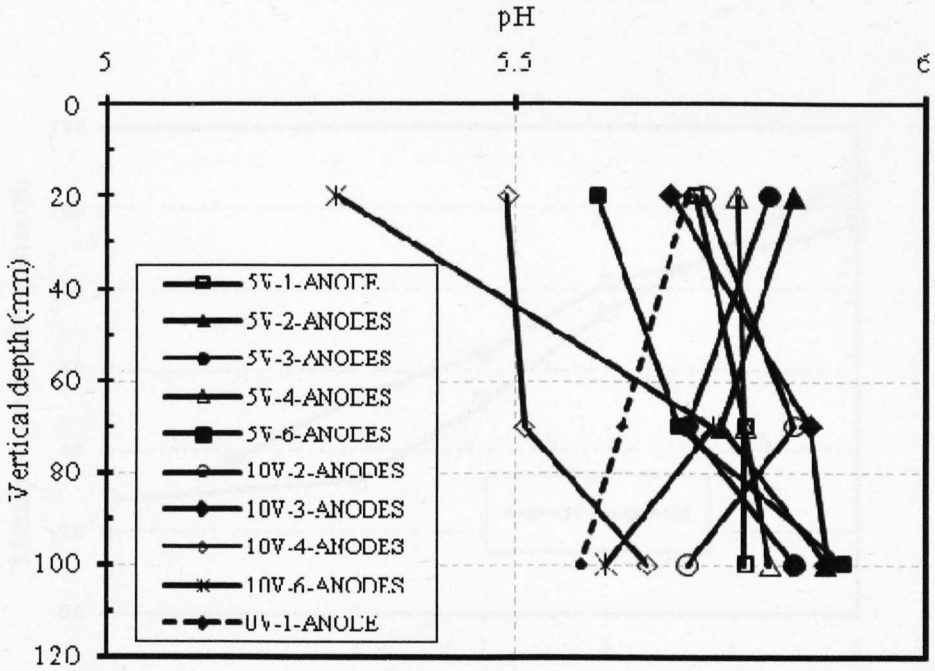

Figure 4- 20: Variation of pH with depth below the pipe invert using different number of anodes

4.3.5 Pulling test results with number of anodes

Figure 4- 21 shows the results of the vertical pulling tests conducted to investigate the effects of number of anodes on the soil resistance to pipe vertical displacement after the EK treatment. The resistance increases with the number of anodes. Figure 4- 22 indicates that there is a gradual increase in the maximum pulling force with increase in number of anodes.

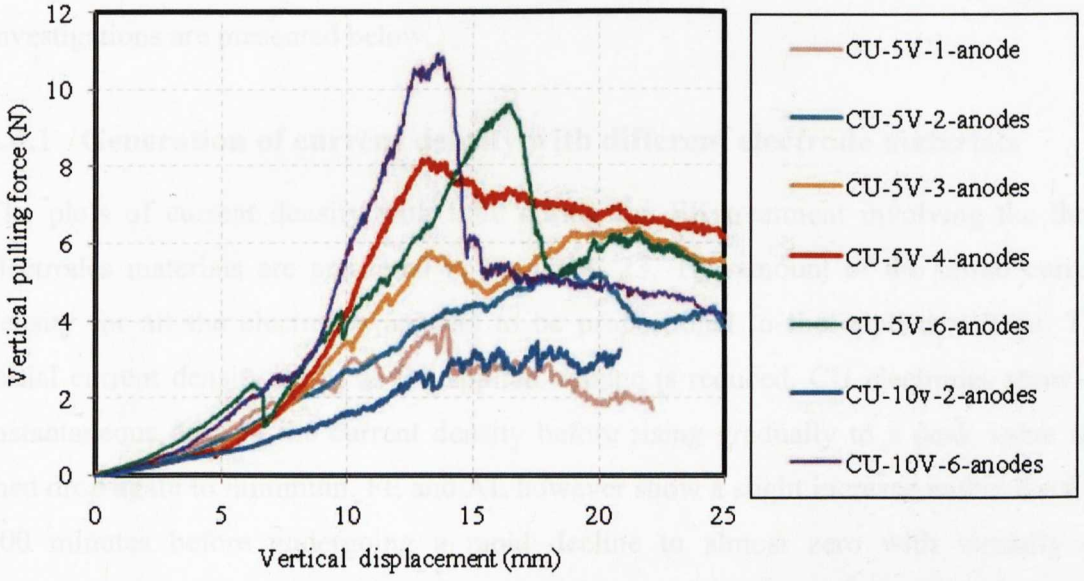

Figure 4- 21: Vertical pulling test results using different numbers of anodes

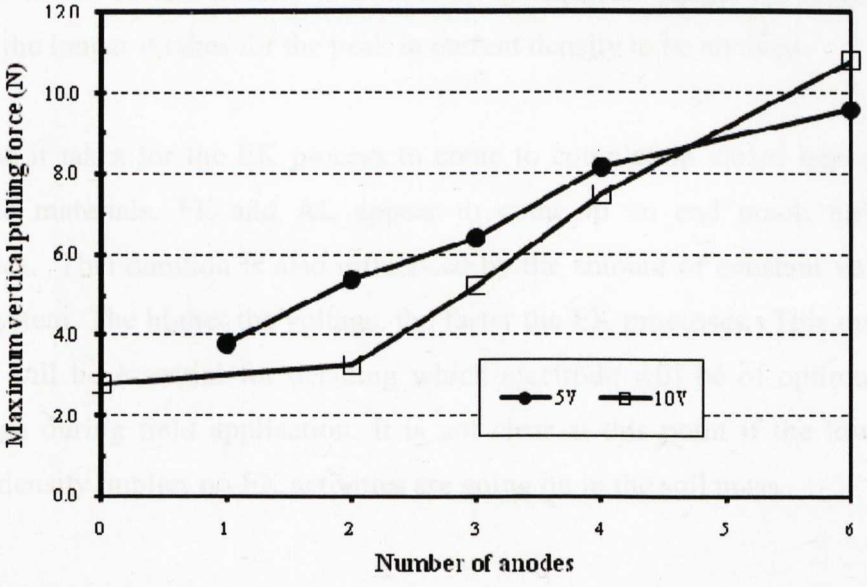

Figure 4- 22: Plot of maximum vertical pulling force with number of anodes

4.4 Effect of using different electrode materials

The selection of appropriate electrode material is vital for both economic viability and treatment efficiency of the EK process. Three electrode materials, namely copper (CU), iron (FE) and aluminium (AL), were chosen to investigate the effects of the electrode material on EK modification of the model soil and hence pipeline stability. For each test involving a particular electrode material, both the anode and the cathode were the same type. Test series TV-EM, TV-DT and TV-WC were designed to investigate the impact of electrode materials during the EK treatment. The results of the various aspects of the investigations are presented below.

4.4.1 Generation of current density with different electrode materials

The plots of current density with time during the EK treatment involving the three electrodes materials are presented in Figure 4- 23. The amount of the initial current density for all the electrodes appears to be proportional to the applied voltage. The initial current density drops as the applied voltage is reduced. CU electrodes show an instantaneous drop in the current density before rising gradually to a peak value and then drop again to minimum. FE and AL however show a slight increase within the first 500 minutes before undergoing a rapid decline to almost zero with virtually no subsequent increase as the process continues to completion. The rapid drop in the current density using FE and AL could suggest a rapid increase in the soil resistivity due to the chemical changes in the soil. CU electrodes also indicate that the time to reach the peak in the current density is a function of applied voltage; the lower the applied voltage the longer it takes for the peak in current density to be attained.

The time it takes for the EK process to come to completion varied between the three electrode materials. FE and AL appear to come to an end much faster than CU electrodes. This duration is also influenced by the amount of constant voltage applied to the system. The higher the voltage, the faster the EK processes. This duration of EK process will be essential for deciding which electrode will be of optimum economic advantage during field application. It is not clear at this point if the lower/minimum current density implies no EK activities are going on in the soil mass.

4.4.2 Pipe settlement with different electrode materials

A plot of the relative pipe settlement with time during the EK treatment and the maximum pipe settlement at the end of the EK treatment involving the three electrode materials are presented in Figure 4- 24 and Figure 4- 25 respectively. It can be seen that a gradual settlement of the pipe with time occurs using CU and AL electrodes while a slight uplift of the pipe occurred using FE electrodes. At higher applied voltage more uplift is obtained. This uplift also coincides with the peak in current density noted in Figure 4- 24.

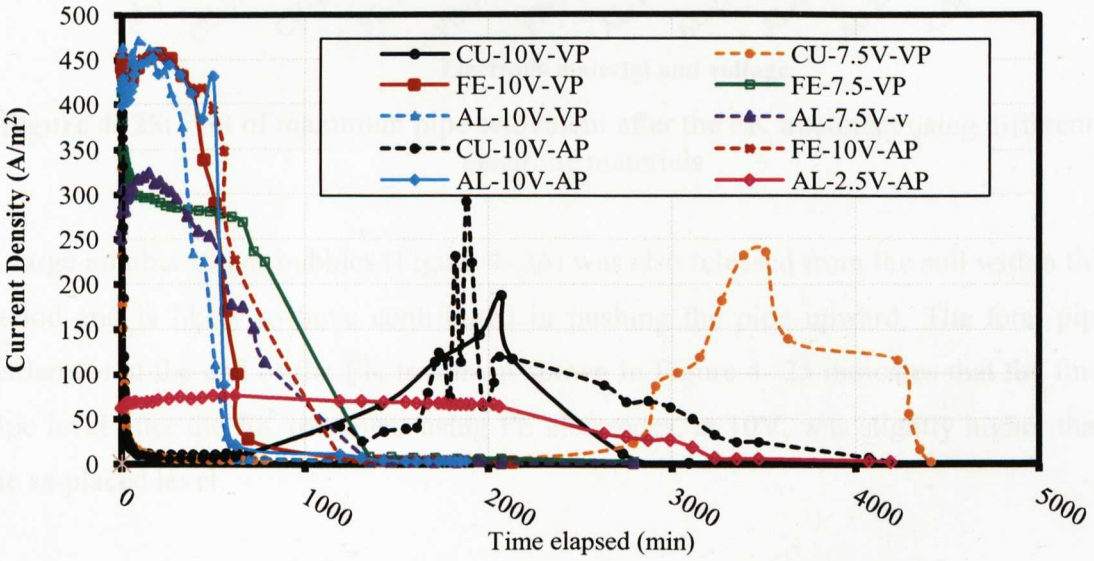

Figure 4- 23: Variation of current density with time during the EK treatment

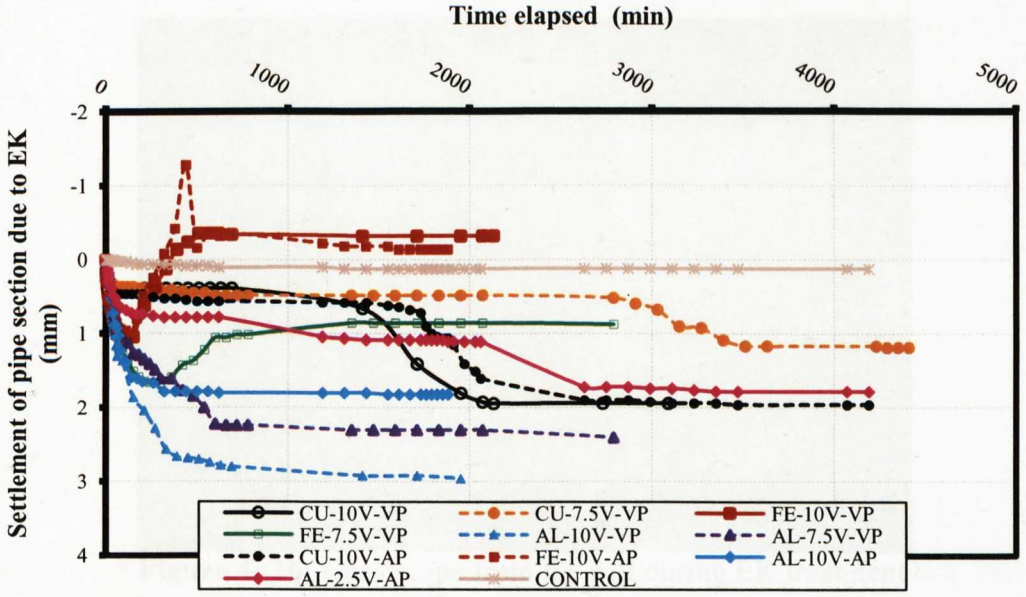

Figure 4- 24: Plot of relative pipe settlement with time during the EK treatment

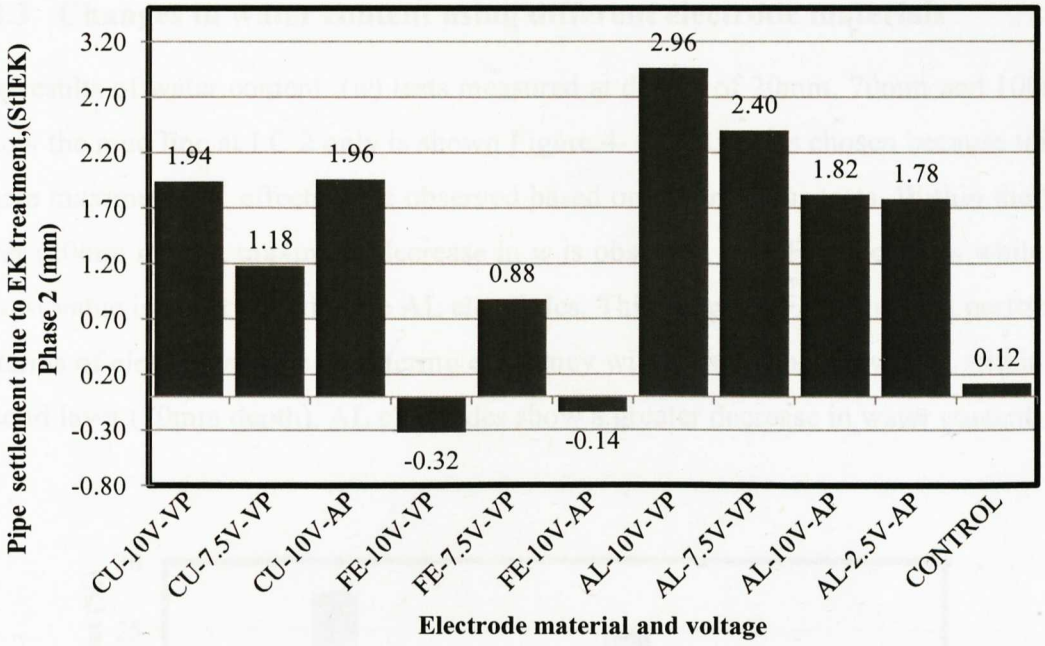

Figure 4- 25: Plot of maximum pipe settlement after the EK treatment using different electrode materials

A large number of gas bubbles (Figure 4- 26) was also released from the soil within this period and is likely to have contributed in pushing the pipe upward. The total pipe settlement at the end of the EK treatment shown in Figure 4- 25 indicates that the final pipe level after the EK treatment using FE electrodes, at 10V, was slightly higher than the as-placed level.

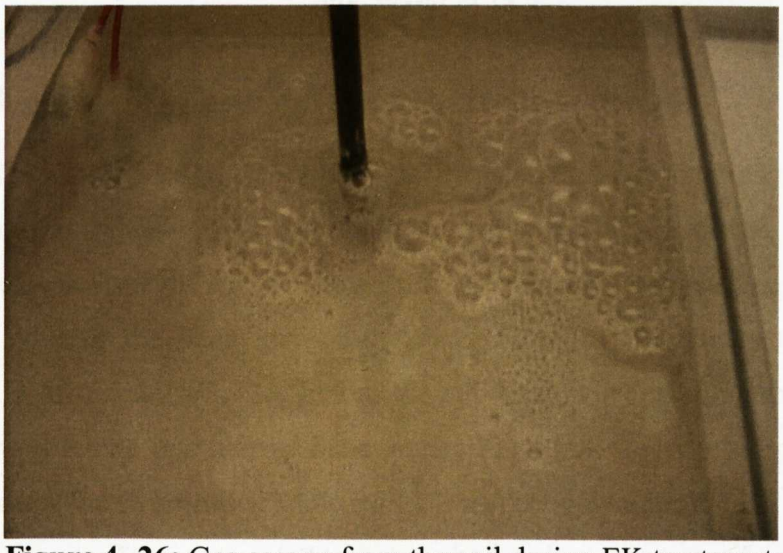

Figure 4- 26: Gas escape from the soil during EK treatment

4.4.3 Changes in water content using different electrode materials

The results of water content (w) tests measured at depths of 20mm, 70mm and 100mm below the mud line at LC 2 only is shown Figure 4- 27. LC2 was chosen because this is where maximum EK effects were observed based on the previous tests. Within the first layer (20mm depth), maximum decrease in w is observed with FE electrodes while the lowest value is observed with the AL electrodes. This suggests FE is the best performer in terms of electro-osmotic dewatering efficiency within that zone. However, within the second layer (70mm depth), AL electrodes show a greater decrease in water content.

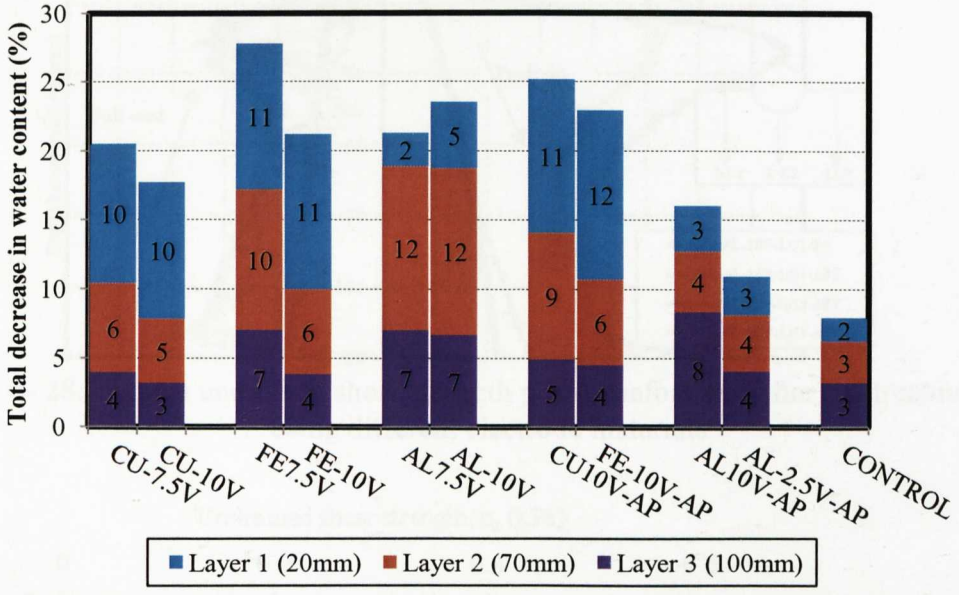

Figure 4- 27: Decrease in water content against electrode materials at depths below pipe invert at LC2

4.4.4 Development of c_u with different electrode materials

Figure 4- 28 shows a typical trace of the c_u profile using the AL electrode material. Both the peak strength and the remoulded strength were investigated. However, in subsequent plots, only the peak strength will be shown for ease of comparisons since it is the peak strength that governs the behaviour of the pipe. Figure 4- 29 shows the undrained strength profile of the soil samples before the EK treatment including the average c_u. The strength profiles lie in a narrow band generally within +/- 15%. Figure 4- 30 and Figure 4- 31 show the c_u profile at LC1 and LC2 respectively after the EK treatment. At LC1 where the least effect is expected to occur, the maximum increase in c_u is measured for the FE electrode while the least increase was recorded using AL electrodes.

Maximum effect of EK is observed at LC2 where AL causes up to 600% increase in strength. About 200% and 100% increase is measured for FE and CU electrodes respectively. The peak c_u is also directly related to the applied voltage. It does appear from the plots that FE electrodes actually stiffen the soil at the surface while the AL stiffens more at greater depth. It also indicates that the EK effects using AL reaches down to the base of the tank.

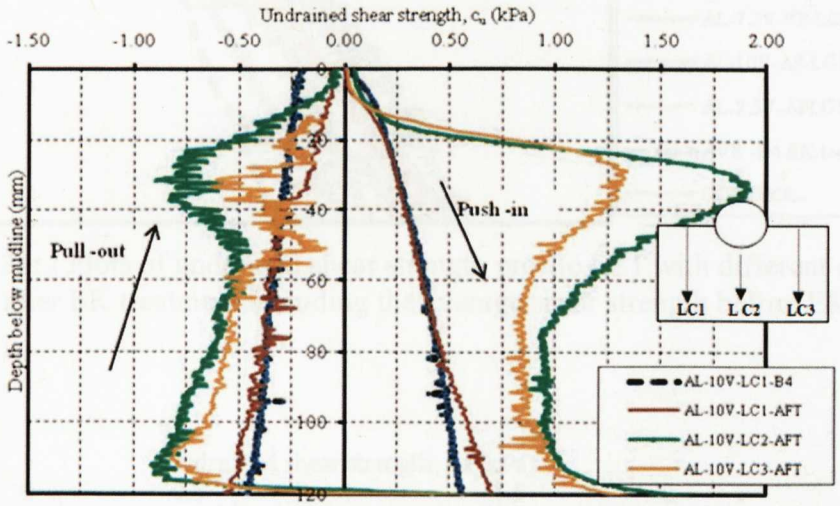

Figure 4- 28: Typical undrained shear strength profile before and after EK treatment using different electrode materials

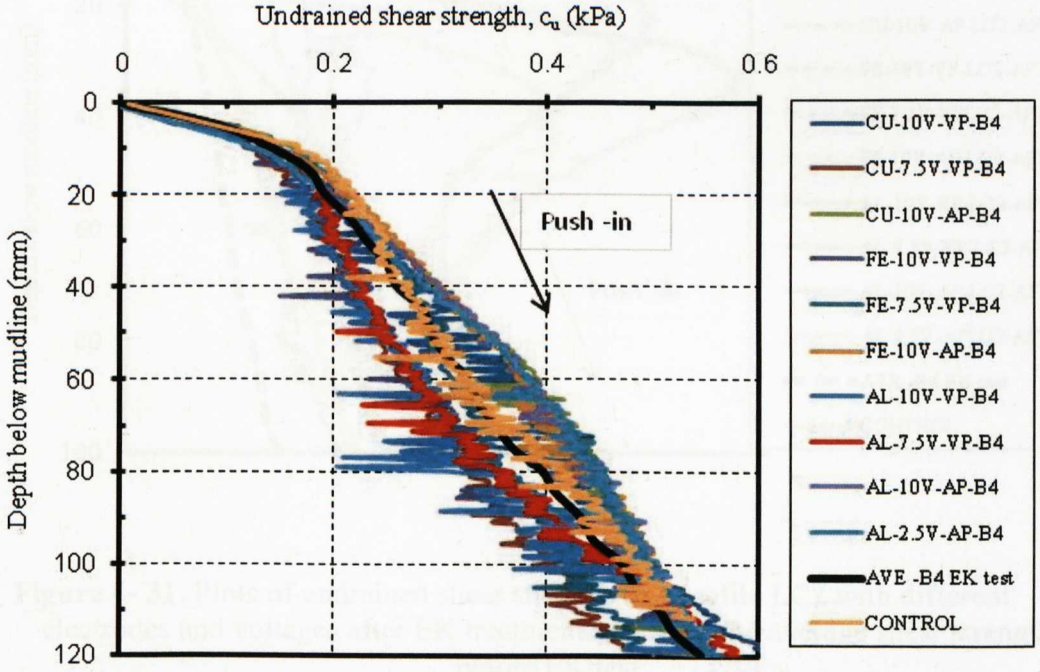

Figure 4- 29: Plots of undrained shear strength profile for all tests with different electrodes and voltages before EK treatment of the soil

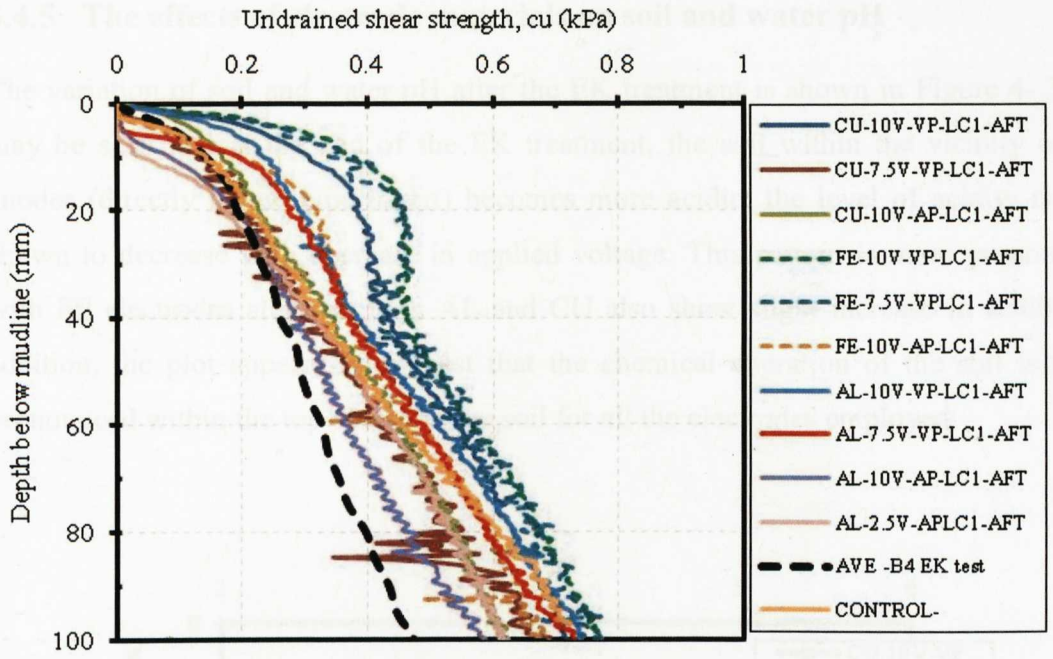

Figure 4- 30: : Plots of undrained shear strength profile LC1 with different electrodes after EK treatment including the average shear strength before EK test

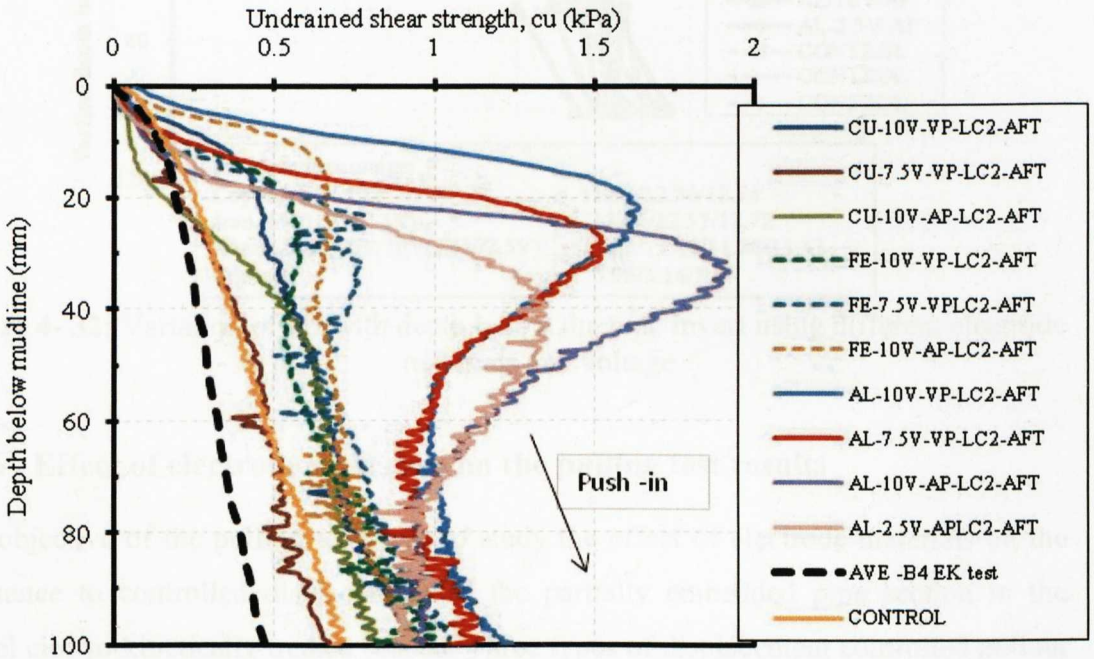

Figure 4- 31: Plots of undrained shear strength (c_u) profile LC2 with different electrodes and voltages after EK treatment including the average shear strength before EK test

4.4.5 The effects of electrode materials on soil and water pH

The variation of soil and water pH after the EK treatment is shown in Figure 4- 32. It may be seen that at the end of the EK treatment, the soil within the vicinity of the anodes (directly below pipe invert) becomes more acidic; the level of acidity is also shown to decrease with decrease in applied voltage. This pattern is more pronounced with FE electrodes although both AL and CU also show slight increase in acidity. In addition, the plot appears to suggest that the chemical alteration of the soil is more pronounced within the top 60mm of the soil for all the electrodes employed.

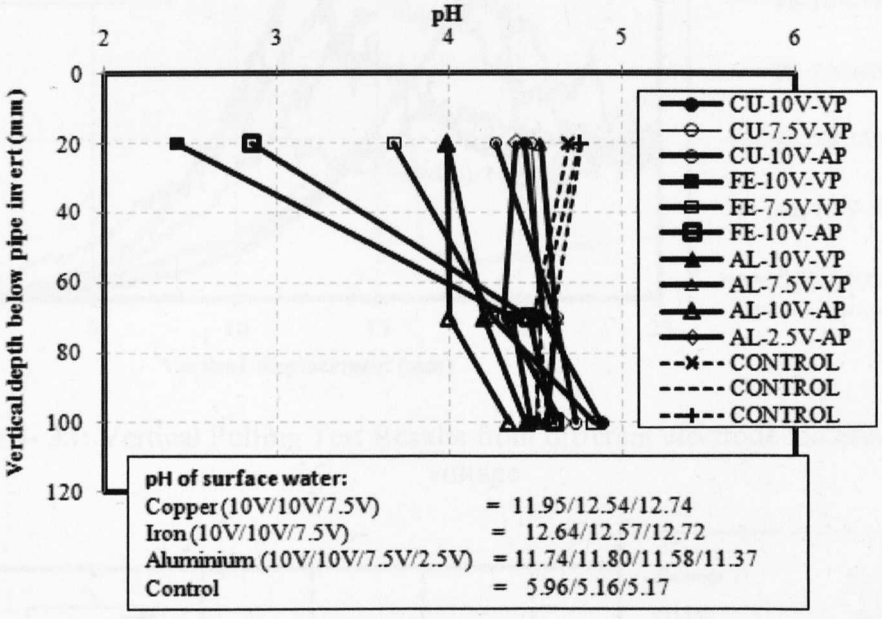

Figure 4- 32: Variation of pH with depth below the pipe Invert using different electrode materials and voltage

4.4.6 Effect of electrode materials on the pulling test results

The objective of the pullout tests was to study the effect of electrode materials on the resistance to controlled displacement of the partially embedded pipe section in the model electro-kinetically treated seabed. Three types of displacement controlled pullout out tests were conducted namely: vertical, axial and lateral pullouts as explained in detail in §3.3.6. Figure 4- 33 shows the results of vertical pullout test conducted using the three electrodes. The control test is also shown for purposes of comparisons. The peak resistance of the soil at failure is indicated with the arrow. In order to quantify the impact of the EK treatment on the soil, the peak resistances of the soil at failure are expressed as percentage of the peak from the control test at failure. The calculated

percentage increase is also included as an insert in the plot. It can be seen from the plot that while FE electrodes show the maximum increase in vertical breakout of the pipe, the AL electrodes show the least value decreasing to even a negative value (.i.e. less than the control test) at higher applied voltages.

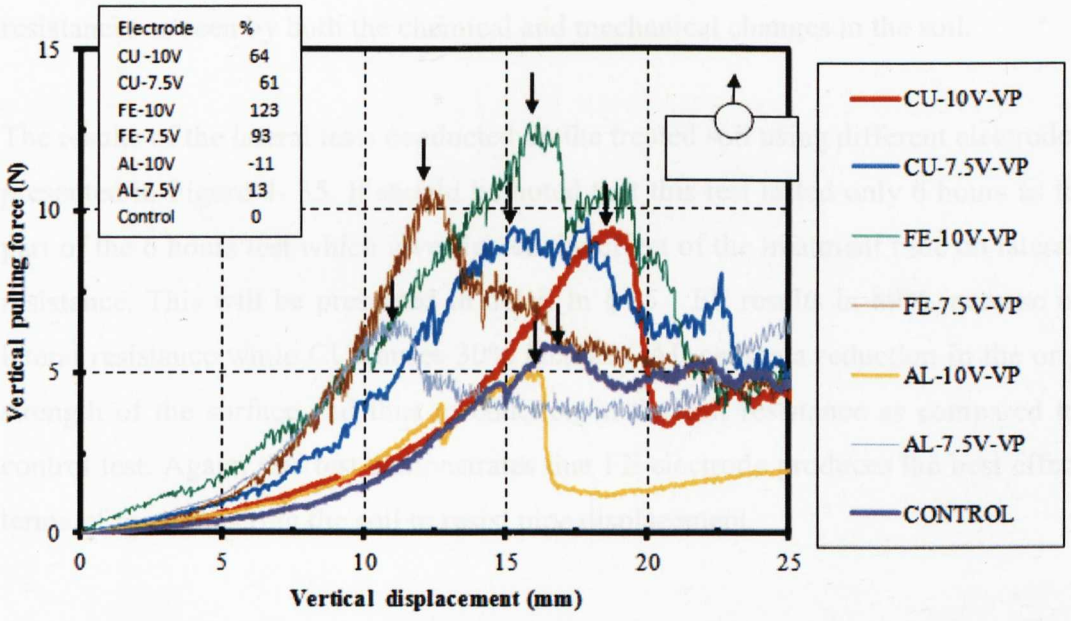

Figure 4- 33: Vertical Pulling Test Results from different electrode materials and voltage

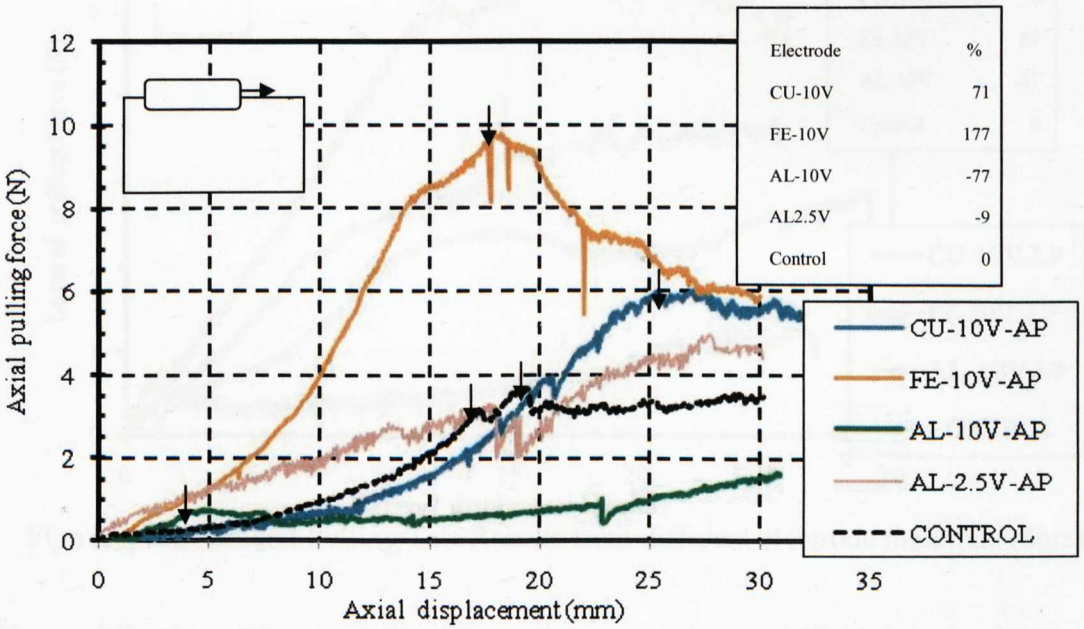

Figure 4- 34: Axial Pulling Test Results using different electrode material

Results of the axial pulling test involving the three electrodes are presented in Figure 4-34. There is in excess of 170% increase in soil resistance to axial pipe displacement using FE electrode compared to about 70% for CU electrodes. AL again shows a reduction in the pullout resistance. It should be noted here that depth of embedment of the pipe was 30mm for all the tests conducted and it is the combination of both physycal and chemical changes in the soil that lead the to the overall changes in the treated soil resistances as seen by both the chemical and mechanical changes in the soil.

The results of the lateral tests conducted on the treated soil using different electrodes are presented in Figure 4- 35. It should be noted that this test lasted only 6 hours as it was part of the 6 hours test which investigated the effect of the treatment time on lateral soil resistance. This will be presented in detail in §4.5 FE results in 89% increase in the lateral resistance while CU causes 30% increase. AL causes a reduction in the original strength of the surface and thus a reduction in the soil resistance as compared to the control test. Again, this test demonstrates that FE electrode produces the best effects in terms of re-engineering the soil to resist pipe displacement.

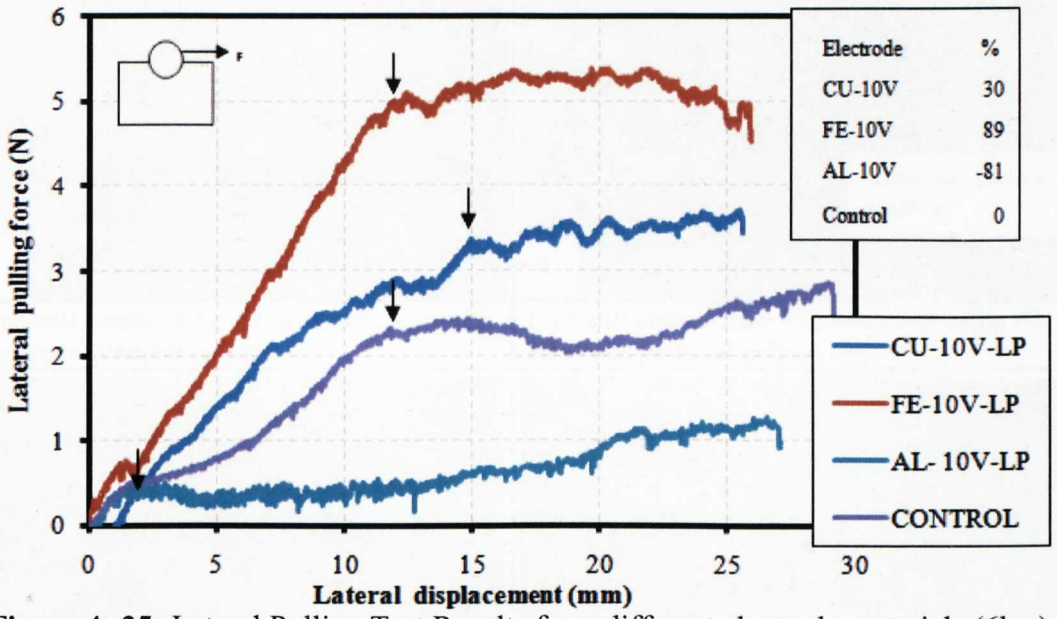

Figure 4- 35: Lateral Pulling Test Results from different electrode materials (6hrs)

The modification of the top soil was more pronounced even with visual examination of the pipe-soil contact after the pulling tests. It was observed that the treated soil was firmly attached to the pipe section as seen in Figure 4- 36 using FE and CU electrodes.

However, this was not observed during tests with AL, instead the top layer of the soil (about 12mm thick) appears much softer than the original soil before the test Figure 4-36e). For the axial pull, there is also a clear peak when using FE and CU electrodes, whereas in AL and the control tests, the soil builds up resistance due to progressive increase in the passive resistance only with significant increase in the pipe-soil adhesion.

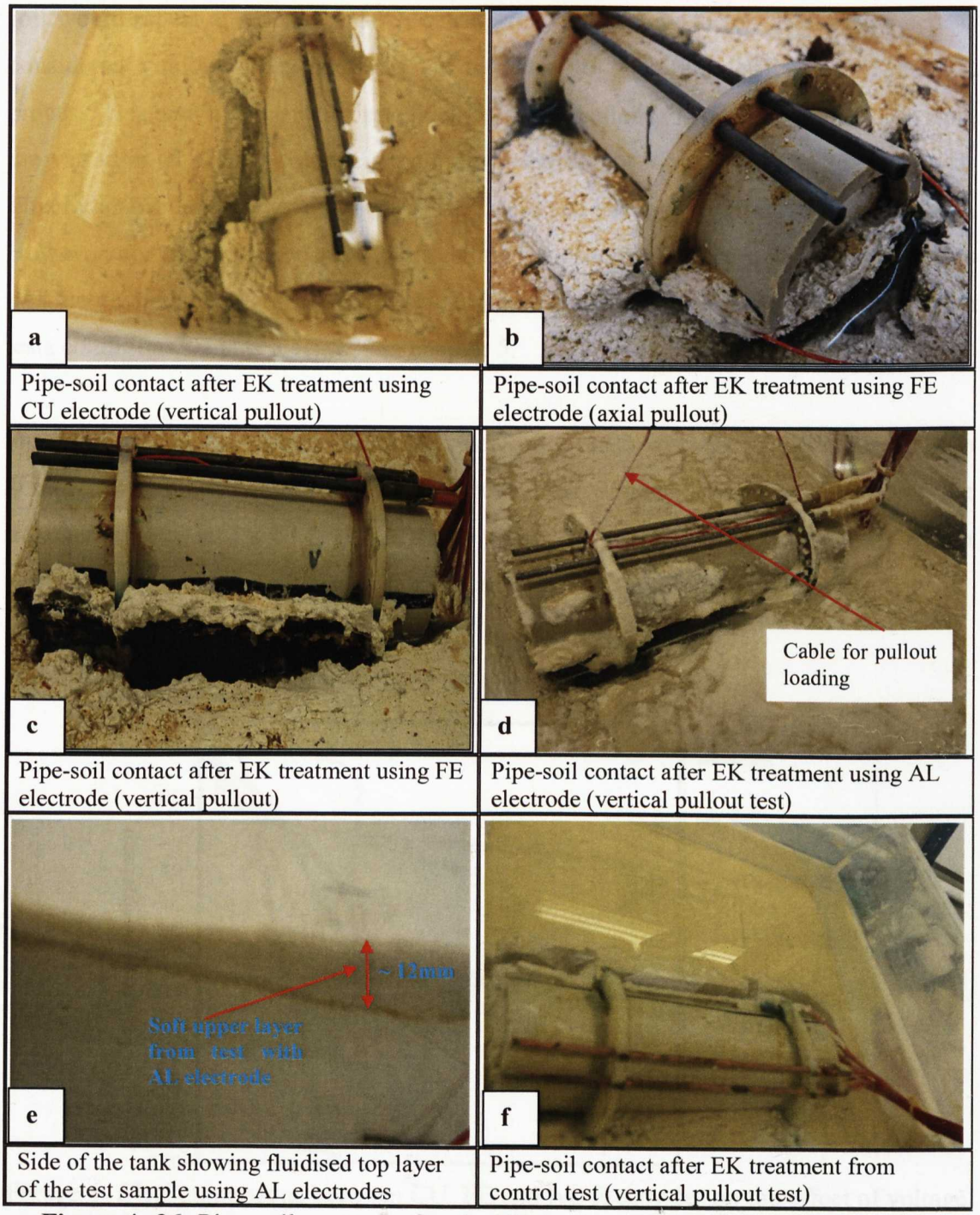

Pipe-soil contact after EK treatment using CU electrode (vertical pullout)

Pipe-soil contact after EK treatment using FE electrode (axial pullout)

Pipe-soil contact after EK treatment using FE electrode (vertical pullout)

Pipe-soil contact after EK treatment using AL electrode (vertical pullout test)

Side of the tank showing fluidised top layer of the test sample using AL electrodes

Pipe-soil contact after EK treatment from control test (vertical pullout test)

Figure 4- 36: Pipe-soil contacts after the EK treatment using different electrodes

4.5 Effect of treatment time

In this section, the results of the tests conducted to study the effect of the duration of EK treatment are presented. The effects of treatment on the development of soil strength using the three electrodes were studied by exposing the soil to 6hours, 12 hours and end of (i.e. till zero current was reached) EK treatment. It should be noted that this assessment was made with respect to the specific dimensions of the electrodes employed in the small scale tests. However, it is assumed that that these changes in the soil would repeat at an enlarged scale using relevant scaling factor. This assessment is considered vital in order to determine the time to maximum efficiency of the EK process. It is also necessary for practical field applications. Typical c_u profiles showing the variation of c_u with treatment time are presented in Figure 4- 37 to Figure 4- 41. This indicates that the development of the undrained shear strength increases with time. However, for the AL electrodes, the treatment appears to be completed from 12 hours treatment which may suggest that this could be the effective treatment duration for these tests conditions. This is discussed in chapter 5.

From the c_u profile in Figure 4- 39 (AL electrodes only), average strength over the top 30mm showed a higher c_u than the average over 75mm. This is because after the treatment, the c_u increased from the top to a maximum of about 1.9kPa at about 35mm depth before gradually reducing again to about 1kPa at approximately 75mm.

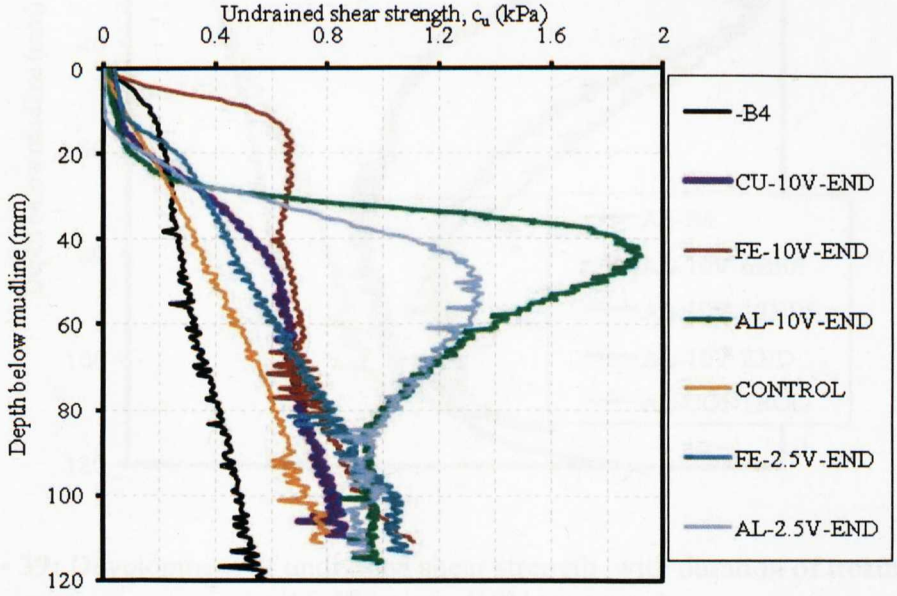

Figure 4- 37: Comparisons between CU, FE and AL Electrodes on the effect of voltage on total treatment time

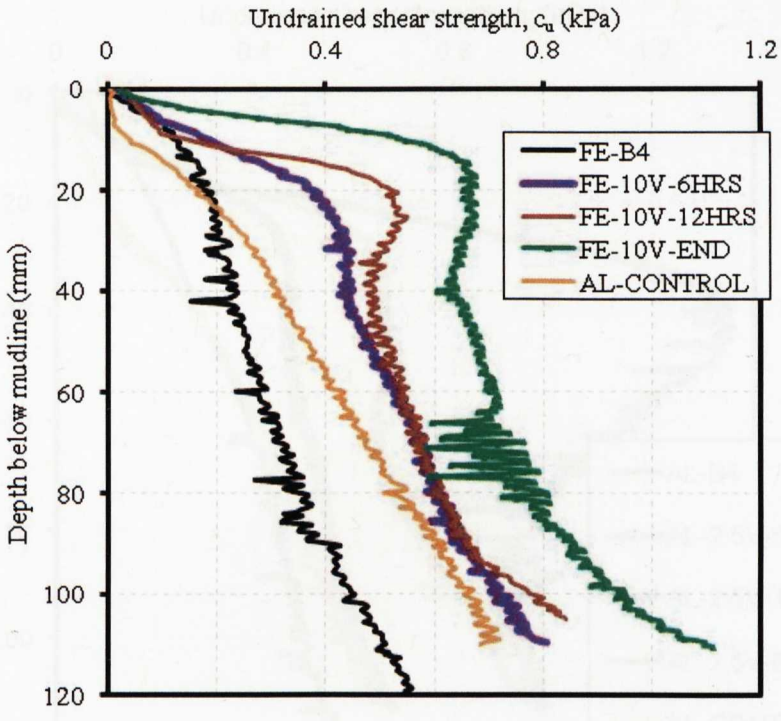

Figure 4- 38: Variation of c_u with duration of treatment for FE-Electrode (10V treatment) Test series TV-DT

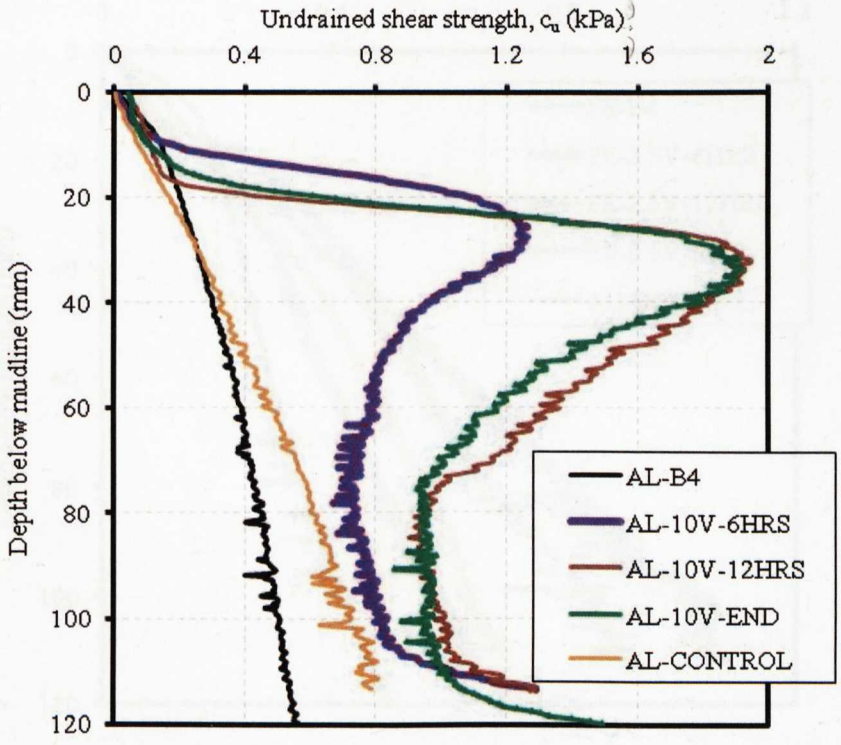

Figure 4- 39: Development of undrained shear strength with duration of treatment for AL-Electrode (10V treatment)

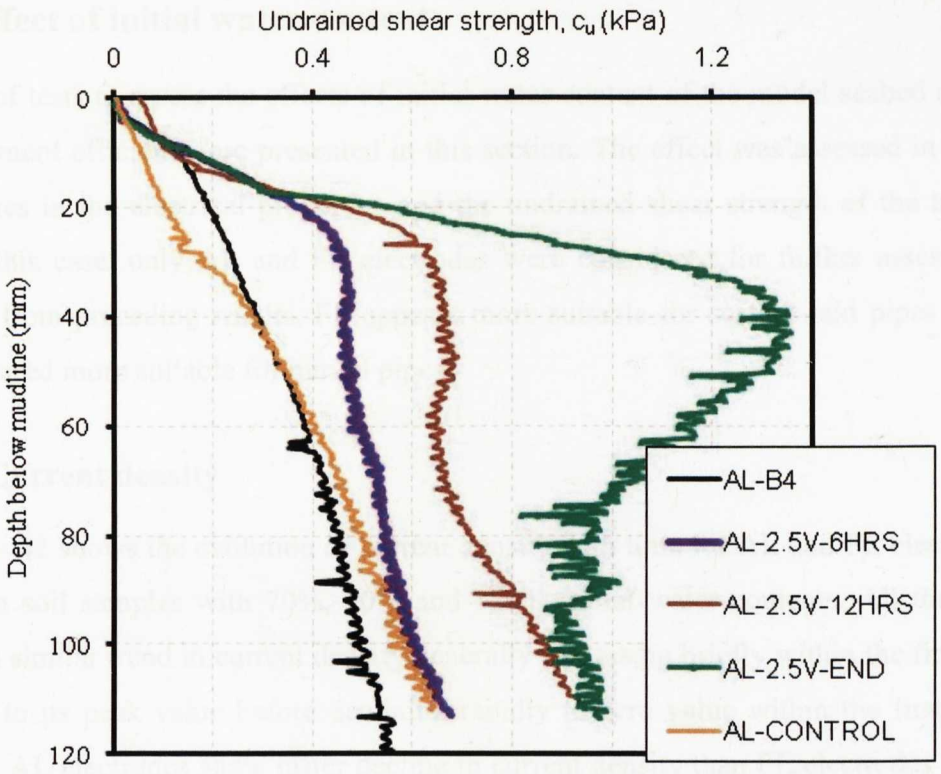

Figure 4- 40: Variation of c_u with duration of treatment for AL-Electrode (2.5V treatment)

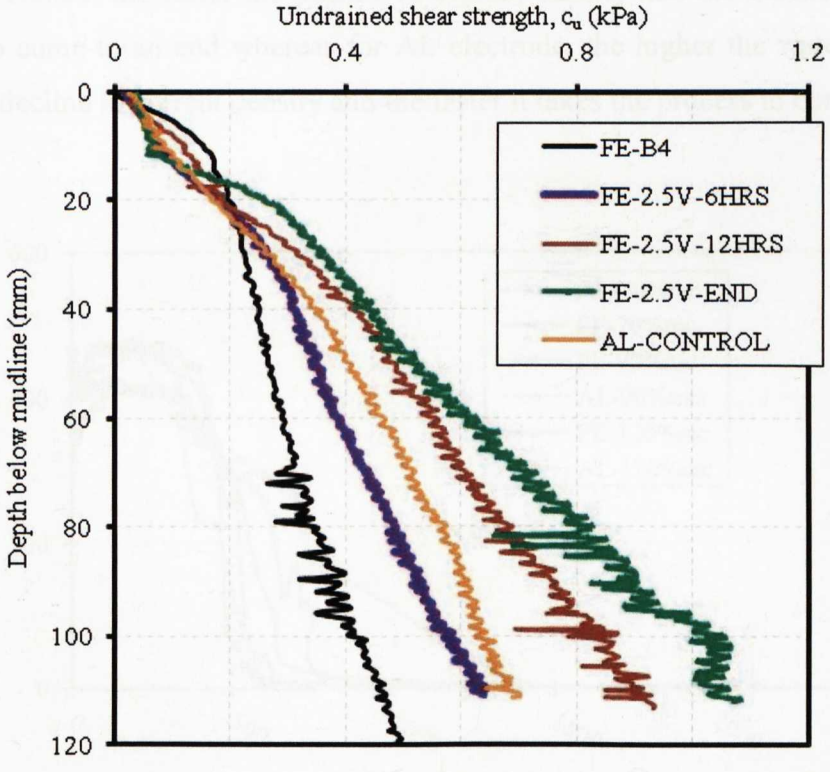

Figure 4- 41: Variation of c_u with duration of treatment for FE-Electrode (2.5V treatment)

4.6 Effect of initial water content

Results of tests to assess the effects of initial water content of the model seabed on the EK treatment efficiency are presented in this section. The effect was assessed in terms of changes in the electrical properties and the undrained shear strength of the treated soil. In this case, only AL and FE electrodes were considered for further assessment because from preceding results, FE appears more suitable for surface-laid pipes while AL appeared more suitable for buried pipes.

4.6.1 Current density

Figure 4- 42 shows the evolution of current density with time for AL and FE electrodes tested on soil samples with 70%, 90% and 120% initial water contents. All the tests exhibit a similar trend in current density generally increasing briefly within the first 500 minutes to its peak value before declining rapidly to zero value within the first 1500 minutes. AL electrodes show faster decline in current density than FE electrodes for all the three water contents considered. It does also appear that for FE electrodes, the lower the water content the faster the decline in current density and the quicker it is for the process to come to an end whereas for AL electrode, the higher the water content the faster the decline in current density and the faster it takes the process to complete.

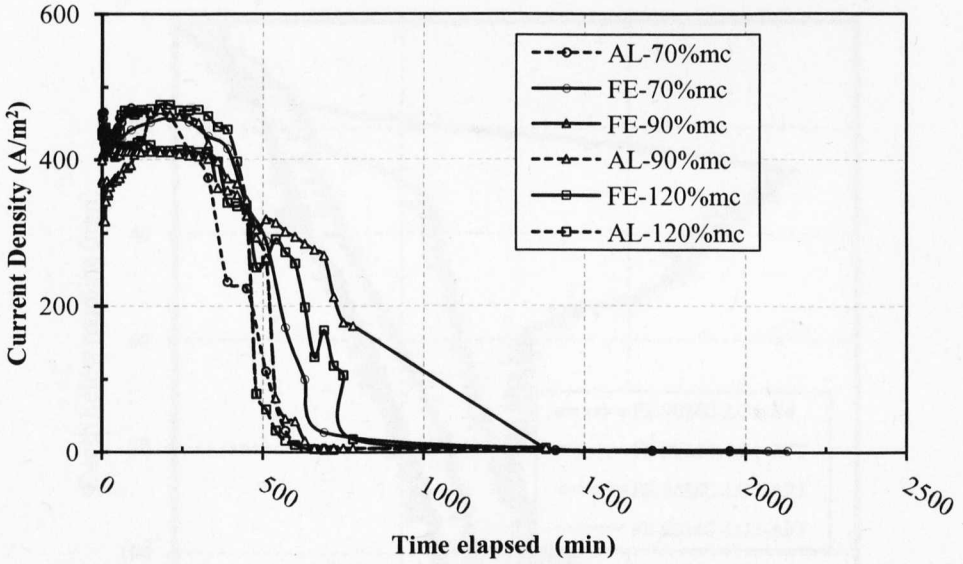

Figure 4- 42: Variation of current density with time using AL and FE at different water contents

4.6.2 Water content and undrained shear strength

Typical c_u plots showing the c_u profiles at different initial water content before and after the EK treatment are presented in Figure 4- 43 to Figure 4- 46 .

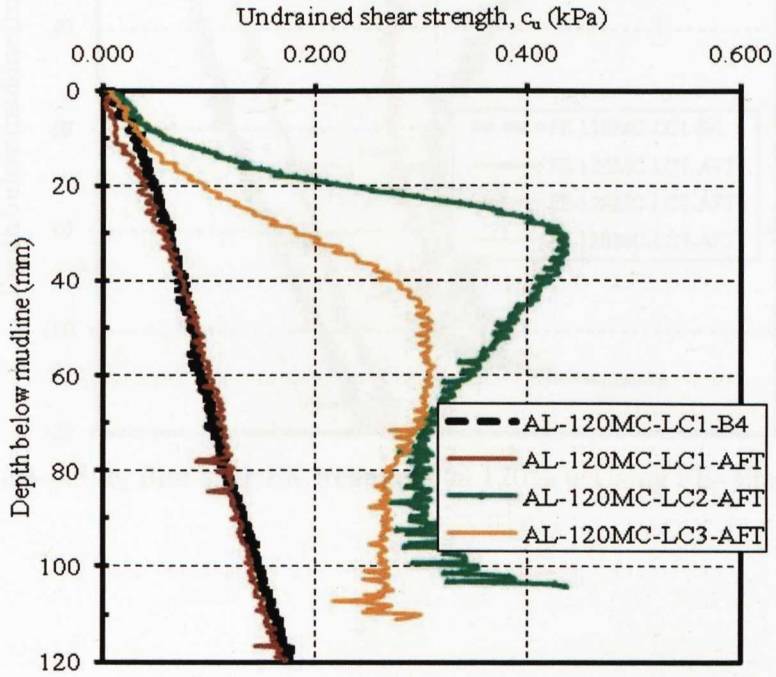

Figure 4- 43: c_u Plot after EK treatment @ 120% Water Content Using AL- Electrodes Test Series TV-WC

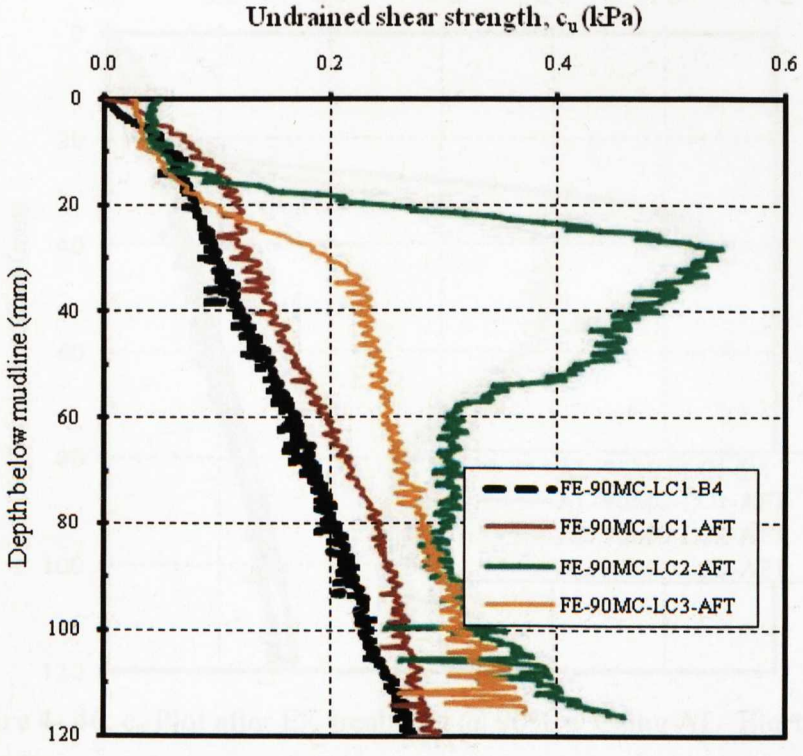

Figure 4- 44: c_u Plot after EK treatment @ 90% water content Using FE- Electrodes

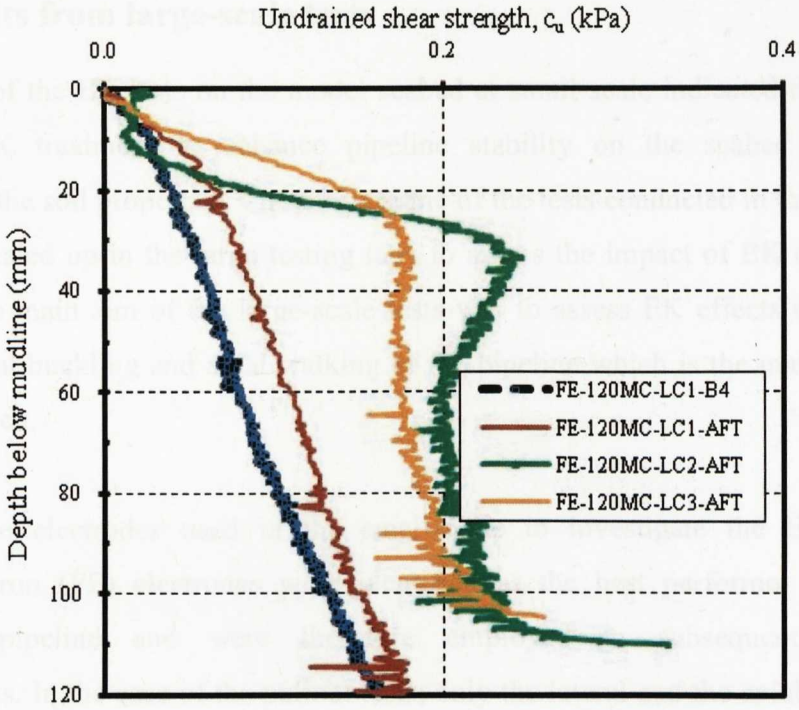

Figure 4- 45: c_u Plot after EK treatment @ 120% *w* Using FE- Electrodes

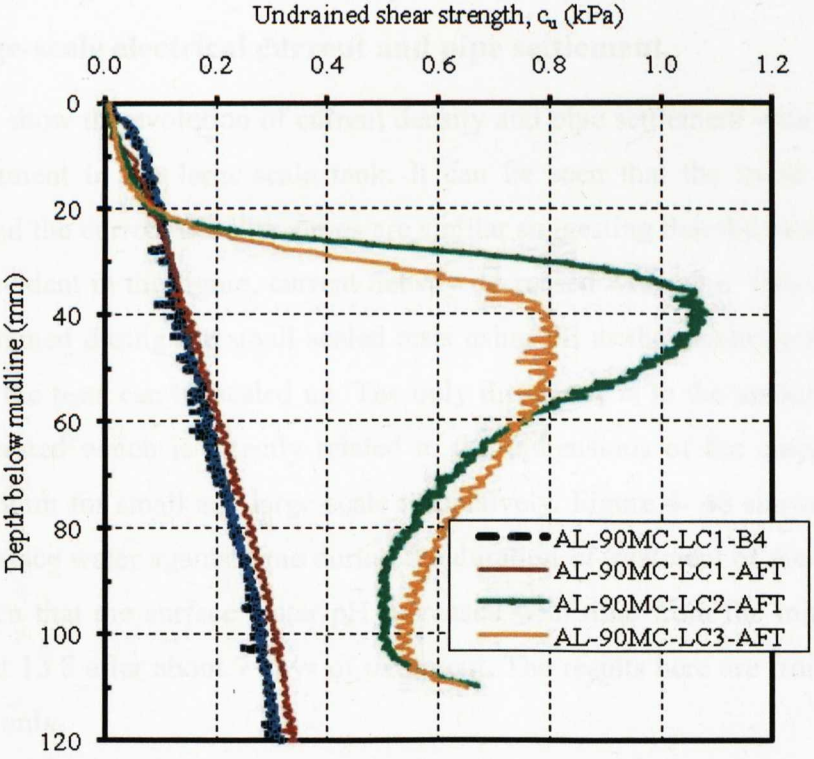

Figure 4- 46: c_u Plot after EK treatment @ 90% *w* Using AL- Electrodes

4.7 Results from large-scale tests

The results of the EK tests on the model seabed at small-scale indicated the feasibility of using EK treatment to enhance pipeline stability on the seabed through re-engineering the soil properties. Therefore, some of the tests conducted in the small-scale tank were scaled up in the large testing tank to assess the impact of EK on the model seabed. The main aim of the large-scale tests was to assess EK effects on mitigating against lateral buckling and axial walking of the pipeline which is the main aim of the whole research.

Of the three electrodes used in the small-scale to investigate the EK treatment efficiency, iron (FE) electrodes were identified as the best performer for partially embedded pipeline and were therefore employed in subsequent large-scale investigations. In the case of the pullout tests, only the lateral and the axial pulling tests were conducted in the large scale as the pipe-soil testing rig used in the pipe-soil interaction study could not simulate vertical pullout. Details of the large-scale testing facility and the pulling mechanisms are explained in §3.3. Results of the large-scale tests are presented below.

4.7.1 Large-scale electrical current and pipe settlement

Figure 4- 47 show the evolution of current density and pipe settlement with time during the EK treatment in the large-scale tank. It can be seen that the trend of the pipe settlement and the current density curves are similar suggesting that the two are directly related. As evident in the figure, current density decreased with time. This is similar to the trend obtained during the small-scaled tests using FE as the electrode thus proving the fact that the tests can be scaled up. The only difference is in the amount of current density generated which is directly related to the dimensions of the electrode used - 3mm and 7.6mm for small and large-scale respectively. Figure 4- 48 shows the plot of pH of the surface water against time during the duration of treatment of the soil sample. It can be seen that the surface water pH increased with time from the initial value of ~7.4 to about 13.8 after about 7 days of treatment. The results here are from the lateral pulling tests only.

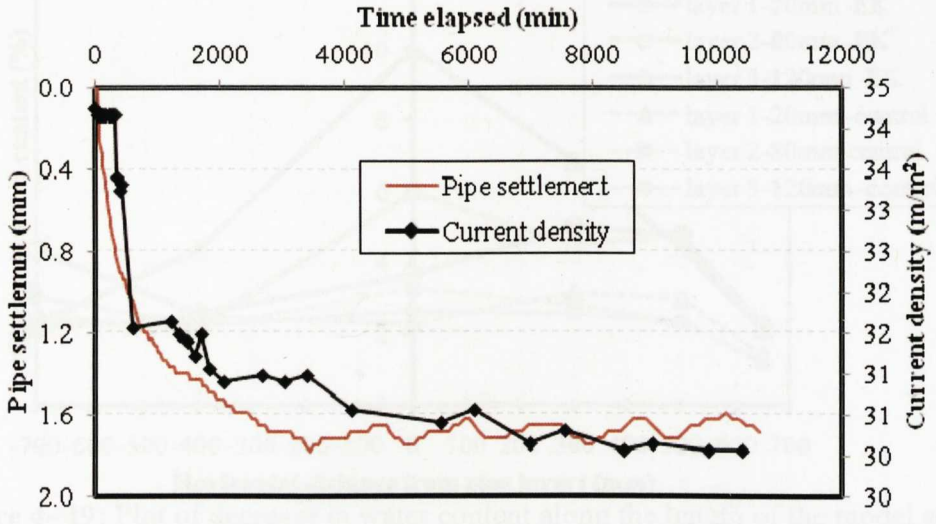

Figure 4- 47: Plot of pipe settlement and current density with time from the pilot-scale EK test

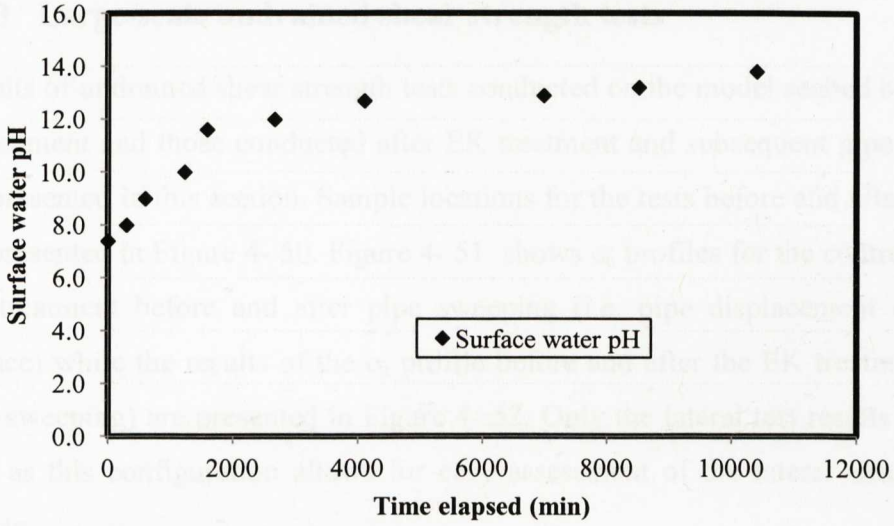

Figure 4- 48: Plot of pH with time during the large-scale EK test

4.7.2 Large-scale water content tests

Figure 4- 49 shows the plot of the decrease in water content for the electro-kinetically treated and untreated bed of clay in the large-scale tank. The initial water content across the length of the tank was almost uniform ranging between 72% at the top level to 68% at the base level. After the EK treatment, it can be seen just below the pipe invert, a decrease of 10% and 3% in water content for the EK treated and control test respectively was obtained due to EK effect. The highest decrease in water content occurs below and near the pipe invert and diminishes away from it.

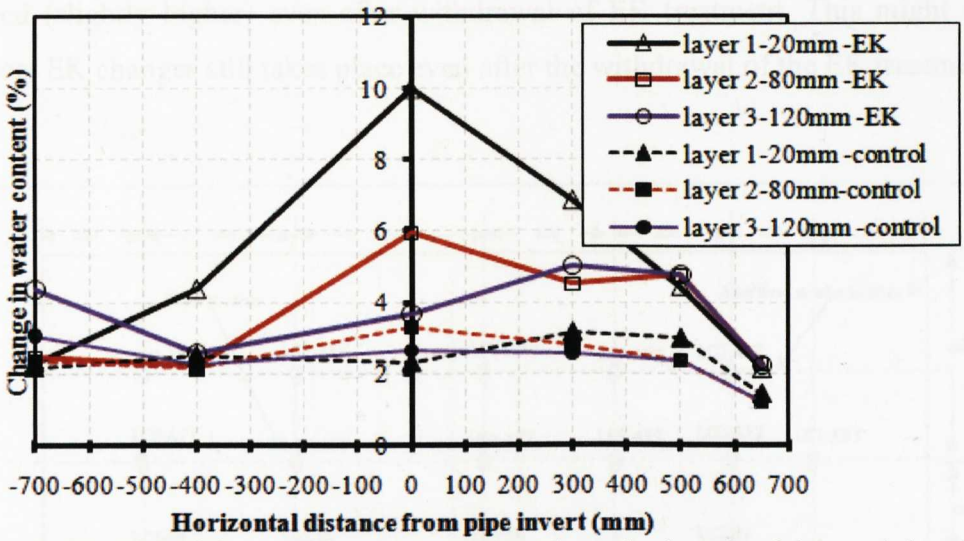

Figure 4- 49: Plot of decrease in water content along the length of the model seabed for control and after EK treatment in the large-scale tank

4.7.3 Large-scale undrained shear strength tests

Results of undrained shear strength tests conducted on the model seabed before the pipe embedment and those conducted after EK treatment and subsequent pipe displacement are presented in this section. Sample locations for the tests before and after the EK tests are presented in Figure 4- 50. Figure 4- 51 shows c_u profiles for the control test with no EK treatment before and after pipe sweeping (i.e. pipe displacement over the clay surface) while the results of the c_u profile before and after the EK treatment (and after pipe sweeping) are presented in Figure 4- 52. Only the lateral test results are presented here as this configuration allows for easy assessment of the lateral extent of the EK effects.

It can be seen from the control tests that no significant changes occur in the c_u before and after soil sweeping (and after the pipe sweeping) especially below the pipe invert. LC4-control and LC5-control denote c_u test locations after the pipe sweeping. However, significant increase in the c_u occurs in the treated soil after the EK treatment especially near the pipe invert. The lateral extent of the EK effect on the soil can also be seen from Figure 4- 53 where the chemical front migrates from the pipe invert and spreads laterally away from the pipe invert. The model seabed was left in a submerged state for three months after which c_u tests were conducted to assess the changes in strength after withdrawal of the EK application. The profiles of c_u conducted after three months on the same bed of clay are also included in the plot. It can be seen that the strength is still

retained (slightly higher) even after withdrawal of EK treatment. This might suggest that post EK changes still takes place even after the withdrawal of the EK treatment.

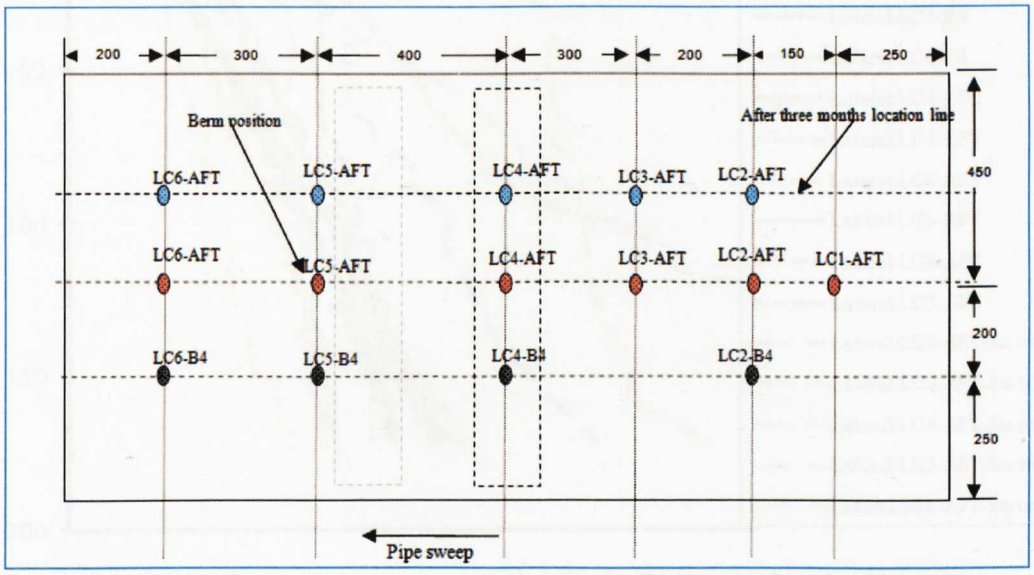

Figure 4- 50: Sample location for T-bar test before and after EK tests

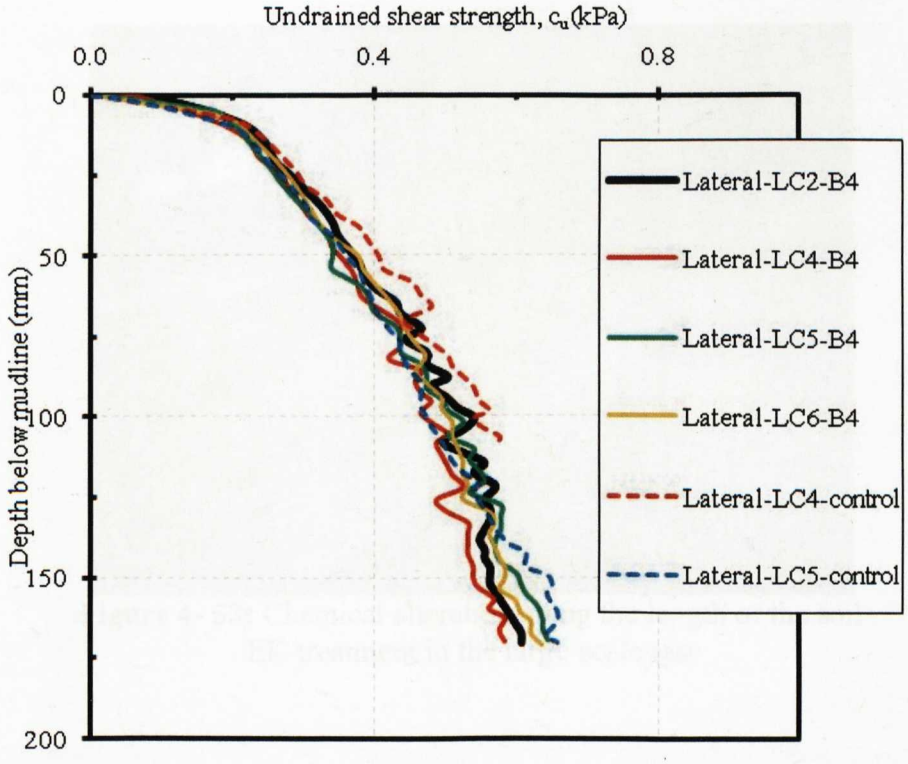

Figure 4- 51: Undrained shear strength profile for the control test in the large-scale test

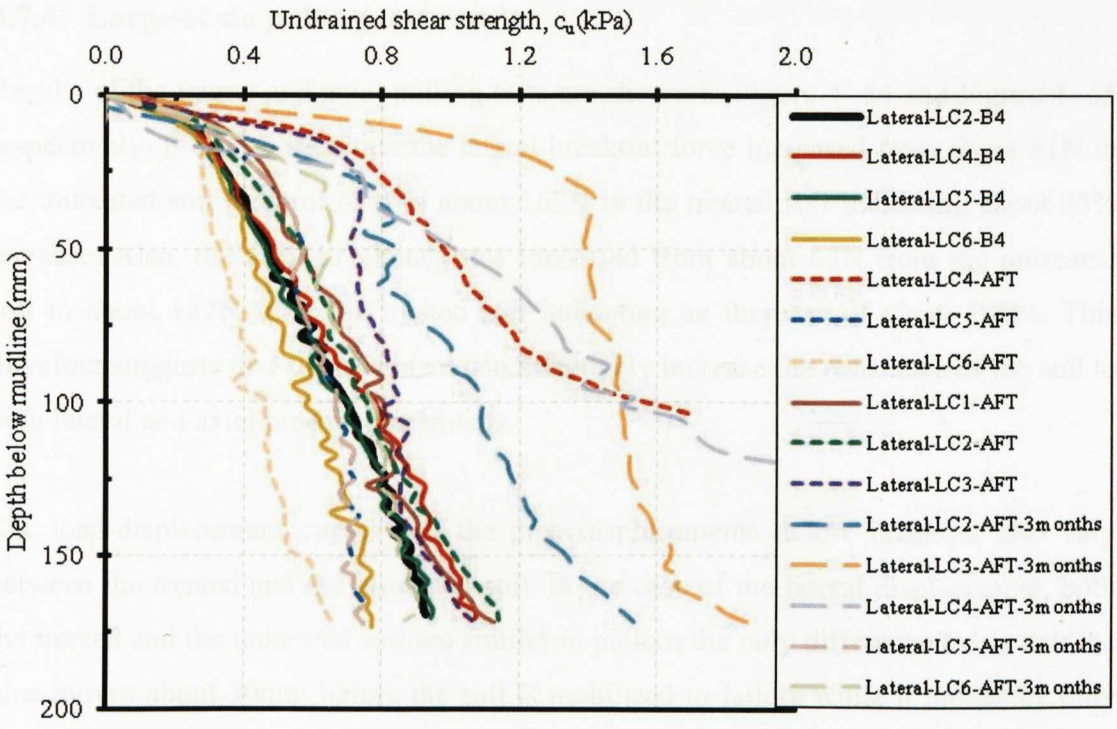

Figure 4- 52: Undrained shear strength profile before and after the EK treatment including profile after three months test

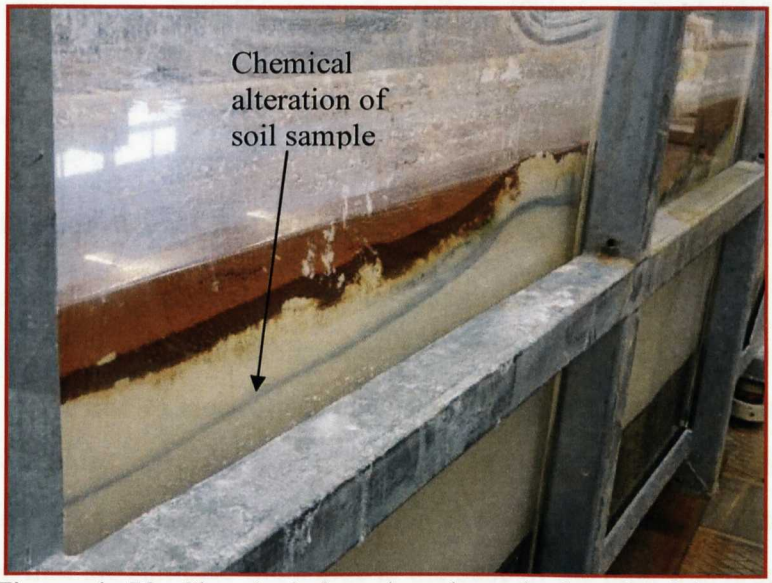

Figure 4- 53: Chemical alteration along the length of the soil EK treatment in the large-scale test

4.7.4 Large-scale pulling test results

Results of the lateral and axial pulling tests are shown in Figure 4- 54 and Figure 4- 55 respectively. It can be seen that the lateral breakout force increased from about 81N in the untreated soil (control test) to about 162N in the treated soil indicating about 98% increase. Also, the axial breakout force increased from about 63N from the untreated soil to about 182N from the treated soil indicating an increase of about 190%. This therefore suggests that EK treatment can effectively increase the resistance of the soil to both lateral and axial pipe displacements.

The load-displacement curves and the pipe displacements before breakout also vary between the treated and the untreated soil. In the case of the lateral displacement, both the treated and the untreated soil are similar in pattern the only difference being that the pipe moves about 30mm before the soil is mobilised to failure while it moves by only 9mm before failure in the control test. This is possibly due to stiffening of the soil around the pipe due to EK effect. On the contrary, there is a distinct difference between the axial curves for the control and treated soils. In the case of the untreated soil the resistance gradually builds up after breakout due to progressive increase in passive resistance of the soil as the berm of soil is created whereas in the treated soil, the axial resistance underwent a gradual decrease after failure. This is probably due to reworking of the area of the soil previously modified by the EK treatment as well as severing of the pipe-soil bonding.

4.7.5 Visual observations during the EK tests

Visual observations were carried out throughout the duration of the EK treatment. At the start of the test, lots of gas bubbles were released from the soil underneath the pipe to the surface water due to electrolysis of water. The volume and the frequency of the gas bubbles were also observed to reduce with time. After the EK test, the soil in between the electrodes and near the pipe section was visually inspected for any changes. It was observed that the soil near the anode at the base of the pipe was much harder than that of the soil around it (Figure 4- 56). Water content testing of the sample gave w of 27% (~43% decrease in w). This was firmly adhered to the pipe section. The anodes also show considerable level of corrosion with the overcall diameter decreasing from 7.9mm to about 5.6mm, approximately 29% reduction. It should be noted here that the

corrosion of the anode should reduce the overall weight of the pipe and hence the pulling force may likely have been reduced.

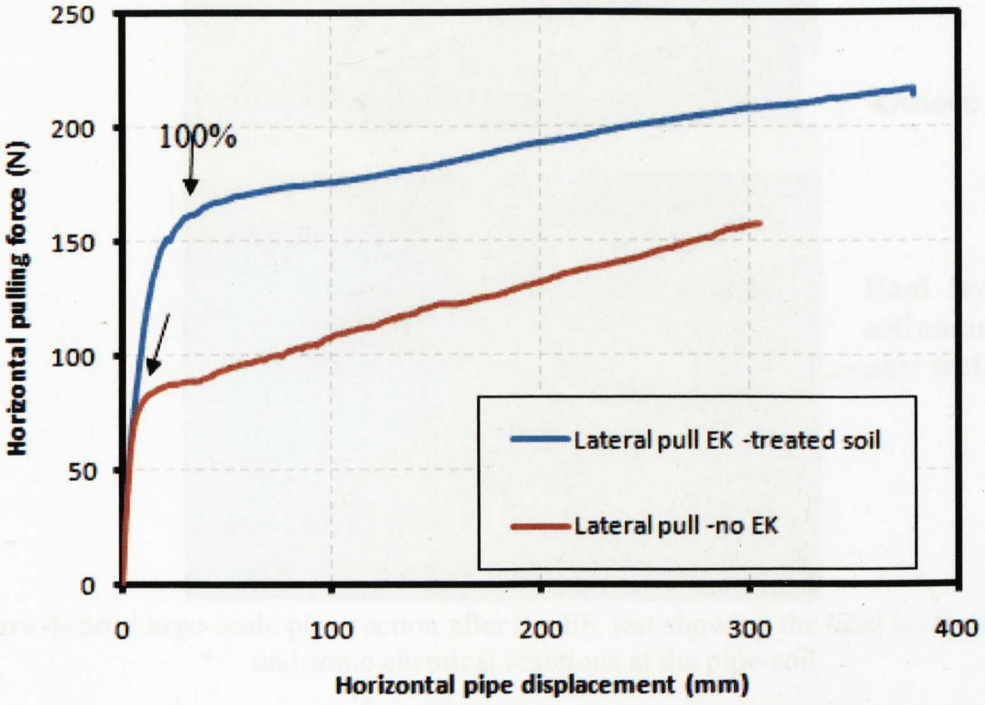

Figure 4- 54: Large scale lateral pulling test result

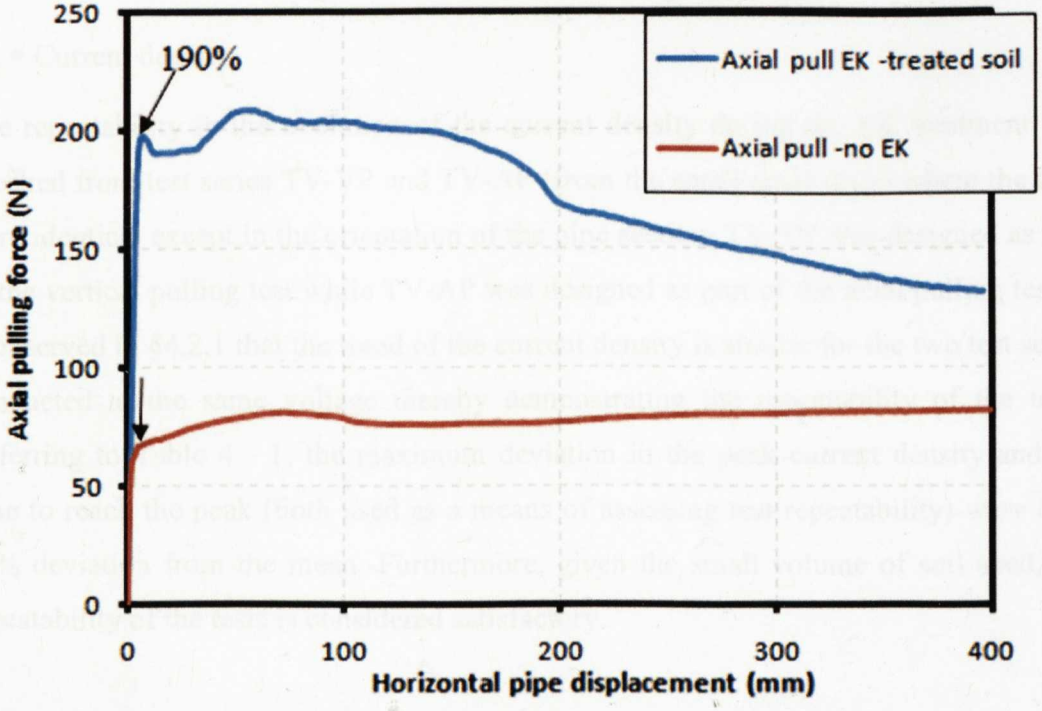

Figure 4- 55: Large-scale axial pulling test result

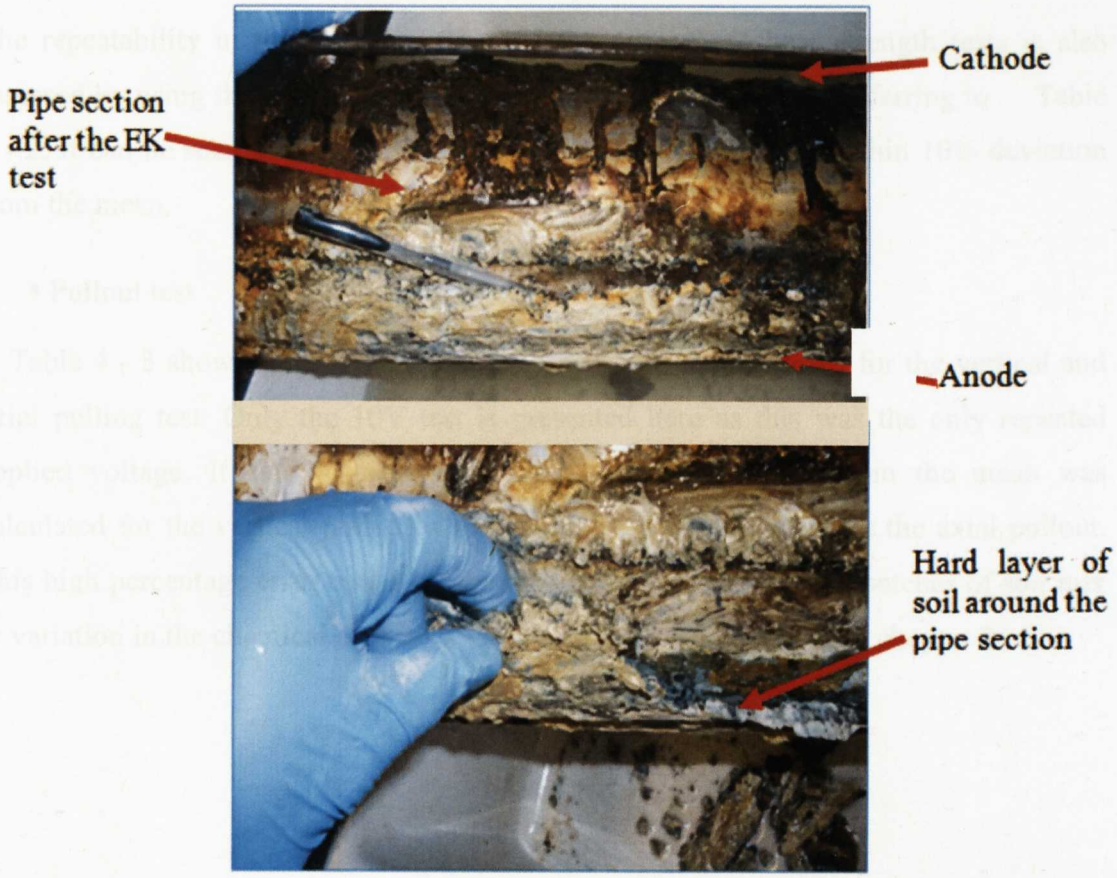

Figure 4- 56: Large-scale pipe section after the EK test showing the hard layer of clay and some chemical reactions at the pipe-soil

4.8 Reproducibility and repeatibility of the test results

- Current density

The repeatability in the evolution of the current density during the EK treatment was checked from test series TV-VP and TV-AP (from the small-scale tests) where the tests were identical except in the orientation of the pipe section. TV-VP was designed as part of the vertical pulling test while TV-AP was designed as part of the axial pulling test. It is observed in §4.2.1 that the trend of the current density is similar for the two test series conducted at the same voltage thereby demonstrating the repeatability of the tests. Referring to Table 4 - 1, the maximum deviation in the peak current density and the time to reach the peak (both used as a means of assessing test repeatability) were both 10% deviation from the mean. Furthermore, given the small volume of soil used, the repeatability of the tests is considered satisfactory.

- Water content and undrained shear strength

The repeatability in the water content and the undrained shear strength tests is also assessed by using the two results from series TV-VP and TV-AP. Referring to Table 4 - 2, it can be seen that both the water content and the c_u were within 10% deviation from the mean.

- Pullout test

Table 4 - 3 show the comparison of the maximum pullout force for the vertical and axial pulling test. Only the 10V test is presented here as this was the only repeated applied voltage. It can be seen here that the 11% deviation from the mean was calculated for the vertical pullout while about 47% was recorded for the axial pullout. This high percentage error could be due to the effect of variation in batches of soil mix or variation in the chemical activities within to be discussed further in chapter 5.

Table 4 - 1: Comparison of the peak in current density and time to attain the peak during EK treatment

Applied voltage (V)	Peak current density (A/m^2)				Time to peak in current density (minute)				Error computations					
	Test series								Average peak	Average time to peak	Max.dev. from average peak	Max dev. From average time to peak	% dev-Peak	% dev-Time to peak
	TV-VP	TV-AP	TV-A	TV-EM	TV-VP	TV-AP	TV-A	TV-EM						
10	102	94	114	94	1940	2370	1850	1740	101	1975	13	395	13	20
12.5	127	148			1820	1460			138	1640	11	180	8	11
15	306	220			1760	1100			263	1430	43	330	16	23
17.5	470	425			620	470			448	545	23	75	5	14
Average deviation (error)													10	10

Table 4 - 2: Comparison of water content and undrained shear strength during EK treatment

Water content (%)			Undrained shear strength (c_u) kPa		Error computations					
Applied voltage	Test series				Average w	Ave c_u	Max dev. from Ave-w	max dev from Ave-c_u	%Dev-w	%Dev-c_u
	TV-VP	TV-AP	TV-VP	TV-AP						
10	13	10	0.23	0.27	12	0.25	2	0.02	13	8
12.5	11	10	0.28	0.31	11	0.30	1	0.02	5	5
15	12	10	0.38	0.32	11	0.35	1	0.03	9	9
17.5	12	13	0.33	0.37	13	0.35	1	0.02	4	6
								Average deviation error	8	7

Table 4 - 3: Comparison of maximum vertical and axial pullout forces during EK treatment

Applied voltage (V)	Vertical pullout force (N)		Axial pullout force (N)			Error computations					
	Test series					Average peak	Average time to peak	Max.dev. from average peak	Max dev. From average time to peak	% dev-Peak	% dev-Time to peak
	TV-VP	TV-A	TV-EM	TV-AP	TV-EM						
10	12	11	9.3	16.5	6.1	11	11.25	1	5.25	11	47
									Average deviation (error)	11	47

4.9 Summary of Findings

Overall the results of the investigation revealed the following:

a) Current density and soil settlement

- The evolution of current density during the EK treatment occurs in four stages and the effect of voltage is more noticeable in the second phase where the peak occurs.
- The peak occurs sooner for higher applied voltage than lower voltage.
- This trend is also noticed in the large-scale test where FE electrodes were used. This suggests that the effect can be scaled up
- There is a gradual increase in pipe settlement with increase in applied voltage although the effects appear less significant from about 5V application.
- It is suggested from the results that increasing the applied voltage can compensate for increasing the number of anodes.
- If the number of anodes is less than three, the EK effects on the soil are minimal.
- Gradual settlement of the pipe section occurred using CU and AL electrodes while slight pipe uplift occurred using FE electrodes, the higher the applied voltage the higher the uplift.
- FE electrode completes the EK process quicker than AL and CU.
- For FE electrodes, the lower the initial water content the faster the decline in current density and the quicker it takes for the process to complete whereas for AL electrodes the higher the water content the faster the decline in current density and the quicker it takes the process to complete.

b) Changes in water contents

- Maximum decrease in water content occurs below the pipe invert and reduces laterally away from it. This pattern is not very prominent at greater depth within the soil mass.
- The effect due to consolidation alone from the control test show very minimal decrease in water content.
- The decrease in water content appears to converge at 100mm depth for applied voltage greater than 12.5V
- Very little correlation exists between applied voltage and decrease in water content. This could suggest that the overall dewatering of the soil depends on other factors

and not entirely on the applied voltage. For example, as long as the EK process is allowed to progress to completion irrespective of the applied voltage, the overall dewatering will be significant especially in the top layer.

- Results suggest that for most of the recorded maximum pipe settlement, the maximum decrease in water content is between 10 and 14%. This is not in agreement with the theoretical basis that the higher the settlement the more the decrease in water content.
- At the top soil level, the maximum decrease in water content is obtained using FE electrodes and less using AL electrode. However, in the second layer, AL electrodes record the maximum decrease in water content.

c) Undrained shear strength

- Significant increase in undrained shear strength occurs after EK treatment with the maximum effect occurring below the pipe invert and reducing laterally and with depth down to about 80mm.
- FE electrodes appear to stiffen the soil at the top level while AL electrode stiffens the soil at lower level. The increase in strength using AL electrodes reaches down to the base of the testing tank.
- Increase in undrained shear strength during EK treatment is water content dependent and thus the effects will be site condition dependent.
- The large-scale test also confirms increase in the undrained shear strength due to EK treatment.

d) Soil pH

- Lower pH (acidic conditions) occurs directly below the pipe invert and the pH gradually increases with depth.
- The higher the applied voltage the lower the pH at the base of the pipe
- Of the three electrode materials used, FE give most acidic condition followed by CU and then AL.
- Surface water pH increase with time of treatment from neutral state to alkaline
- Chemical alteration of the soil is more pronounced within the top 60mm.

e) Pullout test

- There is between 70% and 210% increase in vertical pullout and between 90% and 209% increase in axial pullout due to EK treatment effect. In all, the two pulling tests indicate an average of about 140% increase in pipe resistance to displacement as a result of EK treatment.
- FE electrodes show the maximum increase in the three pullout tests while AL electrodes show the least.
- FE electrode appears to give the maximum pipe-soil adhesion force
- A combination of both physical and chemical changes leads to the overall changes in the treated soil resistance to pipe displacement.

4.10 Concluding remarks

In this chapter, results of investigations to study the feasibility of using electro-kinetic processes to increase the stability of partially embedded pipe section have been presented. The results have provided some of the benchmark basis for further work in this area. Some significant trends relating some of the variables have also been identified although this is considerably obscured by the rather low strength of the soil samples used in this study. Reasonable repeatability between experiments suggests that EK phenomenon can be employed to reengineer subsea soils and thus increase the stability of subsea pipelines. Detail analysis and interpretation of these results in relation to its application to offshore pipeline stability will be discussed in chapter 5.

Chapter 5

ASSESSMENT OF THE IMPACT OF ELECTRO-KINETIC TREATMENT OF SOIL ON THE PIPELINE STABILITY

5.1 Introduction

The feasibility of using electro-kinetic (EK) treatment of soil to enhance the stability of subsea pipelines has been demonstrated from the experimental results presented in chapter 4. In this chapter analysis and discussions of the results obtained in chapter 4 are presented with the aim of assessing the effectiveness of the EK treatment process and its potential application to increase the stability of subsea pipelines. The chapter initially begins by discussing the electrical aspect of the tests conducted by analysing the current density and the influence of voltage. Then the spatial changes in water content are discussed followed by the development of undrained shear strength due to EK treatment of the model seabed. The effects of the EK treatment on resistances of the soil to various pipes displacements are discussed followed by the effects of treatment time. Finally, an assessment of the zone of influence including the power requirement of the EK treatment on the soil is discussed.

5.2 Electrical aspect and pipe/soil settlement

The main driving force in the EK process is the current density (Shang and Dunlap,1996). This was observed to vary during the EK testing period depending upon the electrode material used and the applied constant voltage gradient. Figure 4- 1, Figure 4- 17, Figure 4- 23, Figure 4- 42 and Figure 4- 47 of chapter 4 all showed the current density with time and are used in the analysis and discussions regarding the evolution of current density (J) in the various tests conducted.

From the results of this study, the entire process of the generation of current (or current density) during the treatment process may be broken down into four main stages or

phases namely: 1) initial current density which is obtained immediately after the prescribed voltage is applied across the sample, 2) initial low in current density (this is observed only with copper electrodes), 3) the maximum or peak current density during the treatment process and 4) the residual current density. The position and occurrence of these points on the current density curves are directly related to applied voltage and the electrode materials used. Figure 5 - 1 shows an idealised form of the current density curve showing the points mentioned above with the peak in the current density increasing with increasing voltage and the residual current density decreases with decreasing voltage.

The most noticeable difference between the two idealised curves is the presence of an initial drop in current density obtained when CU electrodes are used. Upon the application of the voltage across the sample using CU electrodes, the current density immediately rose to a very high value before dropping to a low value. This is the first stage (point 1 to 2 in the idealised curve). The actual reason for this variation in current density is not very clear at this point but could be due to the initial migration of the free ionic species on the surface of the electrodes. It is well known that the generation of current density is controlled by the migration of ionic species to the opposite electrode during EK treatment (Mitchell and Soga,2005) and (Wan and Mitchell,1976). It is also likely that this could be due to the surface chemistry of the CU electrodes compared to the FE and AL electrodes. In contrast, FE and AL electrodes showed a gradual rise in current density within the first 300 minute with no initial drop in current density before reaching the peak value.

Nevertheless, this first stage in current density generation is assumed not to have had a significant effect on the treatment process due to its short duration - less than 30 minutes for a 6000 minutes treatment time. This unique response (i.e. within the first stage) in current density using CU electrodes is not reported by previous researchers. This is the only study that involves a partially embedded object where the cathode is not in contact with the soil sample. This is therefore subject to further investigations.

The second stage (point 2 to 3 for CU electrodes) is characterised by a sharp increase in current density. Similar observations (the second stage) were reported by Lo et al. (1991) and Wan and Mitchell (1976) - that after the initial decrease in current to a

minimum value, the current starts to increase again, thereafter it gradually decreases. The third stage- point 3 to 4 shows a rapid fall in current density before the onset of the final stage (point 4 to 5) which is characterised by very low current density as the process continues to the end.

Although the current density was very low throughout the last stage, significant chemical alterations of the soil sample continue to take place evident by the gradual increase in the size of the area of discoloration on the side of the tank even when the current was approaching zero value. It is tentatively concluded that the decrease in current density during the test does not necessarily mean that the EK process within the soil sample has ended. This is because decrease in the current density in this study usually coincides with the electrode depletion. However, some chemical reactions could still continue which might result in further modification of the soil property as explained in §2.11.3.4.

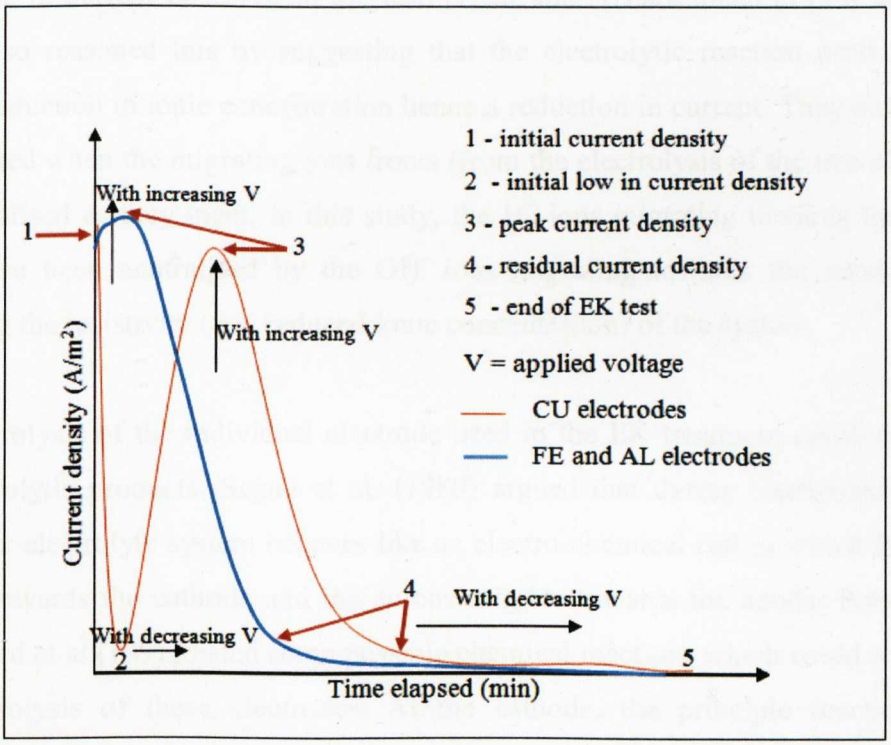

Figure 5 - 1: Idealised stages in current density generation for partially embedded pipe section during EK treatment of the ambient soil

A number of possible explanations have been postulated as to the causes of the observed decline in current density with time during the EK treatment. The most noticeable reason for this is due to the corrosion of the electrode material. In this study,

the electrodes inspection after the tests revealed considerable degradation, about 80% of the weight of the original material. Shang et al. (2004) also attributed the decline in current density to corrosion of the electrode used in their test. During EK treatment, acidic medium was generated at the anode area while alkaline medium existed at the cathode area. Mitchell (1991), Mitchell and Soga (2005) and Lo et al. (1991) also reported similar findings. Therefore, in a more aggressive saline environment, as in this study, this acidic front is aggravated by the salt water thus resulting in the rapid corrosion and decomposition of the anode with time. The rate of this decomposition is also noticed in this study to be related to the applied voltage – the higher the applied voltage the faster the decomposition and vice versa.

Some other causes also exist. Acar and Gale (1992) argued that the dissolution of clay minerals due to electrolysis and pH changes within the soil mass could reduce the current density. It is therefore possible that the dissolution of minerals within the clay mass and from the electrodes evident by the discolouration in the soil could necessitate a decrease in current observed in the test. Acar and Alshawabkeh (1996) and Hamir (1997) also reasoned this by suggesting that the electrolytic reaction products could cause a reduction in ionic concentration hence a reduction in current. They claimed that this resulted when the migrating ions fronts (from the electrolysis of the two electrodes) are neutralised as they meet. In this study, the H^+ ions migrating towards the cathode could have been neutralised by the OH^- ions migrating towards the anode thereby increasing the resistivity (.i.e. reduced ionic concentration) of the system.

The electrolysis of the individual electrode used in the EK treatment could also affect the electrolytic products. Segall et al. (1980) argued that during electro-osmosis, the clay-water electrolyte system behaves like an electro-chemical cell in which the cations migrate towards the cathode and the anions migrate towards the anode. Potter (1956) and Hamed et al.(1991) listed some possible chemical reactions which could result from the electrolysis of these electrodes. At the cathode, the principle reaction is the reduction of hydrogen from water whereas at the anode, a metal corrodes into its oxide and the oxidation of the hydroxide ions forms oxygen. These chemical reactions are also dependent on the characteristic of the pore water and material properties of the electrodes (Barker et al.,2004).

The following equations described the chemical reaction

At the cathode area

$$2H_2O = H_3O^+ + OH^- \quad 5-1$$

$$H_3O^+ + e + M = MH + H_2O \quad 5-2$$

$$MH + H_3O^+ + e \rightarrow H_2\uparrow + H_2O + M \quad 5-3$$

or $$2H_3O^+ + 2e \rightarrow H_2\uparrow + 2H_2O \quad 5-4$$

$$4H_2O + 4e \rightarrow 2H_2\uparrow + 4OH^- \text{ (from water hydrolysis)-reduction} \quad 5-5$$

M is the specific electrode material used in the EK treatment. According to Acar and Alshawabkeh (1996), the reaction will result in an increase in the concentration of hydroxide ions as well as boosting the precipitation of metallic hydroxide and the liberation of hydrogen gas.

At the anode area

$$2H_2O = H_3O^+ + OH^- \quad 5-6$$

$$OH^- + M = MHO + e \quad 5-7$$

$$MHO + OH^- = MO + H_2O + e \quad 5-8$$

$$2MO \rightarrow O_2\uparrow + 2M \quad 5-9$$

or $$4OH^- \rightarrow O_2\uparrow + 2H_2O + 4e \quad 5-10$$

$$2H_2O - 4e \rightarrow O_2\uparrow + 4H^+ \text{ (from water hydrolysis) –oxidation} \quad 5-11$$

The reactions at the anode result in the liberation of oxygen and the production of hydrogen ions. The increase in the hydrogen ions lowers the *pH* at the anode.

If the ions are not removed or neutralised, it may result in the movement of hydrogen ions (acid front) towards the cathode and the hydroxide ions (base front) towards the anode. When these two fronts meet they form a neutralised zone of very low conductivity i.e. reduced current in the system (Acar et al.,1990). The current (or current density) is proportional to the amount of metal species in the system and thus affects the ionic strength (Reddy et al.,2002). Therefore the current density decreases as the ions migrate towards their respective electrodes. The migration of these ions depends on the metal species in the electrolytic system.

The evolution of current density can be improved during the EK treatment. Bergado et al. (2003) demonstrated that current density can be increased by polarity reversal while Micic et al. (2002a), Wan and Mitchell (1976), Micic et al. (2004) and Rittirong (2006) reported an increase in current due to a combination of polarity reversal and current intermittence. However, these means of improving the generated current density were not done as part of this study since it was considered not feasible in practical field situations.

It is important to note here that since these tests were conducted using only a kaolinite-rich clay system, the mode of current generation and the responses of the soil sample to the EK treatment may differ significantly from a natural occurring soil or soil of different mineral compositions (as in different offshore petroleum basins). Grundl and Michalski (1996) conducted a test using naturally occurring calcite and illite-smectite rich glacial till and a kaolinite- rich clay system (usually used in most EK tests) and concluded that the results from the two tests differ significantly and that includes the mode of current generation. In fact, the presence of calcite in the natural clay prevents the formation of low pH conditions in the sediment pore water whereas this was not the case for the kaolinite-rich clay. This was attributed to the presence of the different minerals in the clays which causes the electrolytic system to respond so differently to applications of an electric field.

Therefore, this idealised current generation path observed in this study may only be applicable to partially embedded pipeline in a kaolin-rich clay system. Further work will be required to study the mode of current generation for soils of different species and mineralogical compositions.

In the investigations involving AL and FE electrodes at different initial water contents for soil samples, evolution of the current density also exhibited some differences. AL electrodes show a faster decline in current density than FE electrodes for all three water contents considered (.i.e. 70%, 90%, and 120%). FE electrodes showed a faster decline in current density for lower water content. According to Mitchell and Soga (2005), ions and polar molecules dissolved in the soil pores fluid migrate under an electric field. This could suggest that ionic migration through the pores of the clay sample is faster for

lower MC possibly due to the nature of the FE^{2+} ionic species in the electrolyte system. This could therefore result in rapid reduction in ionic concentration and hence the current density measured.

On the contrary, for AL electrodes, the lower the water content the slower the decline in current density. This again could be due to the speed of migration of the AL^{3+} ions species within the soil mass. The size and nature of these species could play a part. Thus, the lower the water content, the slower the migration of these ions and the slower the decline in current density during the EK treatment. Although no comparative assessments of the rate of migration of the various ionic species through different soil masses have been carried, it is likely, however, that this variation could have affected the pattern in the generation of current densities during EK treatment.

Reddy et al. (2002) demonstrated that the initial water content significantly affects the generation of current by reporting that as the initial water content increased, the current increased which makes it easier for the ionic species to migrate through the pore network of the soil sample. However, their study only focused on one electrode material – graphite. Therefore, this study gives an insight into the effects of initial water content of the test soil when different metallic electrodes materials are employed.

The magnitude of the constant applied voltage across the soil sample also affects the migration of the ionic species in the soil and hence the evolution of current density. It has been shown from the experimental results that the lower the applied voltage the slower the migration of the ions and the longer it takes for a test to come to completion. This was demonstrated by the trend in current density from CU electrodes at 7.5V and 10V which indicated that the 10V application had a shorter time to completion than the 7.5V test. For practical field application the time of treatment is very vital. It was also shown in section §4.3.1 that higher applied voltage can compensate for a larger number of electrodes although this will depend on electrode cost and the cost of power source for a given field application. It should be noted that the higher the applied voltage the faster the corrosion of the electrode due to creation of a more aggressive environment.

5.2.1 Influence of electrode materials on EK treatment efficiency

Lockhart (1983d) concluded from his test on Na-kaolinite clay that the dewatering process was not dependent on electrode materials. However, the general opinion from most researchers e.g. (Mohamedelhassan and Shang,2000; Bergado et al.,2003; Xie and Shang,2006) is that electrode materials affects the EK treatment. The effectiveness of individual electrode materials in EK applications is a function of the conductivity of the materials, the reaction of the various species released during the decomposition of the materials, and durability during the EK treatment.

Furthermore, the electro-osmotic dewatering process using different electrode types is strongly dependent on the nature of the clay mineral used and its subsequent reactions with the electrode materials used in the EK treatment. Therefore, depending on the overall chemical compositions of given offshore clay or site conditions, the product and the effects of the EK treatment on the soil will vary. Lockhart (1983c) reported that for Na-kaolinite clay, most of the electro-osmotic dewatering took place at low voltage (1V and 2V) whereas for Ca-kaolinite clay no significant dewatering took place until 10V. In addition, Al-kaolinite clay required about 25V for significant water flow to take place. Further study on different offshore soils is required in this area. Some possible chemical reactions using the three different electrodes are summarised in the following sections.

(I) Iron electrode

According to Barker et al. (2004) the possible reactions using mild steel electrode as in this study will be as follows:

Oxidation at the anode:

$Fe \rightarrow Fe^{2+} + 2e^-$

Reduction at the cathode

$O_2 + 2H_2O + 4e^- \rightarrow 4(OH)^-$

Combined

$Fe^{2+} + 2(OH)^- \rightarrow Fe(OH)_2$ Ferrous hydroxide

Further reaction:

$Fe^{2+} \rightarrow Fe3+ + e^-$

Micic et al. (2002) concluded that the precipitation of iron compounds onto the soil particles surfaces led to a reduction in soil pore volume resulting in the observed increase in the soil undrained shear strength. Therefore the release of the iron oxides and hydroxides from the FE electrodes into the pore spaces of the soil sample could have caused a reduction in pore volume leading to more dense material as well as acting as the cementing agents that causes the observed increase in the strength of the soil after the EK treatment.

(II) Aluminium electrode

Similarly, the change in the geotechnical properties of the kaolin clay when aluminium electrodes are used is due to the release of aluminium ions due to EK phenomenon. Gray and Schlocker (1969) stated that the aluminium hydroxides generated leach into the pores of the clay causing a reduction in the pore spaces and thus an overall change in the geotechnical properties of the clay. Thus, the relatively higher strength obtained with AL electrodes compared to the electrodes in this study could be due to the reaction of the kaolin clay minerals with the aluminium ions. Such possible reactions are listed below:

$Al \rightarrow Al^{3+} + 3e^-$

$Al + 4OH^- \rightarrow Al(OH)4^- + 3e^-$

$Al(OH)_4^- \rightarrow Al(OH)_3 + OH^-$

The ability of aluminium to co-ordinate with hydroxide in different ways to form hydroxy-aluminium compounds makes it very effective to alter the mineralogy of the clay soils thus increasing the in-situ strength (Gray,1970). Gray (1970) also showed that the resulting compounds can make layers between layers of clay minerals or precipitate externally in the pore spaces as amorphous or crystalline hydroxide e.g. Gibbsite.

According to Kim et al.(2007), an aluminium electrode has more effect in decreasing water content than iron electrodes. This however was with respect to buried electrodes and not a partially buried object where the anode is buried while the cathode is submerged in water. From their experiment involving the insertion of electrodes in clay soil sample to study the migration of leached ions and adsorption in the clay surface, they concluded that the decomposition of the inserted electrodes during EK treatment resulted in the modification of the clay soil.

(III) Copper electrode

The use of copper as an electrode has an advantage in terms that only copper oxide or hydroxide is formed and little gas is liberated (Lo et al.,1991). The high conductivity of copper implies that no significant loss of current or electric potential will ensue during the EK treatment.

Another kind of electrode material which was initially planned to be employed as part of this study is the electro-kinetic geosynthetic electrode, generally referred to as the **EKGs**. Due to logistical reasons, these sets of materials were not investigated. However, in a preliminary investigation on the use of EK treatment to enhance the stability of buried pipelines, Armstrong (2007) reported that EKG anodes lasted considerably longer than exposed steel anodes. While the EKGs lasted up to about 100hrs, the exposed steel lasted for only 24 hrs. Therefore, it is anticipated that using an EKG in place of exposed iron electrodes as the case in this study, may increase the durability of the electrodes and possibly, the efficiency of the EK treatment. This however will need to be substantiated with extensive research.

5.2.2 Interim conclusions –influence of electrode materials

- Chemical reactions at the various electrode materials significantly affect the outcome of the EK treatment and the re-engineering of the soil sample.
- The durability of the electrode materials is best with CU electrodes and least with FE electrodes due to their chemical compositions and reactions during EK tests.
- AL electrodes produces most favourable reactions with the kaolin clay that contributes to the observed increase in the soil shear strength at depth after the EK treatment.
- Chemical compositions of offshore site soil will need to be assessed before application of the EK treatment.

5.2.3 The electric field during the EK test

The distribution and intensity of electric fields in the soil during the EK treatment are dependent on the arrangement of electrodes, applied voltage and soil properties. Rittirong (2006) reported that the effectiveness of the EK treatment is dependent on the combination of electric field intensity and treatment time. As already explained in

§3.2.2.3, an effective way to treat the soil below the partially buried pipe section was to generate the electric field around the pipe by installing the electrodes parallel to it.

In this study the electrodes were placed horizontally around the pipe length (anodes below the pipe within the soil mass and the cathode above the pipe within the seawater). The electric field distribution is simplified to indicate a flow of current from the anode below the pipe section to the surface water above (Figure 5 - 2).

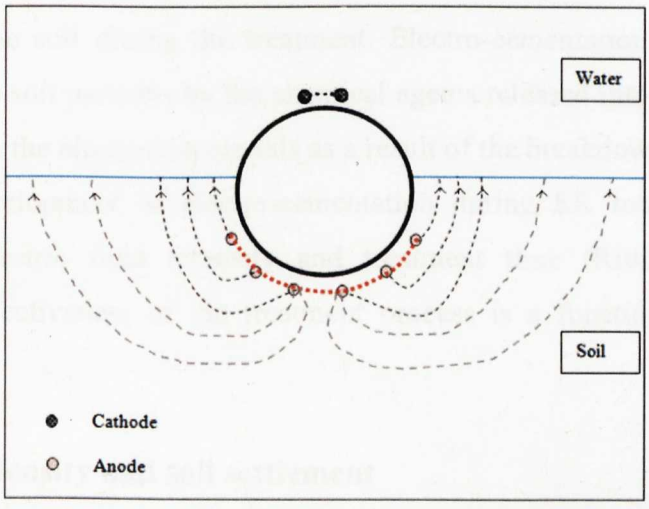

Figure 5 - 2: Assumed simplified electrical field distribution for the pipe-electrode arrangement

Since both the anodes and the cathodes were connected in parallel, they can be simplified as a sheet of metal conductors below and above the pipe. The simplified distance between the anode and the cathode in this case is approximately 50mm resulting in an electric field intensity of between 50V/m for the 2.5V test to 400V/m for the 20V test. Given the fact that the conductivity of the sea water is high compared to the clay, the resistivity of the sea water can be ignored and it can be treated as the cathode.

In terms of the performance of the various electrodes used in this study, the longer the time to the complete decomposition of the electrodes, the more resistant were the electrodes to corrosion during EK treatment. CU electrodes appear to last longer and therefore considered to be more resistant to corrosion. FE electrodes on the other hand corrode fastest and hence are less durable in the aggressive saline environment. The interplay between the duration of the electrodes, the performance/effective of the

electrode material will be vital in selection of an appropriate electrode material for actual field application. Direct measurement of pore water pressure generation during the EK treatment and possible effects from the current density was not done since this preliminary study was only aimed at investigating the increase in strength and pipe-soil adhesion due to EK treatment effects. Further research will be needed to study the pore generation during this treatment.

Apart from the dewatering of the soil sample due to electro-osmotic phenomenon in the soil, another electro-kinetic process, electro-cementation, also contributes to the modification of the soil during the treatment. Electro-cementation here involves the cementation of the soil particles by the chemical agents released into the soil during the EK treatment from the electrode materials as a result of the breakdown of species within the soil. The development of electro-cementation during EK treatment is strongly related to the electric field intensity and treatment time (Rittirong et al.,2008). Therefore, the effectiveness of the treatment process is a function of the electrode configuration.

5.2.4 Current density and soil settlement

The influence of current (or current density) on the settlement of the soil mass was more noticeable in the large-scale test than in the small-scale test. In the large-scale test, the higher effective weight of the pipe section in relation to the soil strength gave better response of the pipe to the corresponding soil consolidation. The current density curve and the pipe settlement curve follow the same trajectory since the driving force for the electro-osmotic process is essentially the current through the soil mass. However, this was difficult to show in the small-scale tests because the light weight of the PVC pipe in relation to the soil strength. Shang et al. (1997) demonstrated that the electric current density is the driving force in electro-osmotic consolidation and that the effectiveness of electro-osmotic consolidation can be improved by increasing the current density. Therefore the direct relation between these two parameters demonstrates the feasibility of EK treatment in this application. Current (or current density) is the driving force for electro-osmotic consolidation. However, an attempt to relate current density with soil consolidation (inferred from pipe settlement) (Figure 5 - 3 and Figure 5 - 4) did not reveal any significant correlation possibly owing to the erratic responses in the generation of current during the test as explained in §5.2.

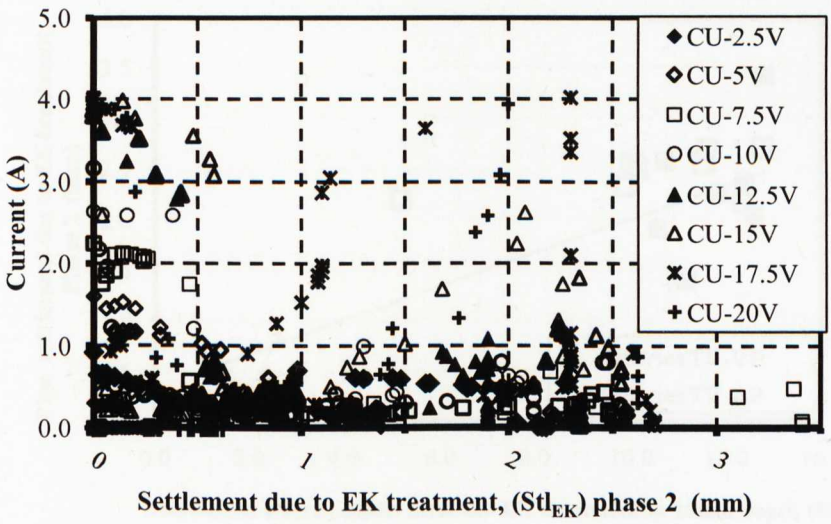

Figure 5 - 3: Plot of current against relative pipe settlement during EK Treatment using copper electrodes

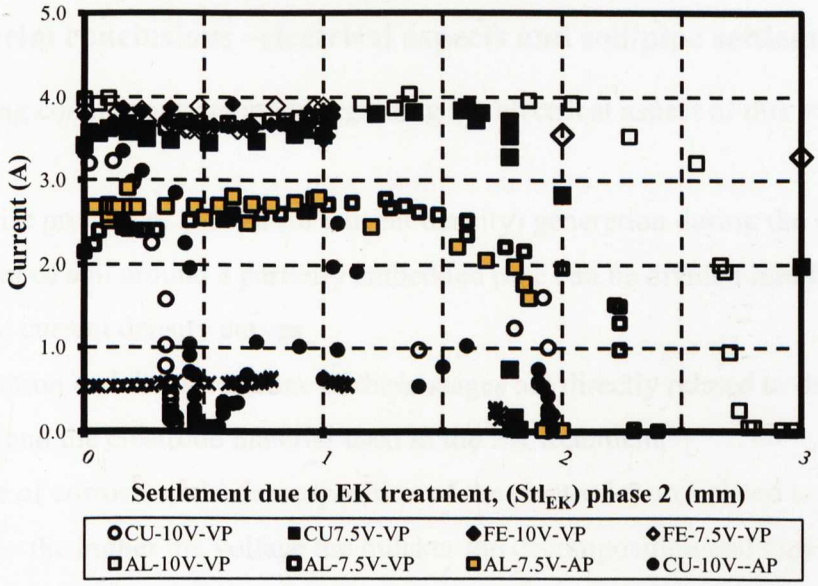

Figure 5 - 4: Plot of current against relative pipe settlement during EK Treatment using different electrode materials

An attempt is made to correlate the observed pipe settlement due to EK treatment with the decrease in water content at 20mm level only as shown in Figure 5 - 5. Although the measured settlement is the cumulative settlement of all the clay, it was however assumed that the decrease in water content with depth below the pipe especially near the surface could be related to the soil settlement. The plot suggests that, for most of the recorded maximum pipe settlement, the maximum decrease in water content is between 10 and 14% near the surface of the soil. This is not in agreement with the theoretical basis that the higher the settlement the more the decrease in water content.

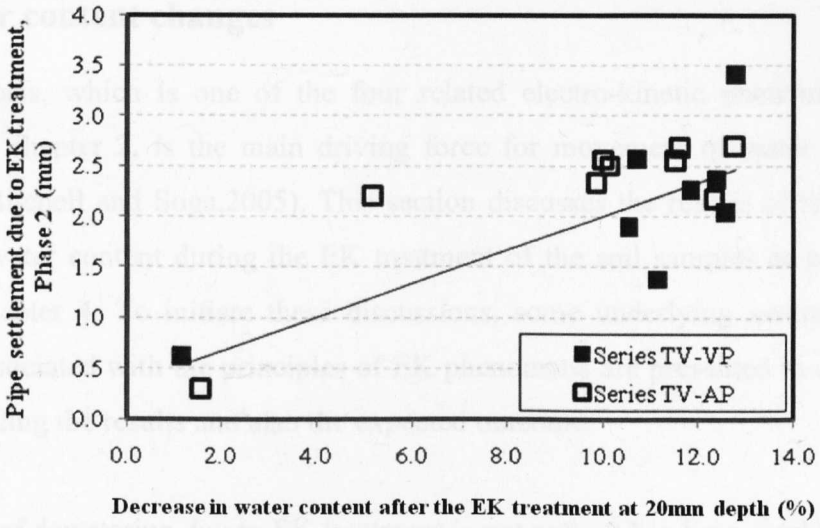

Figure 5 - 5: Plot of relative pipe settlement against decrease in water content

5.2.5 Interim conclusions –electrical aspects and soil/pipe settlement

The following conclusions are made regarding the electrical aspect of this study:

1. The entire process of current (or current density) generation during the EK treatment of soil around a partially embedded pipe can be divided into four stages from the current density curves
2. The position and the occurrence of these stages are directly related to the applied voltage and the electrode material used in the EK treatment.
3. The rate of corrosion and decomposition of the electrodes are related to the applied voltage – the higher the voltage the quicker the decomposition and vice versa.
4. The generation of current density is affected by the initial water content of the soil sample and this is dependent on the type of electrode material.
5. FE electrodes show a faster decline in current density for lower water content while AL electrodes show a slower decline in current density for lower water content.
6. The amount of constant applied voltage across the sample affects the migration of the ionic species in the soil, hence the evolution of current density- the lower the applied voltage the slower the migration of ions and the longer it takes for the test to come to completion.
7. In terms of resistance to corrosion and durability during EK treatment, CU electrodes are more durable while FE electrodes are less durable

5.3 Water content changes

Electro-osmosis, which is one of the four related electro-kinetic phenomena earlier discussed in chapter 2, is the main driving force for movement of water during EK treatment (Mitchell and Soga,2005). This section discusses the results of the observed changes in water content during the EK treatment of the soil samples as presented in §4.2.3 of chapter 4. To initiate these discussions, some underlying assumptions and equations associated with the principles of EK phenomena are presented in order to aid in understanding the results and also the expected outcome.

The process of dewatering due to EK treatment is not new. It has been established from past studies that the application of electrical potential to a wet soil mass causes ionic migrations to the opposite electrodes – cations to the cathode and anions to the anodes. As these ions move, they carry their water of hydration resulting in a net flow of water towards the cathode and dewatering at the anode. These reductions in water content may result in generation of negative pore water pressure and hence increase in the effective stress of the soil hence, increase in the soil strength. A simplified equation for electro-osmotic movement of water through porous soil material (Hamed et al.,1991; Grundl and Michalski,1996; Mitchell and Soga,2005) is presented in equation 5-12 as:

$$q_e = k_e i_e A \qquad \textbf{5 - 12}$$

Where:

q_e = electro-osmotic flow

A = cross sectional area of the soil

k_e= electro-osmotic conductivity and

$i_e = \frac{\Delta V}{\Delta L}$ = voltage gradient.

If both the anode and the cathode have access to free water (open cathode and anode), the soil will function as a porous plug (Mohamedelhassan and Shang,2000). According to Mitchell and Soga (2005), the electro-osmotic induced flow by the open anode and cathode is given by the empirical relationship:

$$Q = k_e E A \qquad \textbf{5 - 13}$$

Where:

Q = electro-osmotic flow rate (m^3/s)

E = electric field intensity (V/m) .i.e. ratio of applied voltage to the distance between the electrodes

k_e= electro-osmotic conductivity and

It should be noted that it was not possible to measure the flow rate during the test hence the flow was only assessed by evaluating the changes in water content profile after the test.

Equation 5 - 13 suggests that the effectiveness of the EK treatment will be a function of the voltage gradient, V/m and the coefficient of electro-osmotic conductivity, k_e. The distance between the anodes and the cathodes was kept constant at approximately 50mm while the applied voltages vary between 2.5 to 20V giving rise to varying voltage gradients. EK tests involving commercial kaolin have been extensively used in previous researches and the k_e ranges between 1.1 x 10^{-5} cms^{-1} per Volts/cm and 5.7 x 10^{-5} cms^{-1} per Volts/cm (Bjerrum et al.,1967; Esrig,1968; Hamir,1997). Casagrande (1952) had also reported a k_e value of 5.7 x 10^{-5} cm^{-1} per Volts/cm for a commercial kaolin at 67.7% water content. Thus the only variable in the test is the value of the applied voltage which was investigated during the test.

The theory of electro-osmotic consolidation originally proposed by Esrig (1968) predicts development of pore pressure (and consolidation) across electrodes embedded in the soil only if the closed anode and open cathode configuration is used (refer to section 2.3.1). Hamed et al. (1991), Acar et al. (1994) and Acar and Alshawabkeh (1996) report consolidation (decrease in w) and development of negative pore pressures in bench-scale experiments with open electrode configuration.

The results of the water content tests presented in Figures 4 – 5, 4 – 6, 4 – 7, 4 – 27 and 4 – 49 all indicated significant decrease in water content. Based on the experimental evidence, a plot of the decrease in water content with depth at different voltage gradients (Figure 4 – 4) is use to assess the effect of voltage.

Although the theoretical expression shows the dependency of the dewatering process of the soil on applied voltage gradient, the results obtained here showed some deviations. At the first level (20mm depth), all the applied voltage gradients show the highest decrease in water content. However, the influence of the applied voltage is not very apparent as the decrease in water content lie approximately between 10 – 14% for all the tests apart from the 5V test which is slightly different. It is therefore possible that although the actual speed of migration of the pore fluid within the soil mass during the EK treatment might have been dependent on the applied voltage gradient, the final change in water content is approximately similar.

Therefore, this could suggest that as long as the process was allowed to come to an end before the water content test was carried out on the sample, the effect of dewatering will be similar if only movement of water is considered. This was also demonstrated by the summary plot of Figure 4 – 8. The EK treatment does not only involve movement of water (electro-osmosis); the final effect of the EK treatment could be different with different applied voltage gradient. (Lo et al.,1991; S.Micic et al.,2002; Mitchell and Soga,2005). The second level (70mm depth) and the third level (100mm depth) also show similar trends in decrease in water content where the influence of voltage gradient is not very pronounced. It is not clear at this point if this unique deviation from the expected trend could be due to the configuration of the electrodes or the partially buried nature of the pipe section used in this study.

The lateral variation in changes in water content is shown in Figure 4 – 6(a-c). Here, it is shown that the greatest reduction in water content is directly below the pipe invert and the reduction reduces with horizontal distance from the pipe. This variation may be related to the distribution of the electric field intensity within the soil mass given the limit of the boundary conditions of this experiment. Again, the influence of the applied voltage is not very pronounced from the results. A similar trend was also obtained from the large-scale test where the maximum decrease in water content was measured at below the pipe invert (Figure 4 – 49).

The effects of the EK treatment below the pipe axis on the development of water content is seen in Figure 4 – 6 where the maximum reduction in the water content was noted near the axis of the embedded pipe and it reduces with distance from the pipe.

This further demonstrates that changes in the water content occur due to EK treatment. By correlating the soil settlement with the observed decrease in water content at the top level of the soil (Figure 4 – 10), the maximum settlement due to EK treatment coincides with about 10 – 14% decrease in water content.

The effects of electrode material in the electro-osmotic flow of water and hence decrease in water content indicates FE electrode as the best performer for the partially embedded pipe. This conclusion arose from the fact that the maximum decrease in water content at the top level of the soil sample was obtained using FE electrodes. The alteration of the soil sample caused by the corrosion and degradation of the electrode materials was also more pronounced in the soil with FE electrodes. Apart from having effects on the soil-pipe adhesion which will be discussed later, it is thought that this is likely to have some influence on the outcome of the water content. This might be due to the nature of the ionic species from irons electrodes and its effects on the chemistry of the soil.

To the contrary, the decrease in water content at deeper levels indicates the AL electrode as the best performer. However, given the position of the anode and the possible electric field generation within the soil mass, this decrease in water content cannot be explained in terms of electro-osmosis alone. Quigley (1980) has reported that the precipitation of iron oxides and carbonate can act as cementing agents, which strengthen soil inter-particle bonds while Micic et al.(2002b) demonstrated the occurrence of pore size and void ratio decrease due to electro-chemical effects on treated soil. Therefore, it is possible that the migrations of the dissolved aluminium ions (which is the main species from the AL electrodes) permeate into the soil pore under gravity, react favourably with the kaolin clay resulting in the reduction in the void ratio, pore size and hence, the decrease in water content obtained. This is however subject to further research before a final conclusion can be arrived at. With this assumption, it implies that the various ions from the dissolution of iron, copper and aluminium electrodes migrate differently and react with the kaolin clay differently. A summary plot showing the variation of water content profile using the three electrode materials is shown in Figure 5 - 6.

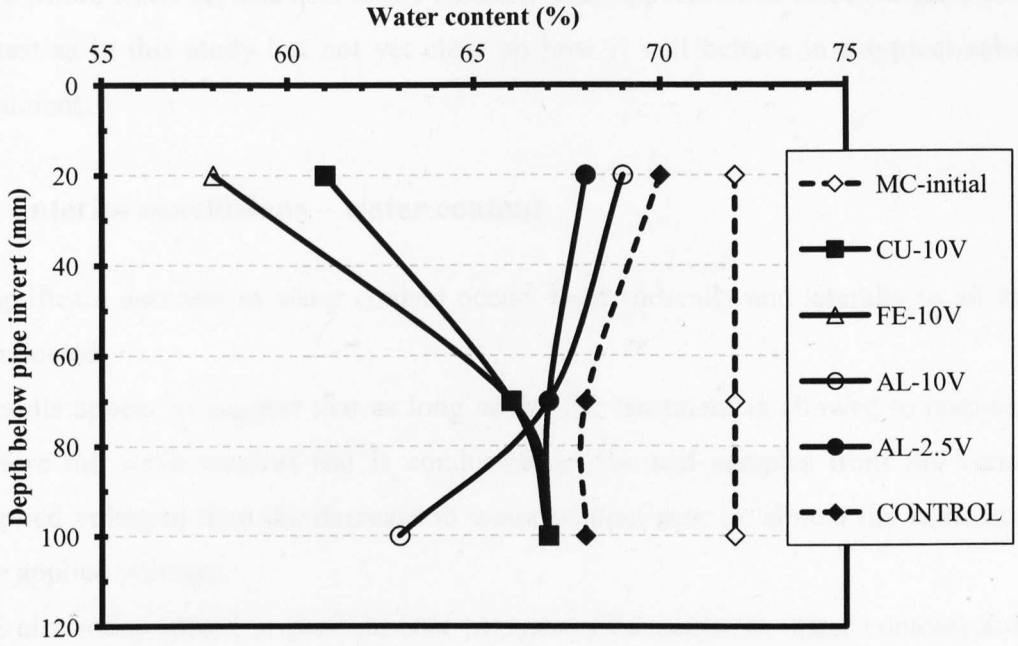

Figure 5 - 6: Variation in water content (w)proile using different electrode materials and voltage after EK treatment

Apart from the AL electrode at 10V, all the water content profiles including the control test roughly converged at around 70mm depth suggesting the possible limit of the dewatering effects due to the EK treatment. The lowest water content is obtained for FE followed by CU. AL at lower voltage also indicates a lower water content than AL at higher voltage. This however is not consistent with the settlement plot (Figure 5 - 6) where higher settlement is noted for AL at higher voltage.

5.3.1 Flow and spatial changes in sample water content

The electro-osmotic flow of pore fluid during the EK treatment is expected to be from the anode, located below the pipe, to the cathode, located above the soil. This is expected to be similar to the direction of flow of the electric field. Therefore, the water will tend to move upward according to the direction of the simplified flow pattern. However, the migrating species from the dissolution of the electrode (mainly the anode) appears to go in an opposite direction, moving vertically downward (under gravity) as evident by the increase in strength of the soil sample below the pipe invert. This pattern of movement was also reported by Alshawabkeh and Acar (1996) where a migrating chemical front resulted in the modification of the soil sample during an EK treatment. Therefore, the strength improvement which was measured below the pipe could be due to the combined actions of chemical alteration and dewatering of the soil. It is assumed

that the whole water surface acts as the cathode. This appears to be effective for a small scale test as in this study but not yet clear on how it will behave in a typical subsea environment.

5.3.2 Interim conclusions – water content

- Significant decrease in water content occurs both vertically and laterally in all tests conducted.
- Results appear to suggest that as long as the EK treatment is allowed to complete, before the water content test is conducted on the soil samples from the various applied voltages, then the decrease in water content may be almost the same in all the applied voltages.
- FE electrodes appear to perform best (in terms of decrease in water content) at the top level of the soil while AL electrodes appear to perform at greater depth below the pipe section.
- Variations exist in the migrations and reactions of the ionic species (released from the disintegrated electrodes) and the kaolin soil sample which affect the water content profile at depth within the soil after the EK treatment.

5.4 Development of undrained shear strength due to EK treatment

5.4.1 Strength profile analysis after EK treatment

This section presents the analysis and discussions of the effects of EK treatment on the undrained shear strength (c_u) of the soil samples using simple classical soil mechanics approaches. Firstly, an assessment of the effects of EK on the treated soil is investigated by subtracting the c_u profiles before the EK treatment at the test locations LC1 and LC2 from their profiles after the EK treatment. The ensuing relative c_u profiles for LC1 and LC2 are presented in Figure 5 - 7 to Figure 5 - 10 for the two test series TV-VP and TV-AP (refer to §4.2.4). These show an increase in strength for the treated soils relative to the control tests. The control tests also show a linear increase in strength with depth up to about 0.4kPa, about 0.04kPa per metre attributed mainly to consolidation. Thus the observed changes in the treated soils include also the effect of consolidation.

Due to the observed slight variations in the c_u profiles from the different batches of clay mix, the EK effects on the soil strength is considered to be best assessed by comparing strength differences in the individual bed of clay. It appears from Figure 5 - 8, which shows the change in strength, that the EK treated soils at LC1 are weaker than the control test from about 30mm depth downwards. Although LC1 is outside the zone of EK influence based on the location of the pipe, this weakening effect on the soil after EK treatment is not fully understood at this point but might be connected to the flow of water during the EK treatment.

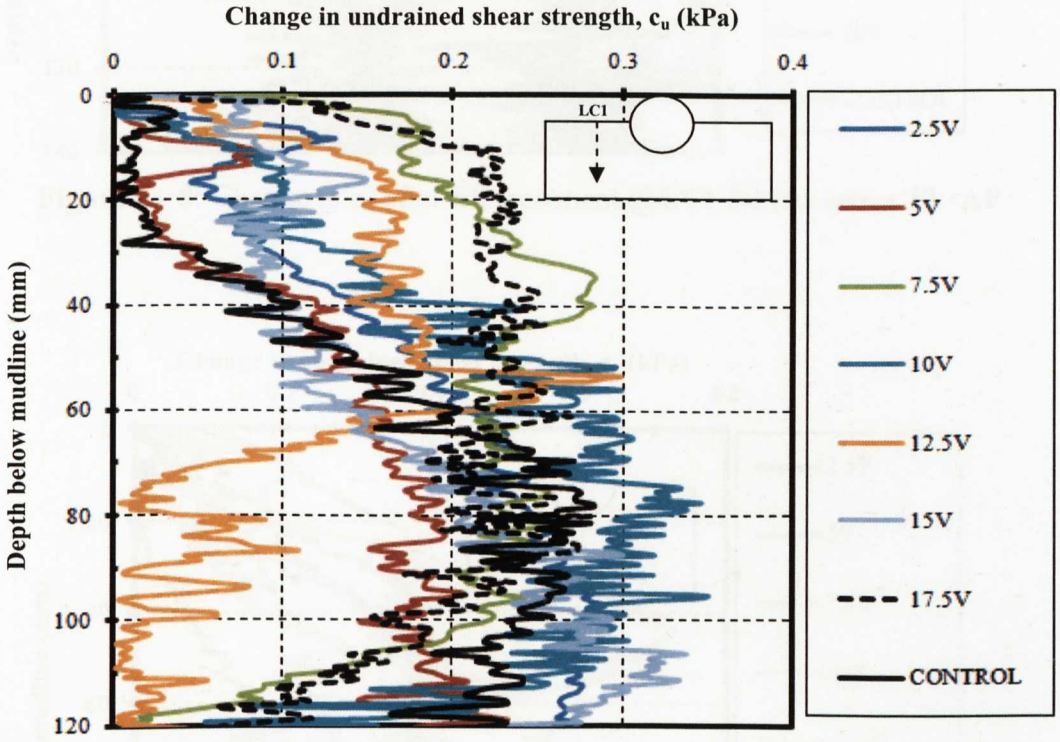

Figure 5 - 7: Change in c_u after EK treatment **@LC1** for Test Series **TV-VP**

In the same way, the effects of the EK treatment using the three electrodes were assessed by subtracting their profiles before the EK treatment from the c_u profiles after the EK treatment at test locations LC1 and LC2. These are presented in Figure 5 - 11 and Figure 5 - 12 for LC1 and LC2 respectively. Here, the maximum increase in c_u at depth after the treatment is observed with AL electrodes. It appears from the results that the effects due to EK are very minimal at LC1-AP (.i.e. axial configuration), implying this is outside the zone of influence of the EK effect.

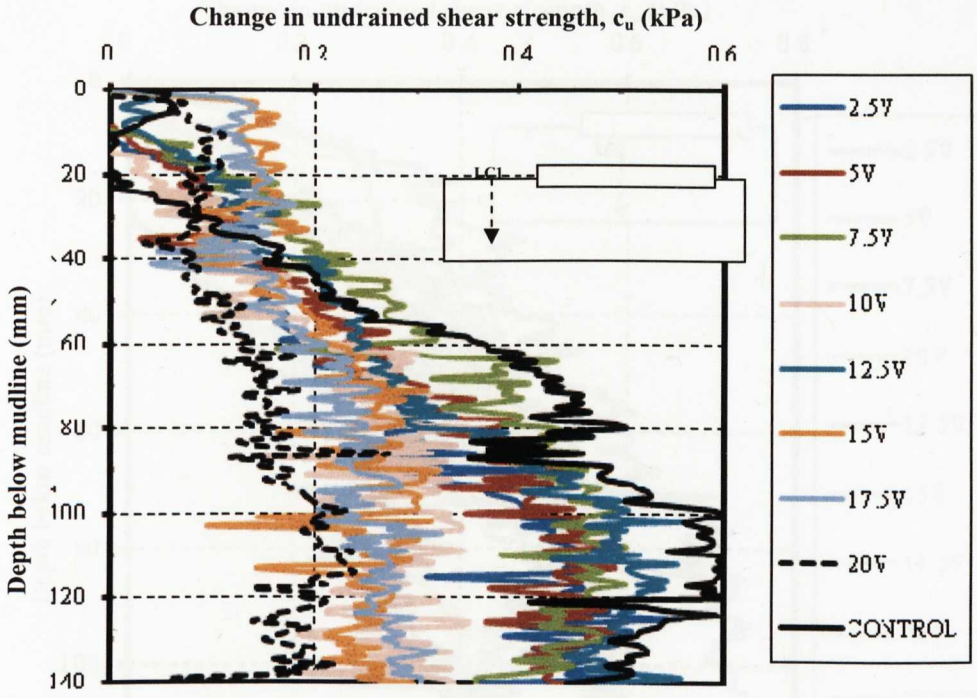

Figure 5 - 8: Change in c_u after EK treatment **@LC1** for test series **TV-AP**

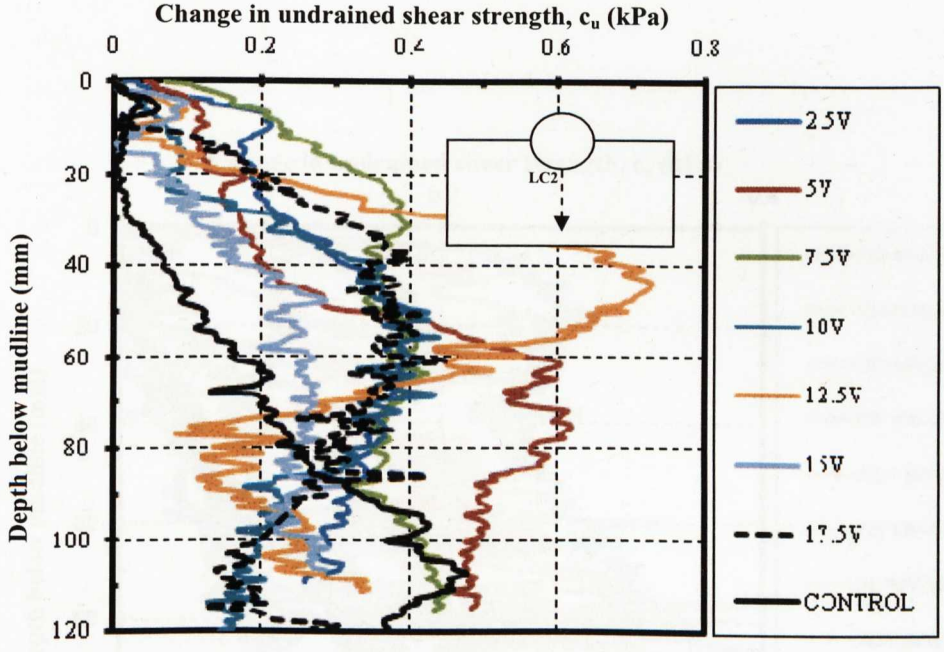

Figure 5 - 9: Change in c_u after EK treatment **@LC2** for test Series **TV-VP**

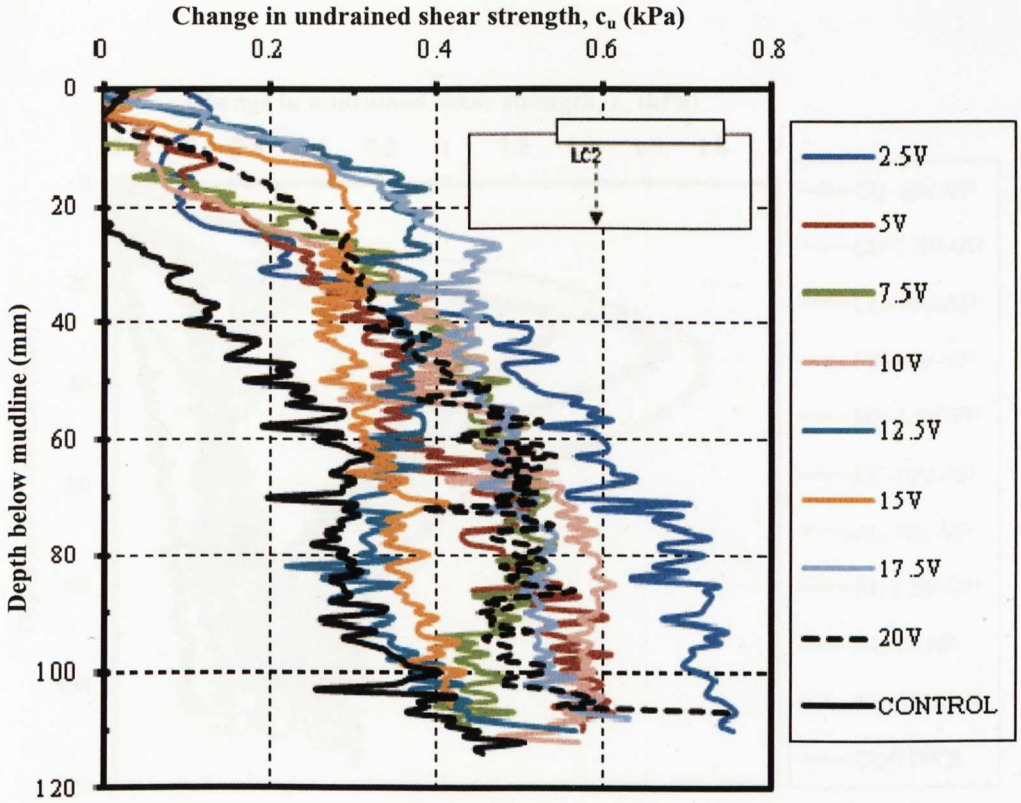

Figure 5 - 10: Change in c_u after EK treatment **@LC2** for test series **TV-AP**

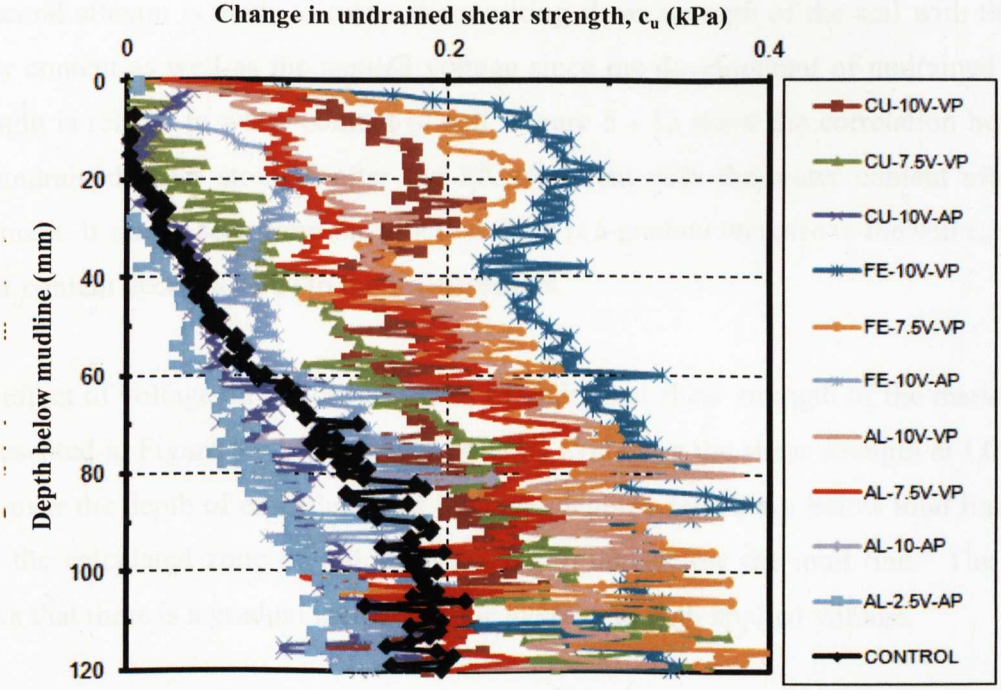

Figure 5 - 11: Change in c_u after EK treatment at LC1 using different electrode materials

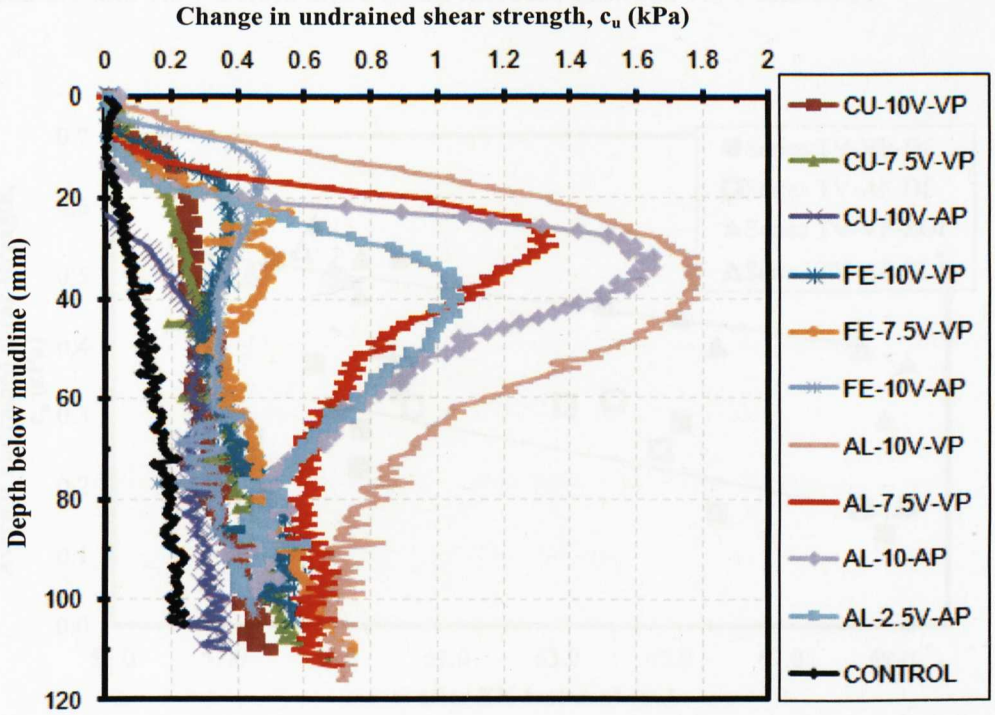

Figure 5 - 12: Change in c_u after EK treatment at LC2 using different electrode materials

5.4.2 Shear Strength / applied voltage / water content

A second attempt is made to relate the resulting shear strength of the soil with the soil water content as well as the applied voltage since the development of undrained shear strength is related to water content of soil. Figure 5 - 13 show the correlation between the undrained shear strength after the EK treatment with the water content after the treatment. It can be seen from the plot that there is a gradual increase in the soil c_u as the water content decreases due to the EK treatment.

The effect of voltage on the development of undrained shear strength of the treated soil is presented in Figure 5 - 14. This was done by averaging the shear strength at LC1 and LC2 over the depth of embedment of the pipe, denoted D_f (30mm below mud line) and over the calculated zone of influence (ZOI_F), 75mm below the mud line. The trend shows that there is a gradual increase in the average c_u with applied voltage.

Similarly, the analysis of influence of voltage on the treatment efficiency of the EK using the three electrodes is shown in Figure 5 - 15. It may be seen that there is a gradual increase in average c_u with increasing voltage. While FE and CU show a

gradual increase with increasing voltage, AL electrodes show almost constant value between 2.5 and 7.5V before and a sharp increase between 7.5V and 10V.

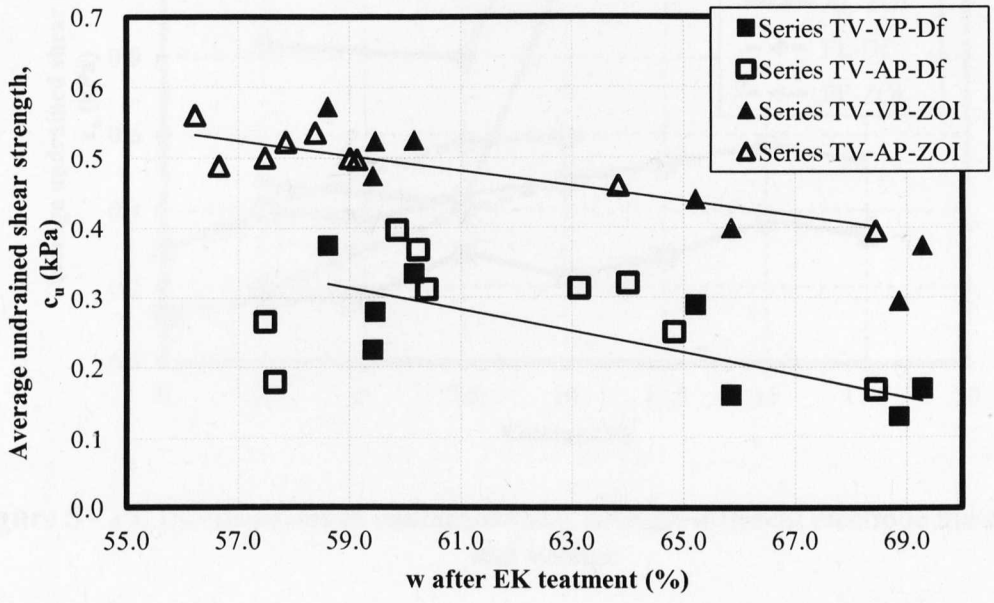

Figure 5 - 13: Development of undrained shear strength (c_u) with decrease in water content within the zone of influence and depth of pipe embedment *(D_f)*

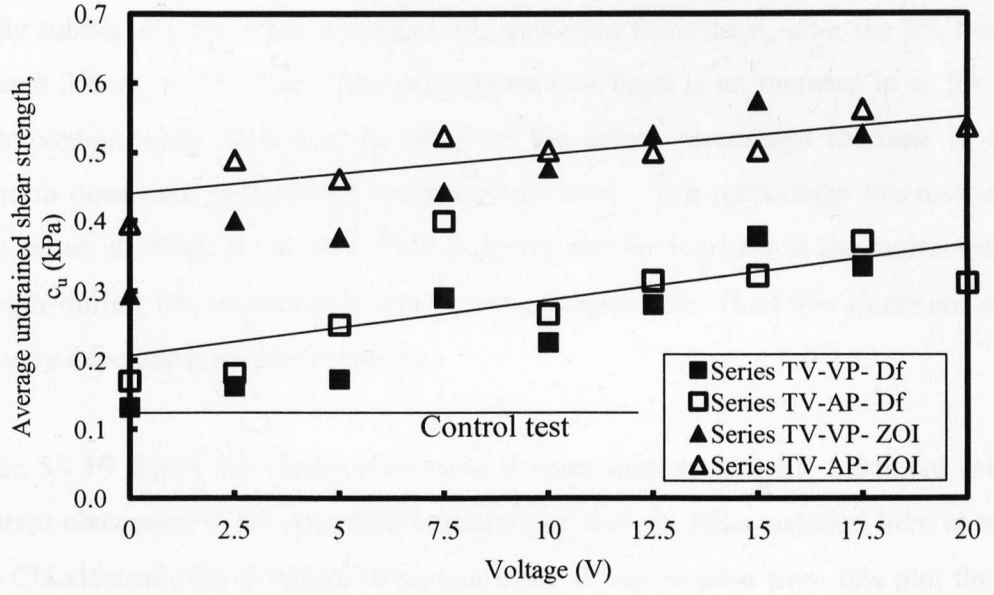

Figure 5 - 14: Development of undrained shear strength (c_u) with voltage within the zone of influence (*ZOI, 75mm*) and depth of pipe embedment (D_f, *30mm*)

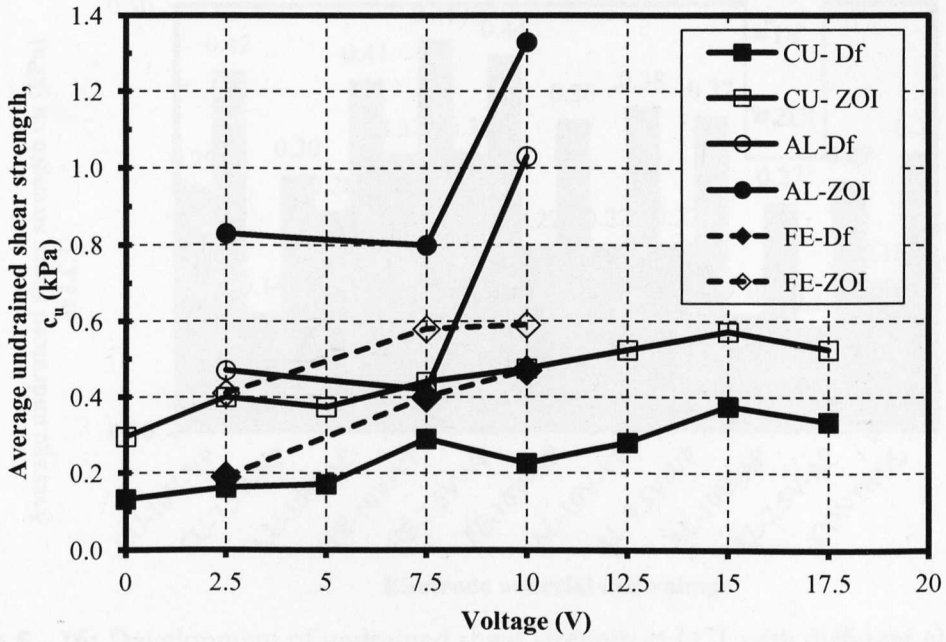

Figure 5 - 15: Development of undrained shear strength different electrode materials and voltage

An analysis of the development of undrained shear strength using different electrode materials is presented in Figure 5 - 16 and Figure 5 - 17 for LC1 and LC2 respectively while the variation of changes in c_u after the EK treatment using AL and FE electrodes at different water contents are presented in Figure 5 - 18. This assessment was carried out by subtracting the initial c_u before EK treatment from the c_u after the EK treatment at depth 30mm, at LC2 only. The plot shows that there is an increase in c_u for all the water content used. However, in terms of the actual percentage increase in the c_u, variation does exist with initial water content used. The percentage increase in c_u is included as an insert in the plot. This suggests that the increase in the undrained shear strength during EK treatment is water content dependent. Thus this treatment process will vary depending on site conditions.

Figure 5 - 19 shows the variation of water content with c_u after EK treatment using the different electrodes at the specified initial water content. Also included here is one test with CU electrode for purposes of comparison. It can be seen from this plot that there are changes in both the water content and c_u using the three electrodes. The greatest changes however are observed with AL electrodes.

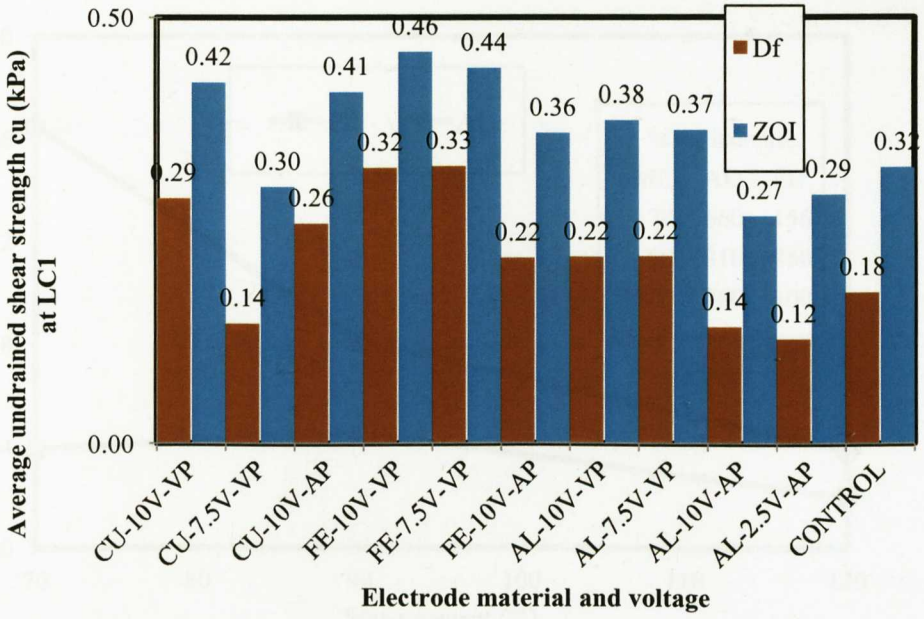

Figure 5 - 16: Development of undrained shear strength at LC1 with different electrode materials and voltage

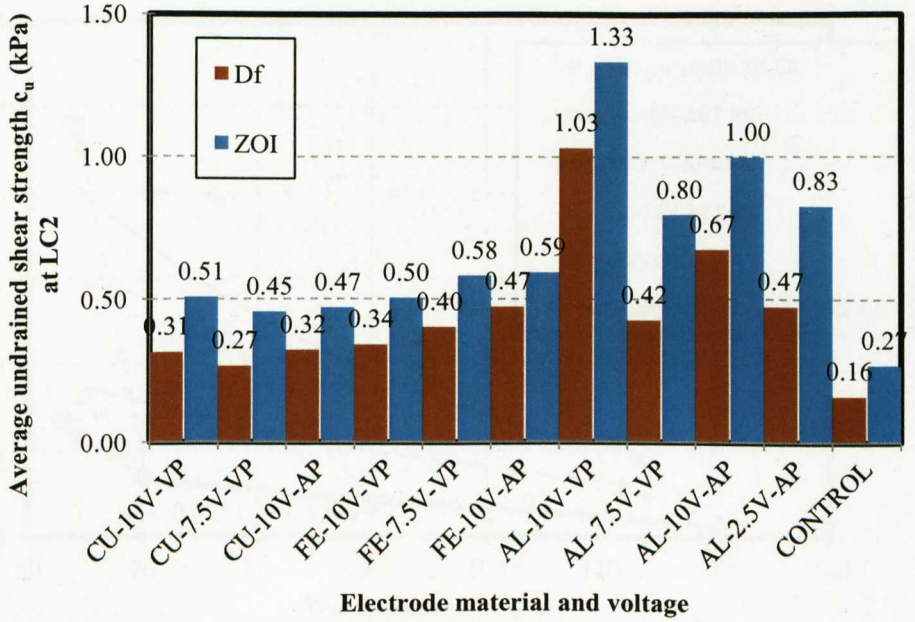

Figure 5 - 17: Development of undrained shear strength at LC2 with different electrode materials and voltage

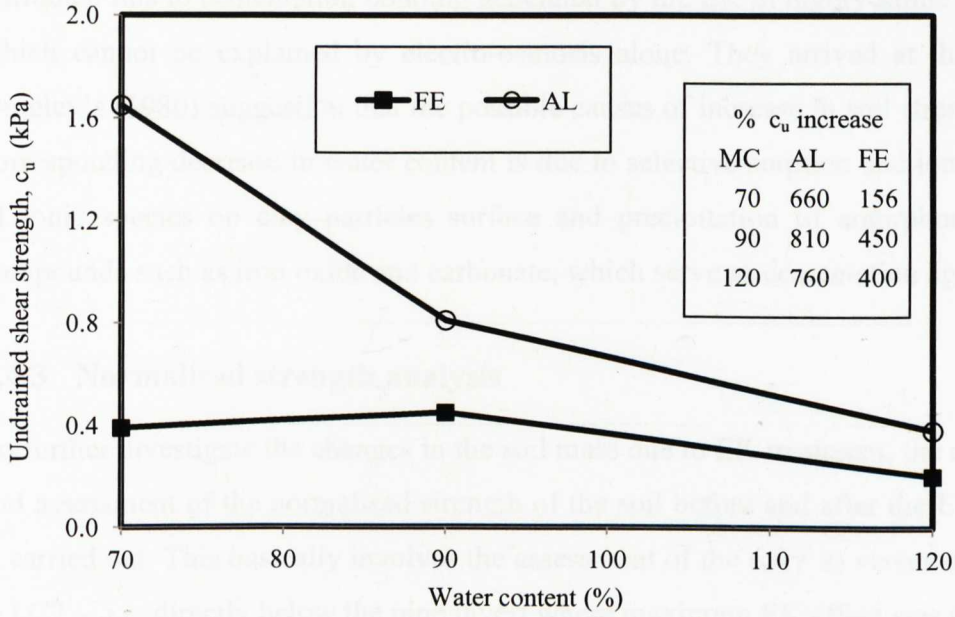

Figure 5 - 18: Variation of c_u with water content using FE and AL Electrodes

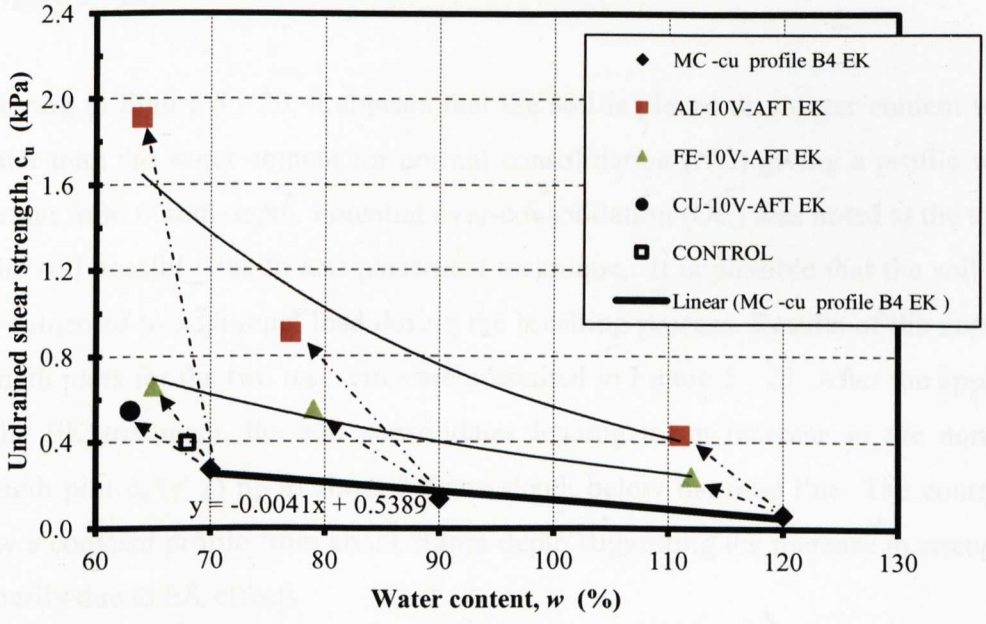

Figure 5 - 19: Development of undrained shear strength and water content using copper, iron and aluminium electrodes after EK treatment

Although the increase in strength should be directly related to decrease in water content (.i.e., if no chemical effects are included), considerable increase in the c_u of the treated soil could still occur without corresponding decrease in water content. Micic et al. (2002a) reported such results in their experiment on natural offshore marine clay. They

attributed this to cementation bonding generated by the EK in highly saline marine clay which cannot be explained by electro-osmosis alone. They arrived at this based on Quigley's (1980) suggestion that the possible causes of increase in soil strength without corresponding decrease in water content is due to selective sorption and ionic exchange of ionic species on clay particles surface and precipitation of amorphous chemical compounds such as iron oxide and carbonate, which serve as cementation agents.

5.4.3 Normalised strength analysis

To further investigate the changes in the soil mass due to EK treatment, the computation and assessment of the normalised strength of the soil before and after the EK treatment is carried out. This basically involves the assessment of the $c_u/(\gamma' z)$ versus depth profile at LC2 – .i.e. directly below the pipe invert where maximum EK effect was noticed. The depth was taken from the mud line in the trench after the extraction of the pipe section. The normalised strength profile of the as-placed soil was denoted as $\mathbf{c_u}$**-P** whiles those due to consolidation effect (from the control test) and those due to EK effects are denoted as **C-**$\mathbf{c_u}$ and **EK-**$\mathbf{c_u}$ respectively. A typical normalised strength profile is shown in Figure 5 - 20.

Referring to Figure 5 - 20, it appears that the soil is placed at a water content which is greater than the water content for normal consolidation (NC) giving a profile which is constant from 60mm depth. Potential over-consolidation (OC) was noted at the top layer of the soil possibly due to soil placement technique. It is possible that the soil surface was subjected to additional load during the levelling process. Results of the normalised strength plots for the two test series are presented in Figure 5 - 21. After the application of the EK treatment, the soil consolidates leading to an increase in the normalised strength plot $c_u/(\gamma' z)$ up to about 100mm depth below the mud line. The control tests show a constant profile from about 20mm depth suggesting the increase in strength was primarily due to EK effects.

The control test curve appears to follow the normal consolidation trend line while the treated soils show significant increase in $c_u/(\gamma' z)$ between depth 20mm and 60mm. In the case of the control test, softening of the soil below the pipe section was probably due to failure caused by the installation of the pipe. This softening can be added to the EK treated soil and hence a slightly higher c_u could have been recorded. Assuming the

soil mass in the tank was uniform given the similarity in the c_u trend for all plots, then the impact of the EK can be assessed by considering the changes in c_u at LC2 only for all the various voltages used.

Similarly, the normalised strength plots for the soil using the three electrode materials are shown in Figure 5 - 22. It can be seen that while the control tests show almost a uniform normalised strength from about 10mm downwards, the treated samples show considerable increase from the top up to about 80mm where they start to converge with the control tests. The plot suggests that the soil is improved down to about 70 - 80mm depth using CU and FE electrodes while the improvement increases down to the base of the tank when AL electrodes are used. In addition, AL electrodes produce the maximum increase while CU produces the least. By comparing the zone of influence due to EK with the theoretical zone of influence (calculated as 75mm) indicate that the two zones are approximately similar.

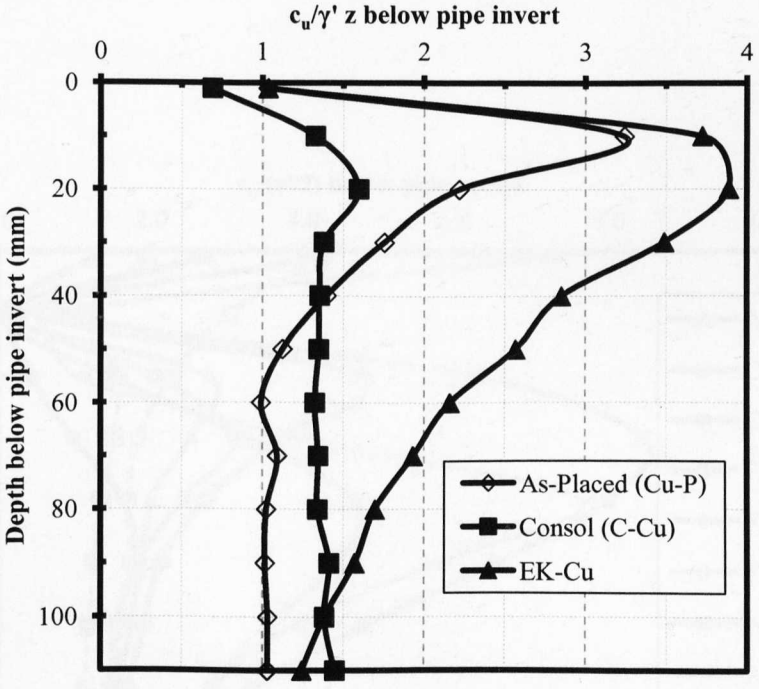

Figure 5 - 20: Typical normalised undrained shear strength plots of the soil before and after treatment

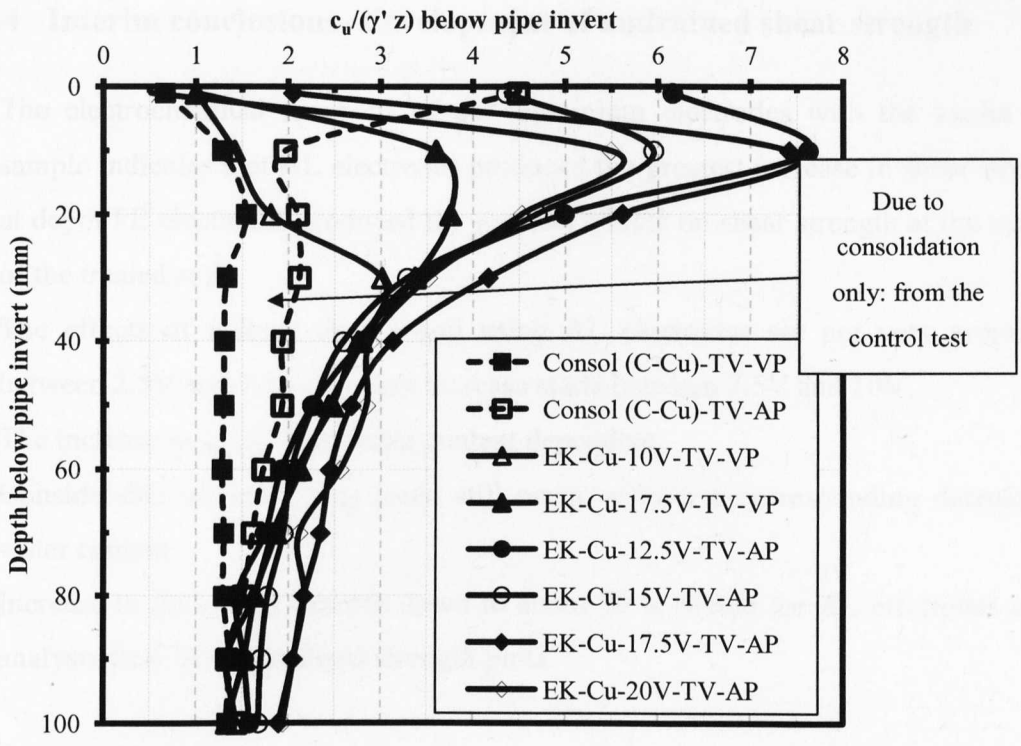

Figure 5 - 21: Normalised undrained shear strength plots of the soil showing control and treated soils

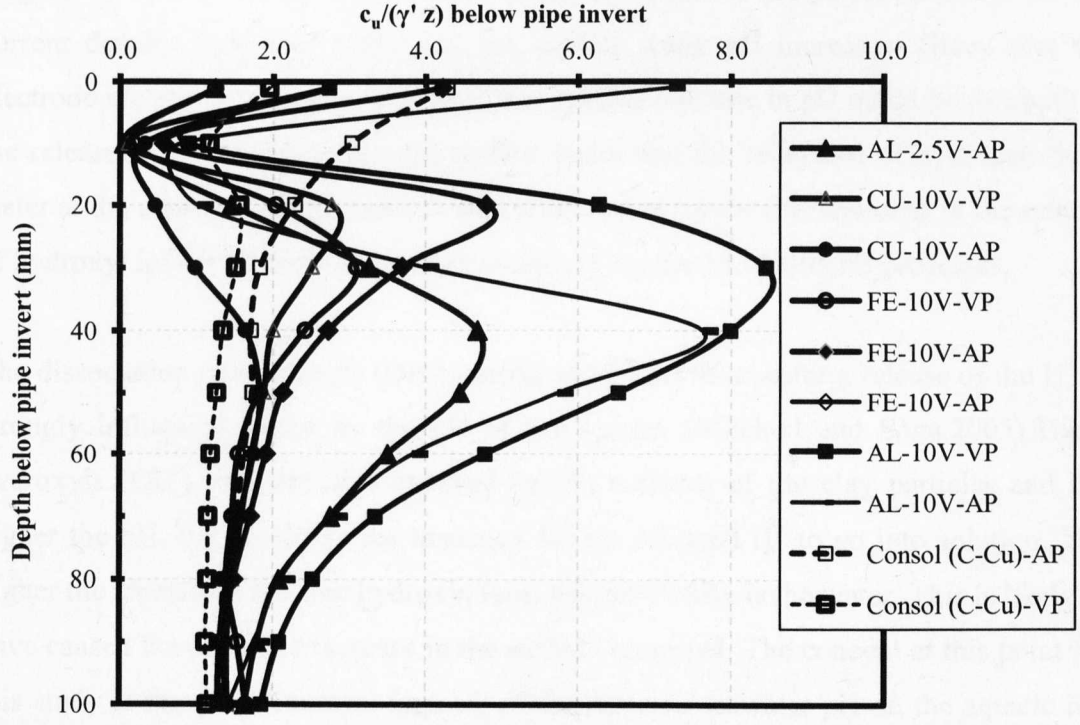

Figure 5 - 22: Normalised strength plot of the soil using different electrode materials showing control and treated soils

5.4.4 Interim conclusions –development of undrained shear strength

- The electrochemical reactions of the aluminium electrodes with the kaolin clay sample indicates that AL electrodes produced the greatest increase in shear strength at depth FE electrodes produced the greatest effects on shear strength at the surface of the treated soil.
- The effects of voltage on the soil using AL electrodes are not very prominent between 2.5V and 7.5V. A sharp increase starts between 7.5V and 10V.
- The increase in c_u is initial water content dependent.
- Considerable increase in c_u could still occur without a corresponding decrease in water content.
- Increase in the soil c_u extends down to about 70 to 80mm for AL electrodes using analysis from the normalised strength plots.

5.5 Soil and water pH

It was shown in chapter 4 that the pH of the soil generally increases with depth below the pipe invert where the soil is more acidic near the anode area (.i.e. close to the embedded pipe section). It was also shown that the higher the current density the lower the pH of the soil. The gradual increase in the surface water pH from the large-scale test (Figure 4 – 48) is shown to be related to the evolution of the current density. As the current density decreases with time, the surface water pH increases. Given that the electrode material in this case was iron, this gradual increase in pH could be due both to the release of iron species into the surface water and the reduction of hydrogen from water at the cathodes (submerged in the surface water) with time resulting in the release of hydroxyl ions (OH^-) into the surface water during the EK treatment processes.

The dissociation of hydroxyls (OH^-) ions in water and the resulting release of the H^+ is strongly influenced again by the pH of the system (Mitchell and Soga,2005).These hydroxyls (OH^-) ions are also exposed on the surfaces of the clay particles and the higher the pH, the greater is the tendency for the released H^+ to go into solution. The higher the amount of the free hydroxyl ions, the more basic is the water. This is likely to have caused the observed increase in the surface water pH. The concern at this point for this study is the environmental impacts of the increase seawater pH on the aquatic life

during real life EK treatment. However, given the volume of water in relation to the pipe footprint in the sea, the effect is likely to be minimal.

There remains a need to assess and quantify these effects, albeit this was not part of this study. The pH level to support aquatic life is generally between 6.5 and 8.5. High pH may mean that the water is low in CO_2 which is necessary to produce oxygen and support aquatic life. However, given the scale of this study, the exact values of resulting seawater pH after EK treatment on a given scale will need to be determined through further research in which the body of water is increased or replenished.

5.6 Analysis and discussions of the pull-out test results

The evaluation of the force required to lift objects, including subsea pipelines, on the seabed is a key requirement in the assessment of the stability of these objects (Vesic,1971). The breakout-force, which is the portion of this force to displace the object in excess of the submerged weight of the object, is generally used in this assessment in offshore operations (Liu,1969; Lee,1973; Byrne and Liam Finn,1978). The pull-out force is approximately equal to the object's submerged weight if it is embedded in cohesion-less soil or at rest on the seafloor without embedment .i.e. no adhesion develops at the soil-object contact (Lee,1973). In undrained conditions where the force is applied rapidly and water has no time to flow into or through the underlying soil, then suction force will develop below the object. It is this suction force that has to be overcome by the applied force to the object.

For an undrained condition to prevail around a penetrating surface foundation, Finnie and Randolph (1994) showed that a non-dimensional velocity of $vD/c_v > 30$ should suffice, with D being the diameter of the foundation, c_v and v being the coefficient of consolidation and the velocity of penetration respectively. In this study, the velocity of pullout is 0.1mm/s while the pipe diameter is 50mm. A c_v value of between $1m^2$/year and $2m^2$/year is typically used for kaolin clay. Lehane and Gaudin (2005) reported a value of $2m^2$/year. This therefore implies that vD/c_v is up to 79 which is greater than 30 suggested by Finnie and Randolph (1994). This therefore suggests that undrained soil behaviour is the prevailing condition during all the pullout tests from this study. Typical range of displacement of subsea pipelines when exposed to elevated temperature and

pressure are between 0.05mm/s to 13mm/s for axial displacement and between 0.2mm/s and 24mm/s for lateral displacement (Denis and de Brier,2010).

The effects of EK treatment on the breakout force using different voltage gradients and electrode materials are analysed and discussed here. The submerged weights of the pipe-electrodes assemblage were kept almost constant for a particular electrode type - 0.68N for copper, 0.61N for iron and 0.22N for aluminium electrode. These were subtracted from the maximum pulling force recorded from the various tests conducted to obtain the breakout force. The key soil parameter that influences the breakout force is the undrained shear strength of the soil. The empirical equation proposed by Muga (1967) and modified by Lui (1969) and then Lee (1973) based on the conventional (.i.e. compressive) bearing capacity equation (Skempton,1951) can be used to predict breakout force from the undrained shear strength although in this case the load is tensile. This is given in equation 5 – 14 and 5 – 15 as:

$$F_{lib} = 1.5A\left[\left(1 - 0.97e^{-2.75D_f/B}\right)F_q\right] + W'' \qquad 5\text{-}14$$

Where,

F_{lib} = the immediate breakout force

A = object plan area

B = object width and

W'' = object submerged weight

$$F_q = 5c_u\left(1 + 0.2\,\frac{D_f}{B}\right)\left(1 + 0.2\,\frac{B}{L}\right) \qquad 5\text{-}15$$

Where,

c_u = undrained shear strength of the soil supporting the object

L = length of the object

D_f = depth of embedment

Given that the pipe dimensions, pipe submerged weight, electrode configurations and the depth of pipe embedment were kept constant in all the tests involving a particular electrode material, equations 5 – 14 and 5 – 15 indicate that the only variable in this

study in terms of the soil resistance to pipe displacement is the undrained shear strength of the soil. Also, taking into consideration the analogy with conventional bearing capacity equation, the failure mechanism of the soil during pipe pullout will involve not only the deformation of the soil at the pipe-soil contact but also failure of soil some distance (vertically and laterally) away from the embedded pipe as the failure surfaces extends away from the pipe. Therefore, the measured soil resistances are due to both the changes (laterally and vertically) in the undrained shear strength of the soil as well as the increase in the pipe-soil adhesion force due to EK treatment.

The correlation between the average undrained shear strength of the soil and the resulting vertical pullout resistance from test series TV-VP is presented in Figure 5 - 23. Assuming symmetry between LC1 and LC3 (.i.e., the EK effect is the same at the two sides of the pipe) the average c_u was obtained by taking the average at LC1 and LC2 only for all tests conducted. The shear strength was averaged over the pipe burial depth *(D_f)* and the zone of influence *(ZOI_F)* obtained using the general foundation theory. The results show slight trend between the peak vertical force and average c_u which demonstrates that increasing applied voltage gradients across the sample promotes increase breakout resistance of the treated soil.

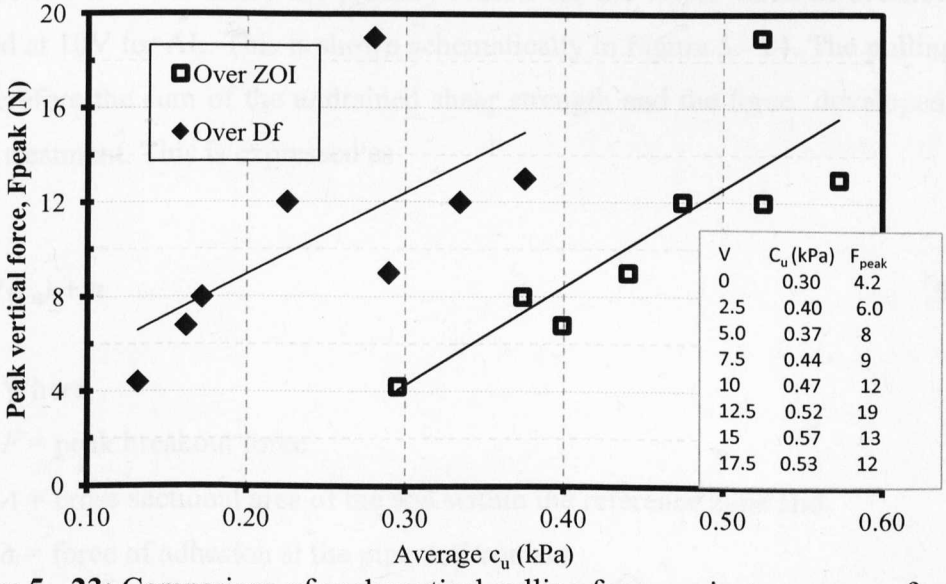

Figure 5 - 23: Comparison of peak vertical pulling force against average c_u for both *ZOI_F (75mm)* and *D_f (30mm)*

It appears that as the average c_u at the sides of the pipe increases, the pipe-soil contact stress increases and the bond between the pipe and the soil also increases resulting in

the increasing resistance to pipe breakout. However, it is expected that the value of the adhesion would depend on the soil type (or site condition) and the type of coating material used on the pipeline. The frictional resistance between coated pipe and uncoated (or rough) pipe is likely to be slightly different.

Erchul and Smith (1970) reported a slight difference in the resistances of coated and uncoated plates penetrated into sediment having cohesion of 7.2kPa. The uncoated pipe has a maximum adhesion of between 17 to 24% of the sediment cohesion while the coated plate had between 15 and 20% of the cohesion of the sediment. The type and nature of the surface coating of the pipe will also affect the pipe-soil adhesion force. Adhesion increases with soil cohesion as well as surface roughness of the embedded object (Chari et al.,1978). It should be noted that adhesion is not considered in this investigation. However, the sharpness of the peaks noted in some of the pullout tests could be related to the level of the adhesion force developed after the EK treatment where higher adhesion could be the reason for sharp peak as it is that noted the load will drop suddenly as the pipe breaks away due to effect of suction.

The top soft level reported for AL electrodes significantly contributed to the low breakout forces measured. Thickness of this layer (about 13mm for AL-10V and about 3mm for AL-2.5V) is likely the primary reason for the lower value of breakout force obtained at 10V for AL. This is shown schematically in Figure 5 - 24. The pulling force, F is therefore the sum of the undrained shear strength and the force developed due to the EK treatment. This is expressed as

$$F = f(c_u) + \alpha \qquad \textbf{5 - 16}$$

Where

F = peak breakout force

A = cross sectional area of the soil within the reference zone and

α = force of adhesion at the pipe-soil contact

$c_{u1} \times A_1 + c_{u2} \times A_2 + \alpha_1 + \alpha_2 = F$

For AL electrodes, c_{u2} is significantly greater than c_{u1}

While for FE electrodes, $c_{u2} \geq c_{u1}$

Therefore, $F_{FE} > F_{AL}$

Although c_u significantly increased at depth using AL-10V and AL-2.5V tests, the pipe-soil adhesion bonding within the pipe-soil contact is greatly reduced due to the top soft layer of the soil by the EK process. During the lateral pulling tests, it is the passive soil resistance and some of the interface friction which contributes to the pullout resistance of the soil whereas during axial pull, it is both interface friction and passive resistance from the soil. Table 5 - 1 presents a comparison of the percentage pullout breakout force measured during this study.

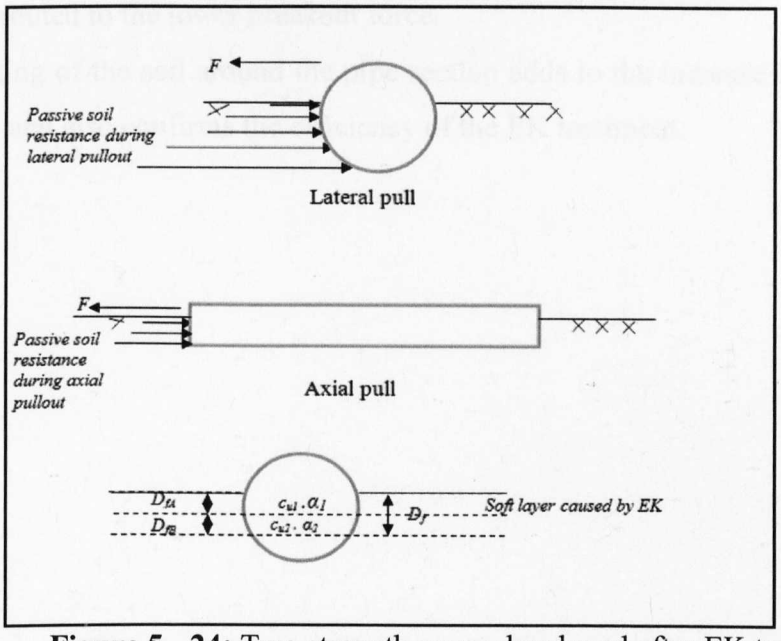

Figure 5 - 24: Two strength zones developed after EK treatment

As stated in §4.7.5, it was observed that the soil around the embedded portion of the pipe section (i.e. anode area) was noticeably altered electro-kinetically. This is due to electro-chemical hardening of the clay around the pipe. In the large-scale test, the pipe section was bare stainless (i.e. no coating) steel pipe section. It does appear that the pipe also acts as the anode even though the electrodes were completely insulated from the pipe section during the test. This is evident by the slight corrosion of the base of the pipe noticed when it was pulled out of the soil. The exact reason for this is not very clear at the moment.

This hardening of the soil and the concomitant increase in the pipe-soil adhesion force at the large-scale confirms the efficiency of the electrode configuration employed in this

study and the potential application of the EK treatment at a full-scale to increase the stability of partially buried subsea. This is consistent with the findings from Milligan (1995) who demonstrated the use of EK to increase the bearing capacity of a metallic steel friction pile in a bridge pier due mainly to electro-chemical hardening of the clay soil around the pipes.

5.6.1 Interim conclusions –analysis of pullout tests results

- FE-electrodes gave the highest breakout force while AL-electrodes gave the lowest breakout force.
- The top weak layer of the soil produced when AL electrodes are used significantly contributed to the lower breakout force.
- Hardening of the soil around the pipe section adds to the increase in the breakout force and also confirms the efficiency of the EK treatment.

Table 5 - 1: Comparison of the results of the pullout tests

Electrode material	Vertical pullout capacity (%)								Axial pullout capacity (%)								Lateral pullout capacity (%)							
	2.5V	5V	7.5V	10V	12.5V	15V	17.5V	20V	2.5V	5V	7.5V	10V	12.5V	15V	17.5V	20V	2.5V	5V	7.5V	10V	12.5V	15V	17.5V	20V
Copper	50	100	125	200	375	225	195		85	164	155	187	136	182	155	200								
Copper		135	61	64								71								30				
Iron			93	123								177								89				
Aluminium			13	-11					-9			-77								-81				
Iron *										190								100						

* = from Large-scale test

5.7 Effect of treatment time

In order to be in position to estimate the efficiency of the treatment process using the different electrode materials, an attempt was made to assess the effect of treatment time on the modification of the model seabed after the EK treatment.

By averaging c_u over the 75mm zone of influence and 30mm depths of embedment, the effects of treatment were assessed and presented in Figure 5 - 25. It can be seen from the plot that the higher the applied voltage the sooner it takes for the process to come to an end. At a constant 10V gradient across the sample, FE electrodes complete the process faster, about 24 hours followed by AL- about 28 hours and finally CU, 60 hours. However, at 2.5V, FE takes the longest time to complete, about 95 hours, followed by AL, 56 hours. For AL at 10V, no significant increase in strength occurs after 12 hours treatment implying that the majority of the EK treatment is only within the first 12 hours of treatment at this applied voltage. A lower applied voltage (2.5V) using the same AL electrode, resulted in a constant increase in strength with increase in treatment time although the final strength is still less than strength at 10V. The 2.5V test was not conducted with CU electrodes.

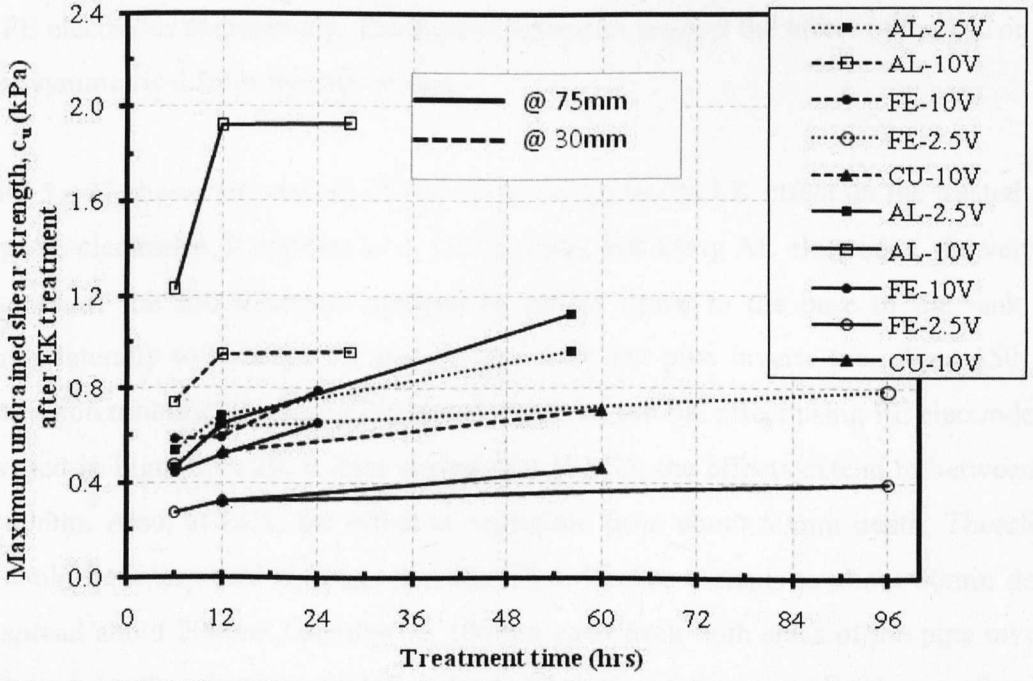

Figure 5 - 25: Effect of treatment time (**6hrs, 12hrs and end of test**) from different electrode materials and voltage

This therefore implies that in terms of speed of the EK process, FE electrodes are the best performers (especially at high applied voltage). This is however a function of the applied voltage gradients, the higher the voltage the faster the treatment process and vice versa.

5.8 Assessment of the zone of influence of the EK treatment

In this section, an attempt is made to assess the combined zone of influence *(ZOI_c)* of the EK treatment on the model seabed. This involves the analysis of the undrained shear strength profiles obtained at the predefined locations (Figure 3 - 10 and Figure 3 - 11) laterally and vertically as well as the use of the normalised strength profiles from the analysis of the c_u profiles. The profiles are extracted from the c_u profiles conducted as part of this assessment. The assessment of this zone is carried out with respect to AL and FE electrodes only since AL electrodes show the best performance in terms of vertical extent of the EK and FE electrodes showed the best performance in terms of lateral extent of the EK treatment.

The lateral and vertical variation in c_u profiles for AL electrode and FE electrodes are presented in Figure 5 - 26 and Figure 5 - 28 respectively. In order to obtain the c_u due to EK effects only, the c_u from the control test was subtracted from the c_u at the various locations and the results presented in Figure 5 – 27 and Figure 5 - 29 for AL electrodes and FE electrodes respectively. The figures appear to suggest the effect of the EK on the soil is symmetrical from the pipe invert.

Figure 5 - 27 shows an analysis of the extent of the lateral EK effect on the treated soil using AL electrodes. It appears from this analysis that using AL electrodes, the vertical influence of the EK treatment appears to extend down to the base of the tank but extends laterally to between 75 and 100mm from the pipe inverts (i.e. about 150 and 200mm horizontally). Similarly the lateral extent of the EK effect using FE electrodes is presented in Figure 5 - 29. It does appear that at LC5, the effects extend to between 70 and 80mm. Also, at LC1, the effect is negligible from about 50mm depth. Therefore, this could be interpreted to mean that the EK influence extends to about 80mm depth and spread about 200mm laterally(i.e. 100mm each from both sides of the pipe invert), depending on the electrode material used. Analysis of the normalised strength plots (Figure 5 - 21and Figure 5 - 22) also confirms the vertical extent of the EK treatment –

about 70 to 80mm below the pipe invert. Therefore it could be concluded that the EK effects using FE electrodes extends laterally more than using AL electrodes. However, the vertical influence is greater when AL electrodes are employed.

If the lateral extent is denoted EK_{lat} and the vertical extent denoted as EK_{Vet}, a non dimensional term which relates the lateral and vertical extents of the EK effects is used to assess the extent of the EK. This combined zone of influence (ZOI_c) could either be elliptical or circular. However, for ease of assessment and comparison, it is simplified as a rectangular and expressed as:

$$ZOI_c = \frac{EK_{lat}}{EK_{vet}} \qquad \textbf{5 - 17}$$

This zone is used in the evaluation of the power requirement (§5.9) of the treatment process for each electrode employed. It gives an indication of the volume of soil treated by the EK process and may be related to the power consumption which is also related to the effectiveness of the EK treatment in terms of cost implications.

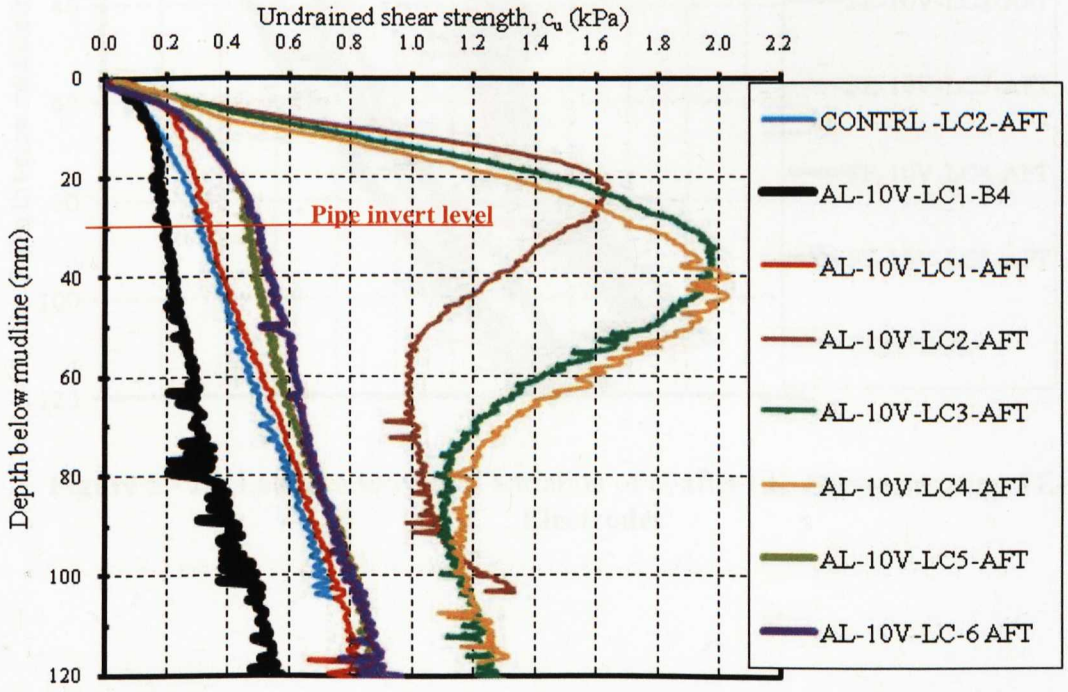

Figure 5 - 26: Lateral and vertical variation of c_u after EK Treatment using **AL-Electrodes**

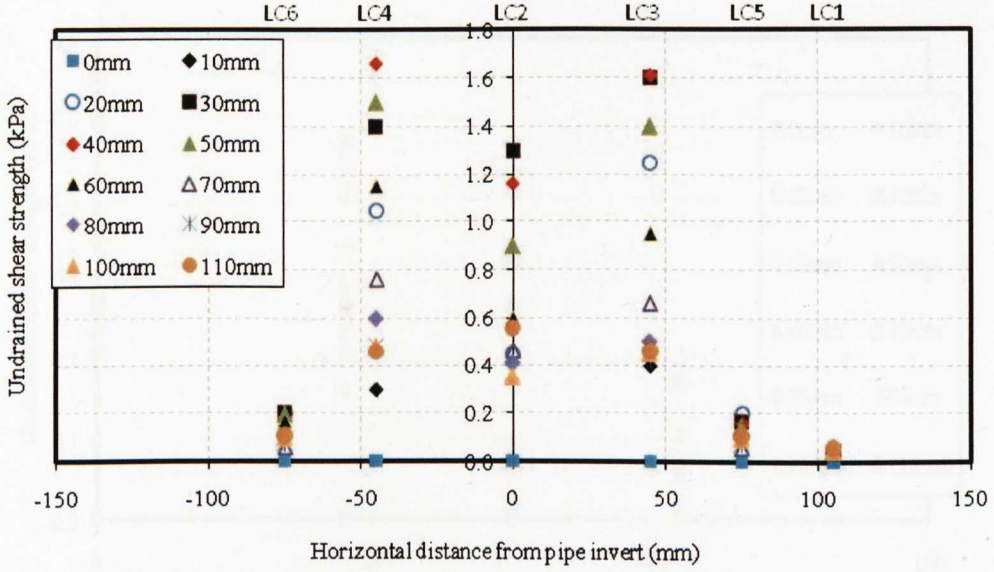

Figure 5 - 27: Assessment of the zone of influence of the EK treatment using AL electrodes

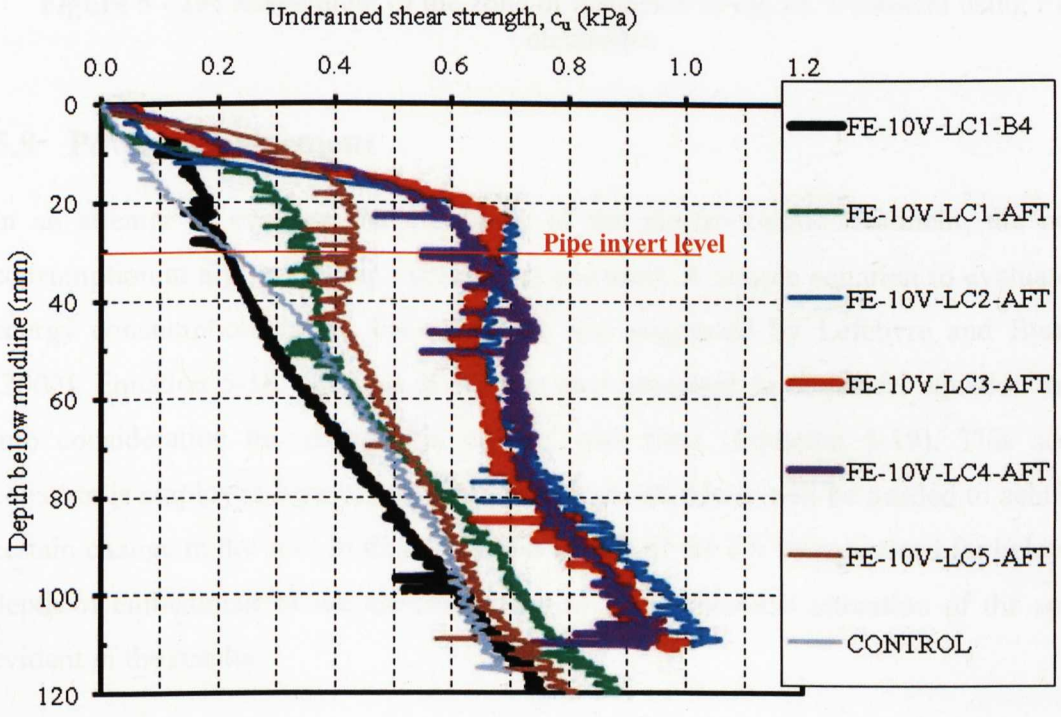

Figure 5 - 28: Lateral and vertical variation of c_u after EK Treatment using **FE-Electrodes**

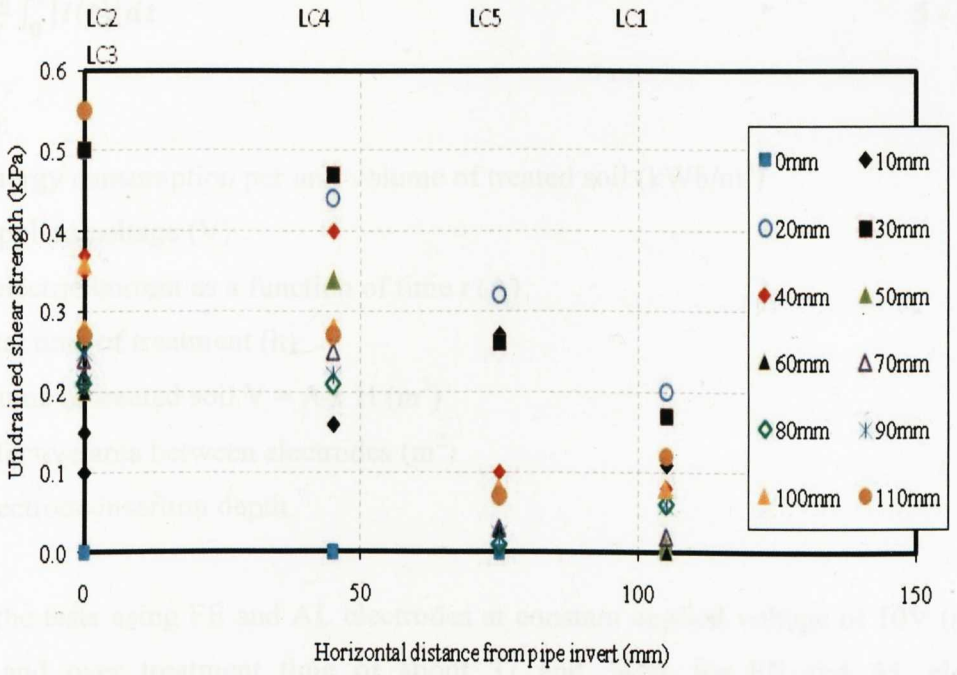

Figure 5 - 29: Assessment of the zone of influence of the EK treatment using FE electrodes

5.9 Power requirement

In an attempt to evaluate the efficiency of the electro-kinetic treatment, the power consumption at a given voltage gradient is assessed. A simple equation to evaluate the energy consumption during EK treatment was suggested by Lefebvre and Burnotte (2002), Equation 5-18. Micic et al.(2003a) also proposed an empirical equation taking into consideration the changes in current with time (Equation 5-19). This second equation is employed here to evaluate the how much power will be needed to achieve a certain change in the soil. In this study, the effects of the EK were noticed far below the depth of embedment of the electrodes due to some chemical alteration of the soil as evident in the results.

$$E = \frac{20VIt}{v} \qquad \textbf{5 - 18}$$

Where:

V = mean applied voltage (V)

I = mean current (A)

t = total time (h)

v = sample volume treated

$$w = \frac{U_o}{V}\int_0^T |I(t)|dt \qquad \textbf{5 - 19}$$

Where:

W = energy consumption per unit volume of treated soil (kWh/m^3)

U_o = applied voltage (V)

$I(t)$ = electric current as a function of time t (A)

T = total time of treatment (h)

v= volume of treated soil V = A x H (m^3)

A = effective area between electrodes (m^2)

H = electrode insertion depth

From the tests using FE and AL electrodes at constant applied voltage of 10V (refer to §5.9) and over treatment time of about 37 and 34hrs for FE and AL electrode respectively, the lateral spread of the EK treatment was 200 mm and 150 mm for FE and AL electrodes respectively. The depth of influence was 80 mm and 100 mm for FE and AL electrodes respectively. The total energy consumption was calculated as 308kWh/m^3 for FE electrode and 302 kWh/m^{3}for AL electrodes. This shows that the energy requirement for the two electrodes is very similar. It should be noted here that while the energy requirement were roughly similar, the ZOI_c varied slightly in terms of lateral spread and depth of influence of the EK using AL and FE electrodes. Further research will be needed to investigate the variation of the power consumption with different applied voltages since this study only investigated the lateral extents of the EK effect using voltage gradient of 10V only due to time constraints.

The amount of power needed to cause a change in the soil properties is assessed as follows: Referring to the undrained shear strength at 30mm D_f at LC2 as a baseline, the power consumption calculated indicates that 308kWh/m^3 is needed to cause a 230% increase in the undrained shear strength of the soil using FE electrode while 302kWh/m^3 is needed to cause about 400% increase in the undrained shear strength using AL electrodes over about 1.5days of treatment.

5.10 Overall repeatability of the EK tests

In order to establish the repeatability of the tests, two identical EK tests (TV-VP and TV-AP) using the same voltage gradients were compared. Various measured parameters such as the current density, changes in the undrained shear strength, water content changes and pullout forces were compared. The results of the comparisons were presented in Tables 4 – 1 to 4 – 3. For instance, the current density from all the tests showed the same trend demonstrating that the experiments were repeatable for the same applied voltage gradient. Referring to Tables 4 – 1 to 4 – 3, it can be concluded that the repeatability of the test results in terms of changes in soil water content, undrained shear strength and the pullouts were satisfactory and repeatable as explained in §4.8.

5.10.1 Interim conclusions –zone of influence and power consumption

- FE electrodes produce the largest lateral zone of influence while AL electrodes produce the most vertical zone of influence.
- The power consumption using AL and FE electrodes are almost similar but not for the same strength.

5.11 Potential electro-kinetic application in pipeline operations

The results and discussions of this research have demonstrated that very soft clay surrounding a seabed offshore pipeline can be successfully treated using EK treatment and therefore provide an alternative approach of mitigation against subsea pipeline instability. However, this approach can only be applied to a new pipeline during the installation process as the cost of its application to an existing pipeline network is not likely to be cost effective. Since EK is potentially a good way of increasing the stability of the pipeline, some suggestions on its possible application to offshore pipeline operations are presented below.

5.11.1 Proposed methods of installation for offshore applications

A preliminary assessment of the shear profile of the site should be carried out and an empirical equation should be use to determine the depth of embedment of the pipeline into the seabed during installation. The next phase should be to couple a series of electrodes around the outer surface of the pipeline using either a geotextile material or appropriate existing offshore pipeline infrastructure. The electrodes could be either

strips of conductive material or woven into a strip of geotextile material e.g. EKGs. These electrodes could either be placed as linear lines along the pipeline, either preinstalled or attached as the pipeline leaves the lay vessel. It is expected that the self weight of the pipeline will cause it to sink into the seabed, bringing the electrodes into direct contact with the soil.

Engineering studies should be conducted in advance of the pipelay operation to determine the lengths of pipeline over which stabilisation will be required. This will have the effect of proving increased contact strength between the pipeline and the seabed at intervals along its length, or throughout its whole length as required. This will enhance the stability of the pipeline at those locations where the pipeline is designed to be anchored and therefore increase the efficiency of the snake-lay configurations (Figure 5 - 30). In addition, the pipeline stability will also be enhanced where the pipeline is to be laid around a curve and over discrete lengths between which the pipeline can expand and contract, without walking. As in this study, the electrode configuration would be such that the electrodes at base of the pipeline and in contact with the soil will be energised as the positive electrode (anodes)will the electrodes at the top portion of the pipeline and within the water medium, will be energised to act as the cathode.

Existing offshore pipeline technology, example (the instrumentations used during pipeline installations) could be used to determine the orientation of the pipeline and possibly give the first indication of depth of embedment. This would guide in determining which electrodes needs to be energised as anode and cathode to provide electro osmosis of the seabed soil. With input from pre-lay engineering studies, the input power requirements and duration of electro osmosis could be determined. During this treatment process the current and voltage could be monitored to give an indication of the progress of the stabilisation. In some circumstances, a subsea power pack and control system may be used with monitoring by acoustic signals; however, in general an umbilical cable could be used as source of power.

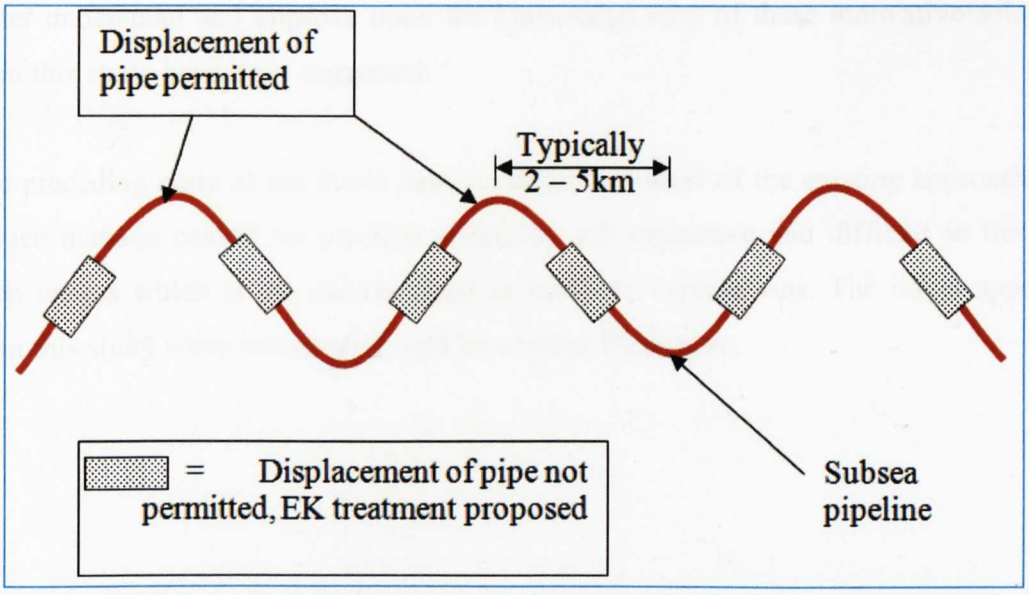

Figure 5 - 30: Schematic representation of plan view of typical lateral buckling design showing possible locations for EK improvement

The most common problem posed with the application of EK treatment in offshore foundations capacity enhancement is the enormous amount of current/power needed to consolidate the soil due the very high conductivity of the seawater. However, in pipeline operations, only a small volume of soil is needed to be consolidated to increase the stability of the pipe and therefore considerably less power will be needed. For example, during axial displacement of the pipeline, only a small volume of soil is involved.

5.12 Concluding remarks

The chapter has presented the analyses and discussions of the results obtained from the electro-kinetic treatment of ambient soil around a model seabed and also demonstrate the potential of using this phenomenon to increase the stability of subsea pipelines. These preliminary results are the first attempt at extending the application of EK in geotechnical engineering to offshore pipelines. The outcomes are very promising and could form a basis for subsequent research in this area.

Although some of the measured effects of EK are not very impressive as compared to the traditional EK treatment onshore, the design of the tests was constrained to closely mimic the actual offshore field conditions and therefore could be improved upon. In addition, some interesting areas for further research which could not be explained using the limited results of this preliminary study have been identified. Possible ways to

better understand and improve upon the knowledge base of these innovative solutions from this study have been suggested.

The preceding parts of the thesis have revealed that most of the existing approaches to reduce damage caused by pipeline instability are expensive and difficult in the very deep waters which is the current trend in offshore explorations. The novel approach from this study when developed could be a better alternative.

Chapter 6

RESULTS, ANALYSES AND DISCUSSIONS OF THE LARGE-SCALE PIPE-SOIL INTERACTION TESTS

6.1 Introduction

This chapter presents in detail the results, analyses and discussions of the large-scale pipe-soil interaction tests described in §3.3. The results of the seabed characterisation tests are presented first followed by the results of the main pipe-soil interactions tests. The results of the lateral pipe-soil interactions are divided into three major sections to assess the influence of the weight of the submerged weight of the pipe, speeds of pipe pulling and the depth of pipe initial embedment during pipe lateral displacement. The results of the axial pipe-soil interaction are also presented. The responses in relation to the generation and development of the soil berm are explained and finally, a summary of the findings and the conclusions of the chapter are provided at end of this chapter followed by discussions of findings in relation to stability of subsea pipeline.

6.2 Test results from the model seabed characterisation

6.2.1 The T-bar and vane test results

The undrained shear strengths (c_u) of the model seabed which were estimated from T-bar and hand shear vane (HSV) tests are presented here. The soil strength from the T-bar penetrometer is achieved by converting the measured soil resistance on the projected area of the bar during the T-bar penetration to the soil c_u using a T-bar factor (N_t) of 10.5 (Stewart and Randolph,1994) as expressed in equation 4-1. It should be noted here the 10.5 factor suggested by Stewart and Randolph (1994) disregards the effects of differences in the surface area during the T-bar penetration and extraction. This appears to suggest the soil strength during extraction of the T-bar is slightly higher.

There is therefore need to assess the effects of this differences with necessary corrections being applied. Figure 6 - 1 shows a typical sets of c_u profiles obtained from T-bar tests, showing both the peak (during pushing in of the T-bar) and the remoulded (during pulling out of the T-bar) undrained shear strength of the model seabed prior to the pipe-soil interaction tests. Note that the lines connecting the two profiles are there because the penetration strength is shown as positive and the extraction strength as negative.

Only the peak strengths, i.e. the penetration strength, are shown subsequently for the purposes of assessing the soil strength. The softening index, S_s (equation 6 -1) of the clay normally expressed as the difference between the strength during the T-bar penetration (peak c_u) and extraction (remoulded c_u) of the soil at the same water content gives an indication of the change in the c_u of the bed of clay due to softening. S_s is usually used to express soil sensitivity to disturbance at constant water content (Craig,2005). From this study, the kaolin used here is indicated to have a S_s ranging between 1.7 and 2.8 which is typical of most normally consolidated clays (Craig,2005).

$$S_s = \frac{peak\ c_u}{remoulded\ c_u} \qquad 6 - 1$$

A total of 25 model seabed (labelled test "a" to test "y") were prepared as part of these tests. T-bar test was not conducted for test-y because the model seabed was assumed very uniform after repeated mixing. For each of the model seabeds investigated, the various c_u profiles from the individual test locations are combined together to obtain an average c_u profile which is taken as the representative shear strength profile of that model seabed (Figure 6 - 2).

Figure 6 - 3a and b show the c_u profiles from the first two model seabeds including results from the hand shear vane (HSV). These two model seabeds are shown because they both include the HSV tests results which were conducted for purposes of comparison with the T-bar. Apart from the first four beds of clay which show relatively higher strength, other model seabeds show slightly reduced strength possibly due to the effect of repeated mixing. There was a slight variation in the spatial variation in the soil c_u across the model seabed in the first seven tests. However, test-h sea bed shows significant uniformity in the soil c_u across tank (Figure 6 - 4b). Therefore test a, b, d and

h are shown here while the remainder of the strength plots are shown in Appendix C. The uniformity in the soil strength with repeated mixing is supported by Figure 6 - 5 which appears to suggest that the homogeneity in soil strength across the tank increases with increasing number of mixes.

Almost all the model seabeds show the average undrained shear strength as being very soft clay with an increase in the c_u of about 0.02kPa/cm down to a depth of 200mm before beginning to increase rapidly with depth. The sudden increase in the strength at about 200mm is mainly due to prolonged exposure to consolidation under its weight since only the top 220mm of the seabed was repeatedly remixed. The HSV data appear to agree with the T-bar results thus the vane were carried out on the first three seabeds only. Also shown in Figure 6 - 2 is the theoretical profile of the c_u for comparison where c_u is predicted from $c_u = 0.3\sigma_v'$ (Muir Wood,1990), assuming $\gamma = 16$ kN/m^3, which is typical of kaolin clay. Although this relationship applies to fresh water soil, no direct relationship exists for saline soil, thus it is assumed valid for saline water.

The predicted soil strength is mainly due to the self weight consolidation of the clay (and is a function of the effective unit weight of the soil elements as well as level of consolidation). This theoretical profile however shows a slightly lower soil strength than the measured strength which might suggest that the soil is slightly over-consolidated with depth. The strength profiles from the tests show that beyond 225mm depth the soil shows increasingly higher strength. Since the calculated zone of influence due to the lateral and axial motion of the pipe is within this depth, its effects on the soil resistance is assumed to be minimal. The determination of the seabed c_u profile is fundamental in estimating the penetration of the pipe into the seabed as well as assessing the lateral and axial resistance of the soil to pipe motion.

In order to assess the influence of consolidation time on c_u from a T-bar test, additional T-bar tests were conducted at 24 hours intervals during test-d (Figure 6 - 4a). These are LC10 to LC12. It can be seen from the plots that the average change in c_u from the T-bar was approximately 0.02kpa per day implying the increase in shear strength ~1%. This reflects that the effect of consolidation time on the c_u after thorough mixing was minimal and therefore between 3 to 7days consolidation time was chosen for all the tests.

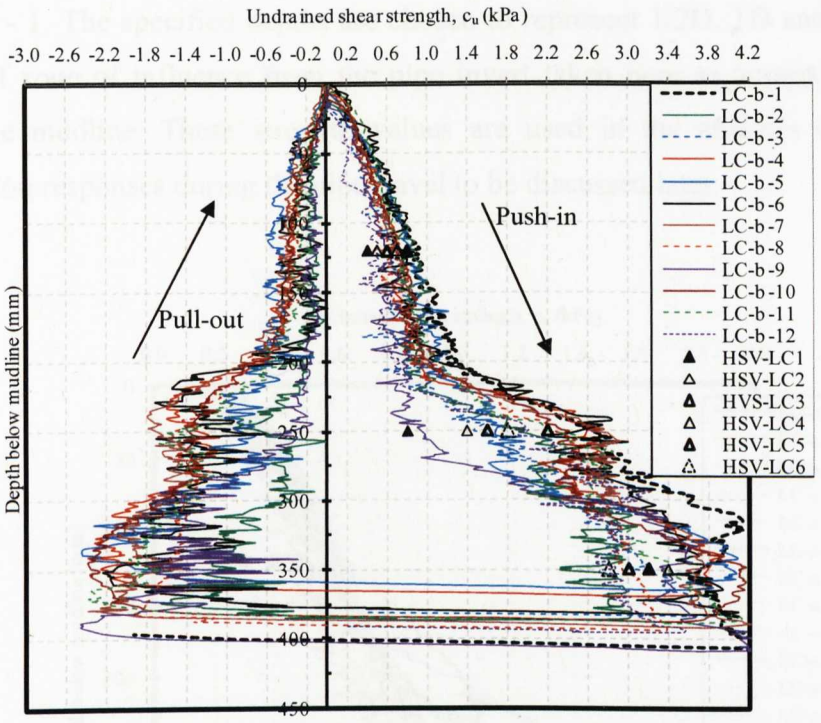

Figure 6 - 1: A typical T-bar response showing the push-in and pull-out soil resistances representing the peak and the remoulded strength profiles of one of the model seabeds

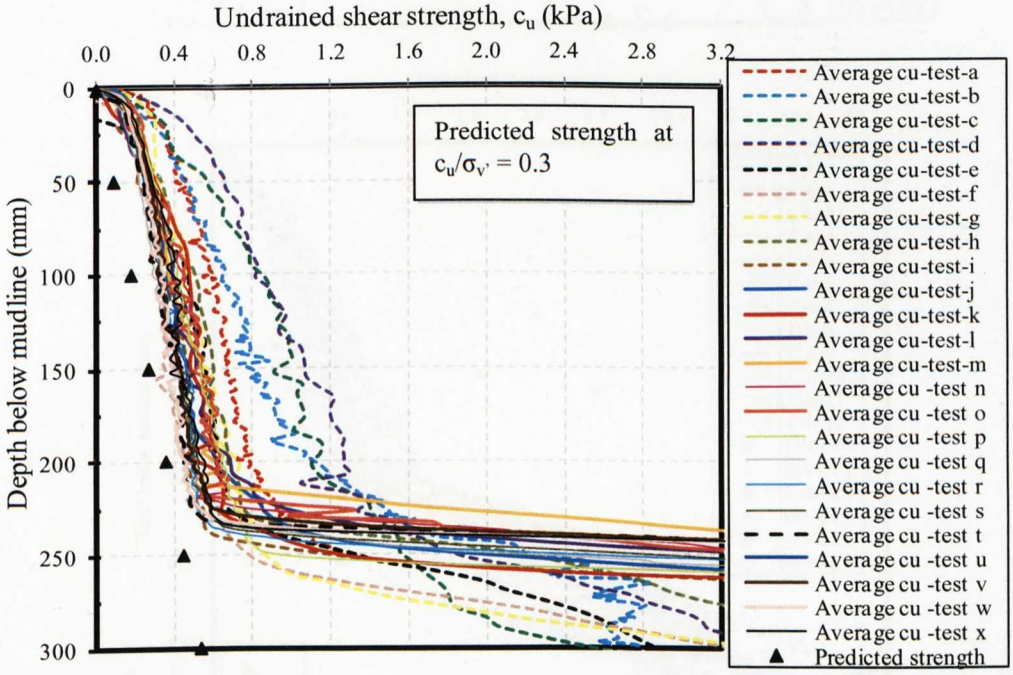

Figure 6 - 2: Plots of average undrained shear strength profiles of the model seabeds investigated

It is a usual practise to normalise the resulting soil resistances during pipe displacement by a representative shear strength value. In order to assess this representative c_u value from the individual seabeds, the soil c_u at depths 65mm (1/2D), 130mm (1D) and 225mm were extracted from the individual averaged c_u profiles and are presented in

Table 6 - 1. The specified depths are chosen to represent 1/2D, 1D and the anticipated depth of zone of influence from the pipe invert taken here as approximately 250mm from the mudline. These strength values are used in the analysis of the pipe-soil interaction responses during the pipe travel to be discussed later.

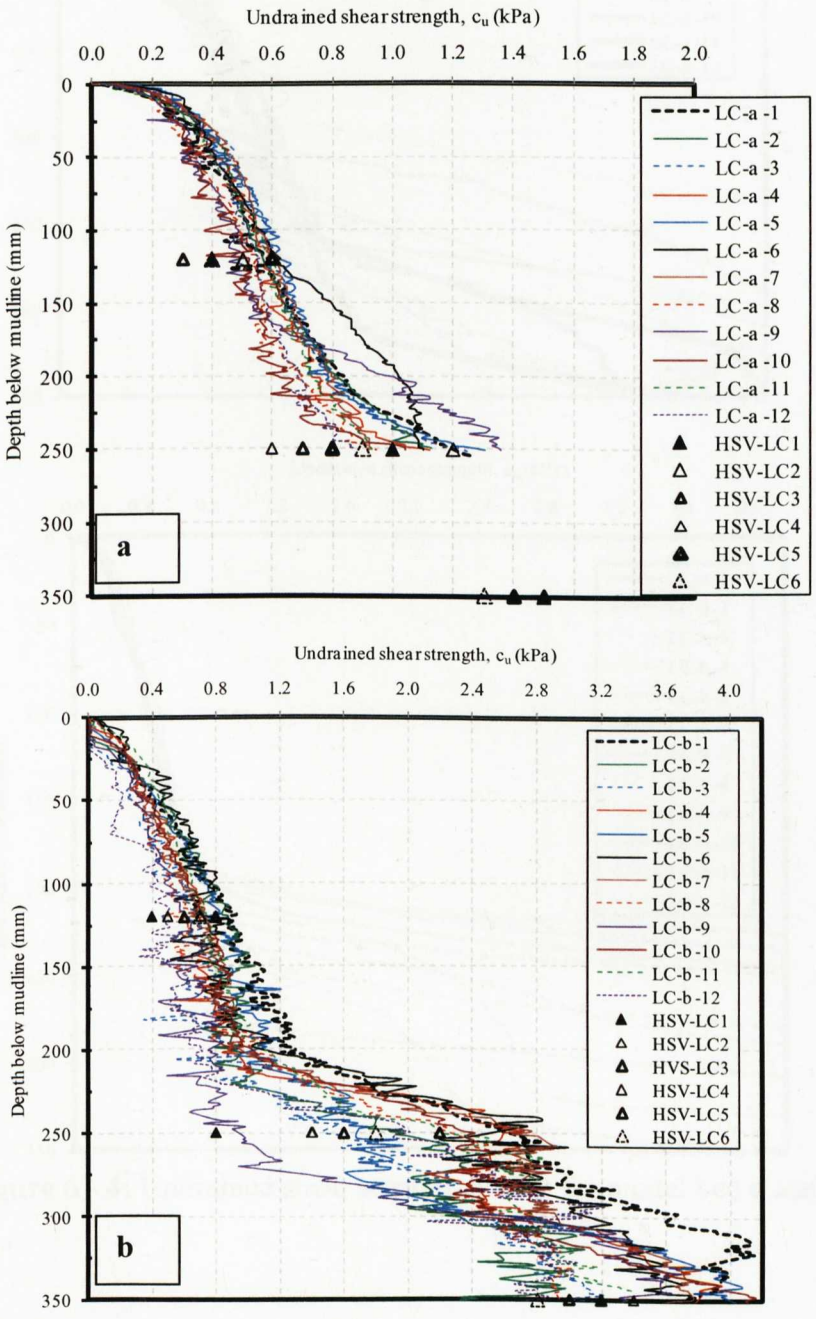

Figure 6 - 3: Undrained shear strength profile for model bed a, and b

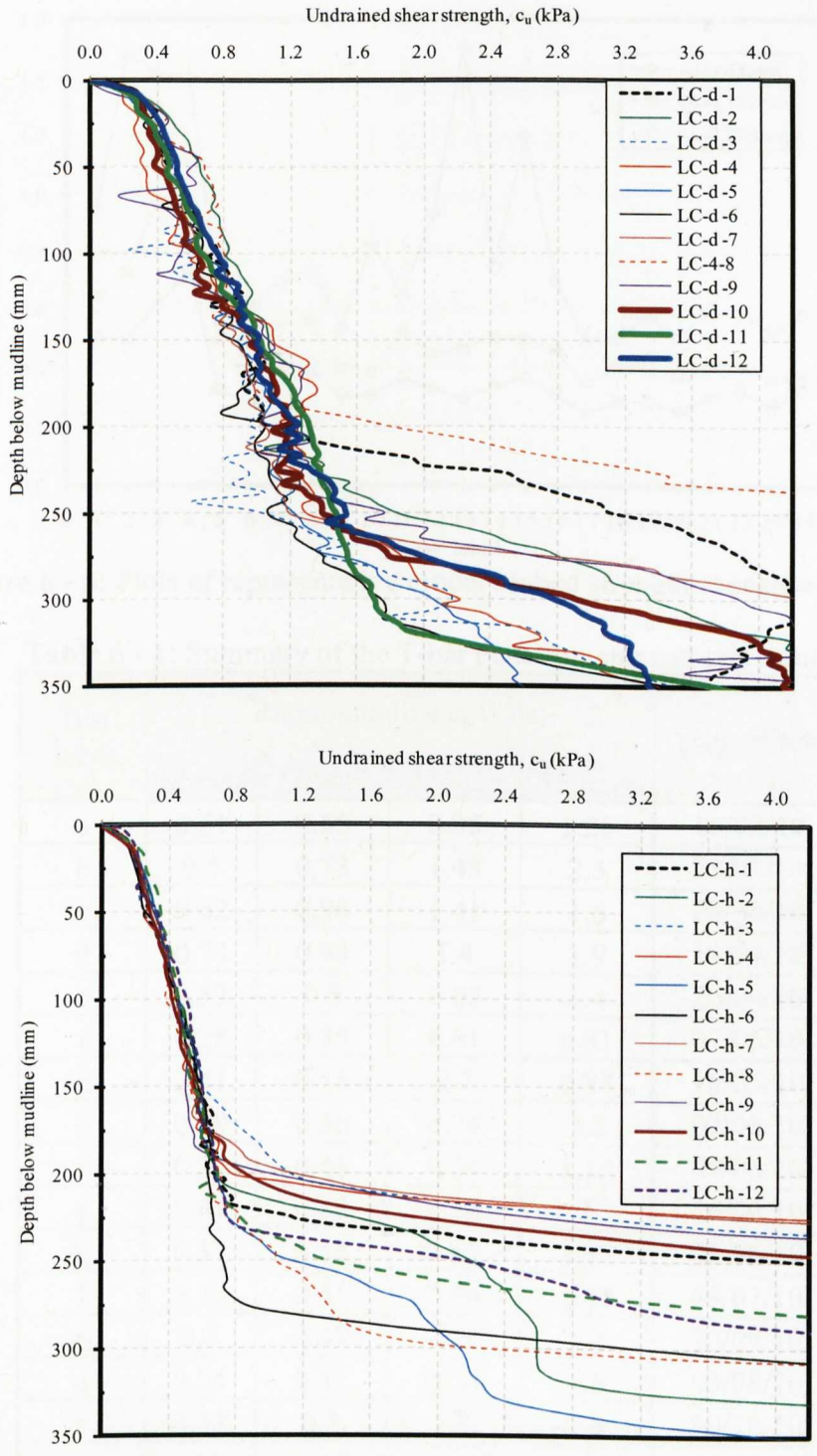

Figure 6 - 4: Undrained shear strength profile for model bed d and h

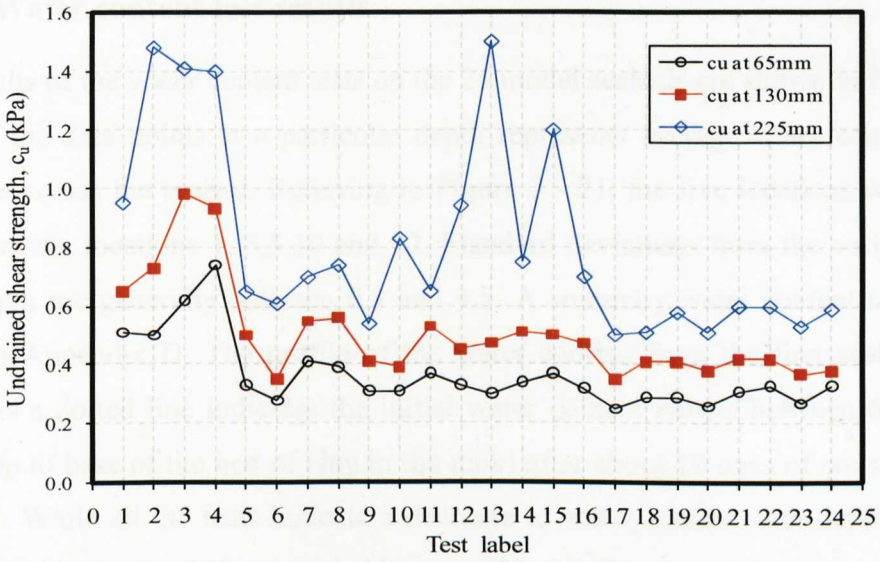

Figure 6 - 5: Plots of representative model seabed strength at selected depths

Table 6 - 1: Summary of the T-bar penetrometer test and results

Test label	Representative c_u (kPa)				Date of test
	65mm	130mm	225mm	250mm	
a	0.51	0.65	0.95	1.25	16/02/10
b	0.5	0.73	1.48	2.3	22/03/10
c	0.62	0.98	1.41	1.6	08/04/10
d	0.74	0.93	1.4	1.9	19/04/10
e	0.33	0.5	0.65	1.4	26/04/10
f	0.28	0.35	0.61	0.81	07/05/10
g	0.41	0.55	0.7	0.87	18/05/10
h	0.39	0.56	0.74	2.2	02/06/10
i	0.31	0.41	0.54	1.13	09/06/10
j	0.31	0.39	0.83	2	16/06/10
k	0.37	0.53	0.65	1.35	23/06/10
l	0.33	0.45	0.94	2.68	09/07/10
m	0.3	0.47	1.5	4.2	20/07/10
n	0.34	0.51	0.75	3.6	03/08/10
o	0.37	0.5	1.2	3.6	10/10/10
p	0.32	0.47	0.7	1.42	15/09/10
q	0.25	0.35	0.5	2	21/09/10
r	0.29	0.41	0.51	2	30/09/10
s	0.29	0.41	0.58	2.4	11/10/10
t	0.26	0.38	0.51	3.8	18/10/10
u	0.31	0.42	0.6	3.8	25/10/10
v	0.33	0.42	0.6	3.9	29/10/10
w	0.27	0.37	0.53	3.8	02/11/10
x	0.33	0.38	0.59	3.9	04/11/10

6.2.2 Water content test results

The results of the water content tests on the 25 model seabeds are shown in Figure 6 - 6. Each of the data points at a particular depth represents average water content over 5 locations across the seabed. Referring to Figure 3 - 21, the five locations were near to the T-bar test locations 1, 3,5,10 and 12. Standard deviations from the various tests at each depth are generally between 0.8 and 4.8. A summary water content table can be found in Appendix D. The profile of the water content from the first seabed (test-a) shown as a dotted line indicates the initial water content ranges between 69 and 63% (from top to base of the bed of clay in the tank) after about 10 days of consolidation in the tank. While all the tests indicate a decrease in water content with depth, the water content within the top 150mm varied between 60 and 78% due to the repeated remixing of the seabed during successive tests.

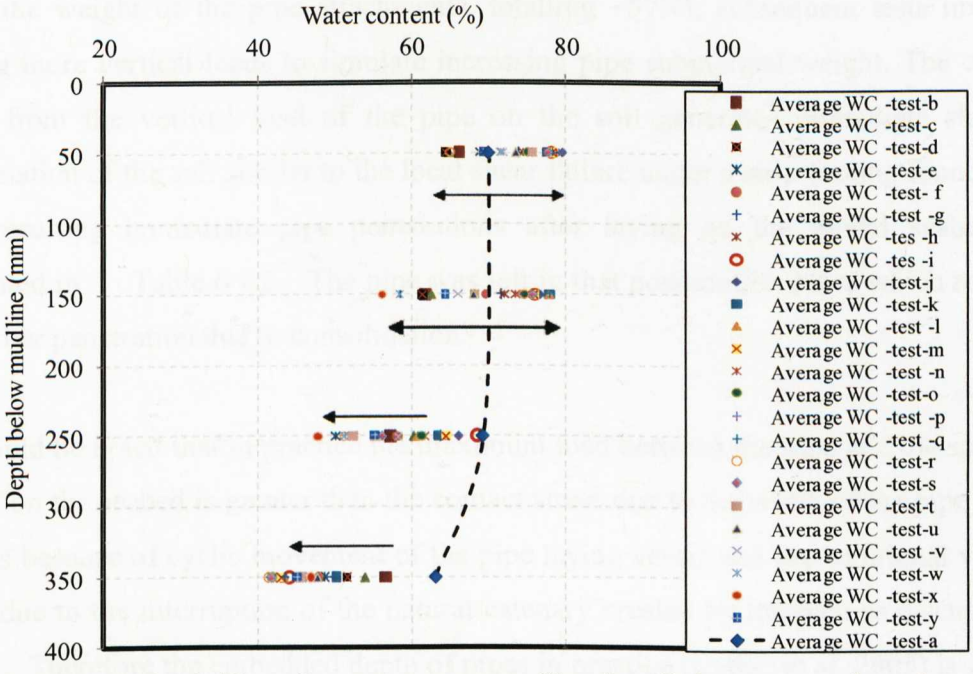

Figure 6 - 6: Plot of water content profiles for all the tests conducted

The constant remixing of the model seabed after each test appears to promote a variation in water content profiles. It can also be seen that in the zone where no mixing took place, the value of the water content constantly decreased with time down to about 42% due to prolonged consolidation of the seabed. It does appear therefore that this method of seabed preparation which involves removal of the surface water after each pipe-soil interaction tests and remixing of the clay bed does not ensure consistency in

the water content as seen in the c_u plots. However, the pipe-soil interaction responses during tests were normalised by the representative c_u for ease of comparison of results.

6.3 Results from pipe-soil interaction tests

6.3.1 Effects of submerged weight of pipe – *Series LP-SW*

In this section, the results of tests to investigate the effects of effective vertical weight of the pipe on soil lateral resistance are presented. Results of the lateral pulling tests are presented first followed by the results of the seabed deformation studies (berm generation) during the lateral movement of the pipe (referred to as pipe sweeping).

6.3.1.1 Results of the lateral pulling tests (pipe sweeping)

The first sweep (from test-a) started by releasing the pipe section from the loading trolley and allowing it to bury gently into the model seabed due to its submerged weight (plus the weight of the pipe attachments, totalling ~57N); subsequent tests involved adding more vertical loads to simulate increasing pipe submerged weight. The contact force from the vertical load of the pipe on the soil generates immediate shearing deformation of the soil similar to the local shear failure under a strip footing foundation. The resulting immediate pipe penetrations after laying on the model seabed are presented in Table 6 - 2. The pipe was left in that position for 24hrs which resulted in further penetration due to consolidation.

It should be noted that in practice the maximum load between the pipe and the soil as it is laid on the seabed is greater than the contact stress due to the width of the pipe alone. This is because of cyclic movement of the pipe laying vessel and the additional vertical force due to the interruption of the natural catenary created by the pipe as discussed in §2.4.1. Therefore the embedded depth of pipes in practice (Cathie et al, 2005) is greater than that due to its weight alone. These additional forces are unknown and are difficult to predict. Therefore, the total penetration of a pipe is a function of the immediate penetration during pipe installation, penetration at the end of consolidation period, and further penetration due to cyclic movement of the pipe. The penetration due to the weight of the pipe can be predicted using classical soil mechanics approaches already discussed in chapter 2.

The force-displacement responses and the pipe trajectories during the lateral sweeps from the five tests conducted in this test series are presented in Figure 6 - 7 to Figure 6 - 11, while the pipe vertical penetrations during the tests are presented in Table 6 - 2. All the plots are presented using the same scale for purposes of comparison of the soil resistances from various submerged pipe weights. For test-a, the immediate pipe penetration into the soil was about 6mm plus a further 0.43mm after 24 hours of consolidation of the soil.

The first sweep was made to start at ~500mm (on the x-axis of the graph) and moved to the left a distance of about 600mm. At the end of the sixth sweep, the maximum pipe penetration was 35mm. Initially the pipe moved horizontally (Figure 6 -7a). Gradually a berm of soil started to build in front of the pipe causing the pipe to rise by about 10mm (equivalent to approximately 1mm uplift per 40mm of lateral displacement). This is consistent with the force-displacement response (Figure 6 – 7b) of the pipe where after the breakout from the as-laid position, the lateral resistance of the soil continue to increase as the berm of soil increases in front of the pipe section. The breakout force was defined in §2.3 as the force in the excess of the pipe's submerged weight needed to lift or move the pipe from its as-laid position.

During the second sweep, the pipe invert level reduced by about 17mm due to the pipe gradual embedment into the soil. The relative reduction in the pipe invert level in subsequent sweeps was less than that in the second sweep. This was possibly due to the increasing shear strength of the soil at greater depth below the mudline; i.e. the soil provided a greater resistance to penetration. In all, a total of 15 lateral sweeps were conducted during test-a. In subsequent tests it was decided to restrict the number of passes to six because the additional passes did not show any further increase in soil resistance.

It is noted that in test-a there was very little variation in the hysteresis loop between passes after the first pass (Figure 6.7.b). Furthermore, the gradient of the force displacement plot as the pipe moved across the trench created by the previous pass was almost horizontal. This pattern was noted in test -b and -c (Figure 6 - 8 and Figure 6 - 9). However, in test d and e (Figure 6 - 10 and Figure 6 - 11) there was a significant increase in the slope of the force-displacement plot. Figure 6 - 12 shows a plot of these

gradients for the first pass only. This tends to suggest that slope of the horizontal force-displacement curve is a dependent on the submerged weight of the pipe. Effectively the pipe slides over the seabed if its weight is less than 87N but acts as a plough if the weight exceeds 87N. As state in §2.2.8, pipes are classified as 'light' or 'heavy' depending on their normalised weight (W'/c_uLD), i.e. with respect to the seabed strength and the pipe diameter. For normalised pipe weight (W'/c_uLD). < ~1.5, the pipe is considered "light" whereas for values > ~2.5, it is considered "heavy"(Bruton et al.,2008). The normalised weight for tests -a – d ranges between 1.1 and 1.5 while that of test-e is 3.1 based on the representative c_u at the respective pipe invert. Therefore, tests -a-d behave as light pipes while test-e as a heavy pipe.

It appears therefore that even within the same category some variations exist in the response of the pipe that would call for reclassification especially with the "light" pipes. Nonetheless, it appears to suggest that the slope of the curve which represents the rate of increase in lateral soil resistance with lateral displacement is dependent on the effective weight of the pipe as seen by the shape of the hysteresis curve. This response is also consistent with the vertical penetration of the pipe where significant pipe penetration with lateral displacement increases significantly in test-e ($W'/LDc_u = 3.1$).

In addition, only test-a ($W'/LDc_u = 1.1$) shows pipe uplift during pipe travel after breakout during its first sweep while test b – d, although classified as "light pipes", do not. It is the opinion of the author therefore that normalised pipe weight from ~3.0 is likely to promote excessive pipe vertical penetration during cyclic lateral displacement. Extreme vertical penetration of pipelines, especially at the crest of the buckles, imposes excessive lateral load on the pipe which could undermined its structural integrity during operation (Friedmann,1989; Bruton et al.,2008). This is because with increasing penetration, the lateral movement of the pipeline is restricted leading additional loading on the pipe. All five tests except test-c were allowed to go over the dormant berm of soil at a point (mostly during the 4^{th} sweep). This was to assess the amount of additional lateral resistance that could be offered by the dormant berm. The dormant (or static) berm is the heap of soil left behind when the pipe changes its direction of movement. For test-a, as the pipe approaches the dormant berm and tries to climb it, the pulling force increases rapidly initially and then become nearly constant as the pipe climbs the berm.

Table 6 - 2: Pipe penetrations during lateral pipe-soil interaction tests

Test label	Immediate pipe penetration (mm)	Total pipe penetration after 24 hrs (mm)	Pipe invert depth before start of lateral sweep (mm)	Maximum pipe depth after 6 cycle lateral sweeps (mm)	Lateral soil force on pipe after embedment (N)	Lateral soil force on pipe before lateral sweep(N)	Remarks
a	5.94	0.43	8.03	35	0.943		
b	6.22	9.85	9.31	111	2.152	4.914	
c	7.06	10.10	11.46	128	0.943	6.122	
d	11.89	16.66	16.26	160	0.691	5.006	
e	20.08	31.08	32.96	151	0.345	4.488	
f	8.00	15.11	17.46	154	1.726	7.423	
g	12.96	20.05	20.08	160	0.863	2.762	
h	5.71	9.57	9.60	152	1.899	5.352	
i	14.01	25.78	25.78	140	0.345	5.524	
j	18.72	28.90	28.97	147	0.691	0	
k	18.00	22.74	22.77	154	1.289	3.36	
l	12.10	1.20	66.39	51	0.771	4.396	Pipe pushed to 65mm(1/2D)
m	10.41	-0.20	130.23	7	2.926	10.299	
n	11.48	0.91	65.43	68	2.59	4.488	
o	8.53	-1.17	128.94	6	0.518	1.381	
p	15.4	0.13	65.43	89	0.691	2.59	
q	10.48	0.10	130.20	5	10.093	9.748	
r	13.92	0.91	66.43	5	0.691	2.762	
s	7.33	0.10	130.14	5	0	1.726	

Vertical cracks are also noted on the soil surface in front of the pipe as it pushes through the berm possibly indicating tensile failure of the soil mass. In contrast, test-b, d and e all indicate a constant increase in the soil resistance as the pipe pushes through the dormant berm of soil. As the pipe maintains a constant climb, the force starts to reduce slightly meaning the lateral restraint from the soil reduces as the advancing pipe climbs upward.

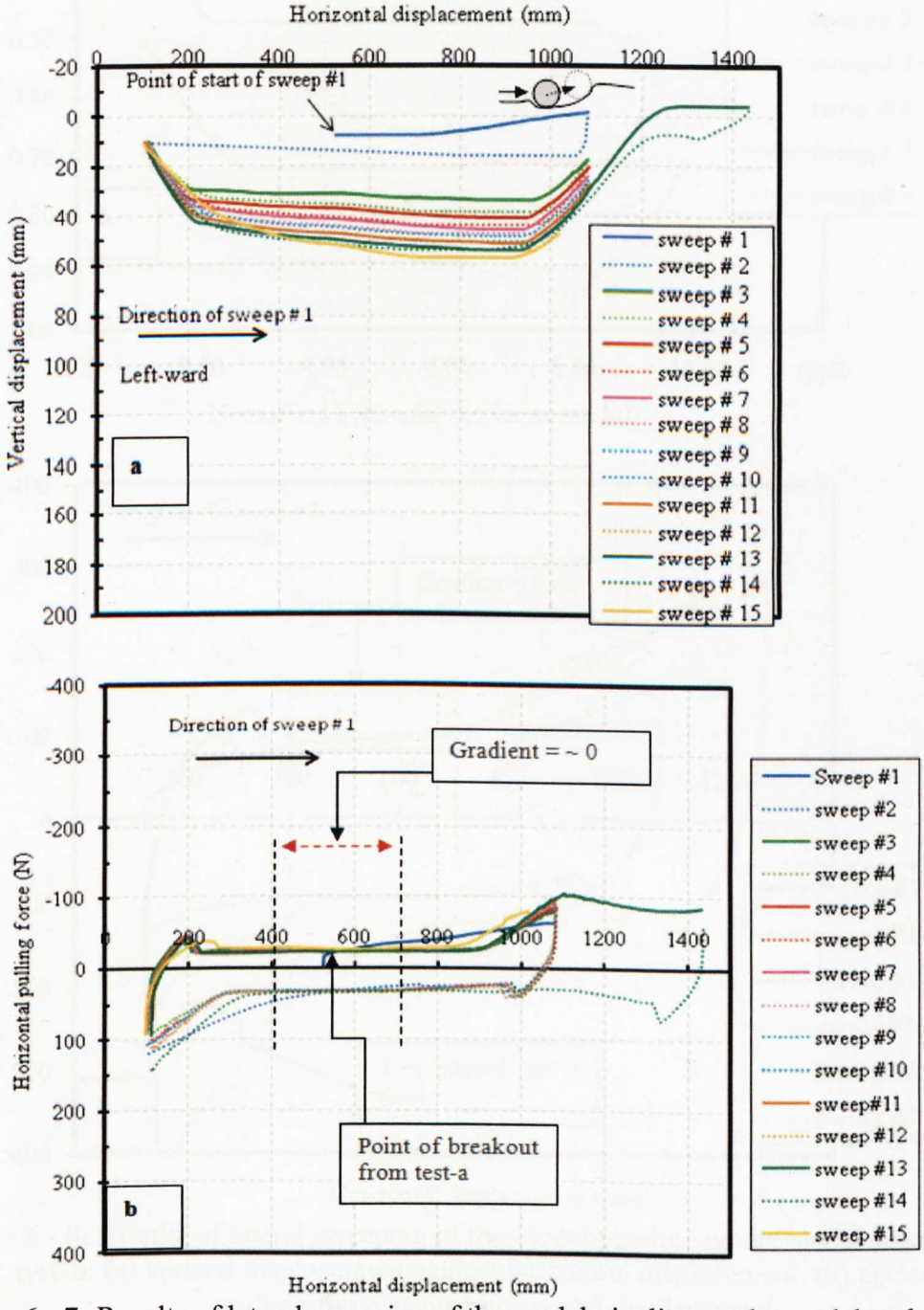

Figure 6 - 7: Results of lateral sweeping of the model pipeline on the model seabed for **test-a**: (a) vertical displacement against horizontal displacement, (b) horizontal pulling force against horizontal displacement

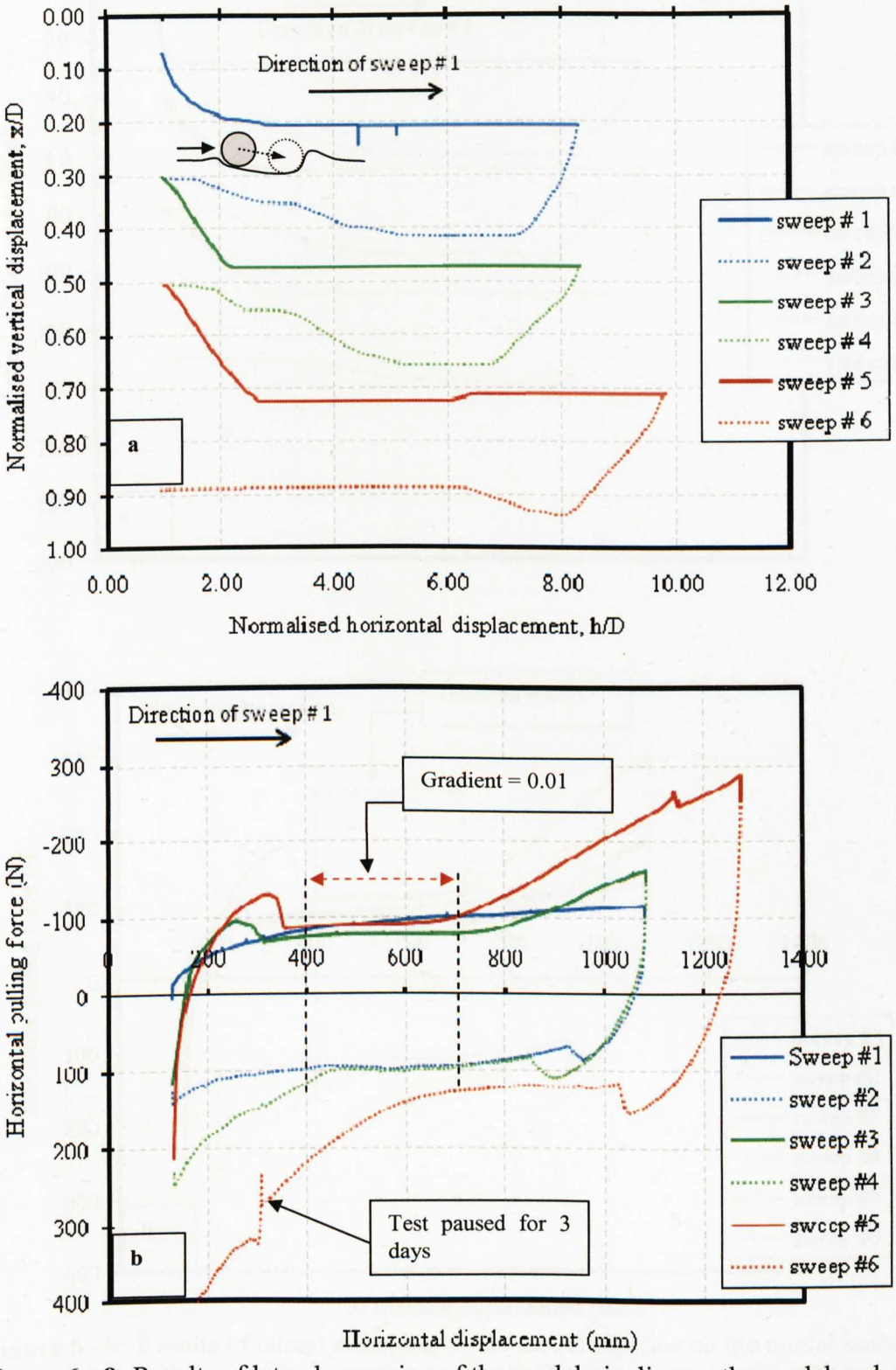

Figure 6 - 8: Results of lateral sweeping of the model pipeline on the model seabed for **test-b**: (a) vertical displacement against horizontal displacement, (b) horizontal pulling force against horizontal displacement

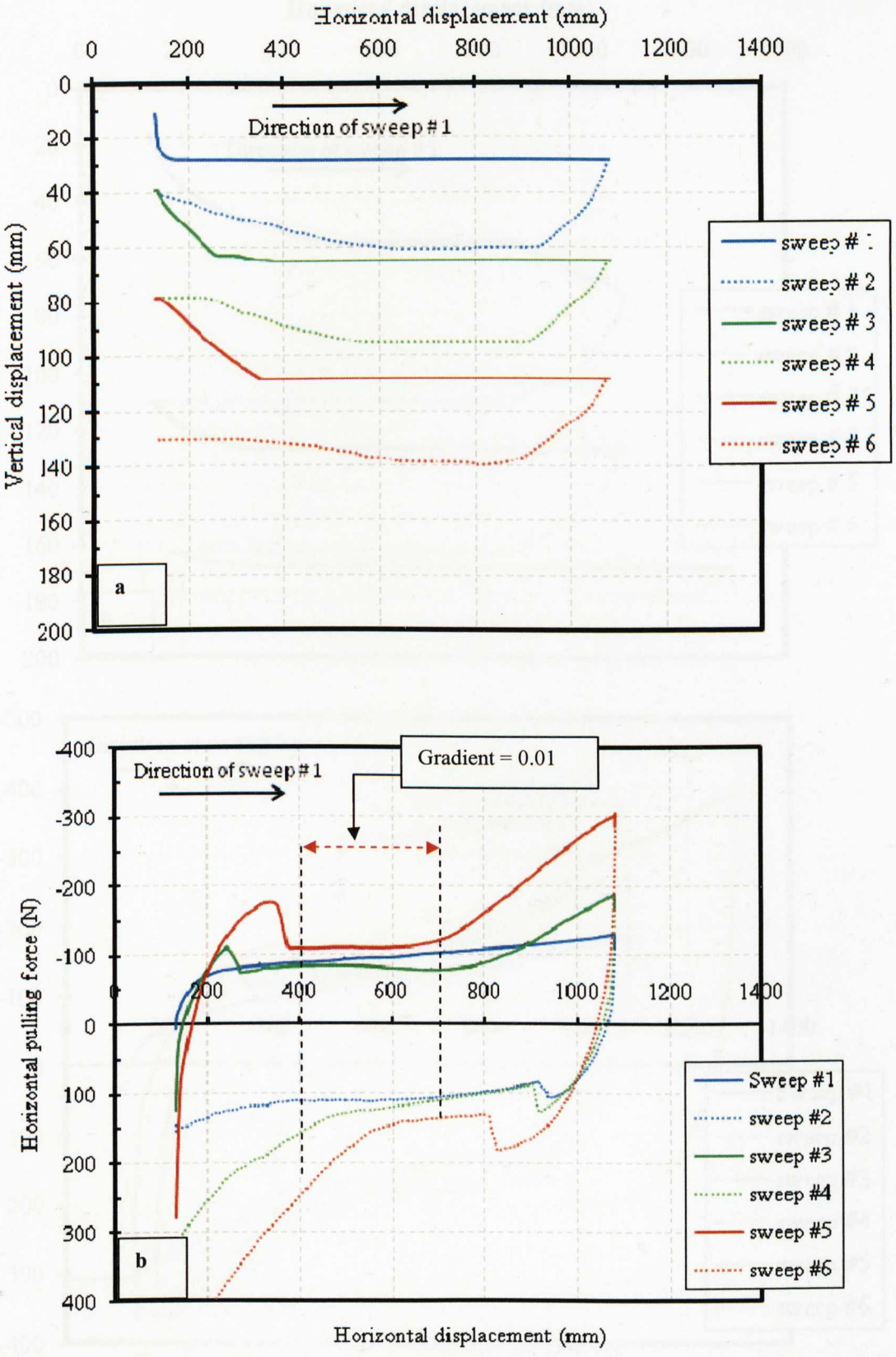

Figure 6 - 9: Results of lateral sweeping of the model pipeline on the model seabed for **test-c**: (a) vertical displacement against horizontal displacement, (b) horizontal pulling force against horizontal displacement

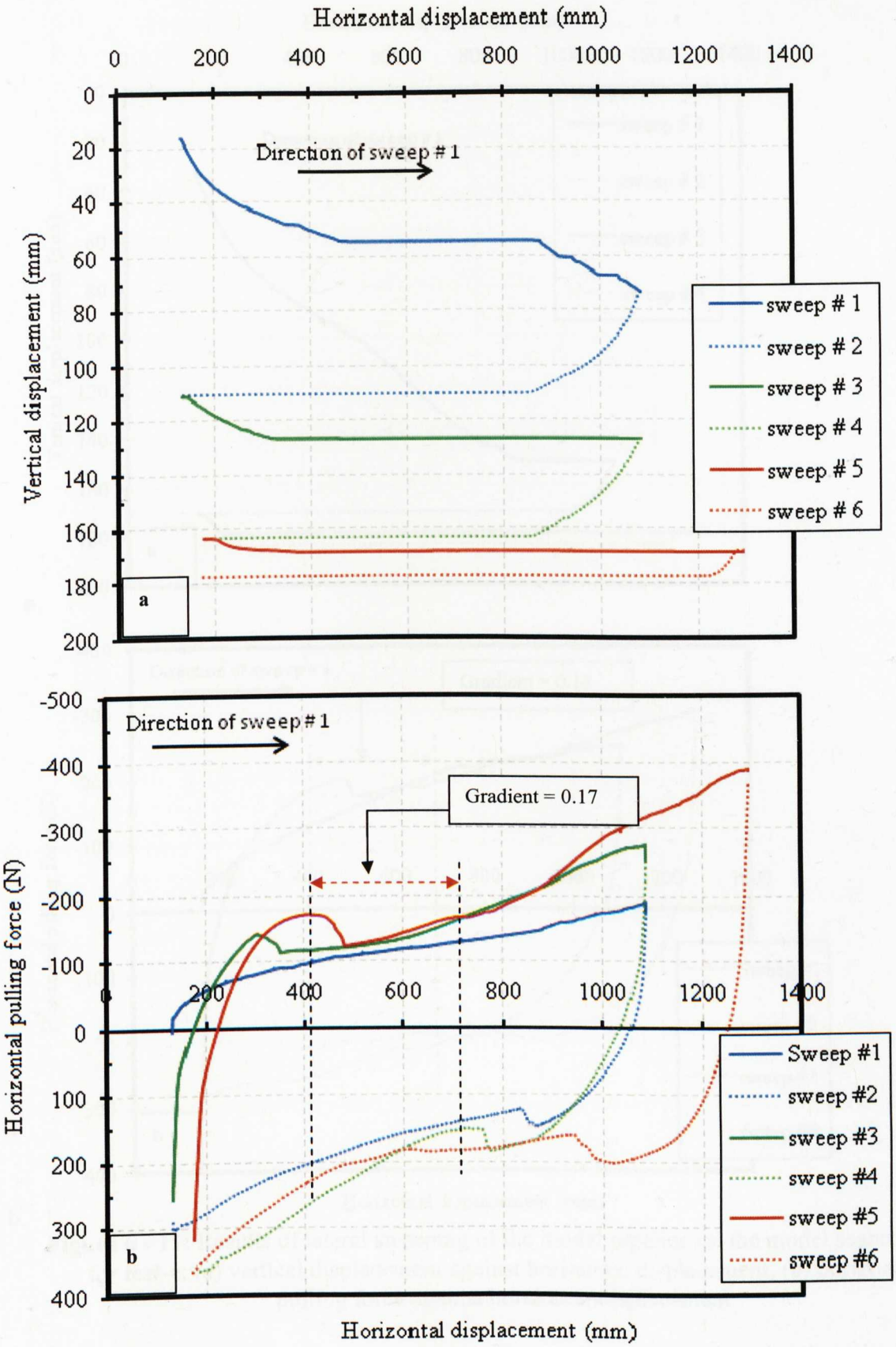

Figure 6 - 10: Results of lateral sweeping of the model pipeline on the model seabed for **test-d**: (a) vertical displacement against horizontal displacement, (b) horizontal pulling force against horizontal displacement

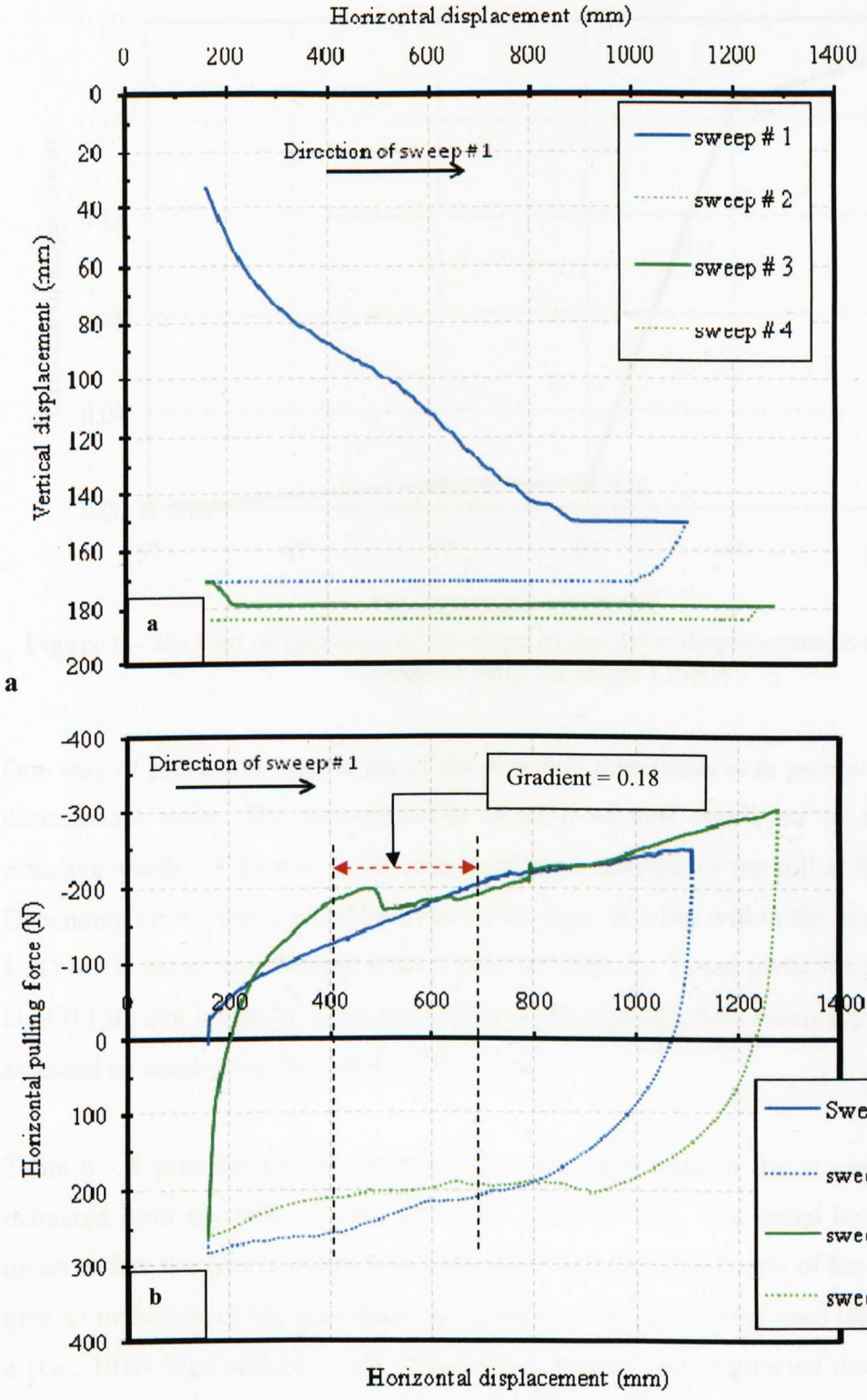

Figure 6 - 11: Results of lateral sweeping of the model pipeline on the model seabed for **test-e**: (a) vertical displacement against horizontal displacement, (b) horizontal pulling force against horizontal displacement

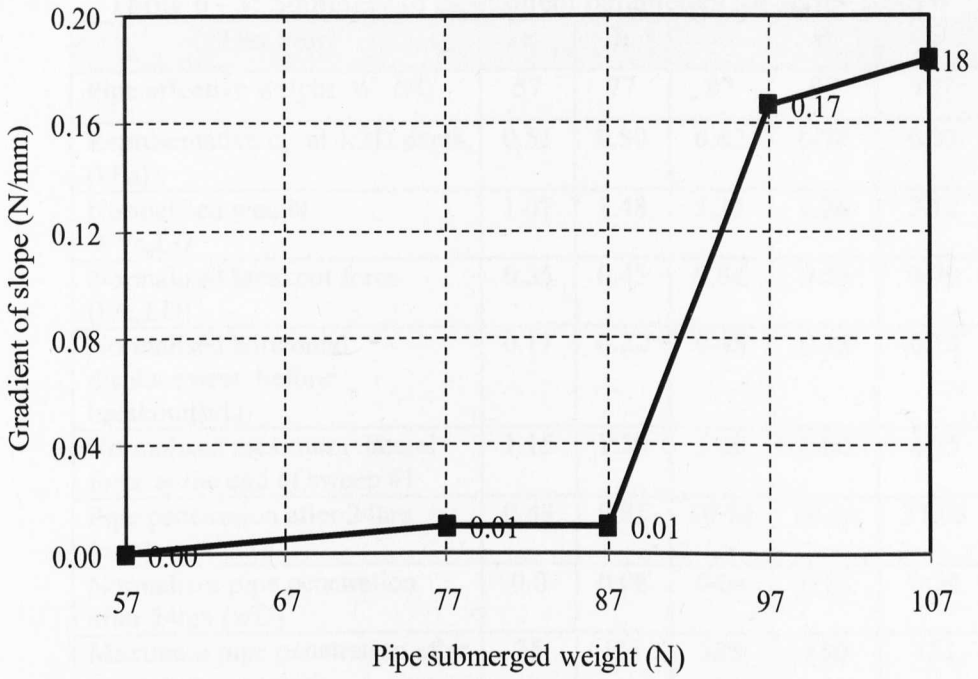

Figure 6 - 12: Plot of gradients of the slope of the force-displacement response from sweep #1 only for series LP-SW

One way of presenting the results of the pipe-soil interaction is to present them in non-dimensional units. The representative strength of soil employed to normalise the effective weight of the pipe is the undrained shear strength of the soil at the pipe invert. Depending on the depth of embedment of the pipe, this lies within the strength range at 1/2D to 1D below the mudline (please refer to Table 6 - 1) and given the pipe diameter, D of 0.13m and length of 0.8m, the effects of the pipe effective (submerged) weight are assessed by combining the results of the 5 tests.

Table 6 - 3 presents the summary of the parameters used in the assessment. This is extracted from the pulling tests results for series LP-SW. The initial level of the pipe invert before the lateral sweep was subtracted from the final levels of the pipe invert to give an indication of the maximum penetration of the pipe during each test. In the test – e (i.e., 107N pipe weight), only four lateral sweeps were conducted due to excessive penetration of the pipe into the soil.

Figure 6 - 13 seems to suggest that while the normalised displacement of the pipe after the six-cycle lateral sweeps increases from test-a to d (.i.e. 55N to 99N vertical load), the normalised vertical displacement appears to be independent of the normalised weight of pipe.

Table 6 - 3: Summary of assessment parameters for series LP-SW

Test label	a	b	c	d	e
Pipe effective weight, W' (N)	57	77	87	97	107
Representative c_u at 1/2D depth (kPa)	0.51	0.50	0.62	0.74	0.33
Normalised weight W'/c_uLD	1.07	1.48	1.35	1.26	3.12
Normalised breakout force (F/c_uLD)	0.35	0.45	0.61	0.53	0.79
Normalised horizontal displacement before breakout(h/D)	0.11	0.22	0.45	0.38	0.18
Normalised maximum lateral force at the end of sweep #1	1.15	1.50	1.20	2.00	4.75
Pipe penetration after 24hrs (mm)	0.43	9.85	10.10	16.66	31.08
Normalises pipe penetration after 24hrs (x/D)	0.0	0.08	0.08	0.13	0.24
Maximum pipe penetration after six sweeps, x (mm)	35	111	128	160	151
Normalised maximum pipe penetration after six sweeps (x_{max}/D)	0.27	0.85	0.98	1.23	1.16

The only deviation is from test -e which shows significantly higher normalised pipe weight with reduced normalised vertical penetration. This could be possible due to the selection of the average c_u used for the normalisation. Also, the model seabed is slightly over consolidated with depth hence reducing the amount of penetration after the initial pipe penetration. Such response will vary depending on the seabed conditions. However, the average seabed strength within the first 1m depth is between 1 – 2kPa, although lateral variations do exist at times, which increases the level of uncertainty in the selection of the appropriate representative c_u for the pipe-soil analysis.

Figure 6 - 14 shows the plot of normalised breakout force against normalised pipe horizontal displacement before breakout. This is one way of assessing the effect of effective pipe weight on the breakout resistance of the soil. Also included as insert, is the maximum normalised lateral load on the pipe at the end of the first sweep from the five tests conducted in this series. Apart from test-e which shows a relatively higher breakout force compared to other pipes, there is a slight increase in the breakout force with increasing pipe effective weight. However, this difference lies within a very narrow band of between 0.3 and 0.6. The excessive increase in the breakout force from test-e is mainly due to the higher frictional component of the force due to the higher

submerged weight of the pipe and less of the passive resistance from the soil. The passive resistance from the soil berm will be dealt with in §6.3.1.2. It is also interesting to note that higher pipe effective weight appears to indicate higher normalised lateral pipe displacement before breakout. The plot also appears to suggest a linear relationship (apart from test-e which appears as an outlier) between the normalised breakout force and the mobilised pipe displacement before breakout for increasing pipe weight. This tends to suggest that higher pipe weight could withstand more lateral displacement before breakout. This negative value on the plot is due to the load cell which measures left-ward pulling as negative force and right-ward pulling as positive.

The effect of the effective weight of pipe on the lateral soil resistance and vertical pipe penetration can be assessed by plotting the normalised vertical displacement against normalised horizontal displacement (Figure 6 - 15a) and normalised horizontal pulling force against normalised horizontal displacement (Figure 6 - 15b) for the five test conducted. It can be seen that only test -a appears to show pipe uplift during the first pass. Test -b and c appears to show almost horizontal pipe trajectory while test-d and e show significant pipe embedment while undergoing the first sweep. This is also consistent with the results of the normalised pulling force where the lateral force for test -b and c are similar while there is significant increase in pulling force for test-e. Test-d differs from test-e by only 10N, but then the amount of penetration during pipe movement is significantly different in test-e. This may appear to indicate that there is likely a combination of pipe weight and soil strength where the magnitude of pipe embedment during pipe lateral displacement will initiate excessive pipe penetration during lateral displacement.

6.3.1.2 Development of soil berm during lateral pipe pulling – Series LP-SW

The stability of offshore pipelines to lateral displacement is a function of the lateral resistance that can be offered by the soil during pipe travel and the frictional resistance between the soil and the pipe. The lateral resistance is dependent on the volume of soil in front of the pipe which in turn is related to the level of the pipe invert and hence depth of penetration of the pipe. The depth of initial penetration and rate of subsequent penetration during pipe displacement has been shown in the preceding section to be affected by the effective pipe weight. It is therefore likely that the effective weight of the pipe could control the formation of the berm of soil since as the pipe moves laterally

an active berm of soil is created in front of the pipe resulting in additional increase in the soil lateral resistance. The height of that berm is dependent on the penetration of the pipe which in turn is a function of the weight of the pipe. The frictional resistance also increases as the pipe penetrates the soil because the shear strength increases.

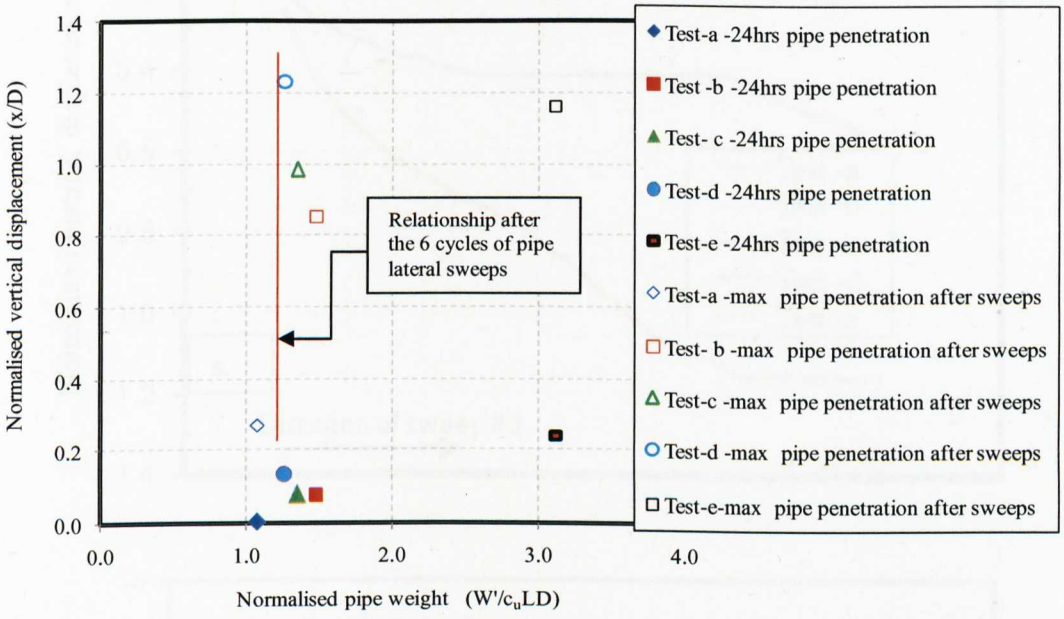

Figure 6 - 13: Plot of normalised vertical penetration of pipe invert before and after cyclic sweeps versus normalised pipe weight for series LP-SW

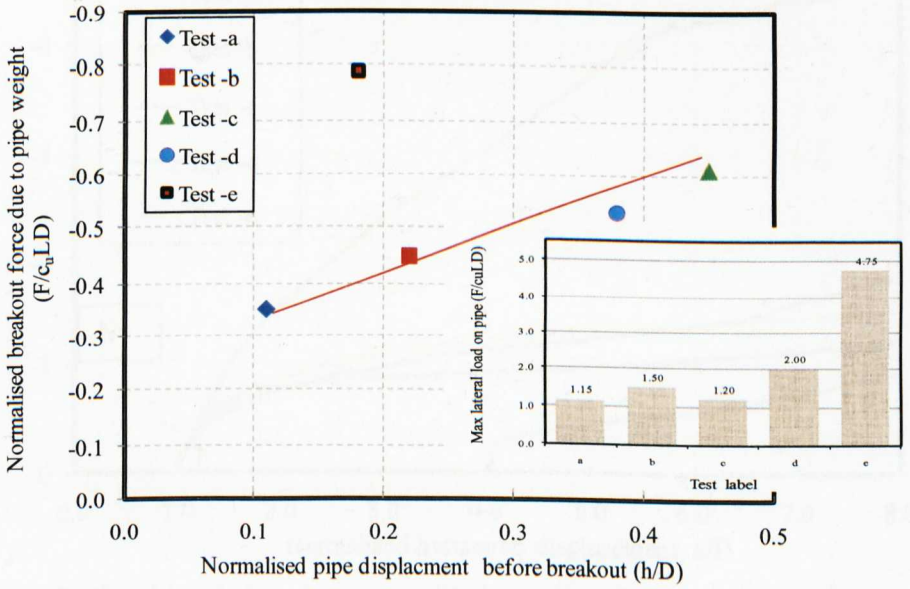

Figure 6 - 14: Plot of normalised breakout force versus normalised horizontal displacement for series LP-SW

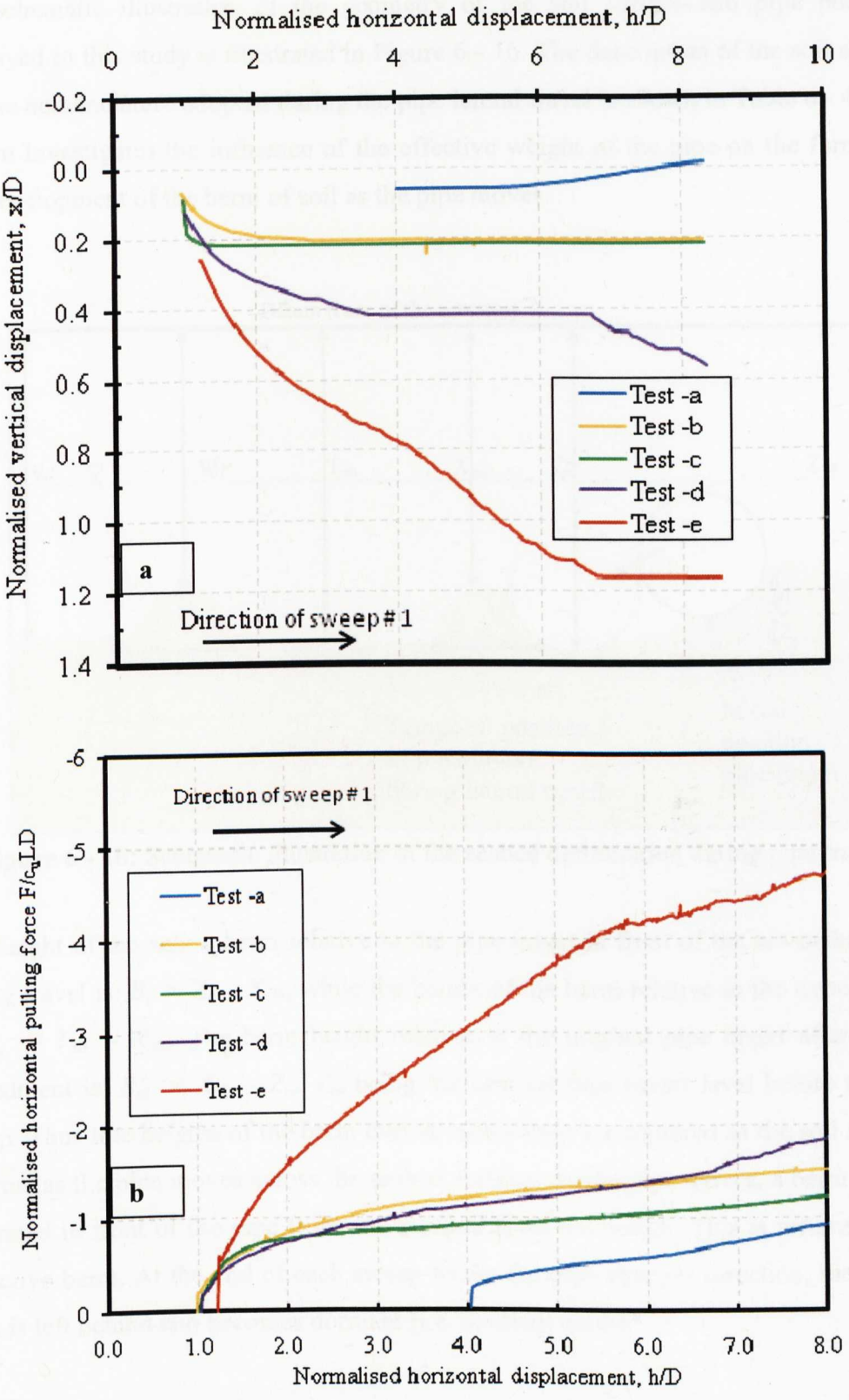

Figure 6 - 15: Combined plots for sweep #1 for series LP-SW, **(a)** normalised vertical penetration of pipe invert versus normalised horizontal displacement, **(b)** normalised horizontal pulling force versus normalised horizontal displacement

The schematic illustration of the geometry of the soil surface and pipe positions employed in this study is illustrated in Figure 6 - 16. The description of the soil surface and the nomenclature adopted during the pipe lateral travel is shown in Table 6 - 4. This section investigates the influence of the effective weight of the pipe on the formation and development of the berm of soil as the pipe moves.

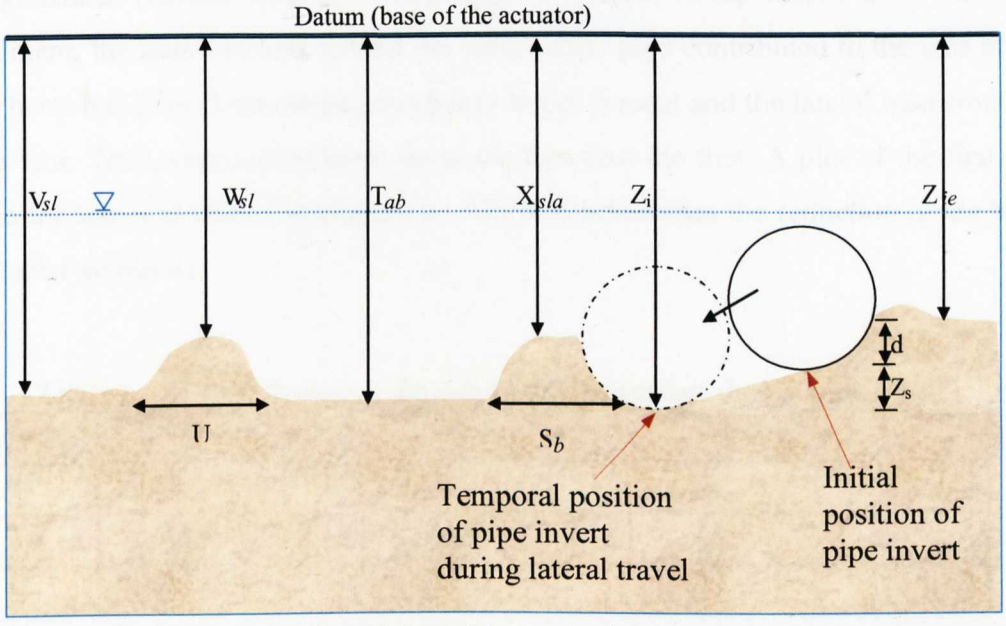

Figure 6 - 16: Schematic illustration of the seabed deformation during pipe travel

The height of the active berm relative to the pipe invert in front of the advancing pipe during travel is: $B_i = Z_i - X_{sla}$, while the height of the berm relative to the trench level is: $B_t = T_{ab} - X_{sla}$. The berm height relative to the original pipe invert after initial embedment is: $B_{oi} = X_{sla} - Z_{io}$, Z_{io} being the original pipe invert level before start of sweep. Thus true heights of the berm during each sweep are captured as the soil surface deforms as the pipe moves across the seabed surface. As the pipe moves, a berm of soil is formed in front of the pipe from soil scraped from the trough. This is referred to as the active berm. At the end of each sweep where the pipe changes direction, the active berm is left behind and becomes dormant (i.e. dormant berm).

Although the berm geometry could be idealised as a semi-circle, the characteristic area of the soil berm is modelled by multiplying the base (width) of the berm with its vertical height. Thus, $(A_{ab}) = S_b \times H_{ab}$. Similarly the shape of dormant berm is $A_{db} = U \times H_{db}$. Table 6 - 5 shows typical data from the seabed bed geometry (including berm) study for test -b sweep 1. These data are plotted in Figure 6 - 17 together with the results of the

other sweeps. It can be seen that only the first two sweeps are shown for the area of the active berm in Figure 6 - 17b. This is because during the 3 to 6 sweeps, deeper penetrations of the pipe obscured the measurement of the base (width) of the berm of soil generated.

It was noted that for the lighter pipe as in test -a, the characteristic shape of the soil berm generated reduced after the first sweep. In the first sweep shortly after the initial embedment, the heave of soil around the sides of the pipe contributed to the size of the initial berm but in the next sweep, this heave is not present and the lateral load from the pipe is less. Thus, subsequent berm areas are less than the first. A plot of the first two sweeps for test -a is shown in (Figure 6 - 18) which indicates the reduction in the berm height after sweep #1.

Table 6 - 4: Description of the model seabed surface during pipe travel

Key	Description
S_b	Width of base of active berm
T_{ab}	Trench level in front of active berm
U	Width of dormant berm
V_{sl}	Soil level in front dormant berm
W_{sl}	Soil level at the dormant berm
X_{sla}	Soil level at the top of the active berm in front of pipe
Z_i	Pipe invert level during lateral travel
Z_{ie}	Soil level after initial pipe embedment
d	Depth of initial embedment of the pipe from the mudline
Z_s	Instantaneous pipe penetration into the soil
H_{ab}	Height of the active berm
H_{db}	Height of the dormant berm
A_{ab}	Area of the active berm of soil in front of the pipe
A_{db}	Area of the dormant berm left behind by the pipe
Z_{io}	The original pipe invert level before start of sweep
B_{oi}	The berm height relative to the original pipe invert after initial embedment

Note: all levels are referenced to below the actuator base level (.i.e. 0mm)

Table 6 - 5: Typical data from soil berm investigation

Test -b-Sweep -1			Levels of active berm (mm BD)			Levels of dormant berm (mmBD)		Width (mm)		Heights of Active berm (mm)			Heights of dormant berm (mm)			*Area (cm^2)	
Time (min)	Time (hr)	Pipe lateral displacement (mm)	Soil level at the top active Berm infront of pipe (X)	Trench level in front of active berm (T)	Level of Pipe invert (Z_i)	Soil level at the top dormant berm (W)	Soil level in front of dormant berm (V)	Width of base of active berm (S)	Width of base of dormant berm at 1000mm (U)	Height of active berm relative to the pipe invert, $B_{i\,(Zi-X)}$	Height of active berm relative to trench level, $B_{t\ (T-X)}$	Height of active berm relative to the original pipe invert, Bo_i $(X - Z_{io})$	Height of dormant berm relative to the pipe invert, B_i	Height of dormant berm relative to trench level, B_t	Height of dormant berm relative to the origianl pipe invert, Bo_i	Area of active berm realtive to pipe invert (A_{Bi})	Area of active berm relative to trench (A_{Bt})
0	0	0	184	184	184		184	0	0	0	0	0				0	0
30		90	148	182	198		184	70		50	34	36				35	24
60	1	180	138	178	200		184	75		62	40	46				47	30
90		270	128	178	202		184	100		74	50	56				74	50
120	2	360	124	178	202		184	130		78	54	60				101	70
150		450	119	178	202		184	175		83	59	65				145	103
180	3	540	116	176	202		184	200		86	60	68				172	120
210		630	114	174	202		184	230		88	60	70				202	138
240	4	720	112	172	202		184	233		90	60	72				209	140
270		810	108	170	202		190	240		94	62	76				225	149
300	5	900	105	170	202		190	242		97	65	79				234	157
330		990															
Test -b-Sweep -2																	
0	0	0	215	215	202	105	190	0	0	-13	0	-31	97	110	79	0	0
30		90	188	203	226	125	190	70		38	15	-4	101	78	59	27	11
60	1	180	168	197	229	128	190	90		61	29	16	101	69	56	55	26
90		270	150	190	229	130	190	140		79	40	34	99	60	54	111	56
120	2	360	140	195	229	130	190	170		89	55	44	99	65	54	151	94
150		450	130	200	227	130	190	195		97	70	54	97	70	54	189	137
180	3	540	125	203	224	130	190	220		99	78	59	94	73	54	218	172
210		630	102	190	221	130	190	245		119	88	82	91	60	54	290	216
240	4	720	107	185	219	130	190	260		112	78	77	89	55	54	292	203
270		810	85	170	216	130	190	265		131	85	99	86	40	54	346	225
300	5	900	73	100	214	130	190	270		141	27	111	84	-30	54	381	73
330		990															

*Note: The area of the berm here is the characteristic shape of the berm

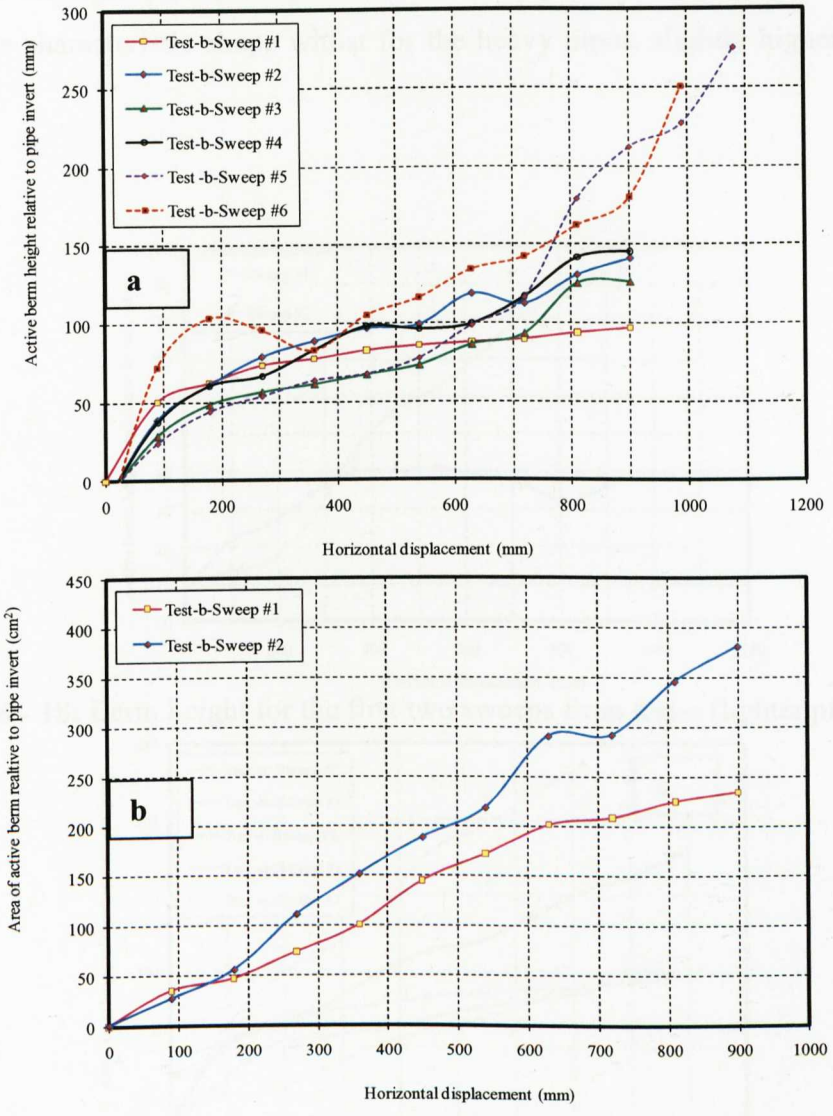

Figure 6 - 17: Typical active berm generation with pipe travel, (a) berm height relative to pipe invert and (b): area (i.e., characteristic shape) of active berm relative to pipe invert

Figure 6 - 19 and Figure 6 - 20 show the combined plots of the generation of the active berm of soil from the series LP-SW for sweep #1 and #2 respectively. The plots are grouped in this manner in order to aid in the comparison of the shape of berm with increasing pipe weights (.i.e. test -a - e). Therefore, the berm of soil formed during the first sweep from different pipe weights is investigated first followed by the berm from the second pass. It can be seen here that the volume of soil scraped from the trench to form the berm as the pipe moves increases with increasing weight of pipe. For the light pipes (test–a - c), the volume of the berm is similar. However, for the heavy pipes (test-d and e), the volume of the berm continues to increase as the pipe moves down into the

seabed. For the light pipe (test-a), the second sweep shows slightly lower soil berm value of the characteristic shape whilst for the heavy pipes, slightly higher values are measured.

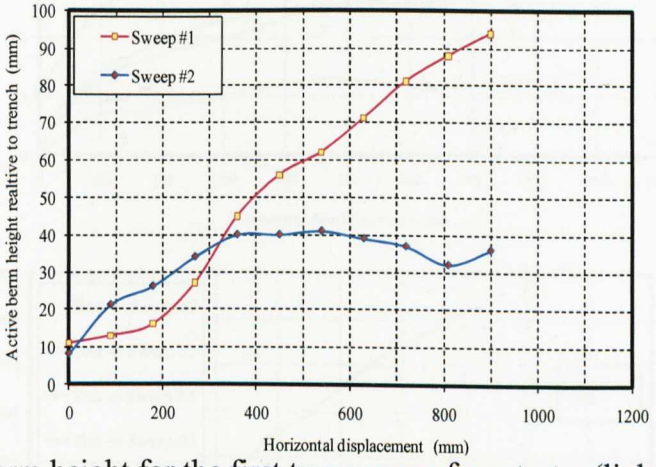

Figure 6 - 18: Berm height for the first two sweeps from test-a (lighter pipe, 57N)

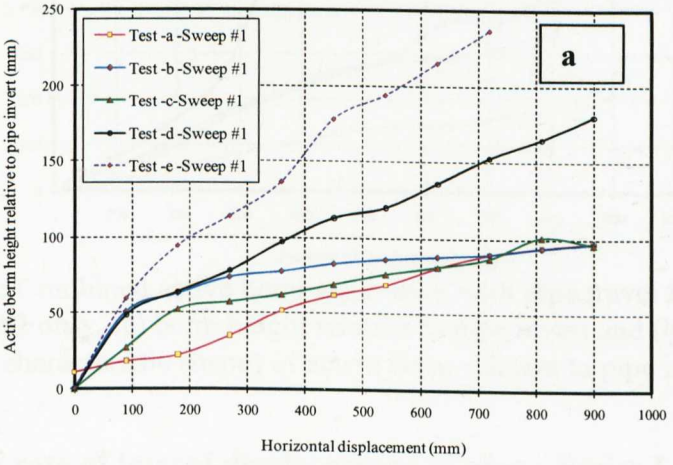

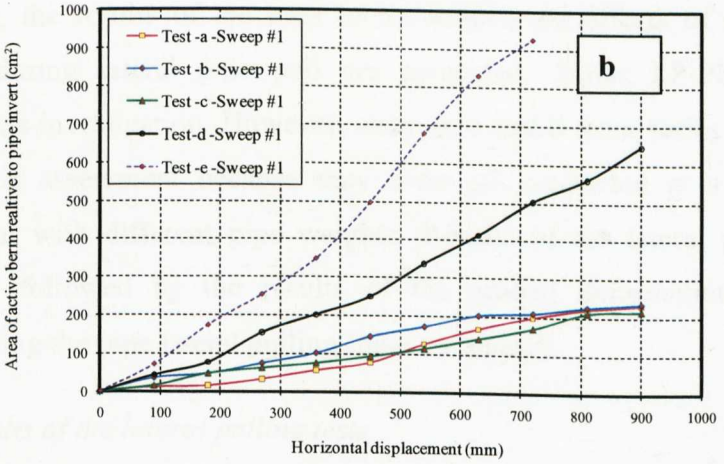

Figure 6 - 19: Combined active berm generation with pipe travel for **test -a - e, sweep#1 only**, a) berm height relative to pipe invert and b): area (i.e., characteristic shape) of active berm relative to pipe invert

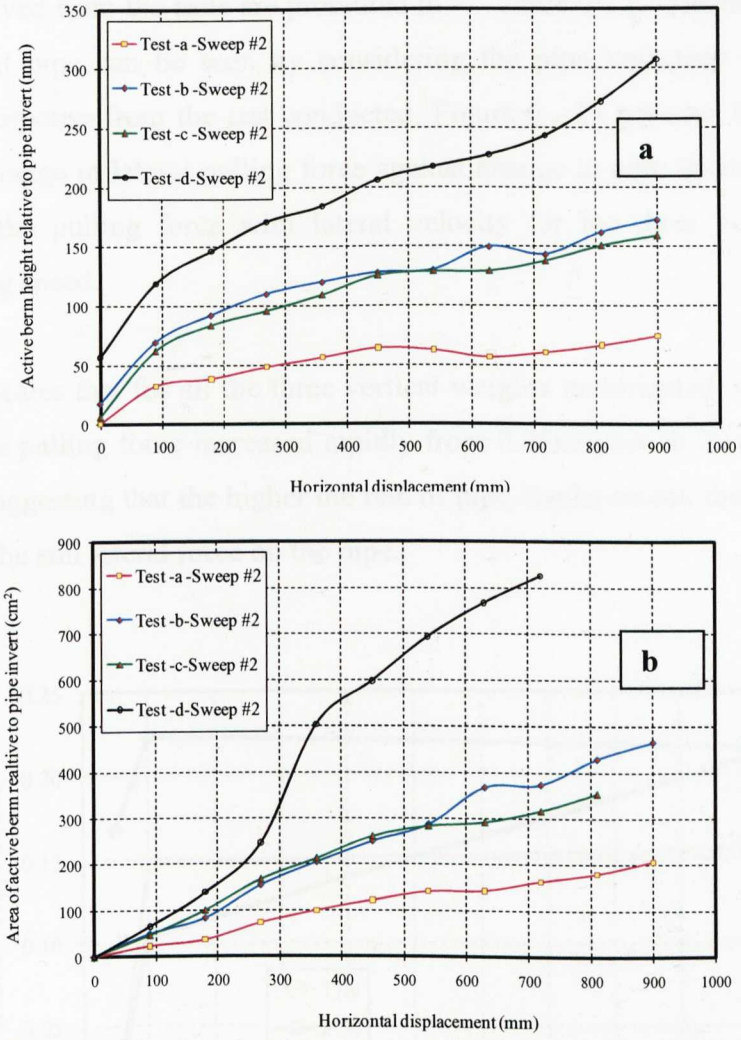

Figure 6 - 20: Combined active berm generation with pipe travel for **test -a - e, sweep#2 only**, (a) berm height relative to pipe invert and (b): area (i.e., characteristic shape) of active berm relative to pipe invert

6.3.2 Effects of rate of lateral displacement of pipe - *Series LP-PS*

In this section, the results of the tests to investigate the effects of the rate of pipe displacement during lateral pipe pull are presented. Series LP-PS was designed primarily for this investigation. However, tests -b, c and d from series LP-SW are also included in this assessment because they were all conducted at a pulling rate of 0.05mm/sec but with different pipe weights. Results of the lateral pulling tests are presented first followed by the results of the seabed deformation studies (berm generation) during the pipe lateral pulling (pipe sweeping).

6.3.2.1 Results of the lateral pulling tests

The results of the force-displacement response and the pipe trajectory during the lateral sweeps from series LP-SP are presented in Figure 6 - 22 to Figure 6 - 27 and the

parameters derived from the tests are presented in Table 6 - 2. The influence of rate of displacement pipe can be seen by considering the pipe trajectory and the force-displacement response from the test conducted. Figure 6 - 21 presents the plots of the gradient (i.e. change in lateral pulling force against change in pipe lateral displacement in N/mm) of the pulling force with lateral velocity for the three vertical loads at different pulling speed.

The figure indicates that for all the three vertical weights investigated, the gradients of the slope of the pulling force increased rapidly from 0.05mm/sec to 0.1mm/sec pulling rate possibly suggesting that the higher the rate of pipe displacement, the higher the rate of build up of the soil lateral force on the pipe.

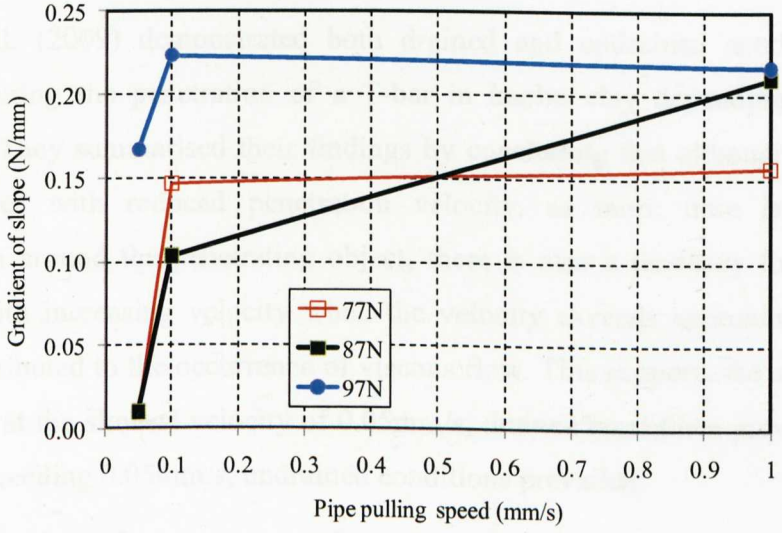

Figure 6 - 21: Plot of gradients of the slope of the force-displacement response from sweep#1 only for series LP-SP

The rate of penetration and the maximum penetration at the end of the first sweep are also influenced by the rate of pipe displacement. For the lower speed (0.05mm/sec), after the initial penetration into the soil, the pipe appears to maintain almost a horizontal trajectory while in the case of the higher speeds (0.1 and 1mm/sec) the pipes underwent a constant penetration in to the soil. This pattern is observed in all the three vertical weights investigated.

It does appear that at a lower speed of lateral displacement, the pipe does not penetrate the seabed but as the speed is increased the embedment of the pipe into the seabed is

increased. The amount of displacement of the pipeline during operation is however dependent on the operating temperature and pressure of the fluid within the pipe in relation to the ambient conditions. There is therefore need to incorporate this effect of the operating temperature on the rate of pipe displacement in the design stage as excessive penetration of pipe during lateral displacement is detrimental to the structural integrity of the pipe during operation. This is because the rate and amount of propagation of the buckles related to the temperature in the pipeline (Hobbs,1984).

The summary of the parameters extracted from the pipe-soil interaction pulling tests which are used to assess the effects of pipe pulling speed are presented in Table 6 - 6. In order to compare the effects of pulling speed, tests with the same vertical loads are grouped together.

Leanne et al. (2009) demonstrated both drained and undrained conditions of soil behaviour during the penetration of a T-bar in kaolin clay depending on speed of penetration. They summarised their findings by concluding that although resistance of clay increases with reduced penetration velocity, as more time is allowed for consolidation around the penetrating object, there is also a tendency for increases in resistance with increasing velocity when the velocity exceeds approximately 1mm/s. This they attributed to the occurrence of viscous flow. This supports the suggestion that in this study at the slowest velocity of 0.05mm/s, drained conditions prevailed while at velocities exceeding 0.05mm/s, undrained conditions prevailed.

It is apparent in Figure 6 – 21 that for the 77 and 97N tests the results are relatively insensitive to pipe pulling speed greater than 0.1mm/s. For the 87N test there is a marked change at 0.1mm/s but the 1mm/s test may be an anomaly. The data suggest that below 0.1mm/s the behaviour is drained/partially drained while above 0.1mm/s is essentially undrained.

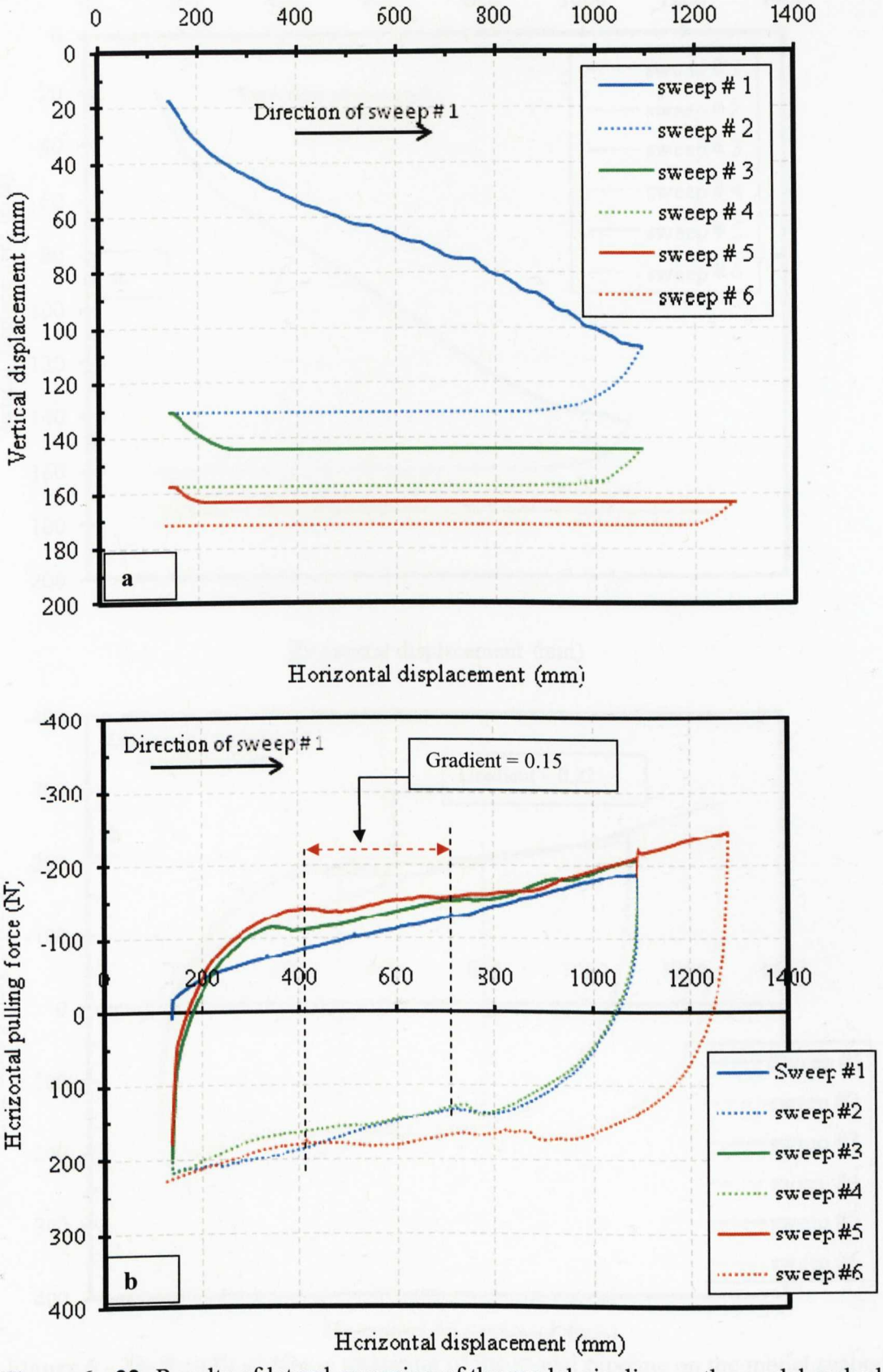

Figure 6 - 22: Results of lateral sweeping of the model pipeline on the model seabed for **test-f**: (a) vertical displacement against horizontal displacement, (b) horizontal pulling force against horizontal displacement

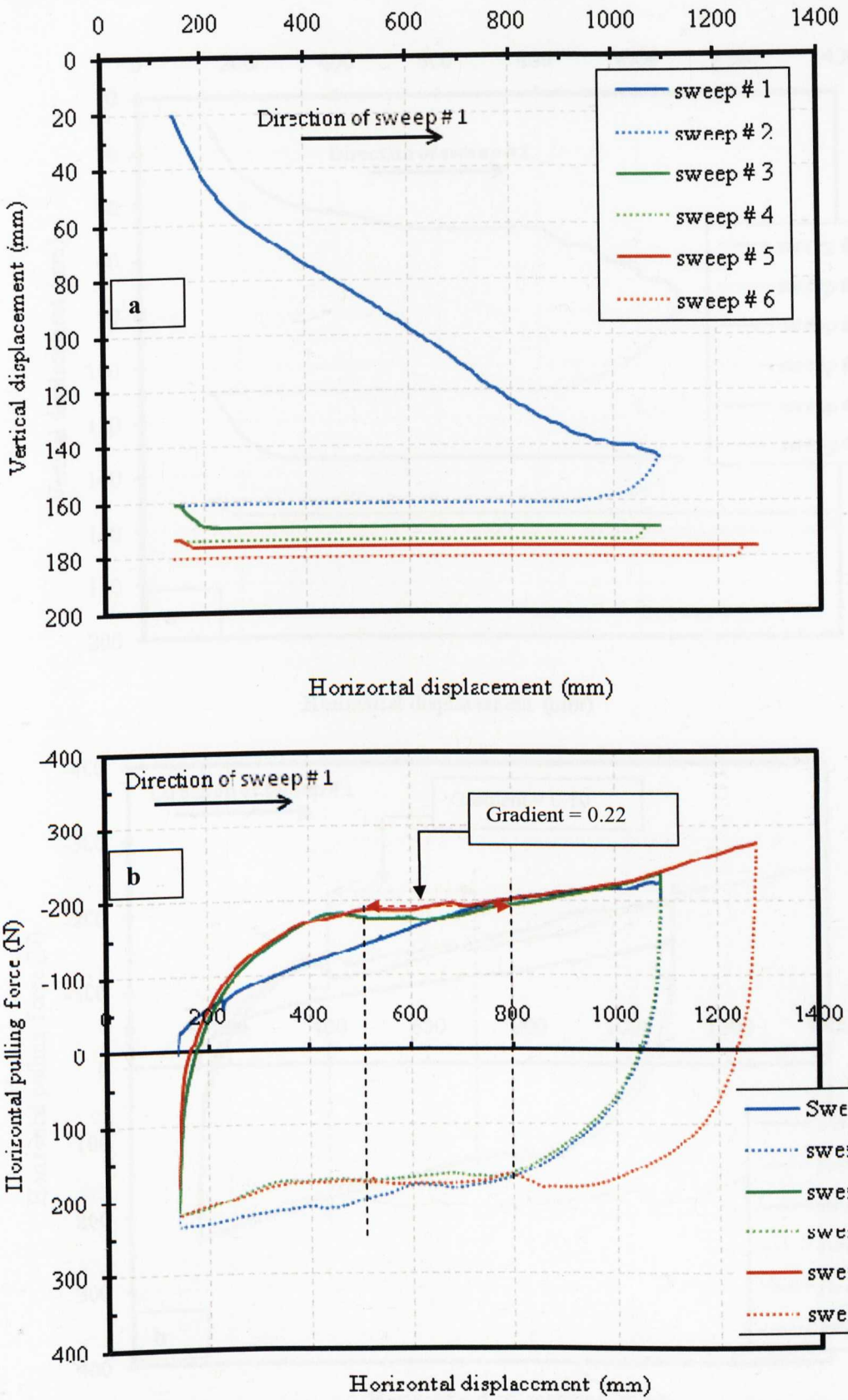

Figure 6 - 23: Results of lateral sweeping of the model pipeline on the model seabed for **test-g**: (a) vertical displacement against horizontal displacement, (b) horizontal pulling force against horizontal displacement

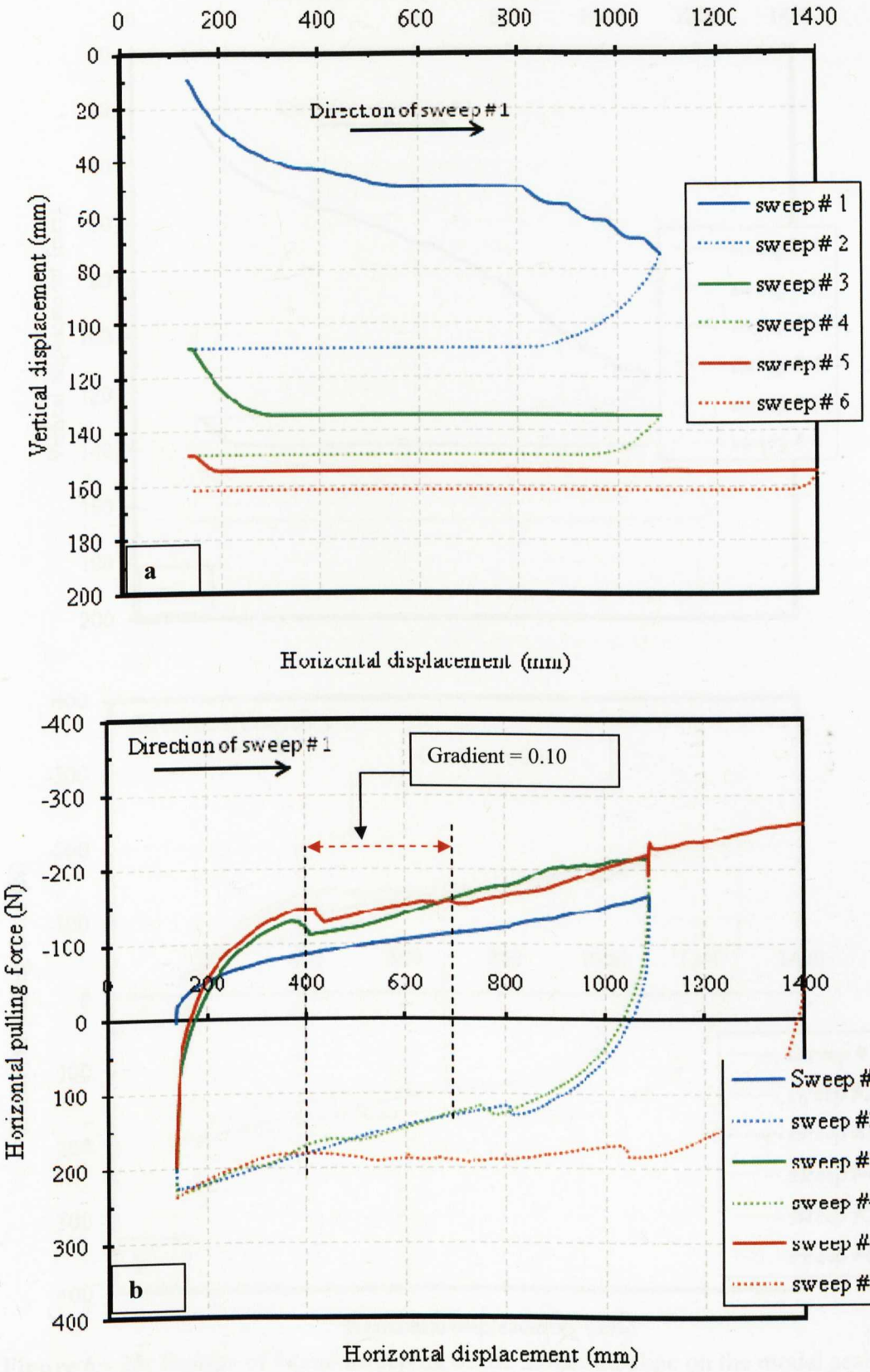

Figure 6 - 24: Results of lateral sweeping of the model pipeline on the model seabed for **test-h**: (a) vertical displacement against horizontal displacement, (b) horizontal pulling force against horizontal displacement

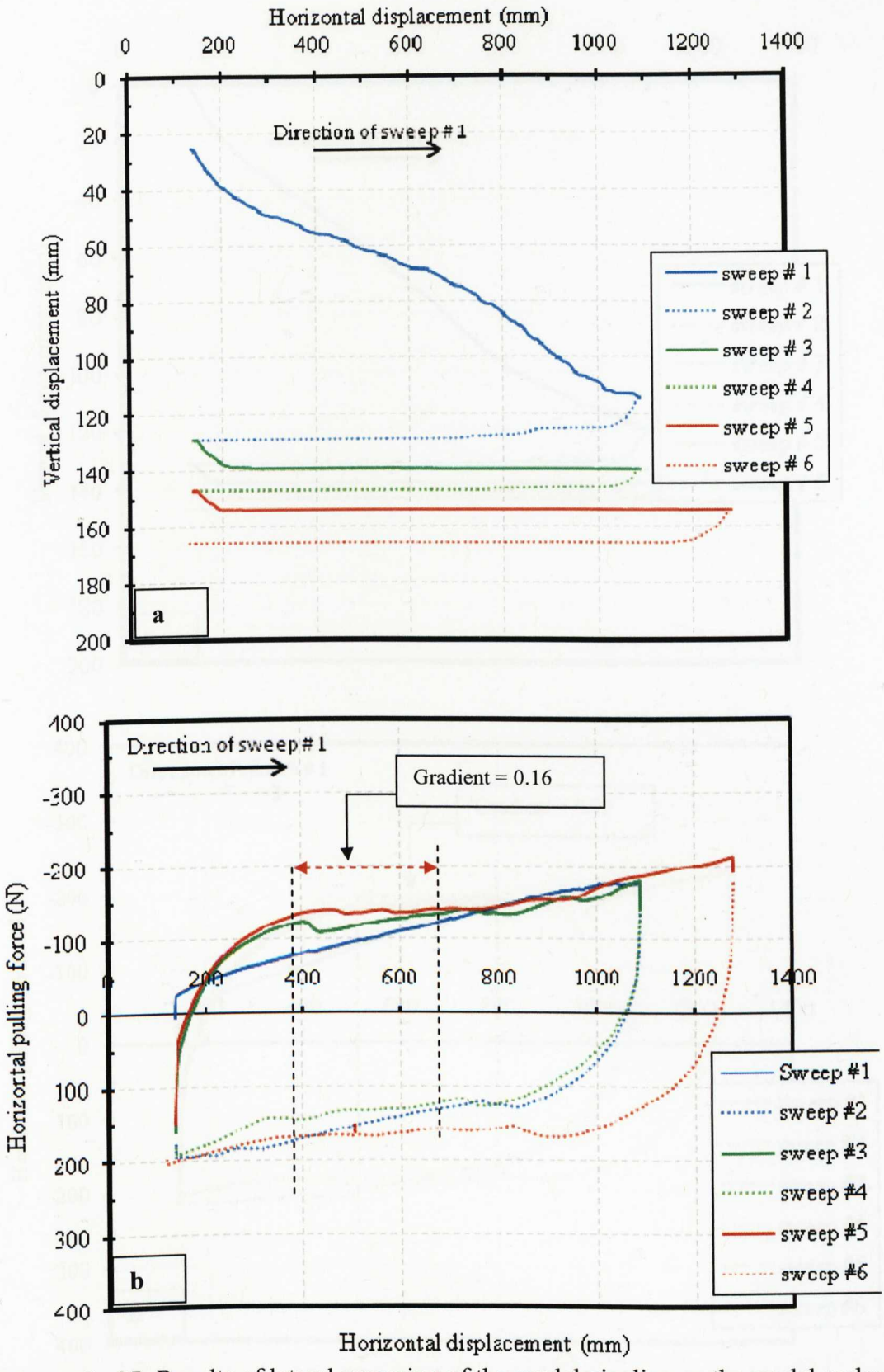

Figure 6 - 25: Results of lateral sweeping of the model pipeline on the model seabed for **test-i**: (a) vertical displacement against horizontal displacement, (b) horizontal pulling force against horizontal displacement

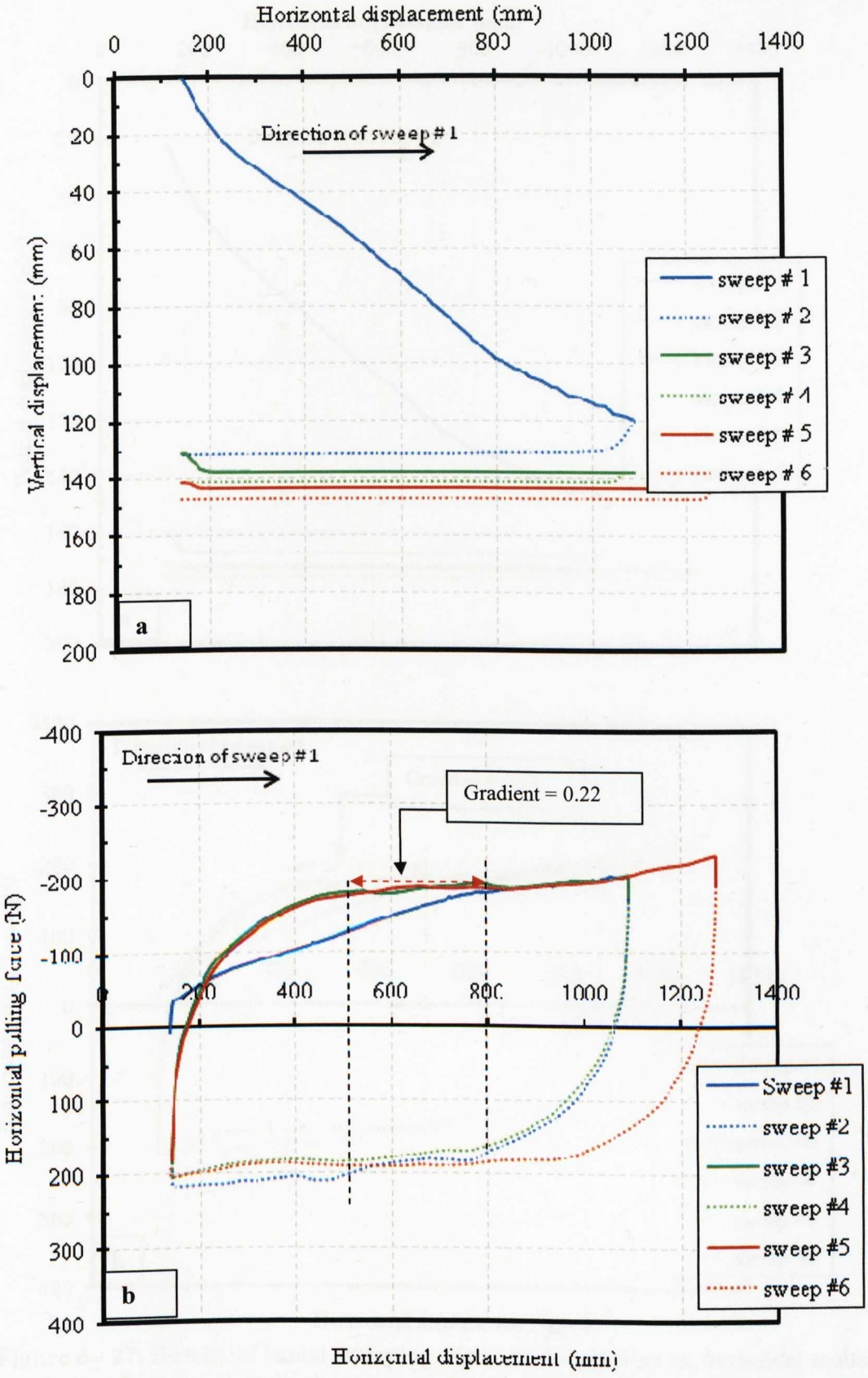

Figure 6 - 26: Results of lateral sweeping of the model pipeline on the model seabed for **test -j**: (a) vertical displacement against horizontal displacement, (b) horizontal pulling force against horizontal displacement

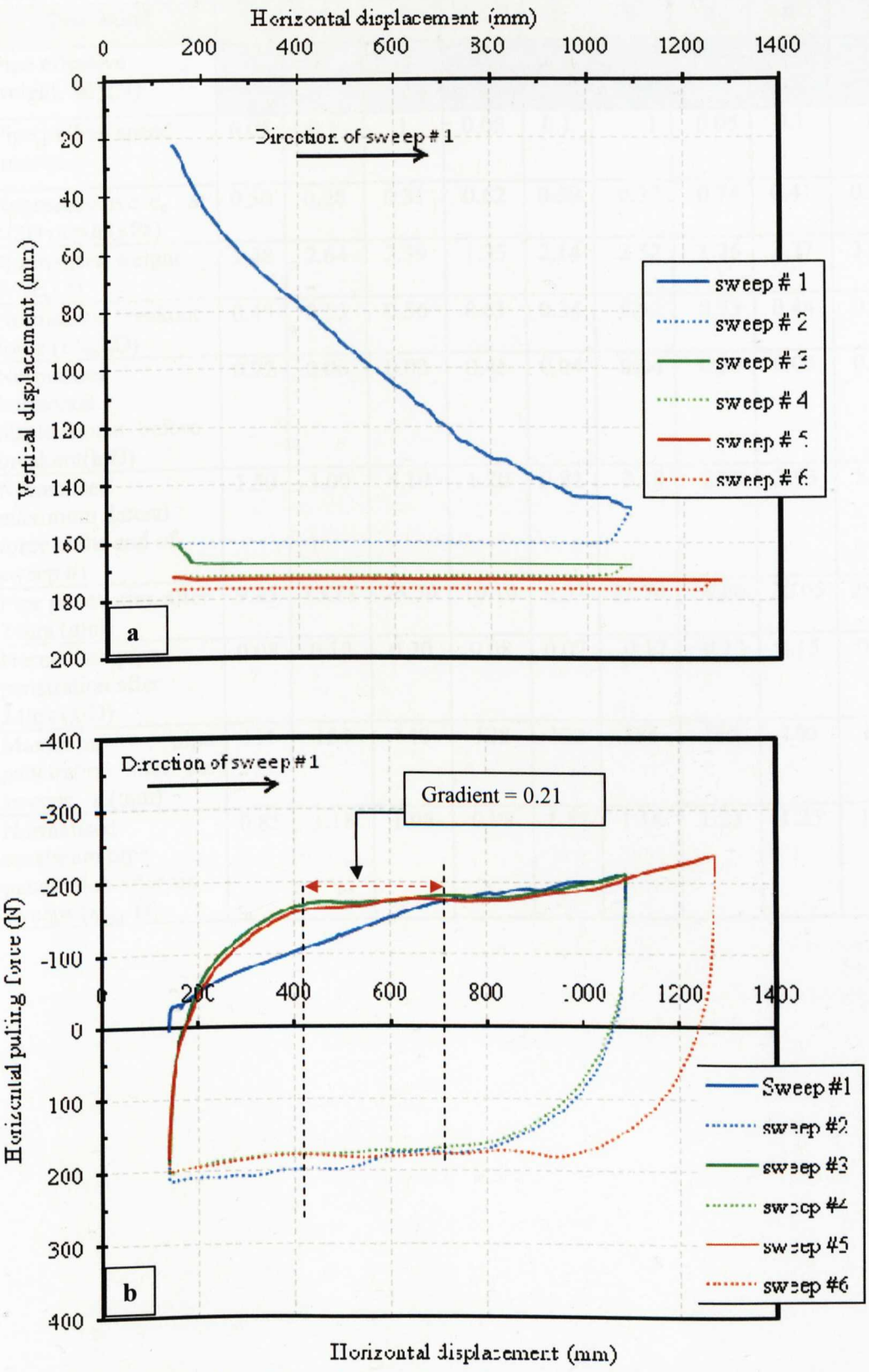

Figure 6 - 27: Results of lateral sweeping of the model pipeline on the model seabed for **test-k**: (a) vertical displacement against horizontal displacement, (b) horizontal pulling force against horizontal displacement

Table 6 - 6: Assessment parameters to investigate effect of pipe pulling speed

Test label	b	f	i	c	h	k	d	g	j
Pipe effective weight, W' (N)	77	77	77	87	87	87	97	97	97
Pipe pulling speed (mm/sec)	0.05	0.1	1	0.05	0.1	1	0.05	0.1	1
Representative c_u at 1/2D depth (kPa)	0.50	0.28	0.31	0.62	0.39	0.37	0.74	0.41	0.31
Normalised weight W'/c_uLD	1.48	2.64	2.39	1.35	2.14	2.52	1.26	2.27	3.01
Normalised breakout force (F/c_uLD)	0.45	0.55	0.56	0.61	0.34	0.52	0.53	0.44	0.87
Normalised horizontal displacement before breakout(h/D)	0.22	0.06	0.03	0.45	0.04	0.04	0.38	0.05	0.05
Normalised maximum lateral force at the end of sweep #1	1.50	5.00	4.19	1.20	2.81	3.18	2.00	3.93	5.01
Pipe penetration after 24hrs (mm)	9.85	15.11	25.79	10.10	9.57	22.74	16.66	20.05	28.90
Normalises pipe penetration after 24hrs (x/D)	0.08	0.12	0.20	0.08	0.07	0.17	0.13	0.15	0.22
Maximum pipe penetration after six sweeps, x (mm)	111	154	140	128	152	154	160	160	147
Normalised maximum pipe penetration after six sweeps (x_{max}/D)	0.85	1.18	1.08	0.98	1.17	1.18	1.23	1.23	1.13

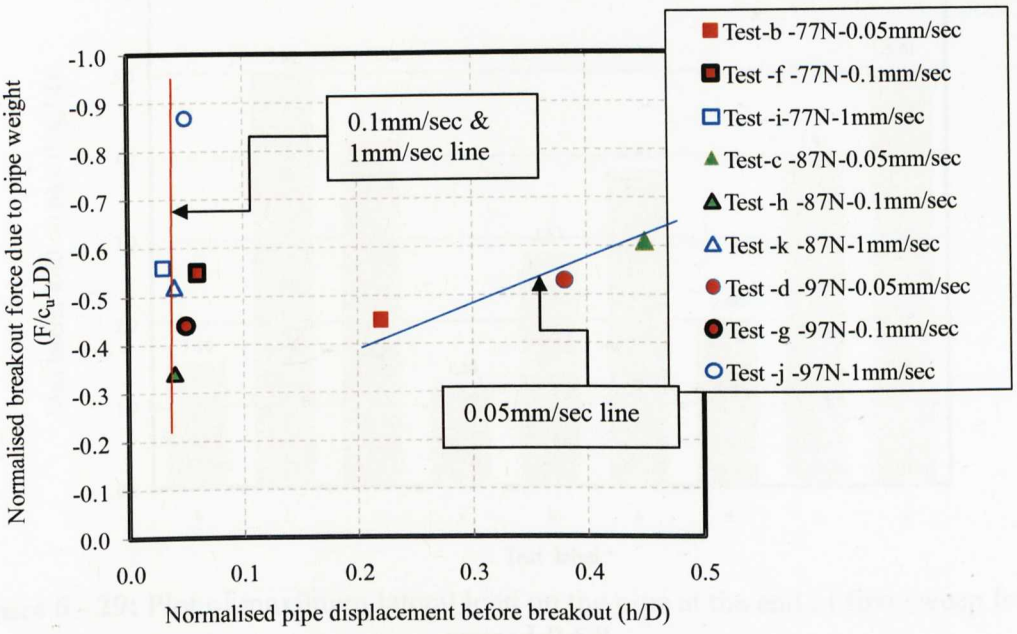

Figure 6 - 28: Plot of normalised breakout force versus normalised horizontal displacement for series LP-SP

It can be seen from Figure 6 - 28 that there are no significant variations in the normalised pipe displacement before breakout between 0.1 and 1mm/sec rate of pipe displacement. Thus only little displacement is noted with increase in the breakout force. However, for the lowest speed (0.05mm/sec), the normalised pipe displacement before breakout appears to show an increase in breakout force with increase in displacement.

The maximum lateral load on the pipe section at the end of the first sweep is presented in Figure 6 - 29. It can be seen here that the maximum lateral load which represents the maximum soil resistance, increases with increasing speed of pipe travel although a small deviation exist for 77N test where 0.1mm/sec loading is slightly higher than 1mm/sec loading. The maximum pipe penetration at the end of the six sweeps also shows the faster pipe speed having maximum vertical penetration at the end of the sweep (Figure 6 - 30). Figure 6 - 31 shows combined plots for the series where the effects of the pulling speed on the pipe trajectory and lateral soil resistances are presented for purposes of comparison.

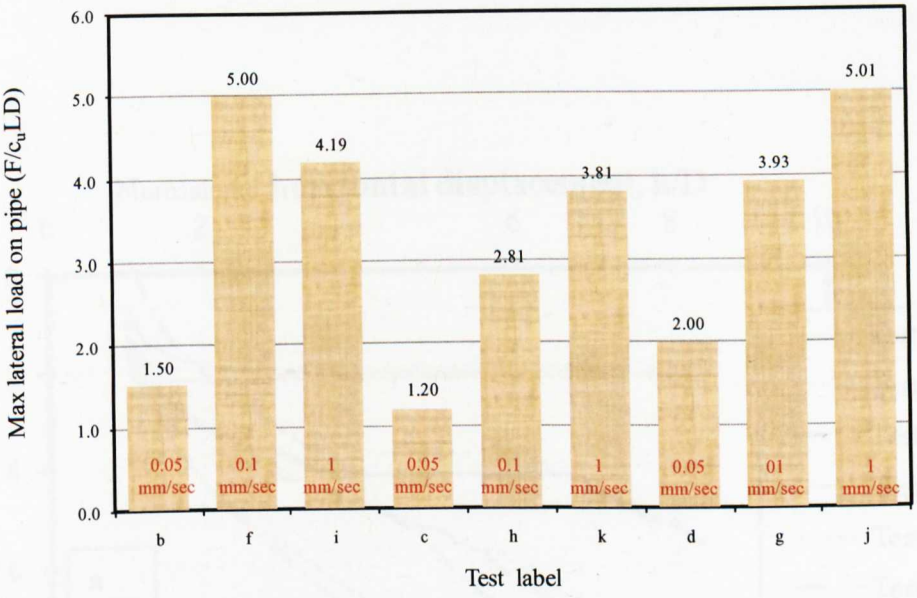

Figure 6 - 29: Plot of maximum lateral load on the pipe at the end of first sweep for series LP-SP

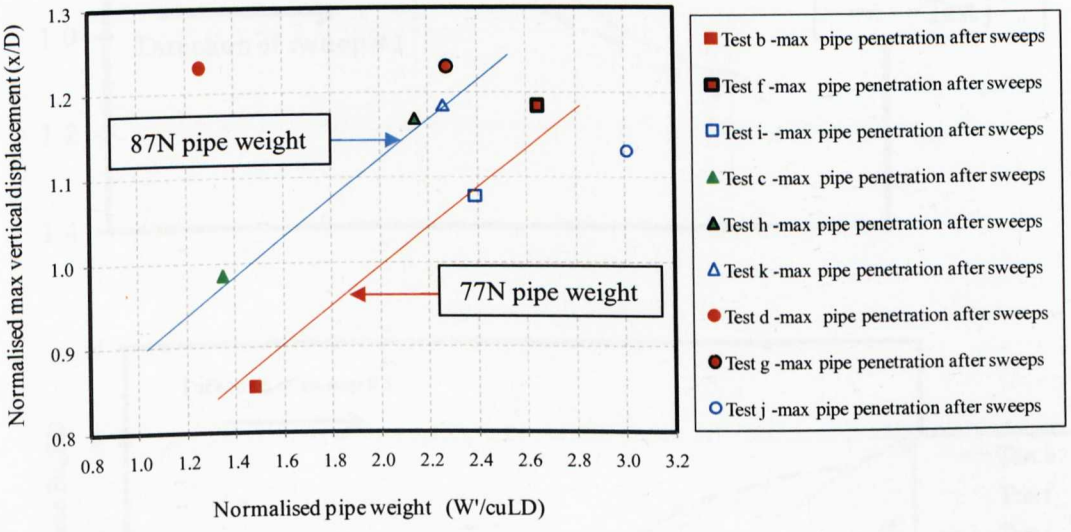

Figure 6 - 30: Plot of normalised vertical penetration of after the six cyclic sweeps versus normalised pipe weight for series LP-SP

6.3.2.2 *Development of soil berm during lateral pipe pulling - series LP-SP*

The effects of pulling speed on the generation and migration of soil berm during lateral pipe displacement is shown in Figure 6 - 32. It can be seen that the higher the speed of travel the greater the volume of soil scraped from the seabed to form the berm of soil in front of the pipe. This could be inferred to imply that higher pipe speed will result in faster generation of soil berm and hence increase in soil resistance to pipe motion. Due to the higher speed of displacement coupled with the excessive penetration in Test -j, the monitoring of berm formation was not possible.

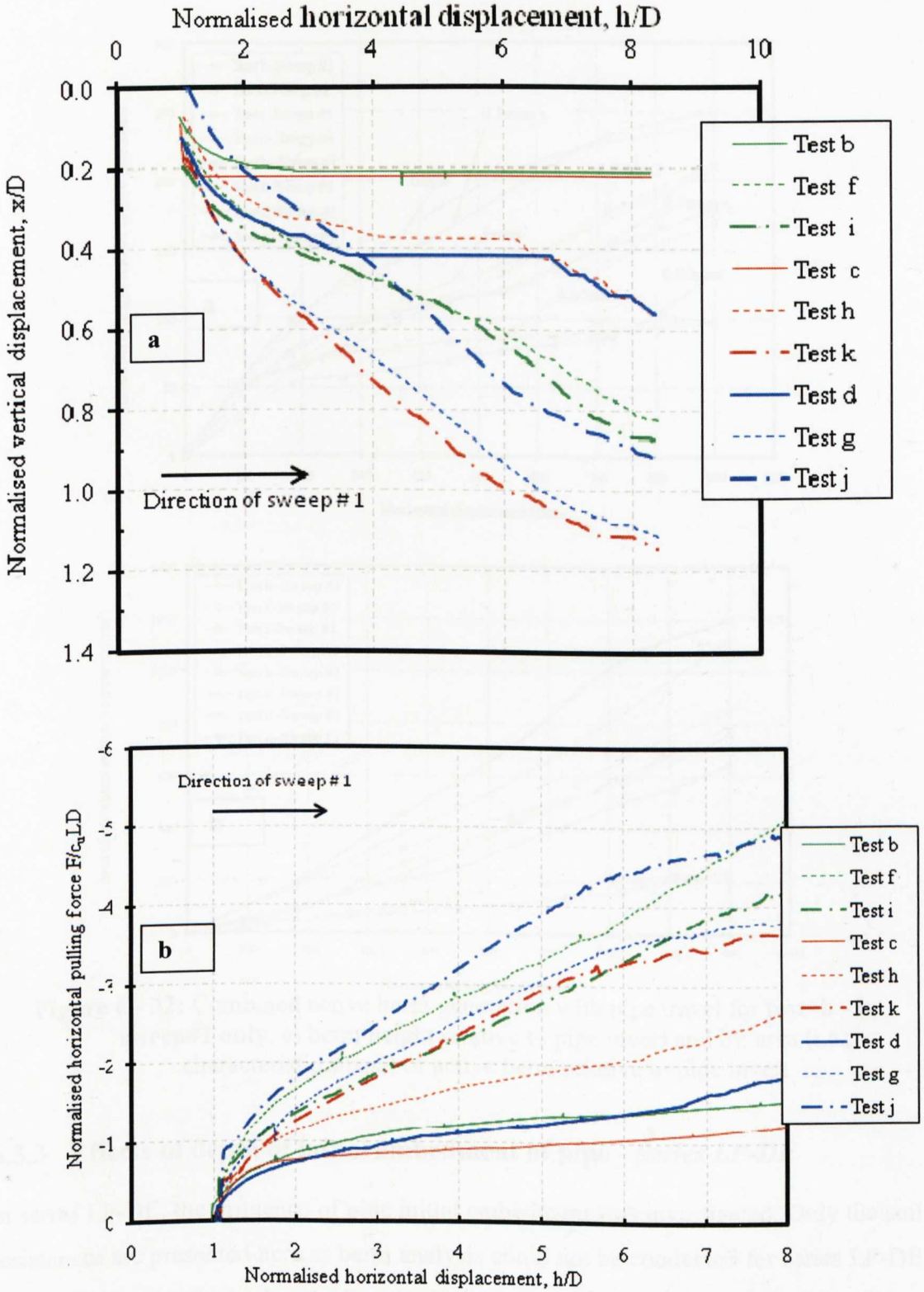

Figure 6 - 31: Combined plots for sweep #1 for series LP-SP, **(a)** normalised vertical penetration of pipe invert versus normalised horizontal displacement, **(b)** normalised horizontal pulling force versus normalised horizontal displacement

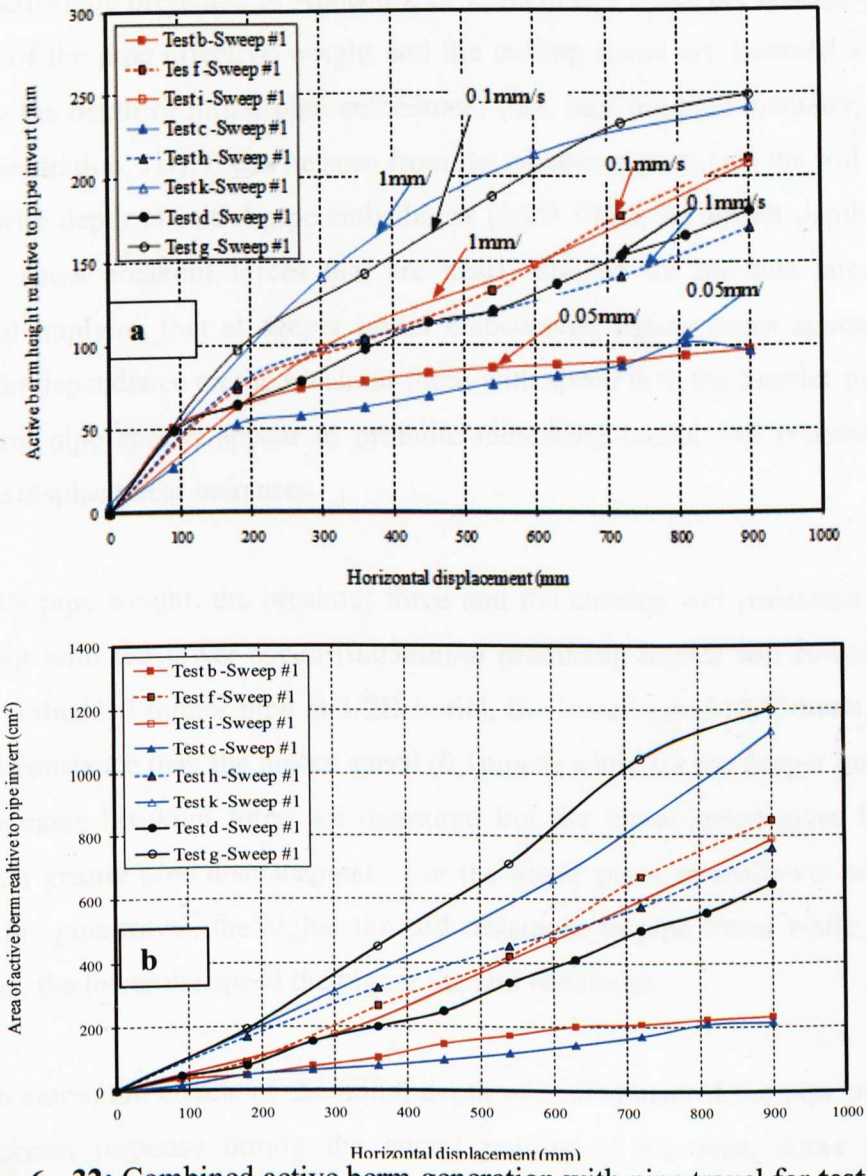

Figure 6 - 32: Combined active berm generation with pipe travel for **test -b - k, sweep#1 only**, a) berm height relative to pipe invert and b): area (i.e., characteristic shape) of active berm relative to pipe invert

6.3.3 Effects of depth of initial embedment of pipe - *Series LP-DE*

In series LP-DE, the influence of pipe initial embedment was investigated. Only the soil resistances are presented here as berm analysis could not be conducted for series LP-DE due to the depth of initial embedment which made it impracticable to study the berm formation during pipe travel.

6.3.3.1 *Results of the lateral pulling tests*

Combined plots of the force-displacement response and the pipe trajectory during the lateral sweeps is shown in Figure 6 - 33 while detail plots of all the tests (test- 1 to s from this series) are presented in Appendix E. Tests in this series are arranged such that the effects of the pipe effective weight and the pulling speed are assessed as they are affected by the depth of initial pipe embedment (.i.e. half the pipe diameter, 1/2D and full pipe penetration, 1D). It can be seen from the combined plots that the soil resistance increases with depth of initial pipe embedment (1/2D <1D). At deeper depth (1D), the 57N pipes show breakout forces that are nearly similar for the two lateral speeds investigated implying that at deeper initial embedment, lighter pipes appear to show only a slight dependence on the breakout force with speed than the heavier pipes. Also, lower lateral pipe speeds appear to promote increasing lateral soil resistance as the lateral pipe displacement increases.

For the 87N pipe weight, the breakout force and the ensuing soil resistance responses are different with the lower speed (0.05mm/s) producing higher soil resistance. For shallower embedded lighter pipe at 1/2D burial, the lower speed (0.05mm/s) produces higher soil resistance than the higher speed (0.1mm/s) while for the deeper buried pipes, almost the same breakout force are measured but the lower speed gives higher soil resistance at greater pipe displacement. For the heavy pipes at shallower embedment, the faster the pipe travel, the higher the soil resistance to pipe travel while for deeper embedment, the lower the speed the higher the soil resistance.

In order to assess the effects of the initial depth of embedment of the pipe on the pipe-soil interaction response during the lateral pulling of the pipe, some parameters extracted from the force displacement plots are summarised in Table 6 - 7. The plot of normalised breakout force versus normalised horizontal displacement for series LP-DE is shown in Figure 6 - 34. It can be seen that the normalised breakout force increases with increasing depth of embedment. For the same depth of initial embedment, the lower the pulling speed, the lower the breakout force and the lower the lateral displacement before breakout. For deeper initial embedment, this pattern is not pronounced. However, higher pulling speed indicates greater distance before breakout. For slightly heavier pipe (87N), this pattern reverses with the lower speed giving higher breakout force and lateral displacement before breakout.

Table 6 - 7: Assessment parameters from the initial depth of embedment

Test label	l	m	n	o	p	q	r	s
Pipe effective weight, W' (N)	57	57	57	57	87	87	87	87
Pipe pulling speed (mm/sec)	0.05	0.05	0.1	0.1	0.05	0.05	0.1	0.1
Representative c_u at 1/2D depth (kPa)	0.33	0.30	0.34	0.37	0.32	0.25	0.29	0.29
Normalised weight W'/c_uLD	1.66	1.83	1.61	1.48	2.61	3.35	2.85	2.88
Normalised breakout force (F/c_uLD)	-1.03	-2.29	-1.15	-2.23	-1.18	-3.32	-1.20	-2.70
Normalised horizontal displacement before breakout(h/D)	0.04	0.10	0.15	0.38	0.17	0.40	0.13	0.34
Normalised maximum lateral force at the end of sweep #1	3.06	3.75	2.35	3.61	2.72	4.39	3.20	4.28
Pipe penetration after 24hrs (mm)	1.20	-0.20	0.91	-1.17	0.13	0.10	0.91	0.10
Normalises pipe penetration after 24hrs (x/D)	0.01	0.00	0.01	-0.01	0.00	0.00	0.01	0.00
Maximum pipe penetration after six sweeps, x (mm)	51	7	68	6	89	5	5	5
Normalised maximum pipe penetration after six sweeps (x_{max}/D)	0.39	0.05	0.52	0.05	0.68	0.04	0.04	0.04

The maximum lateral load on the pipe at the end of the first sweep (Figure 6 - 35) shows that the higher the depth of initial embedment the higher the maximum load on the pipe. The lower the speed the higher the maximum load on the pipe at the end of the first sweep. For slightly higher weight, the lower the speed, the lower the max loads on the pipe at the end of the first sweep. Figure 6 - 36 presents the plot of normalised pipe weight versus normalised vertical penetration of the pipe after cyclic sweeps for series LP-DE. It can be seen that the deeper the pipe initial embedment, the lower the maximum pipe penetration at the end of the first sweep. The faster the pipes speed, the higher the maximum penetration at the end of the pipe first sweep. For deeper embedment, almost no difference exit in the maximum pipe penetration for varying speed.

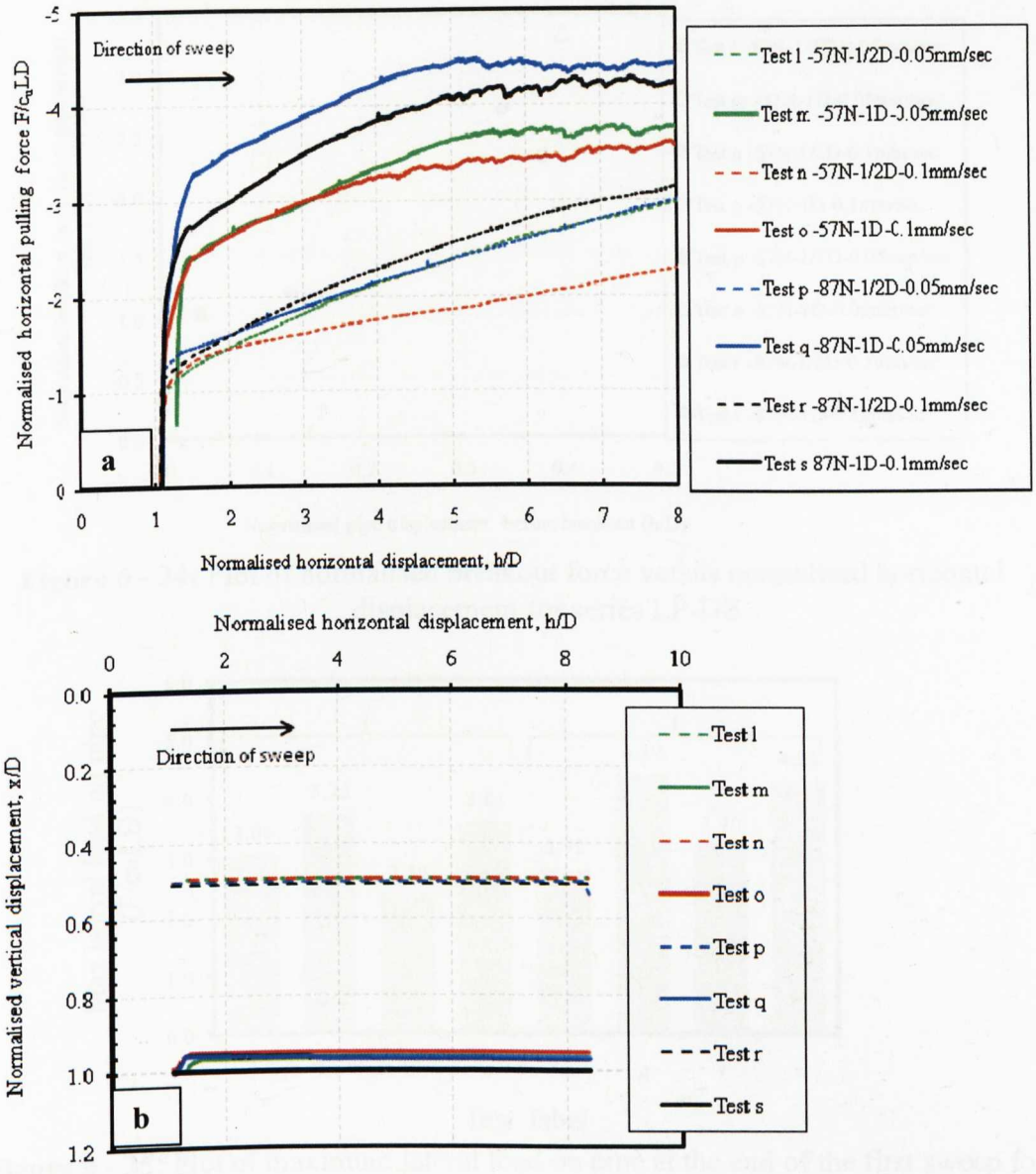

Figure 6 - 33: Combined plots for sweep #1 for series LP-DE, **a)** normalised vertical penetration of pipe invert versus normalised horizontal displacement, **b)** normalised horizontal pulling force versus normalised horizontal displacement

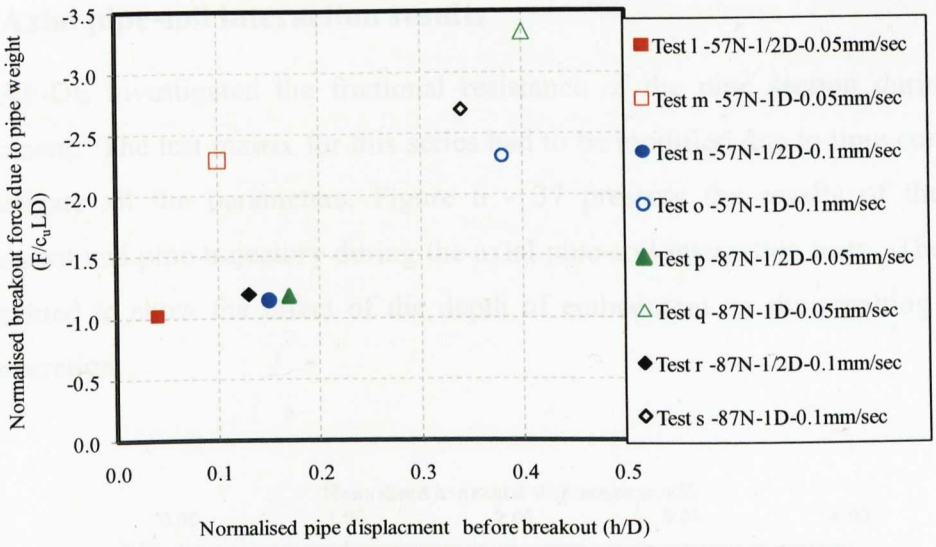

Figure 6 - 34: Plot of normalised breakout force versus normalised horizontal displacement for series LP-DE

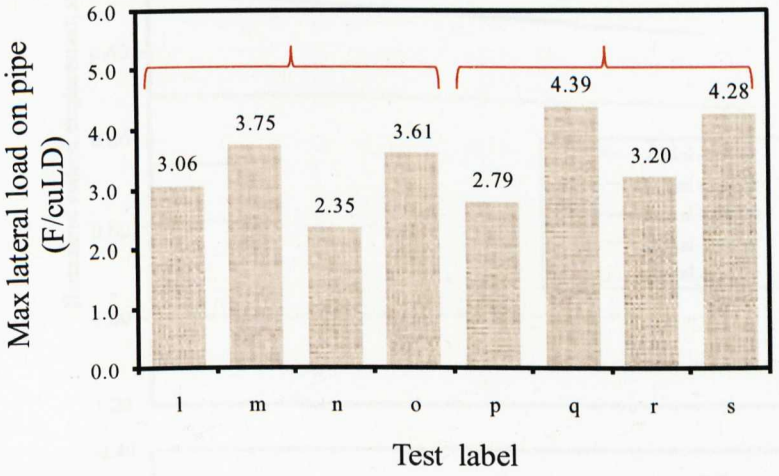

Figure 6 - 35: Plot of maximum lateral load on pipe at the end of the first sweep for series LP-DE

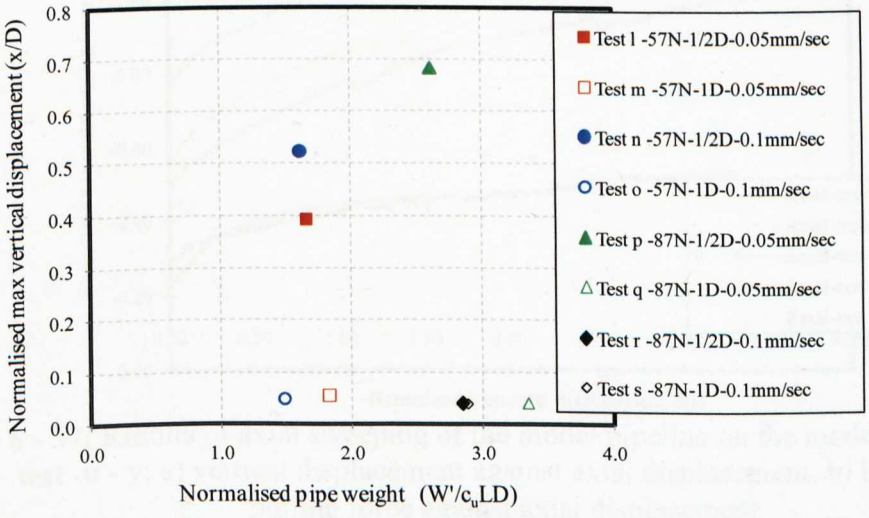

Figure 6 - 36: Plot of normalised pipe weight versus normalised vertical penetration of after cyclic sweeps for series LP-DE

6.3.4 Axial pipe-soil interaction results

Series AP-DE investigated the frictional resistance of the pipe section during axial displacement. The test matrix for this series had to be modified due to time constraints to investigate all the parameters. Figure 6 - 37 presents the results of the force-displacement and pipe trajectory during the axial pipe-soil interaction tests. The results are presented to show the effect of the depth of embedment on the resulting friction force generation.

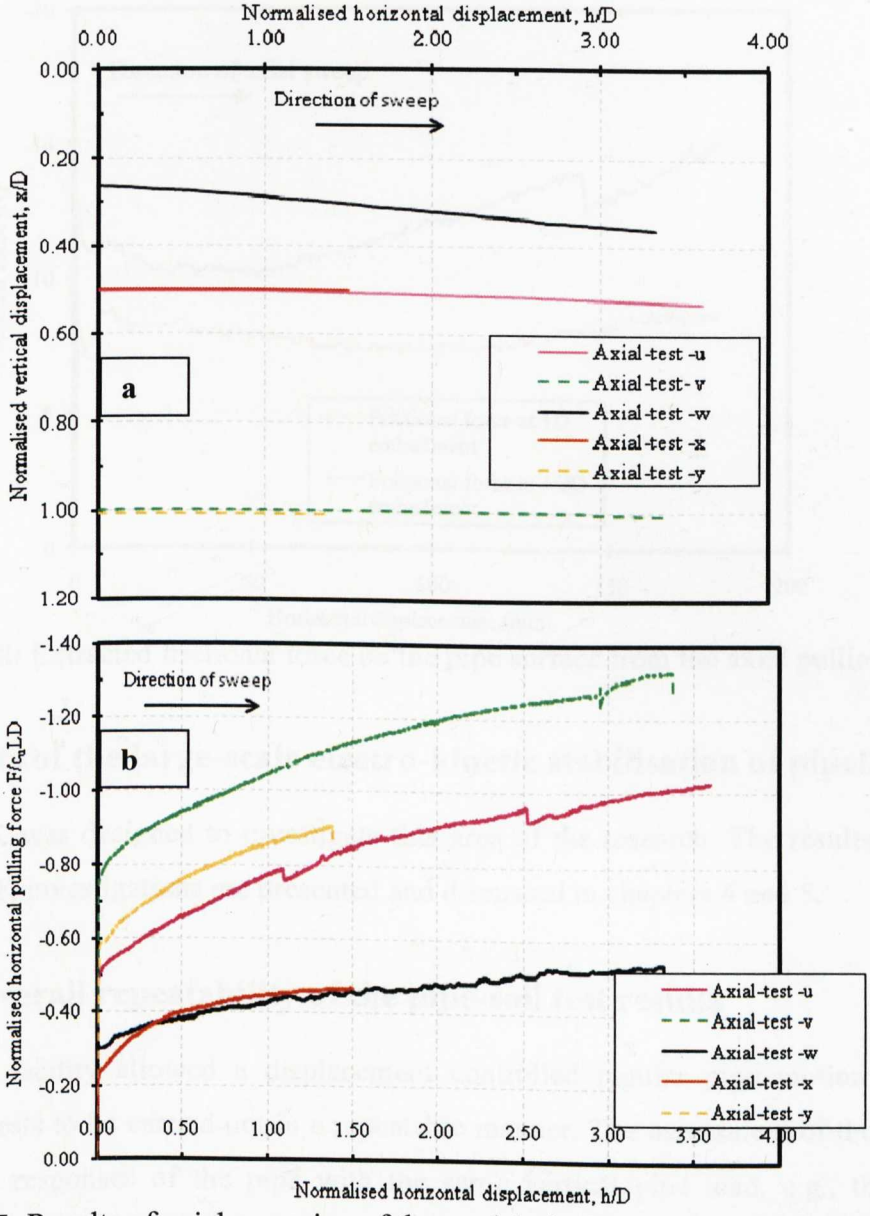

Figure 6 - 37: Results of axial sweeping of the model pipeline on the model seabed for **test -u - y**: a) vertical displacement against axial displacement, b) horizontal pulling force against axial displacement

Referring to Figure 3 - 25 where the proposed determination of the frictional force is schematically illustrated, Figure 6 - 38 shows the friction force on the pipe surface extracted from the force-displacement plots during the axial pull. It can be seen that the higher the depth of embedment, the higher the resulting axial pulling force. However, when the equivalent frictional force on the pipe surface is extracted, the frictional force from the 1/2D embedment appears higher. The reason for this is not understood but could be due to the variation in the soil strength.

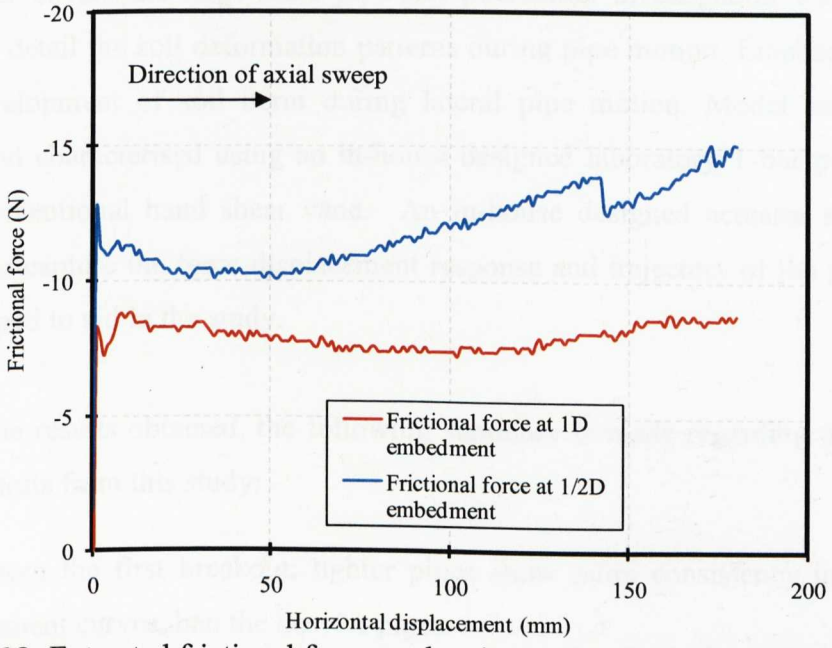

Figure 6 - 38: Extracted frictional force on the pipe surface from the axial pulling tests

6.4 Results of the large-scale electro-kinetic stabilisation of pipeline

Series LS-EK was designed to investigate this area of the research. The results of the large-scale EK investigations are presented and discussed in chapters 4 and 5.

6.5 The overall repeatability of the pipe-soil test results

The test rig facility allowed a displacement controlled regular pipe motion which enabled the tests to be carried out in a repeatable manner. The assessment of the force-displacement responses of the pipe with the same vertical pipe load, e.g., the 87N vertical pipe weight, revealed that the whole pattern repeated itself in all pipe sweeps with the results showing very repeatable load-displacement cycles, thus demonstrating that the tests were repeatable. In the different beds of clay, priority was given to soil

preparation and the pipe displacement control. Sufficient uniformity and repeatability were successfully achieved for each bed of soil. The T-bar, shear vane and the water content tests carried out to check the state of the soil indicated that satisfactory homogeneity and repeatability of the results were obtained. The results from each test bed of soil (e.g., the soil c_u) provided the parameter used in normalising the resulting force-displacement responses of the pipe-soil interaction tests.

6.6 Summary of results of the pipe-soil interaction tests

This chapter covers the large-scale pipe-soil interaction investigation which aims at studying in detail the soil deformation patterns during pipe motion. Emphasis has been on the development of soil berm during lateral pipe motion. Model seabeds were prepared and characterised using an in-house designed laboratory T-bar penetrometer and the conventional hand shear vane. An in-house designed actuator system with capability to capture the force-displacement response and trajectory of the pipe section was developed to aid in the study.

Based on the results obtained, the following summary is made regarding the pipe-soil interaction tests from this study:

- Apart from the first breakout, lighter pipes show more consistency in the force-displacement curves than the heavier pipes.
- The slope of the force-displacement curve is dependent on the submerged weight of the pipe section during lateral motion.
- Some variation exists in the force-displacement responses of pipes classed as "lighter" pipes and therefore required further reclassification in terms of generation of lateral resistance and pipe penetration during pipe motion.
- The lateral resistances from the soil reduces as the pipe tries to climb the soil berm
- Slight increase in breakout force exists with increasing submerged weight of pipe.
- Higher pipe weights shows slightly greater lateral displacement before the actual pipe breakout than the lower weight pipes.
- There is a possible combination of pipe weight and soil strength where the pipe embedment during lateral displacement will initiate excessive pipe penetration during pipe lateral travel.

- The amount of soil berm generation reduces after the first cycle for lighter pipes while it increases for heavier pipes.
- The rate of pipe penetration increases with depth for heavier pipes.
- The volume of soil scrapped from the trench to form the berm during pipe travels increases with increasing pipe weight.
- The gradient of the force-displacement response is dependent on the speed of lateral motion of the pipe.
- The rate of penetration and maximum penetration of pipe are influenced by the rate of pipe displacement. This response varies between light and heavy pipes.
- At lower speeds (0.05mm/sec), the rate of pipe penetration is minimal whereas for elevated speeds (1mm/sec), the rate of pipe penetration is accelerated.
- The maximum lateral load on the pipe at the end of sweep increases with increasing speed of pipe travel.
- Faster pipes show maximum vertical penetration at the end of sweep cycle.
- The higher the speed of pipe travel, the faster the generation of soil berm and hence the higher the soil resistance generated.
- Soil resistance increases with depth of embedment.
- At a shallower depth of initial embedment, the effect of pulling speed is similar. However at greater depths, the difference is more pronounced.
- At a deeper initial embedment, lighter pipes appear to show only a slight dependence of breakout force with speed than the heavier pipes. Also, lower lateral pipe speeds appear to promote increasing lateral soil resistance as the lateral pipe displacement increases.

6.7 Discussions of the large-scale pipeline-soil interaction tests

6.7.1 Introduction

Subsea pipelines operated at elevated temperature may become unstable due to expansion and contraction from start-up and shut-down cycles. Excessive pipe expansion can result in lateral buckling while unplanned/excessive penetration of the pipeline can undermine the structural integrity of the line. Therefore, in order to adequately design these pipelines, a clearer understanding of the pipe-soil responses in terms of soil lateral resistance and pipe penetration in addition to berm formation is

essential. This section discusses the results of the pipe-soil interaction reported in earlier in this chapter with a view to increasing this understanding and therefore increases the available database on pipe-soil interaction.

6.7.2 Seabed shear strength profile

The results from the model seabed have been presented in §6.4. The various seabed strength profiles appear to indicate a near linear profile down to about 225mm depth which is typical of a normally consolidated soil. However, most deepwater seabeds often show a layer of strong crust (~ 10 -15kPa) within the upper 1m depth which is believed to be attributed to biogenic activates (White and Cheuk,2008). This leads to a very high normalised strength (c_u/σ'_v) within this depth and corresponding dilatant behaviour when the soil is sheared. The resulting strength profile from this study did not show this crust which is a limitation of this method of seabed preparation as this profile was difficult to obtain within the time frame of this research.

Another drawback to the model seabed in this study is the disparity in the coefficient of consolidation (c_v) of the kaolin, about $2m^2$/year, as compared to the about $0.3m^2$/year (White and Randolph,2007) for most offshore clays. Also, this value varies significantly depending on the composition and depositional environment of the clay. This variation is likely to have effects on the consolidation and settlement behaviour of the seabed/pipeline when attempt is made to relate results from these tests to typical offshore locations.

6.7.3 Vertical pipe penetration

Various attempts have been made by some researchers to provide prediction methods for assessing the initial embedment of pipeline into cohesive soil. As discussed in §2.4, the Verley and Lund (1995) is the one mostly used in the industry (Equation 2.4). An attempt to compare the results of the initial embedment of the pipe section obtained from series LP-SW, where various pipe weights were investigated, with the proposed prediction method from Verley and Lund (1995) is shown in Figure 6 - 39. The unit weight of the kaolin clay was taken as $16kN/m^3$ which is typical of this clay and is used throughout this study.

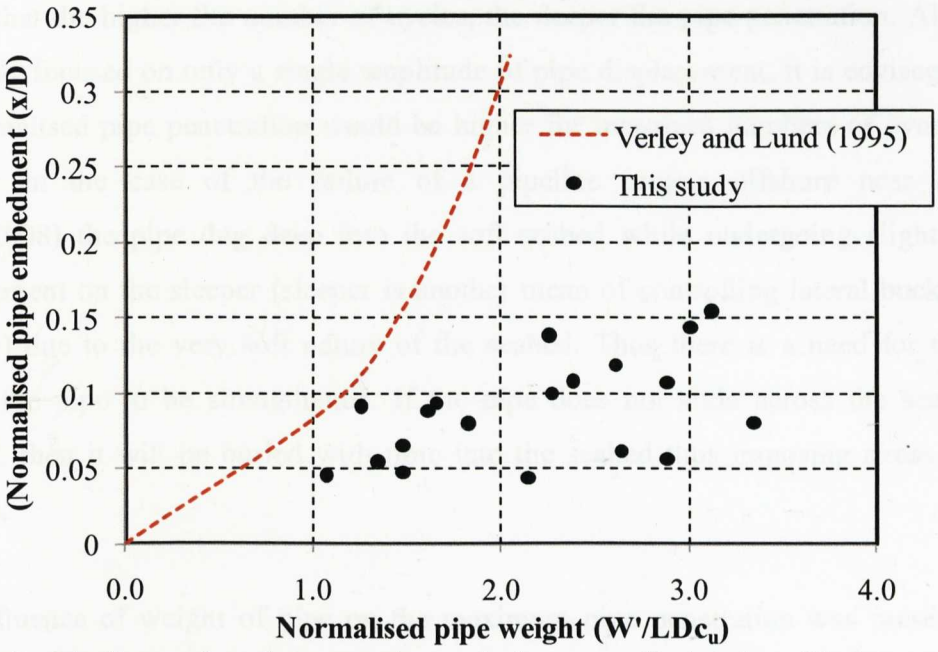

Figure 6 - 39: Comparison between pipe embedment prediction from Verley and Lund (1995) and this study

It can be seen from the plot that the value of pipe embedment for a given pipe weight is less than the predicted value. A possible reason for this variation could be in the selection of the undrained shear strength value used for the normalisation. For ease of comparison, the soil strength at 1/2D embedment of the pipe was used. Within this depth range, the model seabed strength varies between 0.25 and 0.74kPa. However, in the case of the Verley and Lund's (1995) prediction, an average strength value of 0.5kPa was used which made it difficult to correlate with the experimental data due to the variation in the seabed strength used in the various tests. The experimental data indicate a trend which shows increasing depth of penetration with increasing pipe weight.

Referring to Figure 6 – 13, where the normalised vertical pipe penetration was plotted against the normalised pipe weights, the effects of the cyclic motion of the pipe at constant amplitude of displacement can be inferred. It does appear from the plot that the normalised vertical penetration of the pipe is independent of the normalised weight of the pipe after the constant amplitude and cycles of a specified displacement. The effect is however expected to be different if the pipe is moved at varying cycles. The dependence of pipe maximum penetration of pipeline on the numbers of cycles of pipe displacement especially in a soft clay seabed has already been pointed out by previous researchers (Brennodden et al.,1986; Morris et al.,1988; Palmer et al.,1988). They all

agreed that the higher the number of cycles, the deeper the pipe penetration. Although this study focused on only a single amplitude of pipe displacement, it is envisaged that the normalised pipe penetration would be higher for increased numbers of cycles. For instance in the case of the failure of a pipeline project offshore near Angola (Allan,2008) the pipe dug deep into the soft seabed while undergoing slight cyclic displacement on the sleeper (sleeper is another mean of controlling lateral buckling of pipeline) due to the very soft nature of the seabed. Thus there is a need for the soil around the pipe to be strengthened. If the pipe does not slide across the seabed as planned, then it will be buried with time into the seabed thus imposing stress on the pipeline.

The influence of weight of pipe on the maximum pipe penetration was presented in Figure 6-30 which suggests that increasing the speed of the pipeline on the seabed increases the maximum penetration of the pipe for a given cycle and amplitude of displacement. However, this relationship is not significant in the heavier pipe (97N) and the reason could be possibly attributed to the deeper penetration of the pipe due to its weight coupled with the increasing soil strength which obscured the relationship between the rate of displacement and the pipe penetration. The discrepancy is even more obvious in Figure 6 – 36, where the pipe was forced to a specified depth of 1/2D and 1D before the lateral sweeps.

6.7.4 Soil resistance and breakout force

The results presented in chapter 6 indicate that the soil resistance on the pipe section and the breakout force are affected a number of factors including the weight of the pipe, speed of pipe displacement and the depth of initial embedment of the pipe. The prediction method proposed by Verley and Lund (1995) is mostly employed in the industry for the estimation of the breakout resistance of partially buried pipeline. Analysis of the Verley and Lund's (1995) solution clearly shows that the breakout force increases with depth of pipe penetration. A comparison of this solution with other methods has been presented in Figure 2 -8. However, this solution did not consider the mobilised displacement before the breakout of the pipe under varying conditions such as effects of rate of pipe displacement and varying pipe weight.

It is important to note that this study made some interesting observations relating to the breakout force and lateral force on the pipe such as: the greater the normalised pipe weight, the greater the mobilised displacement before pipe breakout (Figure 6 – 14); the quicker the rate of the pipe motion, the lesser the dependency of the breakout force on the mobilised displacement before breakout (Figure 6 – 28); the maximum lateral load on the pipe at the end of the constant amplitude of pipe motion is indicated to be dependent on the rate of pipe motion, where the lateral force on the pipe increases with increasing rate of pipe motion (Figure 6 – 29). In addition, Figure 6 – 34 and 35 conform to the Verley and Lund's (1995) prediction where the breakout force and the lateral load on the pipe are directly related to the depth of the pipe embedment. This additional information is considered vital in reducing the uncertainty relating to the large amplitude of displacement associated with the lateral buckling of partially emended pipelines.

A comparison of the breakout force between the predictions by Verley and Lund (1995), Bruton et al (2006) and the experimental data from the study (Figure 6 - 40) indicates that the experimental data is significantly higher than the prediction model proposed by Verley and Lund (1995) while it is fairly consistent with the model proposed by Bruton et al (2006) for the lighter (57 to 97N) pipes but deviates significantly from the heavy pipe (107N). In this comparison, only the experimental results from series LP-SW (same speed of pipe motion) were used. The various depths of embedment obtained from this study were substituted in the two prediction models to obtain the breakout force. The lower value obtained from the Verley and Lund's (1995) model could be possibly due the fact that this model only predicts the lateral resistance for a given depth of embedment of the pipe, while no provision is made for varying the depths of pipe embedment in the formula.

The results presented from the experimental data and the Bruton et al. (2006) predictions however involve various pipe weights. It should be noted that the peak breakout force is a function of the depth of pipe embedment and the submerged weight of pipe; the higher the pipe weight the lower the breakout resistance (White and Cheuk,2008). However, both the experimental data and the two models show the dependency of the breakout force on the depth of pipe embedment.

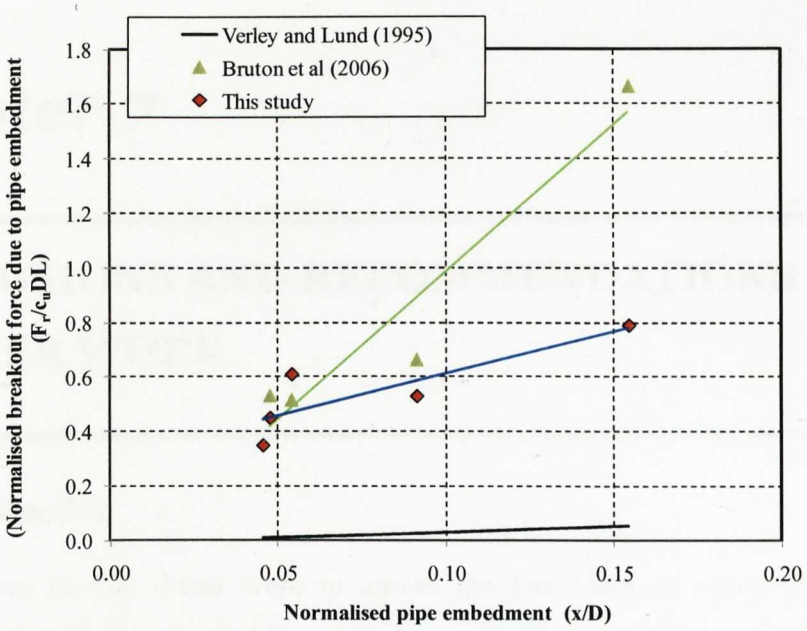

Figure 6 - 40: Comparison of the lateral breakout resistance between the Verley and Lund's (1995), Bruton et al (2006) predictions and the experimental results from this study

6.7.5 Berm development

The resistance of soil to movement of a partially buried pipeline in soft clay has been noted to be affected by not only frictional force at the base of the pipe but also by the passive resistance offered by the wedge of soil (the berm) as the pipe moves laterally. While the first component (frictional force) is relatively well understand and established, the contributions from the berm under varying conditions is uncertain.

This study indicates that the generation of the berm during the lateral motion of the pipe is affected by the weight of the pipe and the speed of pipe motion. Using data from the first sweeps only which give a better platform comparison before the onset of excessive pipe penetration, the effects of pipe weight on the berm generation is assessed. Figure 6 – 19 indicates that the greater the pipe weight, the larger the area of the berm formed assuming plane strain conditions. However, while heavier pipes (Test d & e, 97 N & 107N) show significant variation in the volume of berm generated, the lighter pipes (tests a –c, 57N to 87N) appear to show close response in the behaviour of the berm with increasing tendency to converge with increasing lateral pipe displacement. The influence of pipe speed of displacement (Figure 6 – 32) also indicates that the higher the speed of displacement, the faster the increase in the volume of soil scraped to form the berm and consequently increases in the lateral soil resistance.

Chapter 7

CONCLUSIONS AND RECOMMENDATIONS FOR FURTHER WORK

7.1 Introduction

The objectives of this thesis were to assess the feasibility of using electro-kinetic phenomenon to enhance the stability of subsea pipelines as well as studying pipe-soil interaction on the seabed, especially the deformation of soil during large amplitude pipe displacement and its effects on soil resistance. It was motivated by the ongoing concerns relating to pipe instability problem due to operational conditions. To aid in the study, small-scale EK tests were conducted. Additionally, pilot-scale pipe-soil tests were conducted using a specially designed pipe-soil interaction testing rig. The overall conclusions drawn from the findings of the EK and the pipe-soil interaction studies are detailed in this chapter. Recommendations for further work are presented at the end of the chapter.

7.2 Conclusions

The review of relevant available literature has indicated that the use of engineered buckle solutions to mitigate against subsea pipeline instability has become generally accepted and more frequently used offshore. This is because the other existing mitigating methods are either expensive or impractical in deeper waters. It has also been shown that none of the existing mitigation methods deal with the modification of the ambient soil properties. The use of EK phenomenon which has been explored in this thesis has been identified as an option which could potentially be employed to enhance pipeline stability. The effectiveness of this proposed alternative approach was assessed from the changes in the soil parameters which are summarised below.

7.2.1 Electrical aspects of the EK treatment

Given the configuration of the EK tests adopted for this study, four stages in the generation of current density have been identified as: (1) position of the initial current density, (2) the presence of initial lows in current density, (3) the maximum current density during the EK treatment and (4) the residual current density. Idealised stages in current density generation for partially embedded pipe section during EK treatment of the ambient soil have been presented. The positions and the magnitudes of the four stages on the idealised curve were noticed to be directly related to the applied voltage and the type or nature of the electrode material employed.

It was not confirmed if this trend would be replicated under varying experimental conditions such as different soil type and electrode configurations. Apart from the influence of the electrode materials on the amount of the current density generated, the time it take for the treatment to complete and the influence of the initial water content were indicated to be electrode material dependent which was also shown to influence the rate of corrosion of the electrodes, where copper electrodes were identified as being more durable and iron electrodes less durable.

7.2.2 Changes in soil water contents

A series of water content (w) tests were conducted to investigate the changes in w due to the EK treatment. Findings from this study had indicated that up to 14% decrease in water content was measured with the maximum decrease occurring below the pipe invert. The effects of applied voltage were not pronounced from the various tests conducted to assess this parameter. It appears to suggest that as long as the EK treatment was allowed to come to an end indicated by the complete depletion of the electrodes, then the difference in the changes in the measured water content were not significant probably due to the associated chemical alteration of the soil during the treatment. It was also shown that iron electrodes produced the maximum decrease in water content at the top level of the soil while aluminium electrodes produced maximum decrease at greater depth within the soil mass. The changes in the water content which is directly related to the development of the undrained shear strength of the treated soil also affects the breakout resistance of the soil and hence the pipe stability on the seabed. These changes in w due to the EK treatment supports the fact

that soil engineering properties around a partially buried pipeline could be improved by the application of EK treatment. However, aluminium electrodes appear to weaken the soil at the top level and are likely not to be effective for partially buried pipelines.

7.2.3 Changes in soil undrained shear strength

A significant increase in the undrained shear strength of the treated soil was noted after EK treatment. Iron electrodes stiffened the soil more at the top level while some level of softening of the top level of the soil was noted using aluminium electrodes, although the greatest increase in strength was obtained at depth using aluminium electrodes. In some cases c_u reduced (i.e., less than the c_u increase from the control test) when the soil was treated with aluminium electrodes.

The increase in the soil strength was indicated to be water content dependent which may imply that the treatment efficiency could be site condition dependent. A sharp increase in the soil strength obtained when aluminium electrodes were used was thought to be mainly from the favourable chemical reaction between the kaolin clay and some chemical species derived from the degradation of the aluminium electrodes. Therefore, the observed increase in soil strength was probably mostly due to electro-chemical cementation. It was also shown that considerable increase in strength could still take place without corresponding increase in water content due to continuous electro-chemical reaction within the soil even after the withdrawal of the electric current. Analysis of the normalised strength plot indicates that the strength improvement extends to between 70 and 80 mm depth of the soil which was more than 60% of the soil thickness.

7.2.4 Changes in soil breakout force

Pullout tests were conducted to assess the impact of the EK treatment on the soil using specially designed test rig. Between 70% and 210% increase in the vertical breakout force was noted after the EK treatment while between 90% and 209% increase was noted for the axial breakout force. In the same vein, iron electrodes caused up to 89% increase in the lateral breakout force while copper electrodes caused up to 30% increase with aluminium electrode reduced the breakout force compared to the breakout from the control tests. The greater increase in the breakout force was obtained with iron electrodes. The increase in the breakout force was attributed to the interplay between

chemical alteration and consolidation of the soil which resulted in the increase in the pipe-soil adhesive force. The softening of the top level of soil when aluminium electrodes were used was the reason for the low pullout force measured for aluminium electrodes.

7.2.5 Proposed practical field application of this novel approach

A proposed approach to the actual field application of this novel solution is envisaged to be used in conjunction with the lateral buckle solution for reducing the risk to pipe instability associated with elevated temperature and pressure.

In summary, the preliminary results from this research at extending the applications of EK in geotechnical engineering to offshore pipelines show promising outcomes. The reasonable repeatability between experiments suggests that this preliminary study can form a basis for subsequent research in this area and the results could provide some benchmark for further work in these areas. Furthermore, it is hoped that this thesis would stimulate the pipeline industry to invest in research about the application of EK in pipeline engineering.

7.2.6 Pipe-soil test

The large-scale pipe-soil interaction tests were conducted on E-grade kaolin clay using a specially designed testing rig which was conceived, designed and fabricated to aid in the study. This rig had the advantages of being able to provide uninterrupted loading on the soil during change of direction of pulling as well as using more precision data capturing devices. A laboratory in-house designed T-bar penetrometer was used to measure undrained shear strength profile and the strength values at predefined depths used to normalise the pipe-soil responses. Some interesting observations were made from the pipe-soil interaction tests. Based on the results obtained, the following conclusions are made regarding the pipe-soil interaction tests from this study:

(a) Force-displacement responses and pipe weights

- The force-displacement responses of the "lighter" pipes were somewhat different from that of the "heavier" pipes with regards to the pattern of the displacement hysteresis loop during cyclic pipe sweeps, the displacement distance before the pipe breakout and the rate of pipe penetrations.

(b) Influence of speed of pipe lateral displacement

- The maximum lateral load on the pipe at the end of the predetermined cycles of displacement were observed to increase with the increasing speed of the pipe displacement where the faster the pipe, the higher the vertical pipe penetration at the end of the cycle of displacement.
- It was also observed that the higher the speed of travel the faster the generation of the soil and hence the higher the soil resistance generated.

(c) Influence of depth of initial embedment

- The soil resistances and the breakout force measured were observed to be affected by the initial depth of embedment of the pipe where at deeper initial embedment, the lighter pipes show only a slight dependence on the breakout force with speed than the heavier pipes. Also, the lower pipe speed of displacement appears to promote increasing lateral résistance as the lateral pipe displacement increases.

7.3 Key research findings

The following is a summary of the key findings from the research:

1. Results indicate a distinct pattern of current density generation with time for the three electrodes (copper, iron and aluminium) used in this study. Only copper electrodes show an initial low in current density during the EK treatment.
2. Iron electrodes produced the maximum decrease in water content at the top level of the soil while aluminium electrodes produced maximum decreases at greater depth within the soil mass.
3. As long as the EK treatment was allowed to reach completion the difference in the changes in the measured water content were not significant for c_u probably due to the associated chemical alteration of the soil during the treatment.
4. Aluminium electrodes appear to weaken the soil at the top level and are likely not to be effective for partially buried pipelines while iron electrodes stiffen the soil at the top level. Significant increases in strength were measured at depth using aluminium electrodes.
5. Iron electrodes give the greatest increase in the pullout force compared to copper and aluminium electrodes. The increase in the breakout force was attributed to chemical alteration and consolidation of the soil.

From the pipe-soil interaction studies the following are considered the key research findings:

1. The higher the speed of pipe displacement on the seabed, the higher the maximum lateral load on the pipe at the end of the predetermined cycles of displacement. This implies the higher the speed of travel the faster the generation of the soil berm and hence the higher the soil resistance to pipe movement.
2. The soil resistances and the pipe breakout force depend on the initial depth of embedment of the pipe. For lighter pipes at deeper initial embedment, the breakout force is only slightly affected by pipe speed than compared to the effect for the heavier pipes
3. There appears to be a possible combination of a pipe's vertical load and soil strength where the rate of pipe embedment during pipe motion will initiate excessive pipe penetration.
4. The amount of soil berm generation reduces after the first cycle for lighter pipes while it increases for heavier pipes.
5. Higher pipe weights shows slightly greater lateral displacement before the actual pipe breakout than the lower weight pipes.

7.4 Contribution to the field of knowledge

Through the series of the EK and pipe-soil interaction tests conducted and described in this thesis, the contribution to the field of knowledge are summarised as follows:

- An extension of the application of electro-kinetic phenomenon to enhance the stability of subsea pipelines.
- The suggestion and proposal on possible field application of EK technology in the offshore industry.
- The demonstration of the similarity between the small-scale and the pilot-scale EK treatment of the soil around partially buried pipelines.
- The recognition of the unique nature of the current density generation associated with different electrode materials during the EK treatment of soil around partially embedded pipes.
- The recognition of the influence of electrode materials on the breakout forces during EK treatment of partially buried pipeline, especially the behaviour of aluminium electrode during this treatment.

- The study and presentation of the real time measurement of the berm geometry and its effects on the soil laterals resistance
- The explanation of the favourable electro-chemical reactions which resulted in the significant increase in the undrained shear strength when aluminium was used as electrodes.
- The real time measurement of seabed (berm geometry) deformation during pipe lateral displacement and comments on the effects of pipe weight, rate of pipe displacement, and normalised pipe weights on the seabed deformation and the soil resistances.

7.5 Recommendations for further work

While the results of this study provide a benchmark and insights into the extension of EK phenomenon to offshore pipeline, further studies are still required to apply the results from this study to a wider scope and make them applicable to field situations. Future work should be focused on the following issues:

1. During the EK treatment of the model seabed, it was observed that the chemical alteration of the soil was affected by the nature and composition of the electrode used. It therefore implies that the reactions and subsequent modification would be a function of the reaction of a particular seabed composition and the electrode materials. Further work is necessary to investigate other electrode types with varying compositions as well as soils from different offshore sites. In addition, there is a need to carry out chemical analyses (including pH) of the soil sample before and after the EK treatment for the purposes of accurately modelling the chemical fronts due to the EK effects. This will also aid in assessing the zone of influence as well as electrochemical alteration of the soil sample which could not be accurately assessed in this study. Furthermore, tests should be conducted to assess the rate of depletion of electrodes of different properties and dimensions as this is expected to have an impact on the cost and efficiency of the treatment. This could be another tool to check the efficiency of the individual electrodes on a real time basis.
2. The results from this study indicate that aluminium (AL) electrodes strengthen the model seabed at depth below the pipe section. Since this present research was aimed at only surface-laid pipes, further work is needed to investigate the use of AL for increasing the stability of buried pipelines.

3. The consolidation of the treated soil was inferred from the settlement of the pipe and the changes in the water content. However, direct measurement of the pore pressure development during the EK treatment could be a better way to monitor the consolidation during the EK treatment.
4. Further work is needed to assess the effect of cyclic loading on the electrically modified soil after the EK treatment since the pipeline may be subjected to cycles of lateral and axial displacement after EK treatment. It is not clear what the effect of this cyclic movement would be on the EK modified soil.
5. Finally, this approach is designed to be applicable to new pipeline during installation. However, further studies on the extension of this solution to existing pipelines on the seabed would be useful.

For the pipe-soil interaction tests, there are some issues that require further research work. Firstly, the study of the berm generation assumed that the seabed is horizontal. There is therefore need to investigate the influence of the effect of seabed gradient on the berm generation and soil resistances. Work is also necessary to incorporate the real time study of the berm generation presented in this study to existing pipeline design codes.

Secondly, only one soil type was used in these pipe-soil interaction tests. There is need to test different soils with different chemical and physical characteristics, for example, soil from specific petroleum basins. Observation of the berm formation should also include the measurement of pore pressure build up during the soil deformation and its effects on the ensuing soil resistances.

Finally, only a bare (uncoated) pipe was used in this study There is need to assess the influence of different pipe coatings on the rate of pipe penetration, generation of soil berm and the soil resistances that could be developed.

In spite of the shortcomings implied by the need for further research work, this present research is hoped to form a basis for subsequent research in this area. It has also led to an improved the understanding of the interaction between soil and pipeline on the seabed.

References

Acar, Y. B. and A. N. Alshawabkeh (1996). "Electrokinetic Remediation. I: Pilot-Scale Tests with Lead-Spiked Kaolinite." Journal of Geotechnical Engineering © ASCE **122**(3): 173 - 185.

Acar, Y. B., R. J. Gale, G. A. Putnam, J. Hamed and R. L. Wong (1990). "Electrochemical processing of soils - theory of ph gradient development by diffusion, migration, and linear convection." Journal of Environmental Science and Health Part a-Environmental Science and Engineering & Toxic and Hazardous Substance Control **25**(6): 687-714.

Acar, Y. B., J. T. Hamed, A. N. Alshawabkeh and R. J. Gale (1994). "Removal of cadmium (II) from saturated kaolinite by the application of electrical current." Geotechnique **44**(2): 239 - 254.

Acar, Y. B., H. Y. Li and R. J. Gale (1992). "Phenol removal from kaolinite by electrokinetics." Journal of Geotechnical Engineering-Asce **118**(11): 1837-1852.

Allan, P. G. (2008). Failure of subsea pipeline at Greater Plutonio Field due to soil failure (Personal Communication).

Andreuzzi, F. and A. Perrone (2001). "Analytical solution for upheaval buckling in buried pipeline." Computer Methods in Applied Mechanics and Engineering **190**(39): 5081-5087.

Armstrong, C. (2007). The stiffening of subsea soils using electro osmosis; a new approach to the installation of offshore pipelines in the oil and gas industry. MSc Thesis, Newcastle University.

Aubeny, C. P., C. Gaudin and M. F. Randolph (2008). Cyclic Tests of Model Pipe in Kaolin.

Aubeny, C. P., S. H. and J. D. Murff (2005). "Collapse loads for a cylinder embedded in trench in ohesive Soil." International Journal of Geomechanics ASCE **5**(4): 320 - 325.

Ayers, R. R., D. W. Allen, W. F. Lammert, J. R. Hale and V. Jacobsen (1989). Submarine pipeline on-bottom stability: Recent AGA research. Proceedings of the International Offshore Mechanics and Arctic Engineering Symposium.

Barker, J. E., C. D. F. Rogers, D. I. Boardman and J. Peterson (2004). "Electrokinetic stabilisation: an overview and case study." Ground Improvement **8**(2): 47 - 58.

Bergado, D. T., J. C. Chai, N. Miura and A. S. Balasubramaniam (1998). "PVD improvement of soft bangkok clay with combined vacuum and reduced sand embankment preloading." Geotechnical Engineering Journal **29**(1): 95 - 121.

Bergado, D. T., I. Sasanakul and S. Horpibulsuk (2003). "Electro-Osmotic Consolidation of Soft BangkokClay Using Copper and Carbon Electrodes with PVD." Geotechnical Testing Journal **26**(3).

Bjerrum, L., J. Moum and O. Eide (1967). "Application of electro-osmosis to a foundation problems in Norwegian quick clay." Geotechnique **17**: 214 - 235.

Boulanger, R. W. and R. F. Hayden (1995). "Aspects of compaction grouting of liquefiable soil. Journal of Geotechnical Engineering **121**(12).

Bowles, J. E. (1979). Physical and geotechnical properties of soils. Tokyo, Japan, McGraw-Hill, Inc.

Brennodden, H., J. T. Lieng, T. Sotberg and R. L. P. Verley (1989). An energy-based pipe-soil interaction method. Offshore Technology Conference (OTC). Houston, Texas, USA. **3** , 147-158.

Brennodden, H., O. Sveggen, D. A. Wagner and D. J. Murff (1986). Full-scale pipe-soil Interaction tests. Offshore Technology Conference (OTC). Houston, Texas, USA.

Broms, B. B. and P. Boman (1979). "Lime columns- A new foundation method." Journal of Geotechnical Engineering ASCE **105**: 539 - 556.

Bruton, D. and M. Carr (2007). "The Influence of Pipe-Soil Interaction on Lateral Buckling and Walking of Pipelines - The SAFEBUCK JIP." Proceedings of the 6th International Offshore Site Investigation and Geotechnics Conference 11 - 13 Septmeber, 2007: 133 - 148.

Bruton, D., D. White, C. Cheuk, M. Bolton and M. Carr (2006). "Pipe/soil interaction behaviour during lateral buckling, including large-amplitude cyclic displacement tests by the Safebuck JIP." Offshore Technology Conference: 17944.

Bruton, D. A. S., D. J. White, M. Carr and J. C. Y. Cheuk (2008). Pipe-soil interaction during lateral buckling and pipeline walking - The SAFEBUCK JIP. 2008 Offshore Technology Conference (OTC). held in Houston, Texas, U.S.A.

BS8010 (1993). Code of Practise for Pipelines, Part 3, Pipelines, Subseae Design, Construction and Installation, British Standard Institution, London.

Burnotte, F., G. Lefebvre and G. Grondin (2004). "A case record of electroosmotic consolidation of soft clay with improved soil-electrode contact." Canadian Geotechnical Journal **41**(6): 1038-1053.

Byrne, P. M. and W. D. Liam Finn (1978). "Breakout of submerged structures buried to a shallow depth." Canadian Geotechnical Journal. **15**: 146 - 154.

Carr, M., D. Bruton and D. Leslie (2003). "Lateral Buckling and Pipeline Walking, a Challenge for Hot Pipelines." Offshore Pipeline Technology Conference, 2003, Amsterdam.

Carr, M., F. Sinclair and D. Bruton (2006). "Pipeline Walking - Understanding the Field Layout Challenges, and Analytical Solutions Developed for the SAFEBUCK JIP." Proc Offshore Tech Conf.

Casagrande, L. (1949). "Electro-osmosis in soils." Ge´otechnique **1**: 157 - 177.

Casagrande, L. (1952). "Electro-osmotic stabilisation of soils." Journal of Boston Society of Civil Engineers **xxxix**(1).

Cathie, D. N., C. Jaeck, J. C. Ballard and J. F. Wintgens (2005). "Pipeline geotechnics - State of-the-art." International Symposium on Frontiers in Offshore Geotechnics: 95-114.

Chari, T. R., S. N. Guha and K. Muthukrishnaiah (1978). Adhesive resistance of underconsolidated sediments. Ocean conference Washington, USA.

Cheuk, C. Y., D. J. White and M. D. Bolton (2007). "Large-scale modelling of soil-pipe interaction during large amplitude cyclic movements of partially embedded pipelines." Canadian Geotechnical Journal **44**(8): 977-996.

Chew, S. H., G. P. Karunaratne, V. M. Kuma, L. H. Lim, M. L. Toh and A. M. Hee (2004). "A field trial for soft clay consolidation using electric vertical drains." Geotextiles and Geomembranes **22**(1-2): 17-35.

Chu, J., S. Yan and B. Indraratna (2008). "Vacuum preloading techniques - recent developments and applications." Faculty of Engineering Publication, University of Wollongong, Australia. http://ro.uow.edu.au/engpapers/420.

Craig, I. G., N. W. Nash and G. A. Oldfield (1990). "Upheaval buckling: A practical solution using hot water flushing technique." Offshore Technology Conference, Houston, Texas.

Craig, R. F. (2005). Craig's Soil Mechanics. London, Spon Press.

Dendani, H. and C. Jaeck (2007). "Pipe-Soil Interaction in Highly Plastic Clays " Processdings of the 6th International Offshore Site Investigation and Geotechnics Conference, 11 - 13 Septemeber, 2007: 115 - 124.

Denis, R. and C. de Brier (2010). Deep water tool for in-situ pipe-soil interaction measurement recent developments and system improvement (OTC 20630). Offshore Technology Conference (OTC). Houston Texas, USA.

Dingle, H. R. C., D. J. White and C. Gaudin (2008). "Mechanisms of pipe embedment and lateral breakout on soft clay." Canadian Geotechnical Journal **45**(5): 636-652.

Domone, P. L. (1990). "The properties of low strength silicate/portland cement grouts " Cement and Concrete Research **20**: 25 - 35.

Donnon, F. (1924). "The theory of membrane equilibria." Chemical Reviews 73-90.

Dunlap, W. A., R. Bhojanala and D. V. Morris (1990). Burial of vertically loaded offshore pipelines in weak sediments. Offshore Technology Conference. Houston, Texas, USA: 263 - 270.

Eggestad, A. and T. Foyn (1983). Electro-osmotic improvement of a soft sensitive clay. Proceedings of the 8th ECSMFE, Helsinki, Finland. **2:** 597-560.

Ellinas, C. P., W. J. Supple and H. Vastenholt (1990). "Prevention of upheaval buckling of hot submarine pipelines by means of intermittent rock dumping." Proc 22nd Offshore Tech Conf, Houston: 519-528.

Erchul, R. A. and R. J. Smith (1970). Lubricant and Polymer Reduction of Sediment Adhesion. Proc of ASCE conference- Civil Engrg in the Oceans II 621 - 640.

Esrig, M. I. (1968). "Pore pressures, consolidation, and electrokinetics." Journal of soil Mechanics and Foundation Division, ASCE **94**(4): 899 - 921.

Eykholt, G. R. (1997). "Development of pore pressures by nonuniform electroosmosis in clays." Journal of Hazardous Materials **55**(1-3): 171-186.

Ferguson, G. H. and W. D. Bell (1977). Seafloor cone penetrometer for deep penetration measurements of ocean sediment strength (OTC 2787). Offshore Technology Conference. Houston, Texas, USA.

Finn, L. W. D. and P. M. Byrne (1972). The evaluation of the breakout force for a submerged ocean platform (OTC 1604). Offshore Technology Conference. Dallas, Texas.

Finnie, I. M. S. and M. F. Randolph (1994). Punch-through and liquefaction induced failure of shallow foundations on calcareous sediments. Proceedings of International Conference on Behaviour of Offshore Structures. Boston, pp. 217 -230.

Floodgate, G. and A. G. Judd (1992). "The origins of shallow gas." Continental Shelf Research **12**(10): 1145 - 1156.

Friedmann, Y. (1989). In-service mechanical behavior of heated pipelines laid on seabed surface. Proceedings of the International Offshore Mechanics and Arctic Engineering Symposium. **V** 113 - 119.

Ghazzaly, O. I. and S. J. Lim (1975). Experimental investigation of pipelIne stability In very soft clay. Offshore Technology Conference (OTC). Houston, Texas, USA.

Glendinning, S., C. J. F. P. Jones and R. C. Pugh (2005). "Reinforced Soil Using Cohesive Filland Electrokinetic Geosynthetics." International Journal of Geomechanics, ASCE **5**(2): 138–146.

Gray, D. H. (1966). Coupled flow phenomenon in clay-water systems, PhD Thesis, University of Califonia, Berkley, USA.

Gray, D. H. (1970). "Electrochemical hardening of clay soils." Geotechnique **20**(1): 81-94.

Gray, D. H. and J. K. Mitchell (1967). "Fundamental aspects of electro-osmosis in soil." Journal of Soil Mechanics and Foundation Division **93**(SM6): 209 - 236.

Gray, D. H. and J. Schlocker (1969). "Electrochemical alteration of clay soil." Clay and Clay Minerals **17**: 309 - 322.
Griffin, J. J., H. Windom and E. D. Goldberg (1968). "The distribution of clay minerals in the World Ocean." Deep Sea Research and Oceanographic Abstracts **15**(4): 433-459.

Griffiths, T., D. O'Brien and R. Johnson (2007). Risk mitigation options for UHB design of pipelines in seismic risk area. 30th annual Offshore Pipeline Technology Conference & Exhibition. Krasnapolsky, Amsterdam.

Grundl, T. and P. Michalski (1996). "Electroosmotically driven water flow in sediments." Water Research **30**(4): 811-818.

Hamed, J., Y. B. Acar and R. J. Gale (1991). "Pb(II) Removal from Kaolinite by Electrokinetics." Journal of Geotechnical Engineering. Div. **117**(2): 241 - 271.

Hamed, J. T. and A. Bhadra (1997). "Influence of current density and pH on electrokinetics." Journal of Hazardous Materials **55**(1-3): 279-294.

Hamidi, B., H. Nikraz, K. Yee, S. Varaksin and L. T. Wong (2010). Ground improvement in deep waters using dynamic replacement. Proceedings of the Twentieth (2010) International Offshore and Polar Engineering Conference Beijing, China: 848 - 853

Hamir, R. B. (1997). Some Aspects and Applications of Electrically Conductive Geosynthetic Materials, PhD Thesis. Newcastle upon Tyne, University of Newcastle upon Tyne, United Kingdom.

Hesar, M. (2004). Pipeline-seabed interaction in soft clay. International Conference on Offshore Mechanics and Arctic Engineering. Vancouver, British Columbia, Canada.

Hobbs, R. E. (1984). "In-Service Buckling of Heated Pipelines." Journal of Transportation Engineering **110**(2): 175-189.

Ingles, O. G. and J. B. Metcalf (1972). Soil stabilisation, principles and practice. London, Butterworths.

Ismail, M. A. (2002). "Performance of an offshore stabilised calcareous soil." Ground Improvement **6**(4): 175–186.

Judd, A. G. and M. Hovland (1992). "The evidence of shallow gas in marine sediment." Continental Shelf Research **12**(10): 1081 - 1095.

Karal, K. (1977). "Lateral stability of submarine pipelines." Proceedings of the Annual Offshore Technology Conference **4**: 71-78.

Karal, k. (1983). Time effect on the lateral soil resistance to pipeline movement. Second International Offshore Mechanics and Artic Engineering Symposium, Houston, Texas.

Karim, B., F.-C. Teddy, A. E. Dupas, Y. Berthaud and P. Dangla (2005). " Role of pH in Electro-Osmosis: Experimental Study on NaCl–Water Saturated Kaolinite." Transport in Porous Media **61**: 93 - 107.

Kim, H. O. and D. C. Chang (1999). "Method yields download force to arrest upheaval buckling in offshore lines." Oil and Gas Journal **97**(30): 78-83.

Kim, S. S., J. Y.Kim, B. Y. Kang and K. H.Koh. (2007). The field experimental study on improvement of soft Marine clay by EK-cementation technique. Proceedings of the International Offshore and Polar Engineering Conference.

Kim, S. S., K. Y. Lee, S. J. Han and K. H. Koh (1997). "The study on the electro osmotic consolidation of marine clayey soil." Proceedings of the Seventh International Society Offshore& Polar Engineers: 821-826.

Lambrakos, K. F. (1985). "Marine pipeline soil friction coefficients from in-situ testings." Ocean Engineering **12**(2): 131-150.

Le, M.-H., J.-F. Nauroy, V. D. Gennaro, P. Delage, E. Flavigny, N. Thanh, J.-L. Colliat, A. Puech and J. Meunier (2008). Characterization of soft deepwater West Africa clays: SHANSEP Testing is Not Recommended for Sensitive Structured Clays. Offshore Technology Conference. Houston, Texas, USA.

Le Tirant, P. (1979). Seabed reconnaissance and offshore soil mechanics for installation of petroleum structures, Imprimerie Louis-Jean.

Lee, H. J. (1973). Breakout of Partially embedded Objects from Cohesive Seafoor Soils. Offshore Technology Conference; Paper OTC 1904, Dallas, Texas, USA

Lefebvre, G. and F. Burnotte (2002). "Improvements of electroosmotic consolidation of soft clays by minimizing power loss at electrodes." Canadian. Geotechnical Journal. **39**(2): 399-408.

Lehane, B. M. and C. Gaudin (2005). Effects of drained pre-loading on the performace of shallow foundations on overconsolidated clay. Proceedings of the International conference on Offshore, Marine and Artic Engineering. Halkidiki, Greece.

Lehane, B. M., C. D. O. Loughlin, C. Gaudin and M. F. Randolph (2009). "Rate effects on penetrometer resistance in kaolin." Geotechnique **59**(1): 41- 52.

Lewis, R. W. and C. Humpheson (1973). "Numerical analysis of electro-osmotic flow in soils." Journal of soil mechanics and foundation division **99**(SM8): 603 - 616.

Liming, L., Z. Tianfeng, Y. Xiaogang and D. Menglan (2007). Design of HT subsea pipeline against upheaval buckling by pre-heating before trenched. Proceedings of the International Offshore and Polar Engineering Conference.

Littlejohn, G. S. (1985). "Grouting of platforms and pipelines offshore " International Journal of Rock Mechanics and Mining Sciences & Geomechanics Abstracts **22**(5): 165-165.

Liu, C. L. (1969). Ocean sediment holding strength against breakout of partially embedded objects. Proc. Civil Engrg. in the Ocean II, ASCE: 105 - 116.

Lo, K. Y., I. I. Inculet and K. S. Ho (1991). "Electroosmotic strengthening of soft sensitive clay." Canadian Geotechnical Journal. **28**: 62 - 73.

Lo, K. Y., S. Micic, J. Q. Shang, N. Y. Lee and S. W. Lee (2000). "Electrical strengthening of a soft marine sediment." International Journal of Offshore and Polar Engineering, ISOPE **10**: 137 - 144.

Lockhart, N. C. (1983b). "Electrokinetic Dewatering of Clays. II. It Influence of Salt, Acis and Flocculants." Colloids and Surfaces **6**: 239-251

Lockhart, N. C. (1983c). "Electroosmotic Dewatering of Clays. III. Influences of Clay Type, Exchangeable Cations and Electrode Materials." Colloids and Surfaces **6**: 253 - 269.

Lockhart, N. C. (1983d). "Electroosmotic Dewatering of Clays. I. Influence of Voltage." Colloids and Surfaces **6**: 229 - 238.

Lockhart, N. C. and G. H. Hart (1988). "Electro-osmotic dewatering of fine suspensions: The efficacy of current interruptions." Drying Technology **6**(3): 415- 423.

Lui, C. L. (1969). Ocean Sediment Holding Strength Against Breakout of Partially Embeded Objects. Proc. of Civil Engrg. in the Oceans II, ASCE, .

Lund, K. M. (2000). Effect of increase in pipeline soil penetration from installation. Internationa Conference on Offshore, Mechanics and Arctic Engineering (OMAE). New Orleans, LA.

Lyons, C. G. (1973). Soil Resistance to Lateral Sliding of Marine Pipelines. Offshore Technology Conference. Texas, USA.

Meyerhof, G. G. (1951). "The ultimate bearing capacity of foundations " Ge´otechnique **2**(4).

Micic, S., K. Y. Lo and J. Q. Shang (2004). "Increasing load-carrying capacities of offshore foundations in soft clays." JPT, Journal of Petroleum Technology **56**(2): 53-55.

Micic, S., J. Q. Shang and K. Y. Lo (2002a). "Electrokinetic strengthening of marine clay adjacent to offshore foundations." International Journal of Offshore and Polar Engineering **12**(1): 64-73.

Micic, S., J. Q. Shang and K. Y. Lo (2002b). Electro-Cementation of a Marine Clay Induced by Electrokinetics. Proceedings of the International Offshore and Polar Engineering Conference.

Micic, S., J. Q. Shang and K. Y. Lo (2002c). "Bearing capacity enhancement of skirted foundation element by electrokinetics." Proceedings of the Twelfth (2002) International Offshore and Polar Engineering Conference, Vol 2: 685-692.

Micic, S., J. Q. Shang and K. Y. Lo (2003a). "Improvement of the load-carrying capacity of offshore skirted foundations by electrokinetics." Canadian Geotechnical Journal **40**(5): 949-963.

Micic, S., K. Y. Lo and J. Q. Shang (2003b). A New Technology for Increasing the Load-Carrying Capacities of Offshore Foundations in Soft Clays, OTC 15264 Offshore Technology Conference (OTC) Houston, Texas, U.S.A., 5-8 May 2003.

Micic, S., J. Q. Shang and K. Y. Lo (2003c). Electrokinetic Strengthening of Soil Surrounding Offshore Skirted Foundations. Proceedings of the International Offshore and Polar Engineering Conference.

Micic, S., J. Q. Shang, K. Y. Lo, Y. N. Lee and S. W. Lee (2001). "Electrokinetic strengthening of a marine sediment using intermittent current." Canadian Geotechnical Journal **38**(2): 287-302.

Milligan, V. (1995). "First application of electro-osmosis to improve friction pile capacity - three decades later." Proceedings - ICE: Geotechnical Engineering **113**(2): 112-116.

Mitchell, J. K. (1991). "Conduction phenomena: from theory to geotechnical practice." Geotechnique **41**(3): 299-340.

Mitchell, K. J. and K. Soga (2005). Fundamentals of soil behavior, John Wiley & Sons.

Mohamedelhassan, E. and J. Q. Shang (2000). "Effects of electrode materials and current intermittence in electro-osmosis
Proceedings of the ICE - Ground Improvement **5**(1): 3 - 11.

Mohamedelhassan, E. and J. Q. Shang (2001). "Analysis of electrokinetic sedimentation of dredged Welland River sediment." Journal of Hazardous Materials **85**(1-2): 91-109.

Mohamedelhassan, E. and J. Q. Shang (2002). "Vacuum and surcharge combined one-dimensional consolidation of clay soils." Canadian Geotechnical J. **39**(5): 1126 - 1138.

Morris, D. V., W. A. Dunlap and R. E. Webb (1988). Self burial of laterally loaded offshore pipelines in weak sediments (OTC 5855). Offshore Technology Conference (OTC). Houston, Texas, USA: 421-424.

Muga, B. J. (1967). Bottom breakout forces. Proc. Civil Engrg. in the Oceans, ASCE: 569 - 600.

Murff, J. D., D. A. Wagner and M. F. Randolph (1989). "Pipe penetration in cohesive soil." Geotechnique **39**(2): 213-229.

Narasimha-Rao, S. and G. Rajasekaran (1994). "Lime injection technique to improve the behaviour of soft marine clays." Ocean Engineering **21**(1): 29-43.

Nielsen, N. J. R. and B. Lynberg (2004). "Upheaval Buckling Failures of Insulated Buried Pipelines: A Case Story." 1990 Offshore Technology Conference.

Oliphant, J. and A. Moconochie (2007). "The axial resistance of buried and unburied pipelines." Proceedings of the 6th International Offshore Site Investigation and Geotechnics Conference 11 - 13 September, 2007: 125 - 132.

Palmer, A. C., C. P. Ellinas, D. M. Richard and J. Guilt (1990). Design of Submarine Pipelines Against Upheaval Buckling (OTC 6335). Offshore Technology conference (OTC), 1990. **2:** 551 - 560.

Palmer, A. C., J. S. Steenfelt, J. O. Steensen-Bach and V. Jacobson (1988). "Lateral resistance of marine pipelines on sand." in: OTC '88 Proc. Offshore Technol. Conference., (Houston, U.S.A.: May 2-5, 1988) 4 , Paper OTC 5853: 399-408.

Palmer, A. C., J. S. Steenfelt, J. O. Steensen-Bach and V. Jacobson (1988). Lateral resistance of marine pipelines on sand (OTC 5853). Offshore Technology Conference (OTC), . Houson Texas, USA: 399-408.

Perinet, D. and I. Frazer (2006). Mitigation Methods for Deepwater Pipeline Instability Induced by Pressure and Temperature Variations. Offshore Technology Conference (OTC). Houston, Texas.

Perinet, D. and J. Simon (2011). Lateral buckling and pipeline walking mitigation in deep water (OTC 21803). Offshore Technology Conference (OTC).

Pinna, R., A. Weatherland, J. Grulich and B. Ronalds (2003). Field observations and modelling of the self-burial of a north west self pipeline. International Conference on Offshore Mechanics and Arctic Engineering (OMAE). Cancum, Mexico.

Potter, E. C. (1956). Electro-chemistry- Principles and applications, Cleaver- Hume Press Ltd.

Preston, R., F. Drennan and C. Cameron (1999). Control of lateral buckling of large diameter pipeline by snake lay. International Offshore and Polar Engineering Conference. Brest, France: 58 - 63.

Qian, J. H., W. B. Zhao, Y. K. Cheung and P. K. K. Lee (1992). "The theory and practice of vacuum preloading." Computers and Geotechnics **13**(2): 103-118.

Quigley, R. M. (1980). "Geology, mineralogy, and geochemistry of Canadian soft soils: a geotechnical perspective." Canadian Geotechnical J. **17**: 261-285.

Randolph, M. F. and K. H. Andersen (2006). "Numerical Analysis of T-Bar Penetration in Soft Clay." International Journal Of Geomechanics ASCE / November/December 2006, **6** (6): 411- 420.

Reddy, K. R., R. E. Saichek, V. d. Vegt and P. Ala (2002). "Effects of Soil Moisture and Heavy Metal concentrations on the electrokinetic remdediation." Indian Geotechnical Journal **32** (2): 258 - 278.

Reddy, K. R., A. Urbanek and A. P. Khodadoust (2006). "Electroosmotic dewatering of dredged sediments: Bench-scale investigation." Journal of Environmental Management **78**(2): 200-208.

Rittirong, A., J. Q. Shang, M. A. Ismail and M. F. Randolph (2006). Effect of electric field intensity on electro-cementation of caissons in calcareous sand. International Offshore and Polar Engineering Conference Proceedings**:** 408-415.

Rittirong, A., J. Q. Shang, E. Mohamedelhassan, M. A. Ismail and M. F. Randolph (2008). "Effects of electrode configuration on electrokinetic stabilization for caisson anchors in calcareous sand." Journal of Geotechnical and Geoenvironmental Engineering **134**(3): 352-365.

Rogers, C. D. F. and S. Glendinning (1997). "Improvement of clay soils in situ using lime piles in the UK." Engineering Geology **47**(3): 243-257.

Rose, W. L. (1979). Field applications of electro osmosis to increase offshore pile driveability. Offshore Technology Conference. Houston, Texas, USA**:** 747 - 755.

Micic, S., J. Q. Shang and K. Y. Lo (2002). Electro-Cementation of a Marine Clay Induced by Electrokinetics. Proceedings of The Twelfth (2002) International Offshore and Polar Engineering Conference, Kitakyushu, Japan.

Saowapakpiboon, J., D. T. Bergado, P. Voottipruex, L. G. Lam and K. Nakakuma (2011). "PVD improvement combined with surcharge and vacuum preloading including simulations." Geotextiles and Geomembranes **29**(1): 74-82.

Segall, B. A., C. E. O'Bannon and J. A. J. Matthias (1980). "Electro-osmosis chemistry and water quality. " Journal of the Geotechnical Engineering Division, ASCE **106**(10): 1148 - 1158.

Shang, J. Q. and W. A. Dunlap (1996). "Improvement of soft clays by high-voltage electrokinetics." Journal of Geotechnical Engineering-ASCE **122**(4): 274-280.

Shang, J. Q. and W. A. Dunlap (1998). "Pullout resistance of high-voltage strengthened ground anchors." Journal of Geotechnical and Geoenvironmental Engineering, ASCE **124**(9): 840-845.

Shang, J. Q. and l. Lo, K.Y. (1997). "Electrokinetic dewatering of a phosphate clay." Journal of Hazardous Materials **55**: 117-133.

Shang, J. Q., E. Mohamedelhassan and M. Ismail (2004). "Electrochemical cementation of offshore calcareous soil." Canadian Geotechnical Journal **41**(5): 877 - 893.

Sills, G. C. and S. J. Wheeler (1992). "The significance of gas for offshore operations." Continental Shelf Research **12**(10): 1239-1250.

Skempton, A. W. (1951). The bearing capacity of clays. Proc Building Research Congress. **1:** 180-189.

Skempton, A. W. (1951). The Bearing Capacity of Clays. Proc. Building Research Congress, London, England. London, England. **1:** 180 - 189.

Small, S. W., Tamburel.R.D. and Piasecky.P.J. (1972). "Submarine pipelines supported by marine sediments " Journal of Petroleum Technology **24**: 317- 322.

Srinivasaraghavan, R. and G. Rajasekaran (1994). "Electro-osmotic stabilization of marine clay with chemical piles." Ocean Engineering **21**(2): 207-219.

Stewart, D. P. and M. F. Randolph (1994). "T-bar penetrometer testing in soft clay." Journal of Geotechnical Engineering © ASCE **120**(12): 2230 - 2235.

Terzaghi, K. and R. B. Peck (1948). Soil mechanics in engineering practice, John Wiley & Sons, Inc, New York.

Thevanayagam, S., E. Kavazanjian, A. Jacob and I. Juran (1994). Prospects of vacuum-assisted consolidation for ground improvement of coastal and offshore fills. In: Proc. of sessions sponsored by the Geotechnical Engineering Division of the ASCE in conjuction with the ASCE National Convection Atlanta, Georgia.

Veritec-RP-E305 (1988). On-bottom stability design of marine pipelines, Veritas Offshore Technology and Services A/S.

Verley, R. and K. M. Lund (1995). Soil resistance model for pipelines placed on clay soils. Proceedings of the International Conference on Offshore Mechanics and Arctic Engineering - OMAE. **5:** 225-232.

Vermeulen, H. R. E. (1995). "Theory and Practice of Installing Pipelines by the Pre-Snaking Method." Proceedings of the Fifth (1995) International Offshore and Polar Engineering Conference (ISOPE) **2**: 47 - 52.

Vesic, A. S. (1971). "Breakout resistance of objects embedded in ocean bottom." J. Soil Mech. and Found. Div. **96**(SM4): 1311-1334.

Vesic, A. S. (1971). "Breakout resistance of objects embedded in ocean bottom." Journal of the Soil Mechanics and Foundations Division, ASCE, **97**(9): 1183 -1206.

Wagner, D. A., J. D. Murff, H. Brennodden and O. Sveggen (1989). "Pipe-soil interaction model." Journal of Waterway, Port, Coastal and Ocean Engineering **115**(2): 205-220.

Wan, T. Y. and J. K. Mitchell (1976). "Electro-osmotic consolidation of soils." Journal of the Geotechnical Engineering Division-ASCE **102**(5): 473 - 491.

Wantland, G. M., M. W. O'Neill, L. C. Reese and E. H. Kalajian (1979). Lateral stability of pipelines in clay (OTC 3477). Offshore Technology Conference. Houston Texas, USA.

Wheeler, S. J. (1988). "A conceptual models for soils containing large gas bubbles." Geotechnique **38**(3): 385 - 397.

Wheeler, S. J. (1988). "The undrained shear strength of soils containing large gas bubbles." Geotechnique **38**(3): 399 - 413.

White, D. J. and C. Y. Cheuk (2008). "Modelling the soil resistance on seabed pipelines during large cycles of lateral movement." Marine Structures **21**(1): 59-79.

Wrixon, R. C. and G. A. Cooper (1998). Theoretical and practical application guidelines for using electrokinetics to improve casing support in soft marine sediments. Proceedings of the IADC/SPE Asia Pacific Drilling Technology Conference, APDT.

Xie, L. and C. Shang (2006). "Effects of copper and palladium on the reduction of bromate by Fe(0)." Chemosphere **64**(6): 919-930.

Yan, H. S. and D. Z. Cao (2005). "Application of low-level vacuum preloading technique in offshore projects." Ocean and River Hydraulics **3** . 41-43.